Biosynthetic studies on the non mevalonate pathway to terpenes

Fowler, D. J.

BIOSYNTHETIC STUDIES ON THE NON MEVALONATE PATHWAY TO TERPENES

D. J. Fowler B.Sc. (Hons) Dunelm, GRSC

A Thesis submitted for the degree of Ph.D.

Van Mildert College
University of Durham

2001

COPYRIGHT

DECLARATION

The work contained in this thesis was carried out in the Department of Chemistry at the University of Durham between October 1997 and September 2000. All the work was carried out by the author unless otherwise indicated. It has not been previously submitted for a degree at this or any other university.

ABSTRACT

Biosynthetic studies on the non mevalonate pathway to terpenes

D.J.Fowler B.Sc. (Hons) Dunelm, GRSC

Isoprenoids are a class of secondary metabolites that are widely distributed in Nature. This thesis describes the synthesis and feeding of isotopically labelled enriched substrates to elucidate features of a new mevalonate independent pathway to isoprenoids.

Chapter 2 describes studies with a whole plant system, *Mentha citrata*, which produces the monoterpene linalyl acetate, and a bacterium *Escherichia coli* which produces ubiquinone-8. Feeding experiments with stable isotopically enriched compounds demonstrate that the terpene unit of linalyl acetate is biosynthesised *via* the mevalonate independent pathway. Incorporation of deuterium from [6,6-$^{2}H_2$]-glucose, [$^{2}H_3$]-alanine and [$^{13}C^{2}H_3$]-alanine into linalyl acetate show that the conversion to isopentenyl pyrophosphate does not proceed *via* a series of dehydrations. Feeding experiments with putative intermediates bearing deuterium into *E. coli* show that none of the intermediates are incorporated. This suggests that *E. coli* lacks a kinase to activate exogenously administered substrates fed as the free alcohols.

Chapter 3 outlines biosynthesis studies on a meroterpene rosnecatone produced by the fungus *R. necatrix*. Intact incorporation of ^{13}C from the feeding of [1,2-$^{13}C_2$]-acetate shows that the terpenoid moiety is produced *via* the mevalonic acid pathway and the non-terpenoid unit is polyketide derived. Incorporation of deuterium from [6,6-$^{2}H_2$]-glucose fully describes the pentaketide that delivers the non-terpenoid fragment. The effect on the metabolite production of changing the growth conditions of *R. necatrix* is investigated. Changing from a static culture to a submerged cultures causes an increased rate of growth, an upregulation of the production of cytochalasan E and a cessation of rosnecatone production. Screening of rosnecatone against two Human cancer cell lines shows IC_{50} values of 4.48μM and 5.78μM.

To Mum, Dad and Lisa

"αρχασ εναι τον ηολον ατομοσ και κενον"

"All the world is made of atoms and void"

Democritus

Acknowledgements

I would like to sincerely thank David O'Hagan for his supervision and all his encouragement throughout the PhD and during my studies as an undergraduate. David's boundless energy and excitement for natural product chemistry were some of the key motivations for reading for a PhD and helped me continue when things were going slowly.

The work involving GC-MS would not have been possible without the help of Jack Hamilton (Belfast) who was always ready to analyse samples at a moment's notice and provide candid analysis of the results. Thank you Jack.

Thanks are also due to Jens Nieschalk and Denis Bouvet who synthesised the labelled glycerols and glycerate and for providing assistance with all synthetic matters. Andy Humphrey has been an unrivalled partner and has been a constant source of ideas, discussion and substrates. The O'Hagan group made the lab. a vibrant and exciting place to work and deserve a debt of gratitude for all their help, advice and friendship during this work. Special thanks are due to Helen Smith for support, discussion and companionship whilst writing this thesis.

The NMR staff of Alan, Ian and Catherine require a special mention for running long ^{2}H NMR spectra and for vital, honest and sympathetic discussions about deuterium incorporation.

Ray Edwards (Bradford), Richard Robins (Nantes) and Tony Fawcett (Durham) are duly thanked for donating cultures. Funding by the EPSRC is gratefully noted.

Finally, this work is testament to the support of my family and friends.

Abbreviations

Ac	acetate
ACP	acyl carrier protein
ATP	adenosine triphosphate
Bn	benzyl
Bz	benzoyl
CI	chemical ionisation
CoA	coenzyme A
CDP-ME	4-phosphocytidyl-2-*C*-methylerythritol
CDP-MEPP	4-phosphocytidyl-2-*C*-methylerythritol-2-phosphate
DEPT	Distortionless Enhancement by Polarisation Transfer
DCM	dichloromethane
DHAP	dihydroxyacetone phosphate
DIBAL	diisobutylaluminium hydride
DMA	dimethylallyl alcohol
DMAPP	dimethylallyl pyrophosphate
DMF	dimethylformamide
DMSO	dimethyl sulphoxide
DNA	deoxyribose nucleic acid
DX	1-deoxy-D-xylulose
DXP	1-deoxy-D-xylulose-5-phosphate
EI	electron ionisation
equiv.	equivalent
Et	ethyl
EtOAc	ethyl acetate
EtOH	ethanol
FAD	flavin adenosine dinucleotide, reduced form
FAS	fatty acid synthase
FPP	farnesyl pyrophosphate
FFPP	farnesyl farnesyl pyrophosphate
FMNH	flavin mononucleotide, reduced form
HMG	hydroxy methyl glutarate
GAP	D-glyceraldehyde-3-phosphate

GC-MS	gas chromotography mass spectrometry
GPP	geranyl pyrophosphate
GGPP	geranyl geranyl pyrophosphate
h	hour
HMQC	Hetroatom Multiple Quantum Correlation
Hz	Hertz
IPP	isopentenyl pyrophosphate
IR	infrared
i-Pr	isopropyl
LB	Luria-Bertani
LDA	lithiumdiisopropylamide
Me	methyl
ME	2-*C*-methylerthyritol
MEP	2-*C*-methylerthyritol-4-phosphate
ME-2,4-CDP	2-*C*-methylerythritol 2,4-cyclodiphosphate
ME-3,4-CMP	2-*C*-methylerythritol 3,4-cyclomonophosphate
MeOH	methanol
min	minute
mM	millimolar
MS	mass spectroscopy
MVA	mevalonic acid
NAD	nicotinamide adenine dinucleotide
NADH	nicotinamide adenine dinucleotide, reduced form
NADP	nicotinamide adenine dinucleotide phosphate
NADPH	nicotinamide adenine dinucleotide phosphate, reduced form
NMR	nuclear magnetic resonance
nOe	nuclear Overhauser effect
PKS	polyketide synthase
PLP	pyridoxal 5'-phosphate
ppts	pyridinium *para*-toluene sulfate
pTSA	*para*-toluene sulphonic acid
RNA	ribose nucleic acid
s	second
SAM	*S*-adenosylmethionine

t-Bu	*tert*-butyl
TCA	tricarboxylic acid
temp	temperature
TFA	trifluoroacetic acid
THF	tetrahydrofuran
THP	tetrahydropyran

TABLE OF CONTENTS

Chapter 1

Introduction

1 Introduction

Of all the gifts Nature has to offer, none are as varied or colourful as the natural products that the living planet produces. Man has used this diverse array of metabolites since the start of recorded history. Records found in Egyptian tombs show the use of camphor as a perfume and the extraction of turpentine by distillation[1]. Ancient Britons used the plant pigment woad as war paint and even the Bible chronicles the use of myrrh as a gift to the Infant Christ[2]. In recent times natural products have been found to be as much a blessing as a curse – whilst bioactive drugs such as clavulanic acid (**1**) have greatly reduced disease and suffering, substances such as cocaine (**2**) have caused as much pain as they were originally prescribed to relieve.

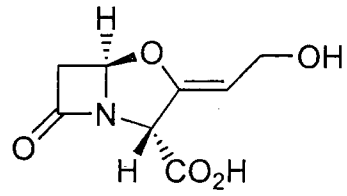

1

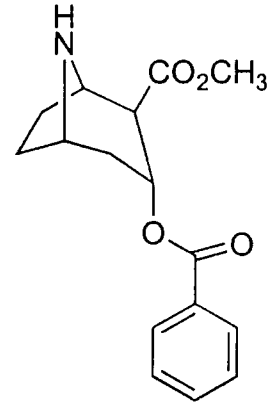

2

1.1 Primary and Secondary metabolism

Primary and secondary metabolism, and hence primary and secondary metabolites, are often generally described as different classes of natural products. Bu'lock[3] describes primary metabolites in plants as "substances which could be detected in all plants" whereas secondary metabolites are "a variety of substances each of which could be obtained from one particular plant species which could be assigned no general function". A more recent and complete definition is provided by Mann[4]; "secondary metabolism is metabolism that is not essential for the growth and reproduction of the organism" i.e. secondary metabolites have a secondary role in the survival of an organism. Secondary metabolites have also been described as species that are produced by an organism but have a specific receptor in a different organism. The enzymes required for primary metabolism are ubiquitous to almost all living organisms whereas the machinery for producing secondary metabolites (idolites) are often unique to one species of a genus. It is difficult to draw a clear distinction between primary and

secondary metabolites, except in the case of bacterial idolites which are described below. Idolites are commonly derived from one of a small number of key intermediates as shown in Figure 1-1.

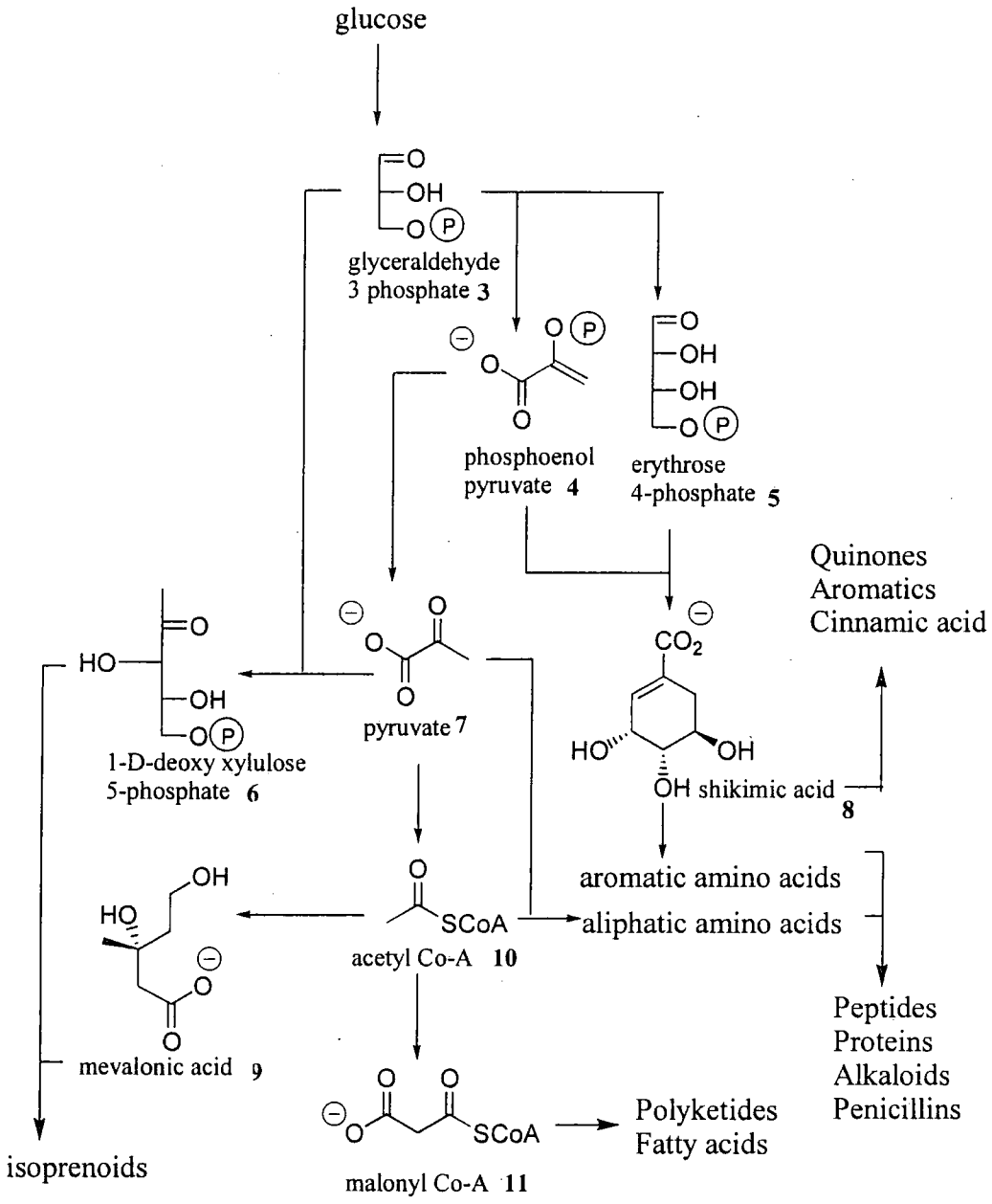

Figure 1-1 Diagram showing the biogenesis of common intermediates and their fate

1.1.1 Bacterial growth and secondary metabolism

Figure 1-2 below shows the growth profile of a bacterial culture with the cell mass plotted against time.

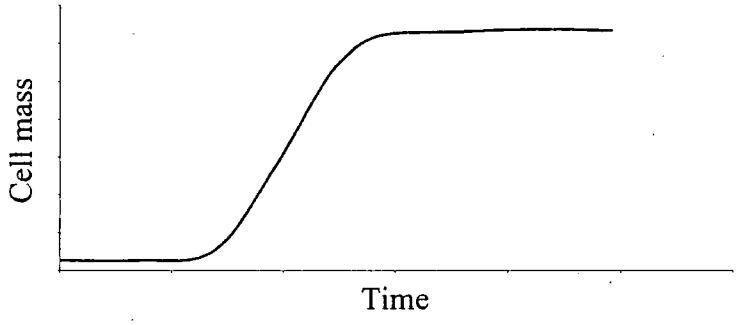

Figure 1-2 Graph showing cell mass versus time for a bacterial culture

Initially cell growth is slow and almost linear until such a point as the organism begins to rapidly proliferate. This is followed by a period of rapid growth that is described as the "log phase" as the cell growth is logarithmic. It is during this time that the organism utilises primary metabolic pathways. These deliver metabolites such as DNA/RNA, proteins, and lipids – metabolites which are essential to life and are made from the exogenous sources such as CO_2, sugars and amino acids by processes such as glycolysis and the tricarboxylic acid cycle (TCA cycle). These primary metabolites are used to manufacture cells and cell machinery.

As the organism exhausts the supply of nutrients the growth is retarded to such a degree that the logarithmic growth rate is halted and replaced by a period where no further growth takes place. This is described as the organism entering the "stationary" phase. The stationary phase is the time when bacteria change the rate at which metabolic pathways are employed by upregulating secondary metabolism at the expense of primary metabolism. This is when secondary metabolite production is maximal. These secondary metabolites, delivered from pathways such as the mevalonic acid pathway, the shikimate pathway and fatty acid biosynthesis, are non-essential to growth as is evident from their late production, but are very important to survival. The late onset of secondary metabolism is essential as many idolites are fatal to developing cells and thus early production would result in severe growth retardation.

Organisms that grow slower than bacteria have a less clear distinction between primary and secondary metabolic production phases. Plants are capable of producing metabolites

that are non-essential for growth long before growth has finished; an everyday example is the smell of garden flowers before they are fully-grown. In systems like these the biomechanical machinery of primary and secondary metabolism is inherently linked and thus the difference between primary and secondary metabolites is expressed in terms of molecular structure rather than biological uses.

1.2 The function of secondary metabolites

The role of secondary metabolites in biological systems has been a source of mystery and controversy. Although secondary metabolites, in particular plant secondary metabolites, have been found to have a variety of functions, the exact reason for their biosynthesis is unknown. The vast array of structures, and thus the number of dedicated enzymes needed to produce the myriad of compounds, naturally leads one to the conclusion that secondary metabolites do perform a valuable function. The precedent for the use of idolites such as azadirachtin (**12**) from the Neme plant and senecionone (**13**) from ragwort (*Senecio jacobaea*) as antifeedants is well established deterring insects and mammals respectively.

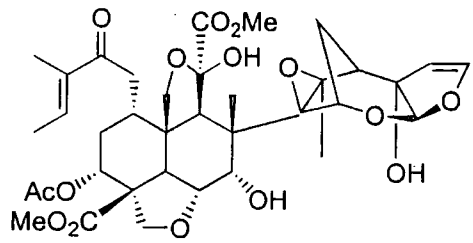

12

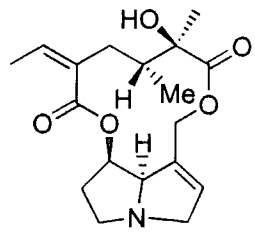

13

Other idolites are known to possess valuable antibiotic activity and have been used by Man. The vast majority of idolites, however, appear to have no obvious purpose or reason for production. This has led to the rationalisation of idolite production in terms of their evolutionary significance. One hypothesis, proposed by Davies[5], is that secondary metabolites, particularly antibiotics, were used as part of defence mechanisms in an RNA world. β Lactam antibiotics are known to target murein peptidoglycan which was present in the first cells, and thus it may appear that the first secondary metabolites were responsible for inter-bacterial chemical defence. This implies that azadirachtin and senecione are evolutionary supercedants which are more sophisticated owing to inter kingdom interaction. Davies' hypothesis has been rejected

by Cavalier-Smith[6] because it fails to account for the initial origin of the required genes and because idolites such as the cytochalasins, which affect eukaryotes, appeared before the organisms that they adversely affect. Furthermore, as the genes coding for idolite production have been conserved over many millions of years the notion that secondary metabolites were used as an evolutionary playground can be dismissed[7]. Over time genes that corresponded to secondary metabolites that give no advantage to the organism to the host would be lost with the result that very few secondary metabolites would be produced.

1.3 Secondary metabolites

1.3.1 Fatty acids and polyketides

Fatty acids are a class of compounds that have a common biosynthesis. Owing to their lipophilic nature, fatty acids are used by Nature in cell membranes as lipids and are employed in energy storage as fats. Both unsaturated and saturated chains are abundant in Nature and chain lengths of between eight and twenty carbon atoms are commonly encountered. One of the key features of fatty acid biosynthesis is that the chain is built up *via* a series of steps that occur on the surface of the fatty acid synthase that mediates chain building. Initially, acetyl-CoA (**10**) is activated to malonyl-CoA (**11**) which is then transferred onto the surface of an acyl carrier protein (ACP) as the thioester. Subsequent decarboxylative condensation of acetyl-CoA with malonyl-ACP produces a β-keto species. Once bound to ACP the chain then proceeds to elongate by decarboxylative displacements of thiol ester bound pendant chains that are present on the ACP (step i). The β-keto ester is then reduced by enoyl-keto reductase to deliver the β-hydroxy acid *via* NADPH (step ii). The elimination of water by β-hydroxy dehydratase delivers the α,β-unsaturated ketone (step iii). The final step of the cycle is reduction of the olefinic bond by an enoyl reductase that produces, on the first iteration, butyryl-CoA. As the carbon chain is built up from acetate units, only even numbered fatty acids are found to occur in Nature.

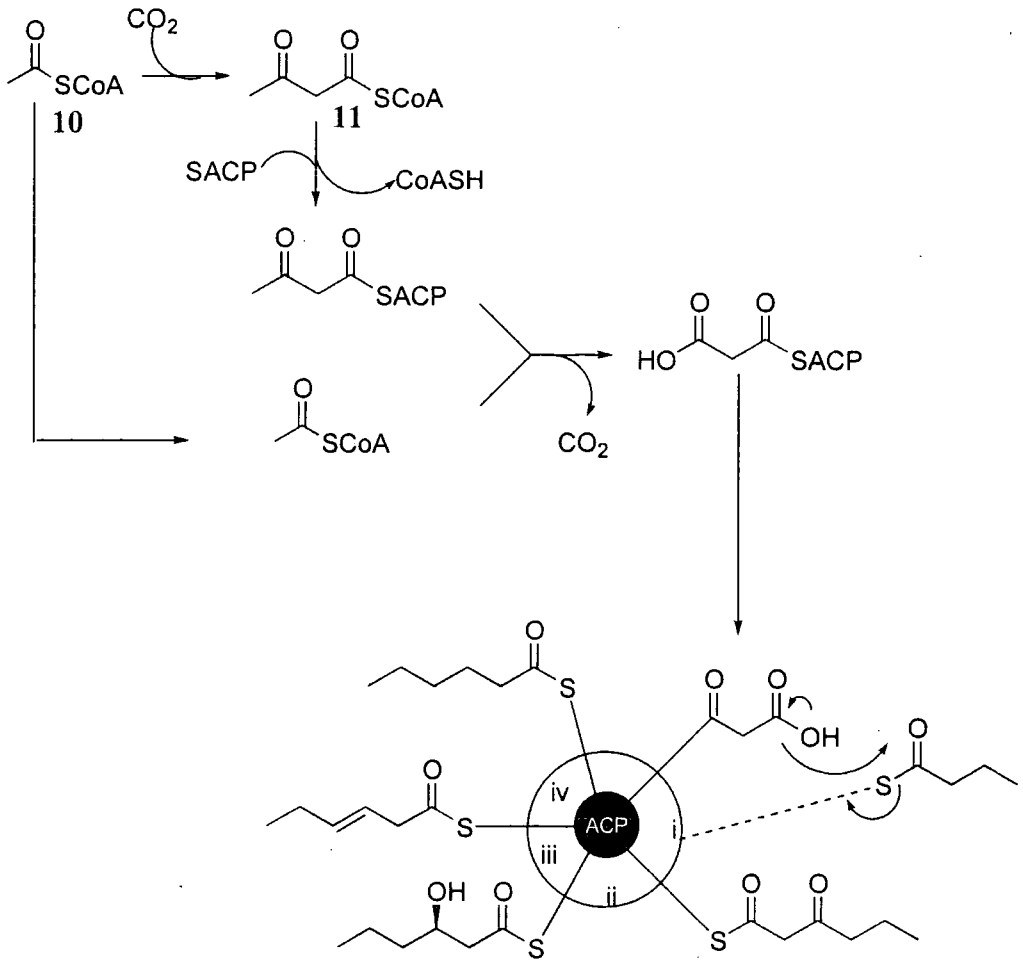

Scheme 1-1 A schematic representation of fatty acid biosynthesis

After the first cycle, the saturated thioester can then react again with malonyl–CoA to repeat the process and increase chain length.

Unsaturated fatty acids are produced using the same machinery as above. Nearly all double bonds produced *via* fatty acid biosynthesis are *cis*, which prevents efficient packing and affords cell wall rigidity. Fatty acids are also responsible for a high proportion of the rare fluorinated natural products, which are most probably derived from the use of fluoroacetate (**14**) as a starter unit[8].

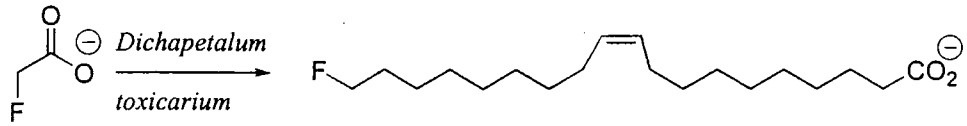

14 15

Scheme 1-2 Fluoro-oleic acid (**15**) from fluoroacetate (**14**) as a starter unit[8]

Polyketides are a class of secondary metabolites that are also produced *via* the condensation of successive malonyl-ACP units. As studies on the isolation and biosynthesis of some polyketide compounds are described later in this thesis, it is pertinent to only briefly outline some features of the polyketide pathway. Polyketides are formed from the condensation of acetyl-CoA (**10**) usually with malonyl-ACP (**11**) units in the same iterative manner as fatty acids (Scheme 1-1). The idea that polyketides could be built from the successive condensation of acetate units was formulated by Collie[9] although the development of the "polyketide hypothesis" was only fully realised by Birch[10] some fifty years later. Birch applied the rationale that polyketides were derived from the repeated condensation of acetate units to show that the proposed structure of eleutherinol (**16**) was incorrect as it could not be described in terms of head-to-tail acetate linkages. The revised structure agreed with findings of degradative experiments.

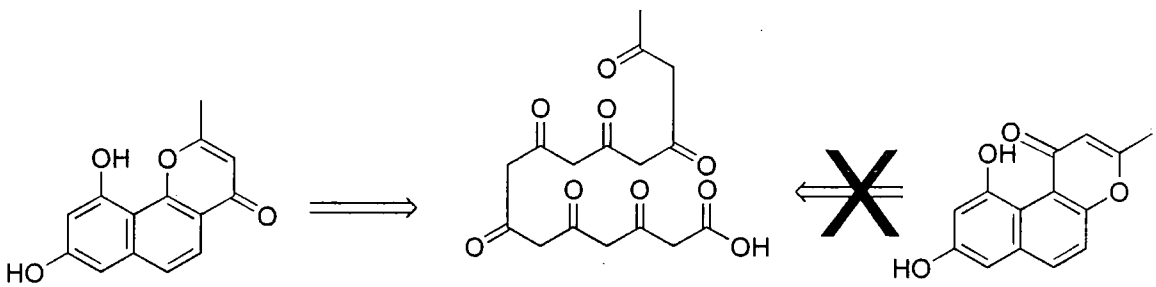

16

Scheme 1-3 Birch's application of the acetate hypothesis to structure elucidation

Polyketides are a structurally diverse class of idolites that are abundant in fungi, particularly fungi imperfecti and are also feature heavily in bacterial secondary metabolism. The range of structures is increased by the use of units other than acetate.

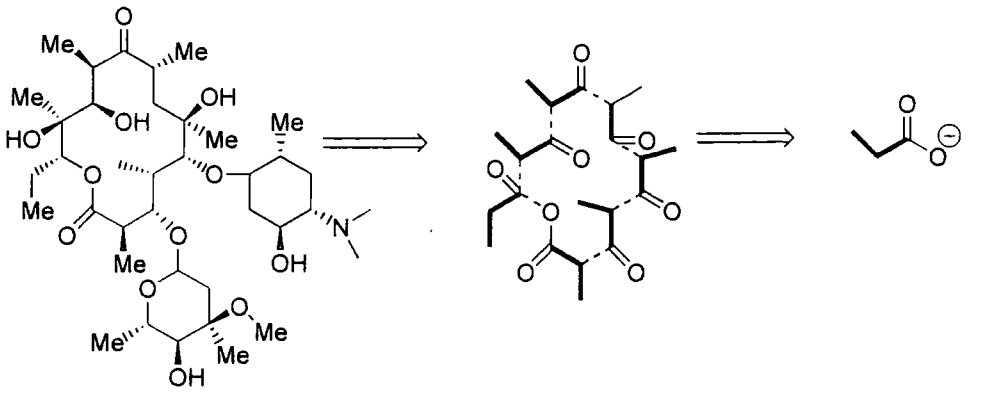

17

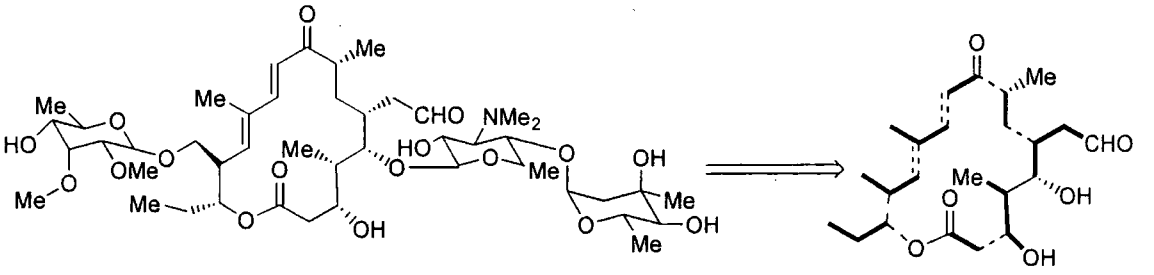

18

Figure 1-3 Disconnection demonstrating propionate build up of erthromycin A (**17**) and tylosin (**18**)

Structures such as the bacterial polyketide erythromycin A (**17**) are derived uniquely from propionate units whereas structures such as the macrocylic component of tylosin (**18**) are formed from acetate, propionate and butyrate units.

Bioactive polyketides are now known to include antibiotics (e.g. erthromycin A,**17**), carcinogens (aflatoxin B1, **19**), nephrotoxins (patulin, **20**) and antifungal agents (variotin, **21**).

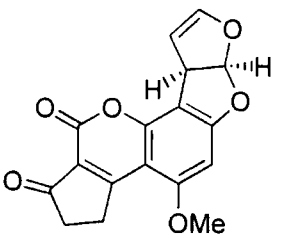

19

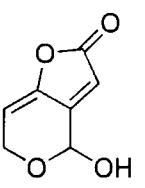

20

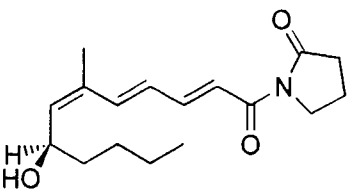

21

1.3.2 Shikimate derived metabolites

The shikimic acid pathway delivers aromatic amino acids to both the primary and secondary metabolic pathways and is important in higher plants and bacteria. The pathway delivers phenylalanine (**22**) and tyrosine (**23**), both of which are abundant in idolites, and tryptophane (**24**), which is used predominantly by primary metabolism.
The pioneering work on the shikimate pathway was performed by Davies, some 70 years after the first isolation of shikimic acid (**8**). The pathway is now well understood and features the condensation of erthyrose-4-phosphate (**5**) with phosphoenol pyruvate (**4**) to produce shikimic acid (**8**).

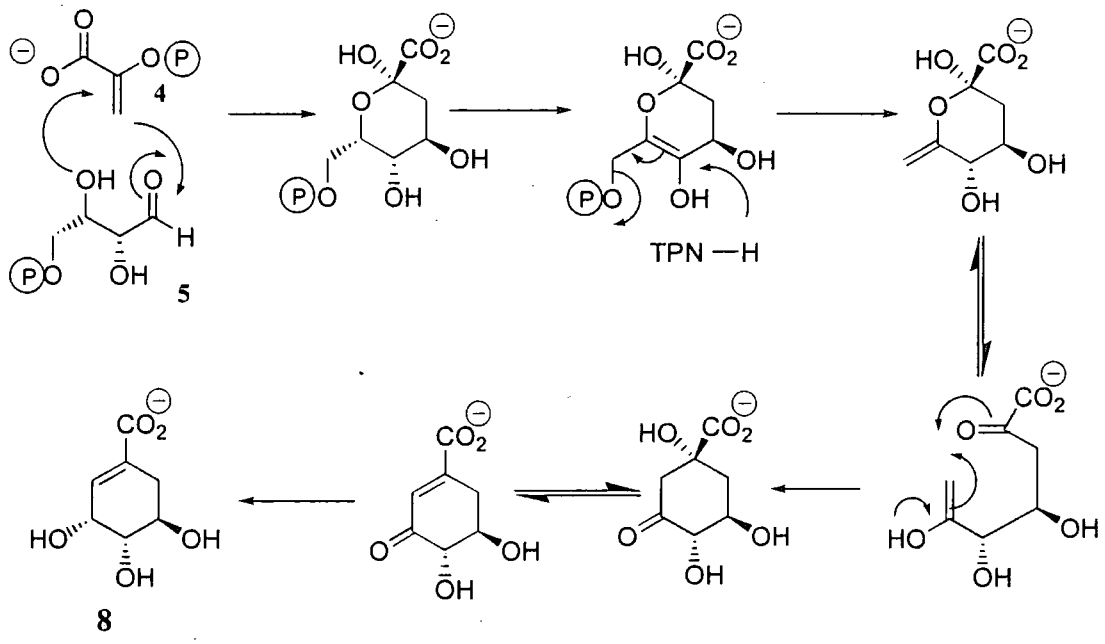

Scheme 1-4 Formation of shikimic acid (**8**)

Shikimic acid (**8**) is then converted to chorismic acid (**25**) by the addition of phosphoenol pyruvate (**4**), which delivers the amino acids phenylalanine (**22**) and tyrosine (**23**) as shown in Scheme 1-5.

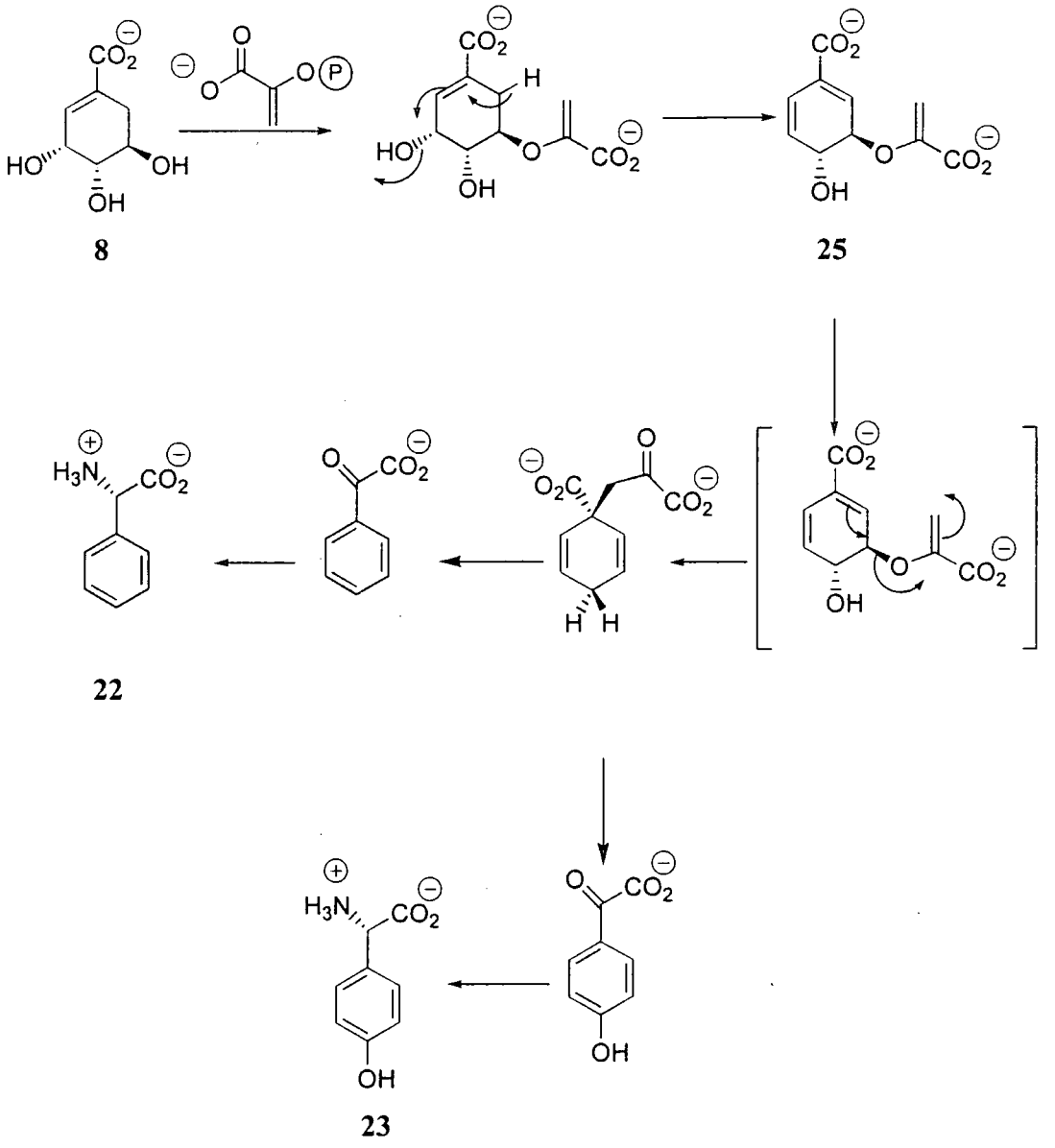

Scheme 1-5 Biosynthesis of phenylalanine (**22**) and tyrosine (**23**) from chorismic acid (**25**)

1.3.3 Isoprenoids

Isoprenoids are a broad class of idolites that include terpenoids, steroids and compounds containing prenyl chains such as carotenoids. It has recently been shown[11] that there are two biosynthetic pathways to isoprenoids and the elucidation of the new terpene biosynthesis is a major focus of this work. Isoprenoids are more fully described in section 1.5

1.4 Elucidation of a biosynthetic pathway

Secondary metabolites are often grouped in terms of their biosynthetic origin. Despite the diverse array of secondary metabolites, almost all are derived from one of a small number of pathways with structural modifications performed later. Knowledge of a biosynthetic pathway can lead to new target compounds for drug discovery as specific inhibitors can be designed to knock out key enzymes. In order to understand fully a pathway, a number of techniques are available.

1.4.1 Incorporation of isotopically labelled precursors

It is often difficult to trace the biosynthesis or catabolism of a secondary metabolite. However, atoms or bonds can be followed, either by single or multiple labelling with isotopes. Typically the organism is grown in the presence of an appropriately isotopically labelled precursor and the resultant metabolite is extracted and analysed by NMR or MS techniques.

1.4.2 Radioisotopes

The post war production of ^{14}C and ^{3}H as nuclear by-products heralded a new age in biosynthetic elucidation by providing ready sources of [1-^{14}C] and [2-^{14}C]-acetate. Pioneering experiments by Calvin using $^{14}CO_2$ with photosynthetic algae showed incorporation of ^{14}C into the carbonyl carbon of 3-phosphoglycerate (**26**) demonstrating that atmospheric CO_2 is fixed *via* ribulose-1,5-bisphosphate carboxylase (Scheme 1-6)

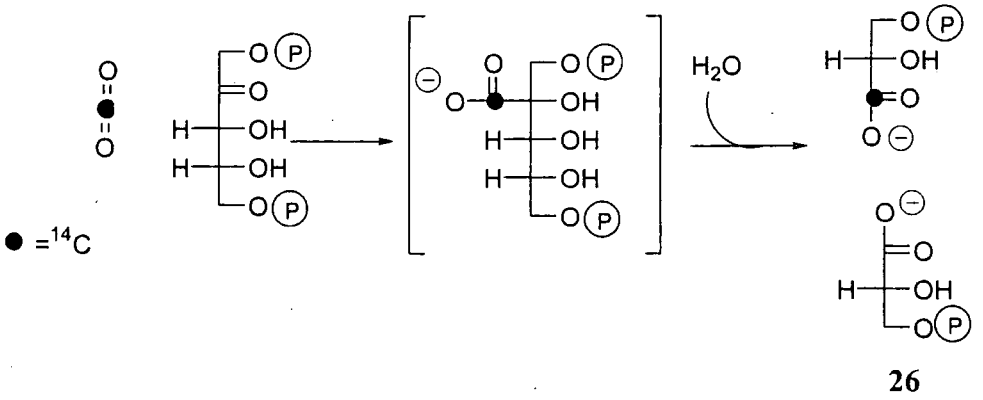

26

Scheme 1-6 Incorporation of ^{14}C labelled CO_2 into 3-phosphoglycerate (**26**)

The Table below shows the properties of the most frequently used radioisotopes.

Radioisotope	*Emission*	*Half life*	*Specific activity (mCi/mA)*
^{3}H	β	12.35 y	2.92×10^{4}
^{14}C	β	5730 y	62.4
^{32}P	β	87.5 d	1.50×10^{6}
^{33}P	β	25.5 d	5.32×10^{6}
^{35}S	β	14.3 d	9.2×10^{6}

Table 1-1 Selected properties of common radioisotopes[12]

Tritium (^{3}H) has been used to trace the biosynthetic course of hydrogen atoms. It has magnetic properties that are similar to that of ^{1}H but it is not found in Nature.

Nucleus	*Natural abundance /%*	*Spin*	*Relative Magnetogyric ratio*
^{1}H	99.976	½	1.000
^{3}H	0	½	1.067

Table 1-2 Comparison of magnetic properties of ^{1}H and ^{3}H

The disadvantage of ^{3}H as a probe is its relatively high levels of radioactivity. Radioisotopes have other associated problems. Being sources of ionising radiation, radioisotopes require careful monitoring in order to minimise exposure. Furthermore, as it is often impossible to discern which of the atoms is bearing the label, each structural motif needs to be isolated and analysed separately *via* degradative techniques. These can be technically demanding and time consuming.

1.4.3 Stable isotopes

Stable isotopes are the most widely used chemical technique employed in the elucidation of biosynthetic pathways. Many compounds are commercially available bearing at least one isotopically enriched atom, typically ^{13}C or ^{2}H. Both nuclei are magnetically observable.

Nucleus	*Spin*	*Natural Abundance/%*
^{2}H	1	0.016
^{13}C	½	1.1

Table 1-3 Magnetic properties of ^{2}H and ^{13}C

Deuterium, like tritium, is conventionally used as a probe to trace the fate of hydrogen atoms and is amenable to detection using NMR spectroscopy although the sensitivity is much lower than for ^{1}H or ^{3}H. An attractive feature of deuterium labelling is that ^{2}H chemical shifts are comparable to proton chemical shifts of the same molecule, which alleviates the need for additional resonance assignments. As ^{2}H is a quadrapolar nucleus, deuterium signals are much broader than proton or triton resonances. Deuterium labelled acetate is commonly used to show that a metabolite is polyketide derived. The position of the deuterium label also shows the orientation of the growing chain[13] as in the case of alternariol (**27**).

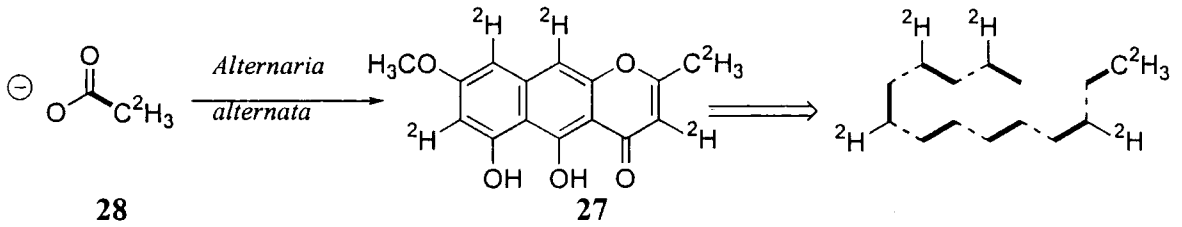

Scheme 1-7 Incorporation of [2-$^{2}H_3$]-acetate (**28**) into alternariol (**27**)[13]

Deuterium incorporation can also be assessed indirectly by ^{13}C-NMR spectroscopy up to one carbon away from the site of enrichment. The heavier ^{2}H nucleus induces a subtle shift in electron density around the carbon nucleus compared to a C-H bond. This causes C-^{2}H carbon resonances to come at higher field than the corresponding C-H

carbon resonances. This one bond shift is described as an α shift. A two bond β shift of 0.06 ppm in a ^{13}C-C-^{2}H system is also observable. Similar shifts are found when using ^{18}O, but these are smaller in magnitude.

Nucleus	*α-shift per atom /ppm*	*β-shift per atom /ppm*
^{2}H	0.35	0.06
^{18}O	0.03	0.001

Table 1-4 α And β shifts caused by ^{2}H and ^{18}O

Oxygen-18 has been used to determine the fate of oxygen atoms along the biosynthetic pathway and is typically analysed *via* mass spectroscopy[14].

Carbon-13 was first fully realised as a potential tool in biosynthesis by Seto and co-workers in 1970[15] thirteen years after the first natural abundance ^{13}C NMR spectrum had been obtained[16]. ^{13}C Enrichments are typically observed *via* the increase in peak heights in the ^{13}C NMR spectrum. This allows the position of the label to be established and, by comparison with other signals in the spectrum, the level of enrichment can be calculated. The use of single labelled carbon precursors is generally limited to late intermediates on a pathway as early intermediates such as [1-^{13}C] and [2-^{13}C]-acetates result in low incorporations due to other metabolic processes that occur. The correspondingly small increase in ^{13}C-peak height may be below the detectable threshold of ^{13}C-NMR.

The use of double-labelled substrates provides much greater sensitivity and can provide additional information. For example, [1,2-$^{13}C_2$]-acetate is routinely used in "bond labelling" whereby the fate of carbon-carbon bonds is followed[17]. If the acetate unit is incorporated intact then adjacent ^{13}C nuclei will couple to each other, resulting in a doublet about the natural abundance ^{13}C peak in the ^{13}C-NMR spectrum. If the acetate unit is catabolised then no doublet will be observed.

The use of multiply labelled ^{13}C and ^{2}H acetates provides a powerful tool for detection of the carbon-deuterium bonds[18]. A $^{13}C\{^{1}H\}$ NMR spectrum shows the carbon resonance corresponding to ^{13}C-^{2}H as a multiplet whereas a $^{13}C\{^{1}H, ^{2}H\}$ NMR spectrum shows the same resonance as a singlet. Subtracting one spectrum from the other shows carbon nuclei with intact C-^{2}H bonds. The α-shift in the $^{13}C\{^{1}H, ^{2}H\}$ NMR spectrum is also additive and hence shows the number of deuterium atoms present

1.4.4 Cell free extracts

Cell free extracts allow the study of biosynthetic reactions by providing the biosynthetic machinery in an *in vivo* setting. Cell free work allows investigation into such features as co-factor requirements in enzyme chemistry. It has the advantage over the feeding of isotopically enriched compounds that substrates are "turned over" directly by the appropriate enzyme rather than requiring activation or metabolic conversion. This has proved to be a very useful method in the study of the new terpene pathway and is discussed later.

1.4.5 Blocked mutants

A biosynthetic scheme can be considered in terms of a series of consecutive steps, each of which is mediated by a unique enzyme. Disabling one of the enzymes in a mutant organism can result in the accumulation of the preceding metabolite such that it can be isolated and analysed.

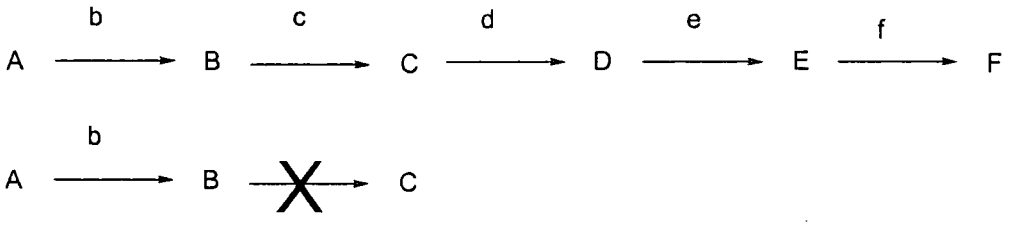

Figure 1-4 Use of blocked mutants to effect metabolite isolation

1.5 Isoprenoids

The term isoprenoids is used to describe terpenes, terpenoids (oxygen containing terpenes), steroids, sterols (steroids containing an alcohol functionality), and carotenoids. The name "terpene" derives from the 14th century, and is a debasement of the Medieval Latin *terbentina*, from *terebinthus*, the tree from which oil of turpentine was collected. Historically terpenes have fascinated Man and the mapping of their biosynthesis and properties reads as a "who's who" of eminent chemists and biochemists of the last century.

1.5.1 Terpene classification

Terpenes are described according to the number of contiguous carbon atoms they possess.

Number of carbon atoms	Class
10	monoterpenoids
15	sesquiterpenoids
20	diterpenoids
25	sesterpernoid
30	triterpenoids
40	tetrapernoids
>40	polyterpenoids

Table 1-5 Classification of terpenoids according to carbon chain length

Early studies observed that many terpenes known at the time could be described as being built up from two molecules of the C_5 isoprene unit. Isoprene (**29**) was known at the time to be a volatile emitted by plants. A retrosynthetic analysis of limonene using a Diels-Alder type reaction reveals two molecules of isoprene. Pyrolysis of monoterpenes supports this hypothesis yielding two molecules of isoprene (**29**).

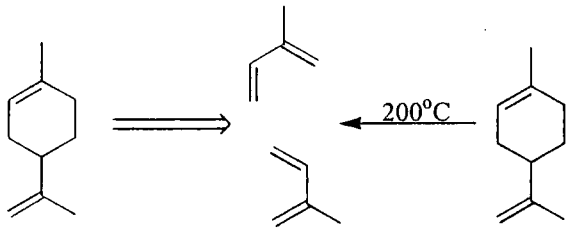

30 **29** **30**

Scheme 1- 8 Disconnection and pyrolysis of limonene (**30**) to produce two molecules of isoprene (**29**)

This approach was successfully applied to all terpenes that were known at the time as only simple monoterpenes had been isolated and characterised. In 1887, Wallach[19] formally proposed the "isoprene rule" which stated that all terpenoids could be described in terms of being assembled from a number of isoprene units linked together

in a head-to-tail fashion. Terpenoids that meet the isoprene rule are described as regular terpenoids. However, with the advent of greater analytical sophistication increasing numbers of irregular terpenoids were isolated, such as eremophilone (**31**)[20], that could not be rationalised by the isoprene rule.

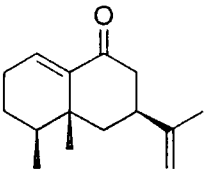

(**31**)

Eremophilone cannot be disconnected to give three molecules of isoprene although Robinson[20] suggested that the structure could be rationalised by the following scheme (Scheme 1-9).

The key step is the formation of a carbocation which promotes a transansullar methyl shift. The resultant carbocation is then neutralised in an elimination reaction.

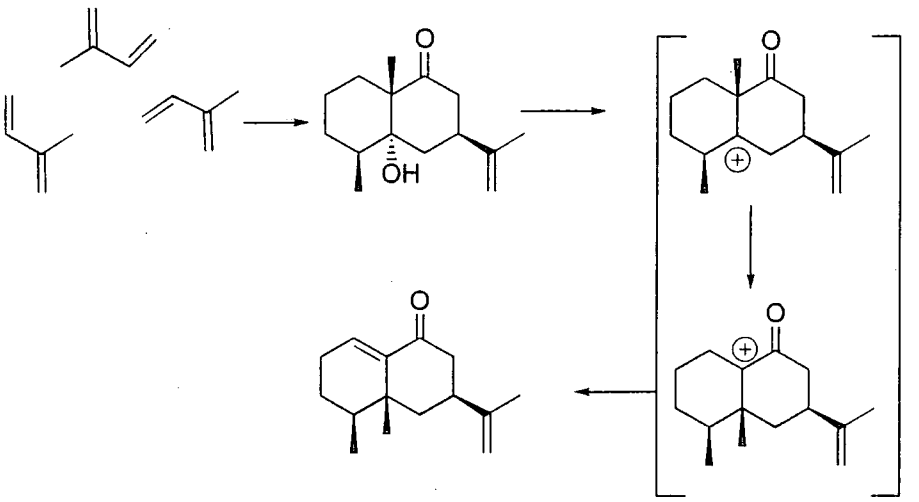

(**31**)

Scheme 1-9 The connectivity of eremophilone (**31**) explained in terms of a rearrangment

Such irregular terpenes led to the formulation of the "biogenic isoprene rule" by Ruzicka[21]. This states that all terpenes can be described in terms of assembly from isoprene with structural modifications provided by simple transformations such as proton shifts. The biogenic isoprene rule has proved useful in the classification of terpenoids. Thus the irones, a class of C_{15} terpenoids produced by sword lily rhizomes

may appear to be sesquiterpenes by virtue of the number of carbons although they are actually triterpenoids and are derived from the iridial group[22].

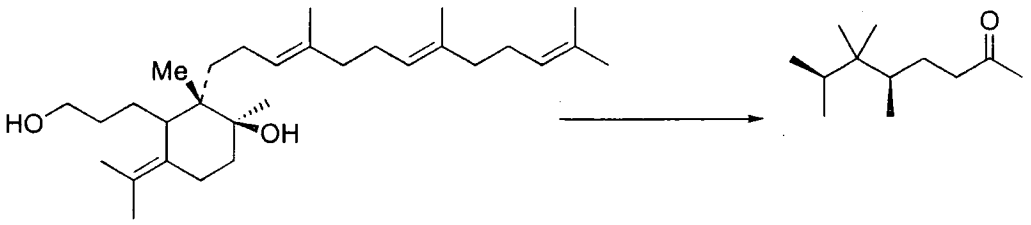

32 33

Scheme 1-10 Conversion of iridial (**32**) to irone (**33**)

The biogenic isoprene rule was correctly inspired and terpenoids are now known to derive biosynthetically from the condensation of C_5 units. These have been identified as isopentenyl pyrophosphate (IPP, **34**) and dimethylallyl pyrophosphate (DMAPP, **35**) which are activated and less volatile forms of isoprene. The condensation of IPP and DMAPP is discussed below.

1.5.2 Formation of terpenes: the interconversion of IPP (34) and DMAPP (35)

34 **35**

It is well established that DMAPP (**35**) is formed from IPP (**34**) by the action of IPP isomerase which stereoselectively removes the *pro*-R hydrogen[23] in the isomerisation reaction. Concurrent with this is the addition of a proton from the medium to the other face of the double bond. As the reaction is stereospecific the methyl groups of DMAPP are non-equivalent. The new methyl group has E-geometry.

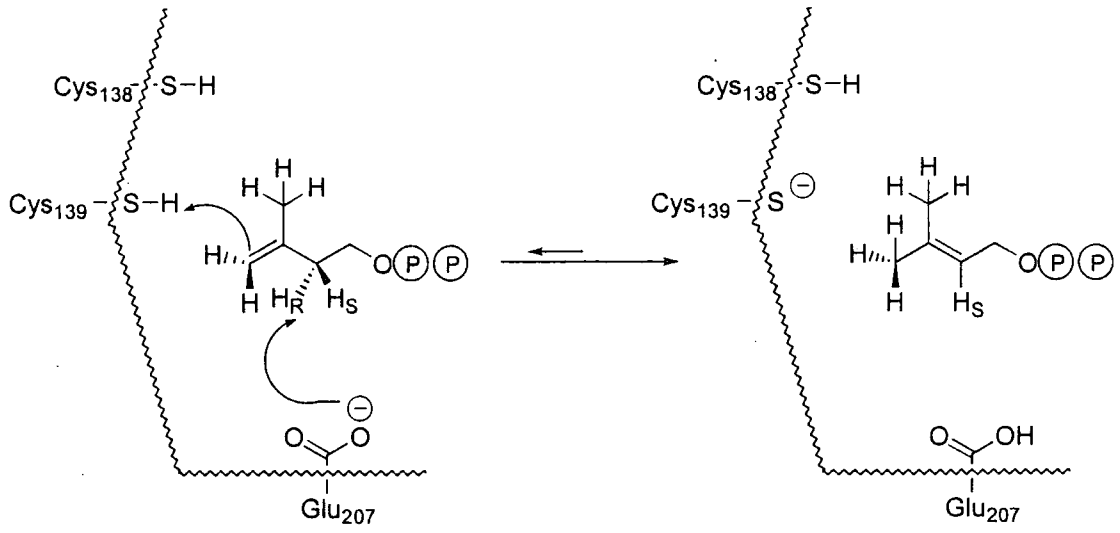

Figure 1-5 Stereochemistry of IPP isomerase[23]

Once DMAPP and IPP have been generated, they are then free to combine to form longer chain terpenoids. The nature of this condensation has been investigated in mammals, although the stereochemical details may differ for IPP and DMAPP generated by the new terpene pathway. The latter is described in Section 2.4.

Cornforth[24] proposed that the condensation of IPP and DMAPP proceeds in a two step manner. The first is the addition of a nucleophilic species, X, across the olefinic bond which is followed by the elimination of X and the *anti* hydrogen atom. The new species, farnesyl pyrophosphate can be used to deliver monoterpenes, or can react with a further molecule of IPP to produce geranyl pyrophosphate (GPP, **36**).

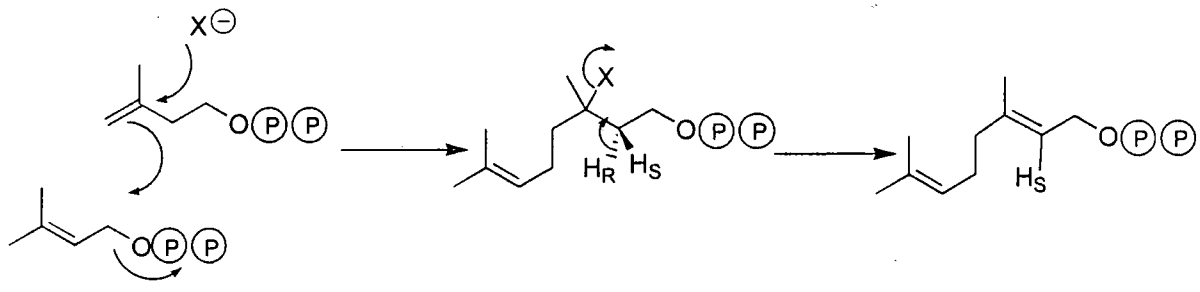

35 **34** **36**

Scheme 1-11 Proposed formation of GPP (**36**) from IPP (**34**) and DMAPP (**35**)

The consecutive addition of IPP to GPP can continue indefinitely in an iterative manner to deliver the higher terpenoids from farnesyl pyrophosphate (FPP, **37**), geranylgeranyl pyrophosphate (GGPP, **38**) and farnesylfarnesyl pyrophosphate (FFPP, **39**).

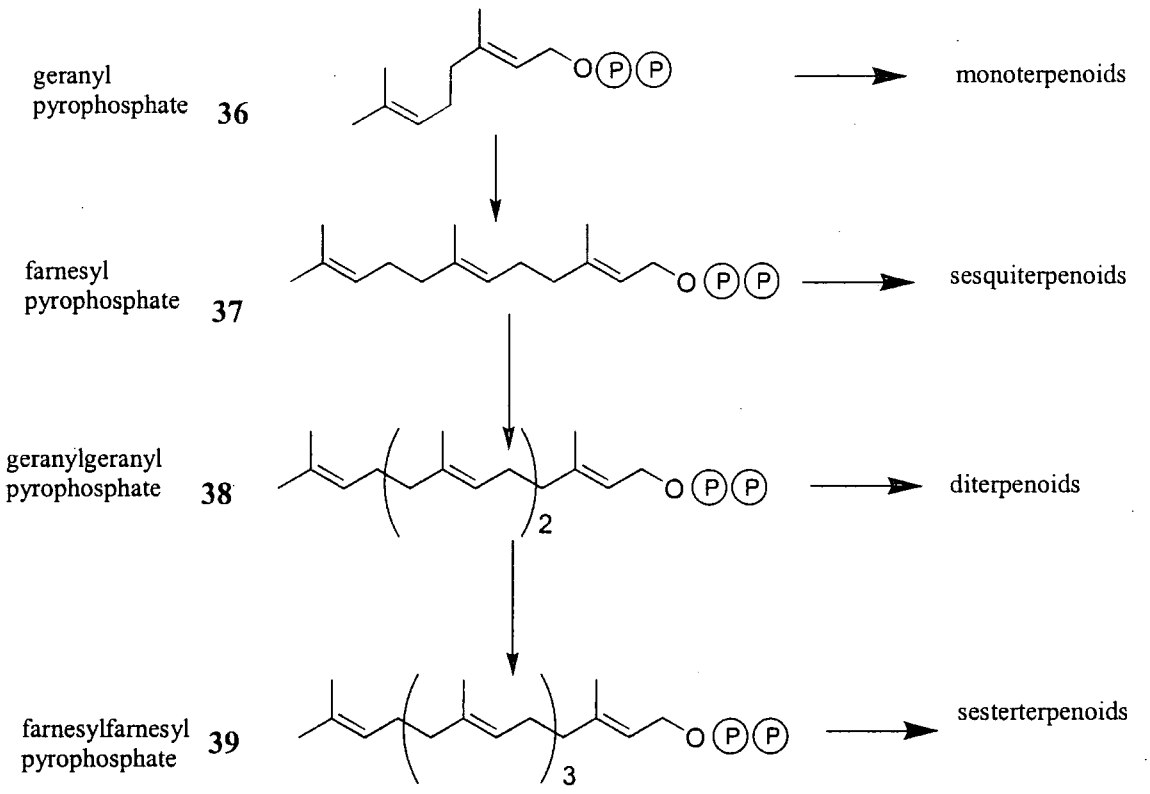

Scheme 1-12 Illustration of how higher terpenes are built up

Two polymers of the general formula $(IPP)_n$ are known - gutta percha (**40**) and rubber (**41**). The two differ in double bond geometry. Rubber possesses *cis* linkages and has free rotation about the methylene linkage that gives rubber its characteristic flexibility. Gutta percha (*trans* polyisoprene) has less rotation and is correspondingly hard and inflexible. It has been known in the West since the nineteenth century and found uses in electrical insulation, dentistry[25], and the preparation of the first golf balls.

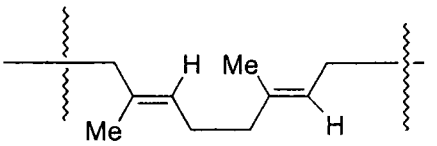

40

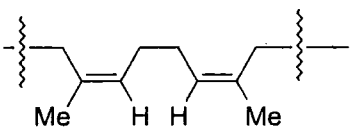

41

1.5.3 Monoterpenes

Monoterpenes are amongst the most widely exploited class of natural products. Owing to their relatively low molecular weight, monoterpenes are fragrant and are used extensively in perfumes and as flavours in foodstuffs. Menthol (**42**) has been known for over 2000 years and thujone (**43**) is the hallucinogen found in the drink absynthe.

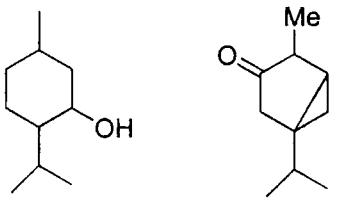

42 **43**

Despite their low molecular weight, monoterpenes display a remarkable structural diversity, which is accounted for by carbocationic rearrangements. Initially GPP isomerases to neryl pyrophosphate (NPP, **44**) which can then deliver terpenoids such as citral (**45**) and linalool (**46**) directly or can eject pyrophosphate to initiate cyclisation *via* the menthane carbocation (**47**)

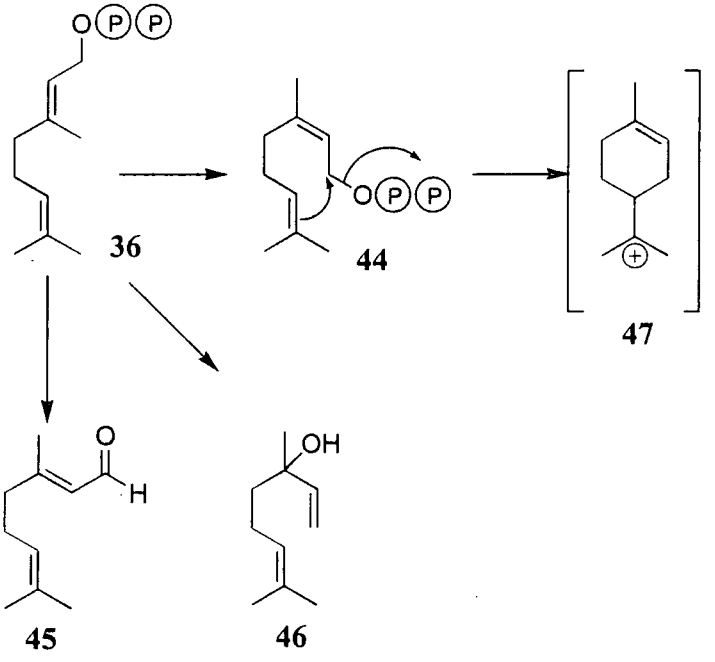

Scheme 1-13 Conversion of GPP (**36**) to NPP (**44**), citral (**45**), linalool (**46**) and the methane carbocation (**47**)

The isomerisation to NPP occurs to bring the cyclising double bond closer to the leaving group. The product of the cyclisation, menthane (**47**), is highly versatile as is evident from the bicyclic products that contain between three and six membered rings. Monoterpenes such as limonene (**30**), thujone (**43**), camphor (**48**) and carene (**49**) are representative examples.

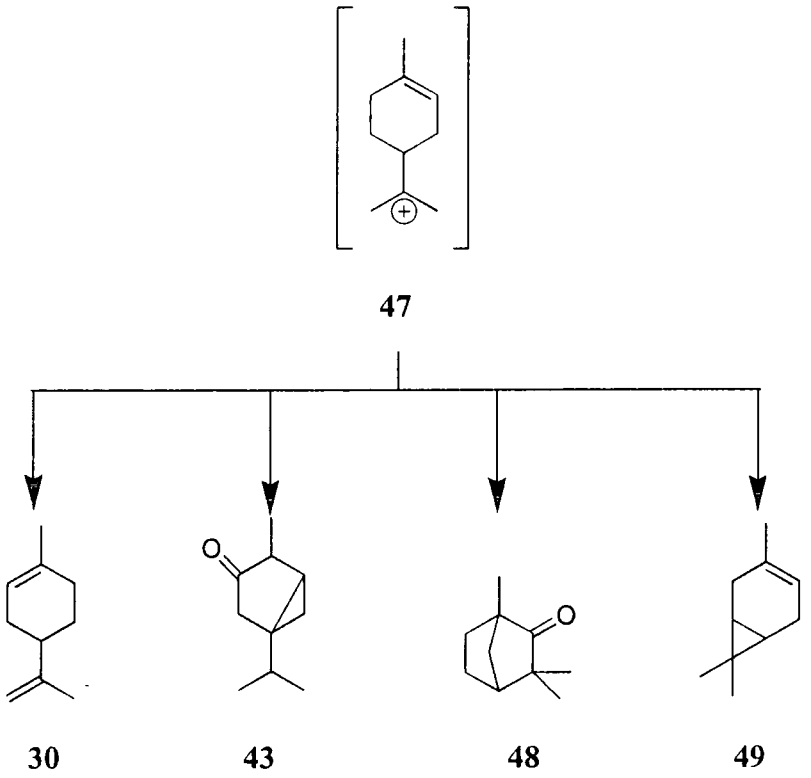

Scheme 1-14 Formation of monoterpenes from the menthane carbocation (**47**)

1.5.4 Sesquiterpenes

Sesquiterpenes are assembled by the extension of GPP by IPP (Scheme 1-12) and like monoterpenes, they are most abundant in higher plants. By analogy to monoterpene biosynthesis, *cis*-FPP (**37**) is isomerised through nerolidyl pyrophosphate (**50**) to *trans*-FPP (**51**). Both isomers undergo cyclisation reactions to deliver a variety of skeletal structures.

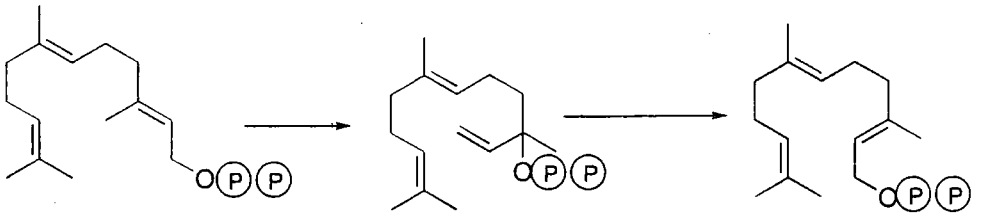

37 **50** **51**

Scheme 1-15 Formation of nerolidyl pyrophosphate (**50**) and *trans* FPP (**51**) from *cis* FPP (**37**)

Sequiterpenes exhibit a range of structural diversity to match that of the monoterpenes owing to the four double bond centres that can participate in ring formation.

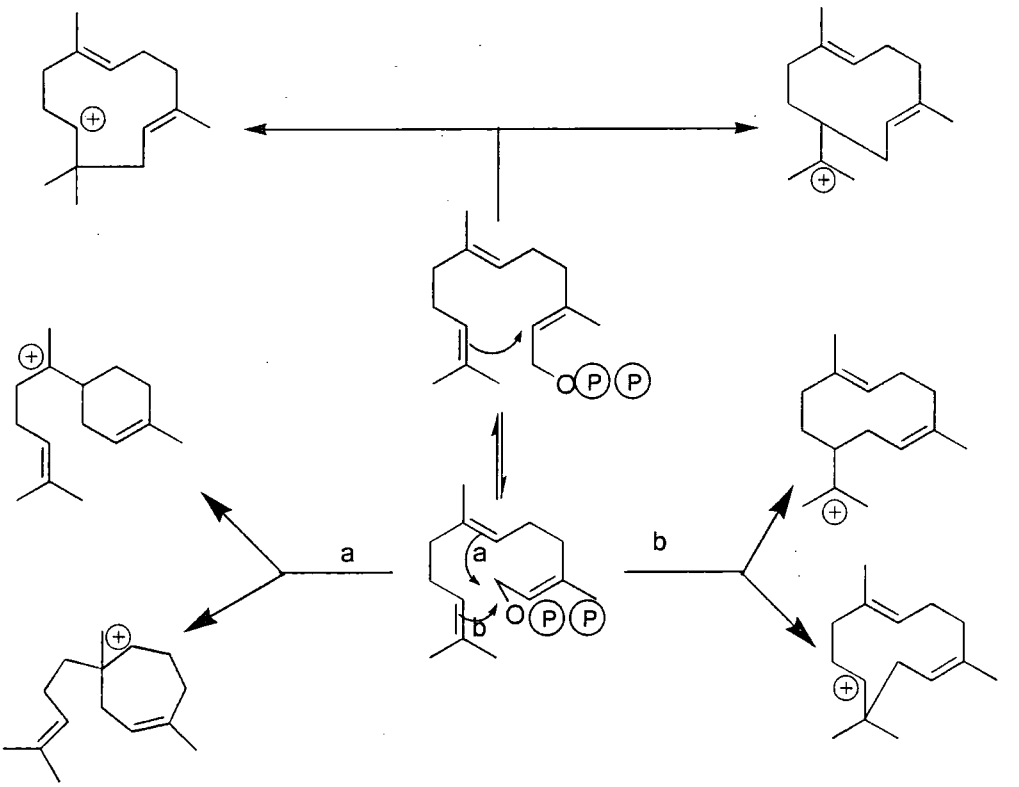

Scheme 1-16 Formation of first generation sesquiterpene skeletons from FPP

Sesquiterpenes are essential for the growth and maturation of insects, and plants have taken full advantage to construct effective defence mechanisms. The sesquiterpene juvabione (**52**) is a known inhibitor of insect maturity and is produced by the balsam fir tree, *Abies balsamea*, in order to prevent insect development. The highly oxygenated plant terpenoid artemisinin (**53**) is a well-known antimalarial drug.[26]

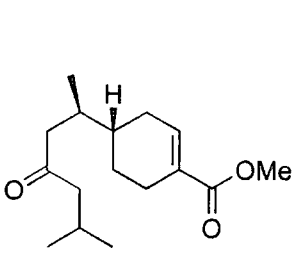

52

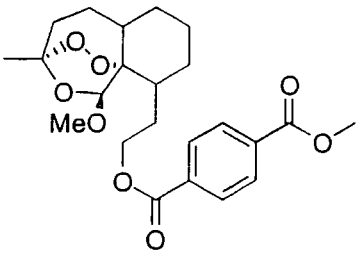

53

1.5.5 Diterpenes

Diterpenes are derived from the coupling of FPP with IPP to form GGPP (Scheme 1-17) and are found in higher plants, fungi, insects and marine organisms. Most are tricyclic compounds.

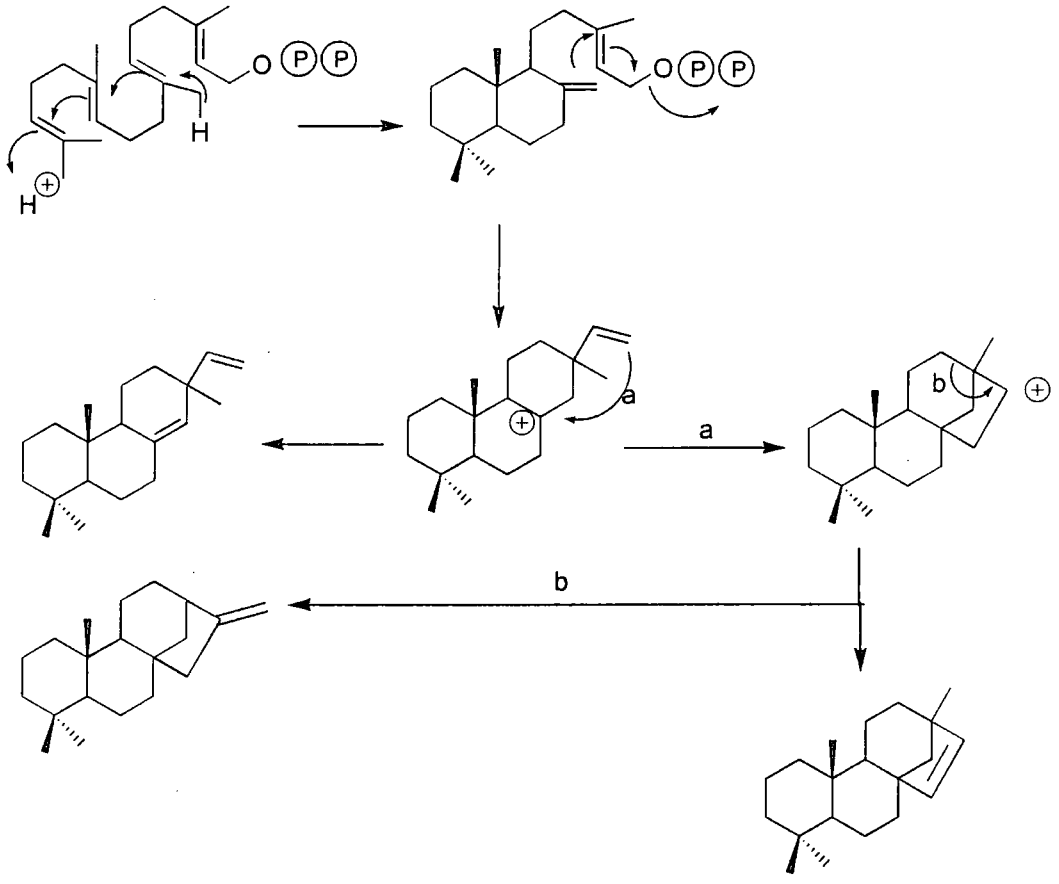

Scheme 1-17 Formation of diterpene skeletons

Diterpenes are important as bioactive agents and three of the most widely studied terpenoids are diterpenoids, namely taxol® (**54**), gibberellic acid (**55**) and vitamin A (**56**).

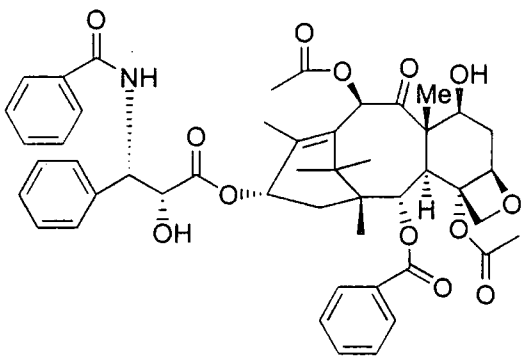

54

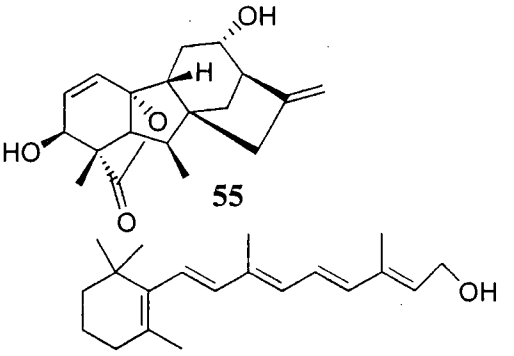

55

56

Taxol (**54**) was first isolated from the bark of the Pacific Yew tree (*Taxus brevifolia*) and is highly effective in the treatment of cancer. As removal of the bark causes the tree to die, semisynthetic analogues are more viable clinical alternatives.

Gibberellic acid (**55**) was the first gibberillin to be isolated and was purified from the broth of the fungus *Gibberella fujikoroi*. *G. fujikoroi* Is responsible for a disease that affects rice in Japan whereby the seedlings grow at a greatly accelerated rate but do not mature which renders the crop useless. Other gibberillins have been found in higher plants and are now recognised as hormones and growth promoters. Gibberillins share the same skeleton and lactone ring as the parent acid with structural variations coming from differing positions of hydroxy and double bonds.

1.5.6 Sesterterpenes

Very few sesterterpenes are known. Their distribution is the same as for the diterpenes and their biosynthesis is analogous with the previous descriptions.

1.5.7 Triterpenes and steroids – the involvement of squalene

Triterpenoids form the largest group of terpenoids although their structural diversity is relatively small, typically having three or four fused alicyclic rings. They are most abundant in higher plants although they are known in animals in small numbers. Squalene contributes their skeletons and is formed from the head-head linkage of two

molecules of FPP[27]. Squalene (**57**) was first isolated from shark liver and has been found to be abundant in fungi, vegetable oils and human earwax. The mechanism of squalene synthase proceeds *via* a carbocationic separated ion pair. Interestingly, the reaction proceeds through a cyclopropane intermediate which is formed by removal of the *pro-S* hydrogen from mevalonic acid. This is followed by ring expansion to a putative cyclobutane cabocation that is opened by the delivery of hydride from NADPH. The ring formation produces the unique head-to-head arrangement of isoprene units found in squalene (Scheme 1-18).

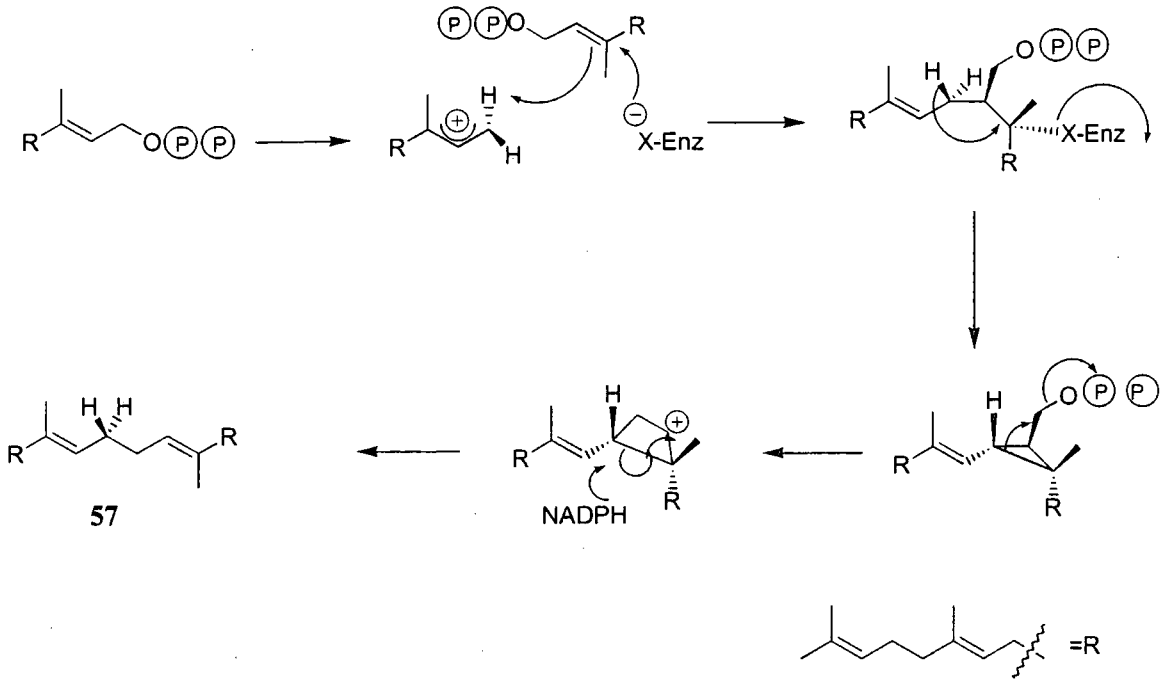

Scheme 1-18 Formation of squalene (**57**)

In 1965 Bloch[28] demonstrated that 2,3-epoxy squalene (**58**) was the precursor of lanosterol (**59**) in animals and cycloartenol (**60**) in higher plants. Triterpenes, such as β amyrin (**61**) are also derived from the folding of 2,3-epoxy squalene.

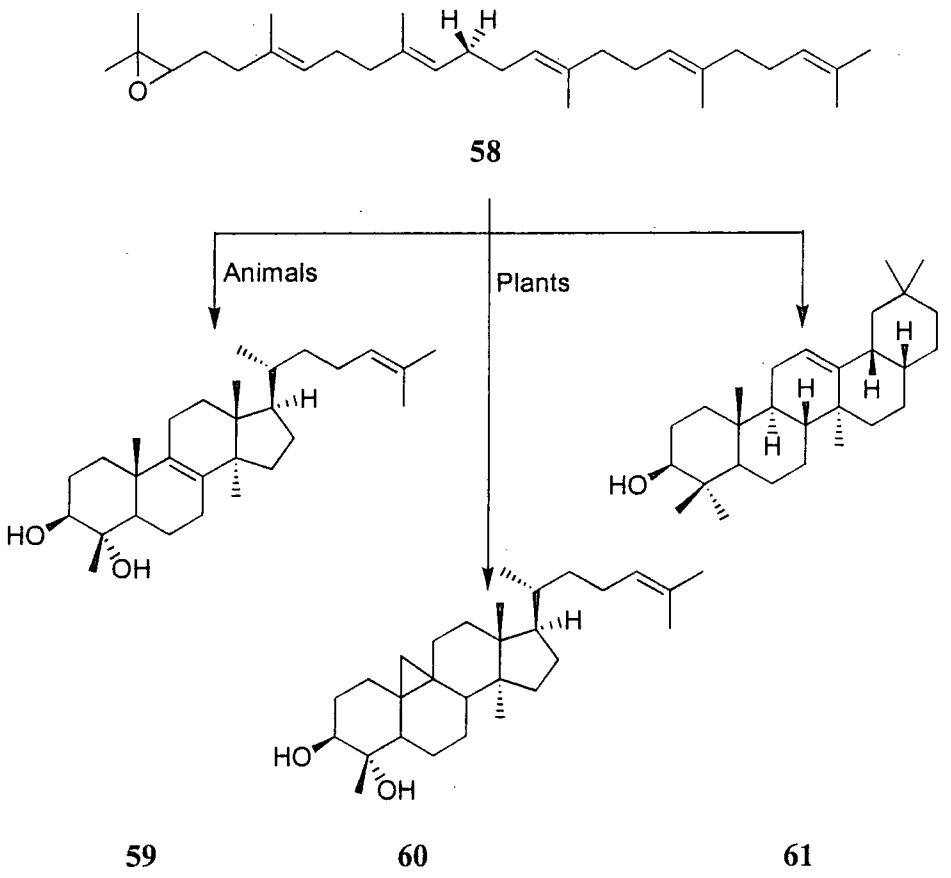

Scheme 1-19 Biosynthesis of lanosterol (**59**), cycloartenol (**60**) and β-amyrin (**61**),

Triterpenoids and steroids have similar applications - both are used in cell membranes to control cell rigidity. Cholesterol (**62**) controls its alignment in membranes *via* its hydroxy group. The prenyl sidechain is non-polar and allows incorporation into lipid bilayers whilst the polar hydroxy head enables it to be incorporated into phospholipid layers. Cholesterol is biosynthesised from lanosterol in nineteen steps. The conversion may be lengthy, but is vitally important as membranes made from lanosterol are much more permeable than the cholesterol containing analogues.

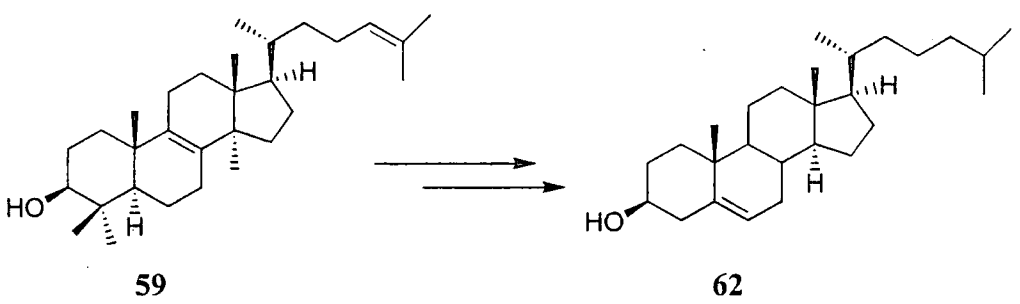

Scheme 1-20 Conversion of lanosterol (**59**) to cholesterol (**62**)

1.6 Terpenoid biosynthesis – the mevalonic acid pathway

1.6.1 Features of the pathway

Ruzicka's isoprene rule provided a rudimentry understanding of the biosynthesis of terpenoids. The first biosynthesis study on terpenoids was performed by Sanderhoff[29] in 1937 who fed sodium [2-$^{2}H_3$]-acetate to yeast. The high level of incorporation of deuterium into resultant sterols suggested acetate as a building block. Progress on the pathway was slow until the intervention of Cornforth, Bloch and Lynden who were later awarded the Nobel Prize for chemistry in 1964. Initial feeding experiments[30,31] with sodium [1-^{14}C]-acetate and sodium [2-^{14}C]-acetate showed the terpenoid skeleton of cholesterol was built from alternating acetate-methyl and acetate-carboxylate carbons, and that the pendant methyl groups were derived from the methyl groups of acetate.

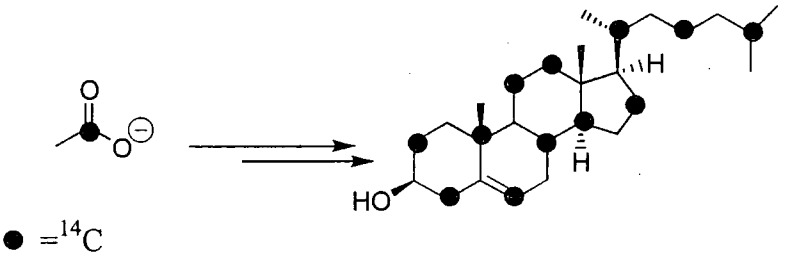

63 **62**

Scheme 1-21 Incorporation of [1-^{14}C]-acetate (**63**) labelled into cholesterol (**62**)

In 1951 it was shown by Lynen and co-workers[32] that acetate is activated *in vivo* to its thiol ester of coenzyme-A to form acetyl-CoA (**10**). Subsequently HMG-CoA (**64**) was identified as an intermediate which is formed from the combination of three acetyl-CoA units. The first step is a Claisen ester type condensation that is then followed by an aldol type condensation. HMG-CoA is an important intermediate as its formation is the rate-limiting step in terpenoid biosynthesis *via* the MVA pathway.

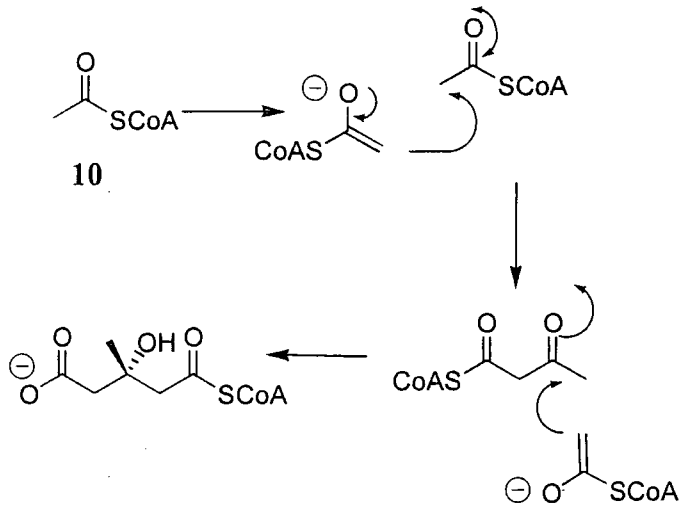

Scheme 1-22 Formation of HMG-CoA (**64**) from acetyl-CoA (**10**)

Conversion of HMG-CoA (**64**) to IPP requires the loss of one carbon atom. This had been noted by Cornforth who observed that isotope from [1-^{14}C]-acetate also produced $^{14}CO_2$, suggesting a decarboxylation process. In 1956, workers at Merck, Sharp and Dohme found that brewing sediment could replace acetate as the carbon source for a mutant strain of *Lactobacillus acidophilus*. Furthermore, when the sediment was fed terpenoids were produced at higher levels. Extraction and isolation of the active material revealed that the growth enhancing substrate was 3,5-dihydroxy-3-methyl valeric acid, which is now described as mevalonic acid (MVA, **9**). Mevalonic acid was firmly established as an intermediate on the pathway when the lactone form of MVA (**65**) was converted by liver extracts into cholesterol.

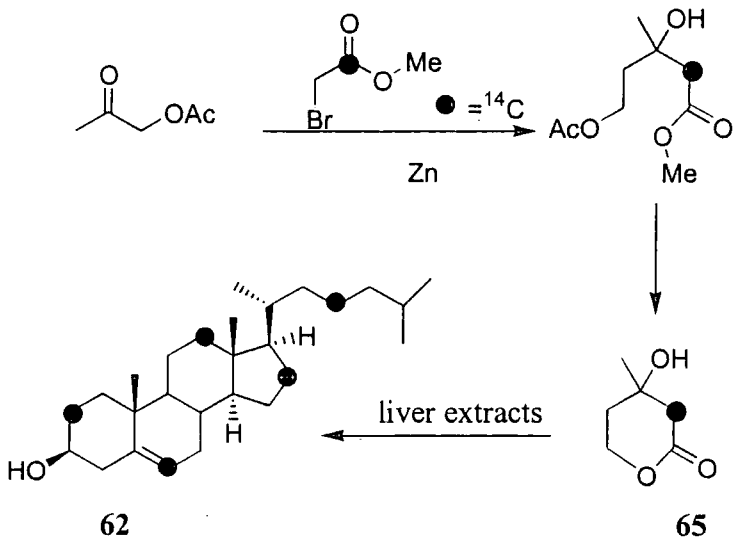

Scheme 1-23 Synthesis and incorporation of [1-^{14}C] mevalonalactone (**65**)

Work by Arigoni showed that only the 3-*R*(-) enantiomer of MVA is produced *in vivo*[33] which was confirmed by feeding experiments with 3-*R*(-)-MVA and 3-*S*(+)-MVA in which only exogenously administered 3-*R*(-)-MVA was incorporated. The final steps that converts MVA to IPP require the alcohols to become activated to phosphate esters, the removal of one carbon atom and the introduction of a terminal double bond. Phosphorylation is catalysed by mevalonate kinases that use ATP and Mg^{2+} to produce the phosphate esters. Subsequent decarboxylation provides IPP as shown in Scheme 1-24 and IPP is then converted to DMAPP as described in Figure 1-5. This sequence of steps, starting from acetate which is processed to HMG-CoA and mevalonic acid to IPP, is described as the mevalonic acid pathway.

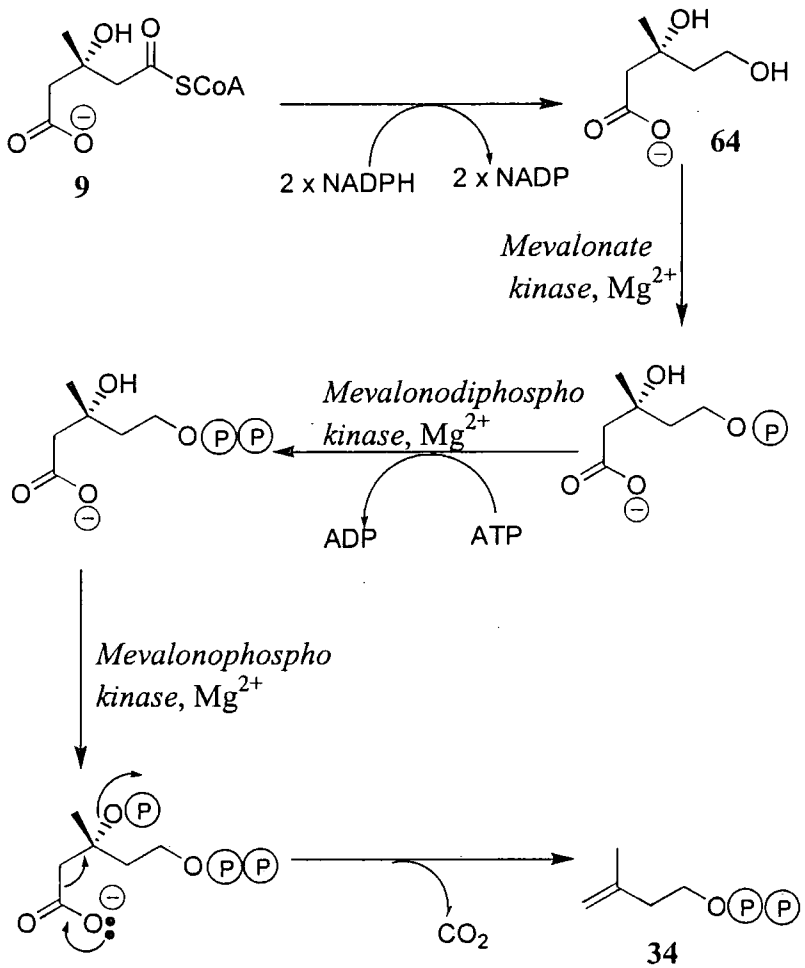

Scheme 1-24 Formation of IPP (**34**) from HMG-CoA (**64**) *via* MVA (**9**)

1.6.2 Other sources of mevalonate

The scheme outlined above represents the major pathway to MVA, but is not the only source of MVA. A minor contribution is from a pathway where leucine (**66**) is converted to HMG-CoA through 3-methylcrotonylcoenzyme A (**67**). The sequence is completed by carboxylation by biotin and finally hydration to produce HMG-CoA (**64**).

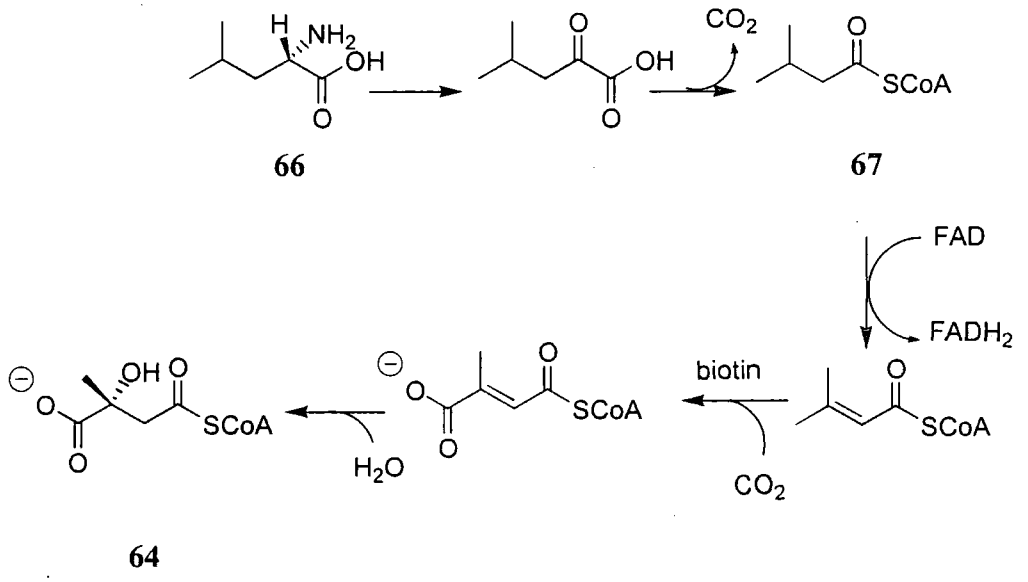

Scheme 1-25 Formation of HMG-CoA (**64**) from leucine (**66**)

1.6.3 Unresolved issues on the mevalonate pathway

Although the sequence and stereochemistry of the steps on the MVA pathway is well known, as early as the 1960's results emerged that appeared to contradict the hypothesis that MVA was the universal precursor to isoprenoids. The incorporation of $^{14}CO_2$ and [2-^{14}C]-MVA into the chloroplasts of seedlings was reported by Treharne and co-workers in 1966[34] who observed that β carotene and phytol were labelled by $^{14}CO_2$ but not [2-^{14}C]-MVA. For sterols, the reverse was true. The conclusion was drawn that as both β carotene and phytol are biosynthesised in the chloroplasts, and sterols are made in the cytoplasm, the difference in incorporations was due to the relative permeability of the chloroplasts and cytoplasm to MVA and CO_2. This agreed with findings[35] that chloroplasts prepared in the laboratory were impermeable to MVA. Similar results were observed for the incorporation of $^{14}CO_2$ and [2-^{14}C]-MVA into monoterpenes and sterols produced by *Mentha piperita*[36]. Incorporation of [1-^{14}C]-acetate into monoterpenes was

also observed to be very low (≤0.01%) which, it was argued, was due to acetate being used for other metabolic pathways. An exhaustive list of incorporations of acetate, MVA and CO_2 into monoterpenes is provided in an excellent review by Banthorpe[37]. In experiments where acetate was incorporated into terpenes, significant scrambling of the tracer occurred[38].

Further evidence for the differences between the MVA pathways in the cytoplasm and chloroplasts was revealed when [2-^{14}C]-MVA was fed to *Thuja occidentalias*[39]. Analysis of the thujone that was produced showed incorporation of the ^{14}C label was two orders of magnitude higher in the IPP unit than the DMAPP unit. Similar asymmetrical labelling was later reported in both enantiomers of camphor[40] and in the sequiterpenes tutin and coriamyrtin[41]. These suggested that two pools of DMAPP existed– a pool that was free and sparsely filled and another that was enzyme bound and full. Further hypotheses were suggested, such as that high concentrations of exogenously administered MVA could inhibit the isomerisation process, resulting in low concentrations of DMAPP.

However, all explanations seemed to overlook that the incorporations were almost insignificantly small (0.01%) and prone to error and contamination. The answer to how plant monoterpenes are biosynthesised is discussed below.

1.7 The 1-deoxyxylulose pathway

1.7.1 Initial studies

The pioneering work on the early stages of the 1-D-deoxyxylulose-5-phosphate (DXP) pathway, or mevalonate independent pathway, was performed by Rohmer and co-workers. The first suggestion that an alternative pathway was operating followed the results of feeding experiments with [1-^{13}C] and [2-^{13}C]-acetate with the bacterium *Rhodopseidomonas palustris*[42]. The aim of the experiment was to determine the origin of a non-terpene sidechain in a hopane. Incorporation showed that the sidechain was derived from a D-pentose but also revealed incorporation of ^{13}C derived from acetate that did not concur with the processing of acetate *via* mevalonic acid. In addition the incorporations were relatively high and showed no evidence of scrambling. The result was explained in terms of compartmentation effects, and that the acetate was processed to MVA but that two non-equivalent pools of acetate existed. Feeding of [1-^{13}C]-

acetate to *E. coli* also showed an identical incorporation pattern into the ubiquinone sidechain to that found in *R. palustris*.

Further experiments[43] in *Zymomonas mobilis* showed identical results. One of the attractive features about using the bacterium *Z. mobilis* is that many glycolytic enzymes are absent and it is capable of growing on a single carbon source. This can lead to relatively high levels of incorporation. Isotopically labelled glucoses were fed and the incorporation into the isoprenoid fraction of the hopanoids was analysed *via* ^{13}C NMR. It was found that C-3 of IPP was derived from C-2 and C-5 of glucose and C-3 and C-6 of glucose gave rise to C-5 of IPP. Similar relationships were found between C-1, C-2 and C-4 of IPP and C-4, C-5 and C-6 of glucose respectively. Feeding experiments with *Methylobacterium fujiawaense* using ^{13}C enriched glucoses labelled IPP in a similar manner to the incorporations in *Z. mobilis*. Both organisms use the Entner-Doudoroff pathway rather than glycolysis for glucose metabolism. In the glycolytic pathway, glucose (**68**) is converted through fructose 1,6 bisphosphate (**69**) to dihydroxyacetone phosphate (**70**) and D-glyceraldehdye-3-phosphate (GAP, **3**). The Entner-Doudoroff pathway metabolises glucose to glyceraldehyde-3-phosphate (**3**) and pyruvate (**7**).

Feeding of [1-^{13}C] and [6-^{13}C]-glucose to *E. coli* and *Alicyclobacillus acidoterrestris*[43] once again showed enrichment of C-1 and C-5 of IPP.

These results inferred the involvement of pyruvate and a C_3 intermediate that would be delivered by the Entner-Doudoroff pathway in *Z. mobilis* and *M. fujiawaense* and *via* glycolysis in *E. coli* to provide a branched C_5 intermediate.

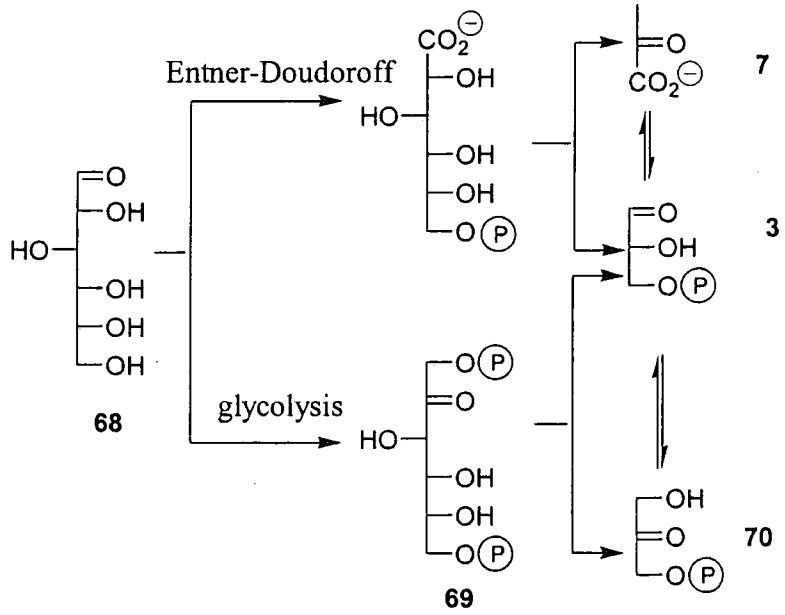

Scheme 1-26 Comparison of glycolysis and the Entner-Doudoroff pathway

The incorporation of [4,5-$^{13}C_2$]-glucose into the ubiquinone of *M. fujiawaense* showed labelling of C-2 and C-4 of IPP with satellites corresponding to ^{2}J ^{13}C-^{13}C coupling. As the carbon-carbon bond was incorporated intact, it was judged that the rearrangement to the branched skeleton is an intramolecular process.

[U-^{13}C]-Glucose fed to *Z. mobilis* showed ^{2}J ^{13}C-^{13}C coupling between C-3 and C-5 in addition to ^{1}J ^{13}C-^{13}C coupling between C-1 and C-2[43]. An enrichment of C-4 was also observed. This proved that the C_2 unit was derived from pyruvate and explained the previously anomalous result of Zhou and White[44] who had observed that [*methyl*-$^{2}H_3$]-lactate was incorporated into the ubiquinone of *E. coli*. In the context of the mevalonate independent pathway, the incorporation represents processing of lactate to pyruvate. Furthermore, the previous incorporations of acetate studied by radiolabelling represent the processing of acetate to pyruvate *via* oxaloacetate and incorporation of pyruvate *via* the DXP pathway rather than direct incorporation of acetate *via* the MVA pathway.

Investigations into the identity of the C_3 unit were conducted using mutants of *E. coli*[45]. In parallel experiments, cultures were supplemented with [1-^{13}C]-pyruvate and unlabelled glycerol or [1-^{13}C]-glycerol and unlabelled pyruvate. Pyruvate was incorporated into C3 and C5 of IPP irrespective of which enzymes were absent demonstrating that two carbons arise from the decarboxylation of pyruvate. The experiment also pinpointed GAP as the C_3 intermediate. Mutants possessing only the enzymes required to convert pyruvate to GAP showed incorporation of ^{13}C from [1-^{13}C]-pyruvate whilst mutants possessing only the enzymes required to convert glycerol to GAP showed ^{13}C enrichment from [1-^{13}C]-glycerol.

1.7.2 The role of 1-D-deoxyxylulose-5-phosphate

The key intermediate on the mevalonate independent pathway, 1-deoxyxylulose-5-phosphate, was first isolated in 1976 from *Streptomyces hydroscopicus*[46]. Its identification as a precursor to terpenoids was stimulated by an observation by Yokota and Sasajima that bacterial and plant cell free preparations were capable of producing DXP from GAP and pyruvate[47,48]. DXP had been shown to be the origin of the C_5 units in vitamins B_1 (**71**) and B_6 (pyridoxone, **72**). Initial feeding experiments with *E. coli* inferred the free triol as the intermediate[49] although more recent studies conducted by Laber[50] and co-workers have shown that the 5-phosphate ester is the active form *in vivo*.

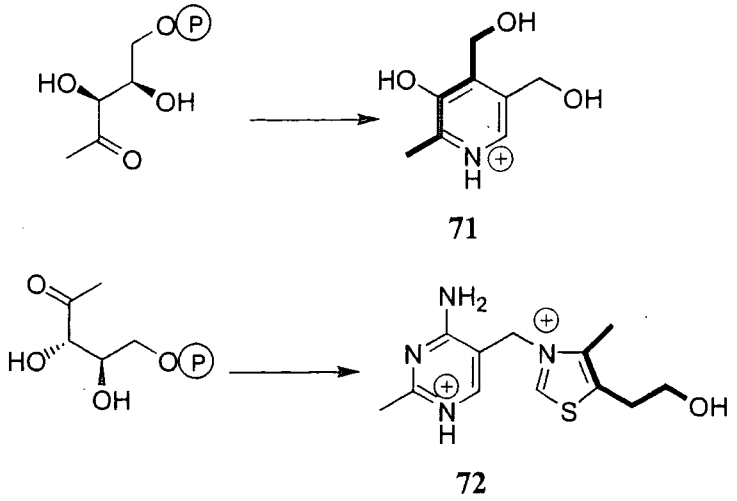

Scheme 1-27 Incorporation of DXP into vitamins B_1 (**71**) and B_6 (**72**)

DXP was shown to be an intermediate on the mevalonate independent pathway by Arigoni[51]. Deuterium incorporation from [5,5-$^2H_2$]-DX was observed into the polyprenyl group of ubiquinone of *E. coli*. The enzyme that produces DXP from GAP and pyruvate, DXP synthase (DXS), was first isolated by Sprenger and co workers[52] from *E. coli*. The enzyme required thiamin as a cofactor which was consistent with an acyloin type condensation of pyruvate and GAP. DXS behaves in a transketolase manner and has a sequence motif that is recognised to bind the thiamin diphosphate cofactor required for pyruvate decarboxylation. When the DXS sequence was compared to other known protein sequences significant homology was found between ORF's in the plant *Arabidopsis thaliana*, the cyanobacterium *Synechocytis sp.* and the Gram positive bacterium *Bacillus subtilis*. A similar result was also reported by Rohmer[53]. DXS has now been cloned from *B. subtilis*[54] and was overexpressed from *E. coli* to upregulate ubiquinone and lycopene production. Following this, DXS was cloned from peppers[55] and peppermint[56] which showed the synthase gene was 2,172 base pairs long. Mechanistically, DXS operates by the thiamin mediated decarboxylative condensation of pyruvate and GAP.

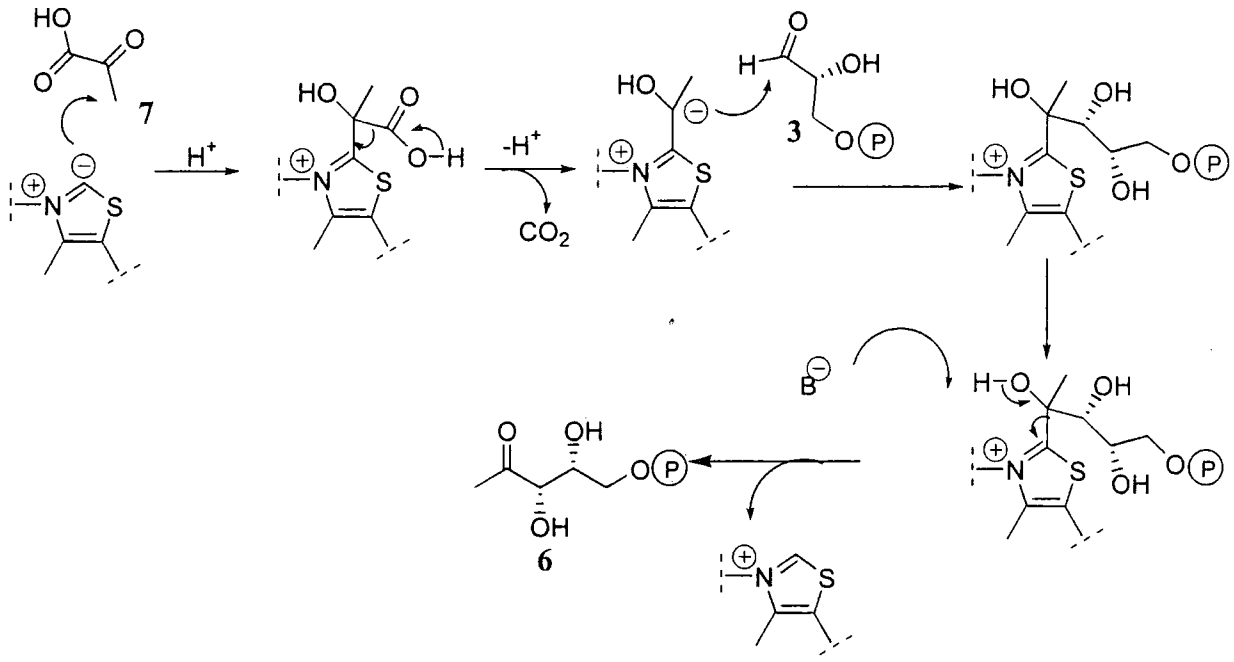

Scheme 1-28 Formation of DXP (**6**) from GAP (**3**) and pyruvate (**7**)

1.7.3 2-C-Methylerythritol-4-phosphate

Clearly DXP must undergo a skeletal rearrangement in order to deliver the branched skeleton of IPP. Rohmer and co-workers[57] identified 2-*C*-methylerythritol-4-phosphate (MEP, **73**) as the next intermediate on the mevalonate independent pathway. MEP had been isolated from various systems as both the 4-phosphate ester and the free tetrol. ^{13}C enriched glucose was fed to *Corynebacterium ammoniagenes* which was known to produce MEP when treated with benzylviologen in the stationary phase. MEP and menaquinone were isolated and the carbon labelling patterns were compared. An identical distribution of ^{13}C labelling was found in both molecules, which suggested a role for MEP as an intermediate.

Synthetic 2-*C*-methyl-D-erythritol and 2-*C*-methyl-L-erythritol were fed to *E. coli*.[58] Incorporation of only the D enantiomer was observed. Further studies[59] showed incorporation of [2,3,4,5-$^{13}C_4$]-DX into β-carotene and ME from *Liriodendron tulipa*. The labelling patterns and levels of incorporation was identical for both molecules. ^{2}J ^{13}C-^{13}C and ^{3}J ^{13}C-^{13}C coupling constants showed that the C_4 backbone of MEP was derived from an intramolecular rearrangement of DXP *via* a pinacol type rearrangement. MEP was shown unambiguously to be the first dedicated intermediate on the pathway when DXP was converted into β carotene *via* MEP by cell free extracts of *Capiscum annum*[60].

MEP is the product of the enzyme, deoxyxylulose reductoisomerase, which initiates rearrangement and employs NADPH to afford aldehydic reduction.

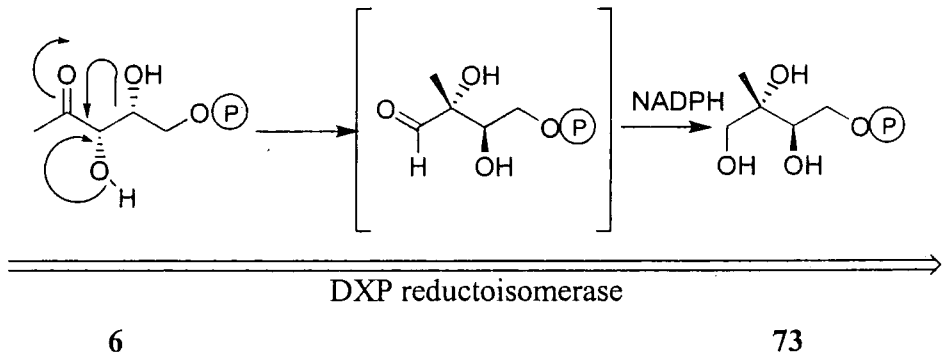

6 73

Scheme 1-29 Formation of MEP (**73**) from DXP (**6**)

Identical transpositions are known in the biosynthesis of branched amino acids such as L-valine. In both reactions the hydride is delivered from the oppposite face to the migrating group[61].

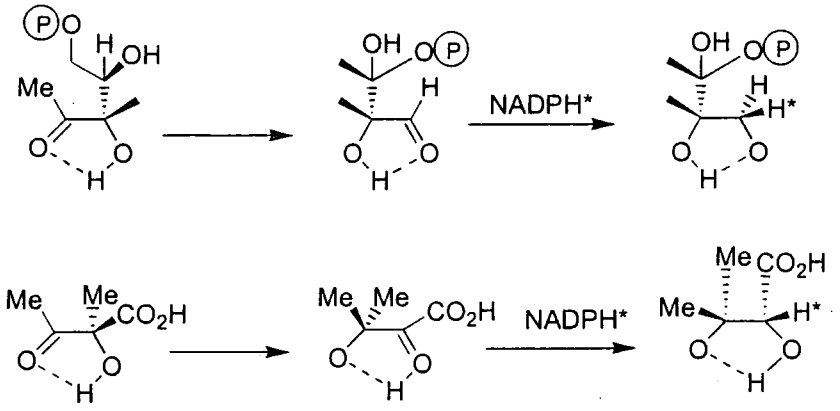

Scheme 1-30 Stereochemistry of reductoisomerases in MEP (top) and valine biosynthesis (bottom) [61]

DXP reductoisomerase has been cloned and expressed from *A. thaliana*[62], *Mentha* x *piperita*[63] and has been isolated from *E. coli*[64]. DXP reductoisomerase isolated from *E. coli* uses exclusively the *pro*-(S) hydride of NADPH which identifies DXP reductoisomerase as a class B dehydrogenase.

1.7.4 Post MEP intermediates

One of the key features of the mevalonate independent pathway is both DX and ME, fed as the free alcohols, are incorporated at very low levels (~0.3%) into whole cells. Consequently, cell free work has been employed to elucidate details of the pathway after MEP.

When *E. coli* extracts were incubated with [2-^{14}C] MEP and ATP a radiolabelled product was formed[65]. Isolation of the radiolabelled product showed MEP had been converted to 4-phosphocytidyl-2-*C*-methylerythritol (CDP-ME, **74**). The enzyme responsible for the conversion was purified and the incubation with [2-^{14}C] MEP was repeated with different co-factors. CTP was found to act more efficiently as a substrate than ATP and that [α-^{32}P] CTP delivered ^{32}P into the product. [2-^{14}C] CDP-ME was incorporated into β carotene when incubated with chloroplasts of *Capsicum annum* which showed it to be an intermediate on the pathway. Identical results were reported shortly afterwards by Seto and co-workers[66]. During these investigations, a previously unannotated gene, *ychb*, was found very close on the genome of *E. coli* to *ygbp*, the gene responsible for CDP-ME synthesis. *Ychb* was overexpressed in a homologous host[67] and the recombinant protein was purified. When CDP-ME was incubated in the presence of ATP and the protein, 4-phosphocytidyl-2-*C*-methylerythritol-2-phosphate (CDP-MEPP, **75**) was formed. [2-^{14}C]-CDP-MEPP was demonstrated to be an intermediate when it was efficiently incorporated into carotenoids produced by *C. annum* chromoplasts. Again, the same result was reported shortly afterwards by Seto[68].

The latest intermediate that has been reported was found using identical methodology to that above[69]. *YgbP*, the gene responsible for CDP-ME synthesis, was found to be fused to another gene, *ygbB* which expressed a protein, *YgbB* that converted CDP-MEPP, in the presence of Mn^{2+} and Mg^{2+}, to 2-*C*-methylerythritol-2,4-cyclodiphosphate (ME-2,4-CDP, **76**) and CMP. *YgbB* was also found to convert MEP-CDP to 2-*C*-methylerythritol 3,4-cyclomonophosphate (ME-3,4-CMP, **77**). Incubation of [2-^{14}C]-ME-2,4-CDP with *C. annum* chromoplasts revealed incorporation into carotenoids whereas [2-^{14}C]-ME-3,4-CMP did not.

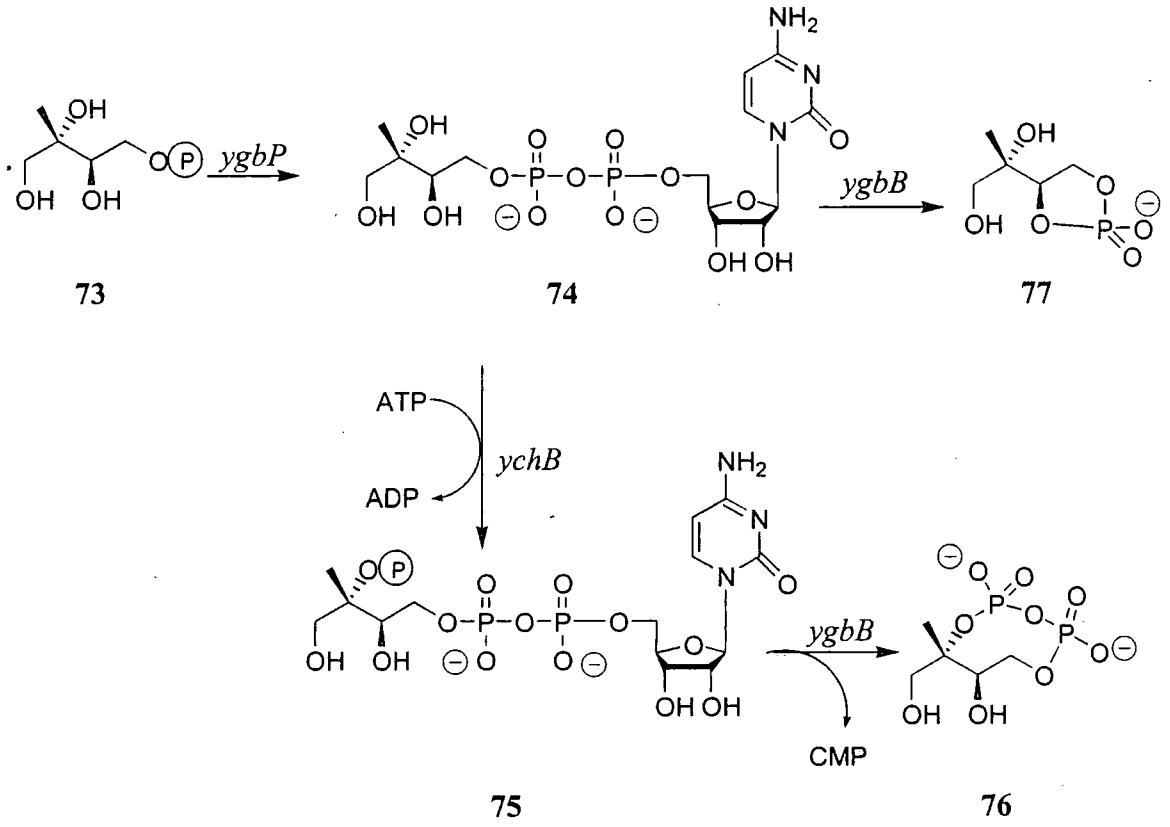

Scheme 1-31 Formation of post MEP intermediates

This results suggests that while ME-2,4-CDP (**76**) is an intermediate on the pathway, ME-3,4-CMP (**77**) is not and may simply be a shunt metabolite. ME-2,4-CDP had been previously isolated from benzylviologen treated *Desulfovibrio desulfuricans*[70] although no connection to the mevalonate independent pathway had been established at that time.

1.7.5 Distribution of the mevalonate independent pathway

In the light of recent feeding experiments it is now known that higher plants and certain Gram negative bacteria, notably Pimelobacteria (cyanobacteria and proteobacteria) use the mevalonate independent pathway. Green algae[71] are also known to use the new pathway. By contrast, animals are known to use the MVA pathway; searches for DXP reductisomerase in mammalian gene sequences have proved fruitless. Furthermore, mevalonin, a known inhibitor of the MVA pathway, has been clinically proven to reduce levels of patients' cholesterol which can only be explained in terms of the MVA pathway.

The pattern that ^{13}C from [2-^{13}C]-acetate was incorporated into sesquiterpenes produced by the liverwort *Heteroscyphus planus* initially suggested a mevalonate origin of the terpene although the level of incorporation was low (0.3% atom)[72] and prone to significant error. Later studies with DX showed operation of the mevalonate independent pathway[73] although a minor contribution from the mevalonate pathway was observed. Similar simultaneous labelling patterns have been found to be common in higher plants. Investigations with plant cultures revealed that the site of terpene manufacture determines the route of biosynthesis. When cultures of higher plants (*Hordeum vulgare, Lemna gibba* and *Daucus carotta*) were fed with [1-^{13}C]-glucose two clearly distinct incorporation patterns were revealed[74]. Sterols were produced *via* the MVA pathway and carotenoids were synthesised *via* the mevalonate independent pathway. Identical results emerged from studies whereby sterols and carotenoids were produced by different pathways. These results can be rationalised in terms of the site of terpene biosynthesis. It is well established that sterols are produced from GGPP in the cell cytoplasm that clearly operates *via* the mevalonate pathway whereas carotenoids and monoterpenes are produced in plant chloroplasts that use the mevalonate independent pathway. However, there appears to be "cross talk" between the two pools and that IPP, FPP and prenyl pyrophosphates can be transported between the cytoplasm and chloroplasts. Striking evidence for this was reported by the group of Arigoni[75]. When gingko embryos were incubated with [1-^{13}C]-glucose, 98% of GGPP was produced by the mevalonate independent pathway. The remaining 2% was of mixed origin; 20% was derived from IPP from MVA and FPP from the mevalonate independent pathway; the rest was composed of FPP produced from MVA and one unit of IPP synthesised *via* the mevalonate independent pathway. Similarly, lima beans showed incorporation of [1-^{13}C]-glucose that were consistent with monoterpenes derived from the mevalonate independent pathway, sesquiterpenes from an equal contribution from both pathways and diterpenes predominantly from the new pathway[76]. In Gram Positive bacteria (those that are non photosynthetic and lack an outer membrane) both pathways have been shown to operate. Indeed, in *Streptromyces aeriouver* both pathways operate simultaneously[77]. During the exponential growth phase the mevalonate independent pathway is used to deliver the prenyl chain of a menaquinone. When monoterpenes are produced in the stationary phase the mevalonic acid pathway is employed. Other Gram Positive bacteria such as *Mycobacteria* use only the mevalonic acid pathway[78].

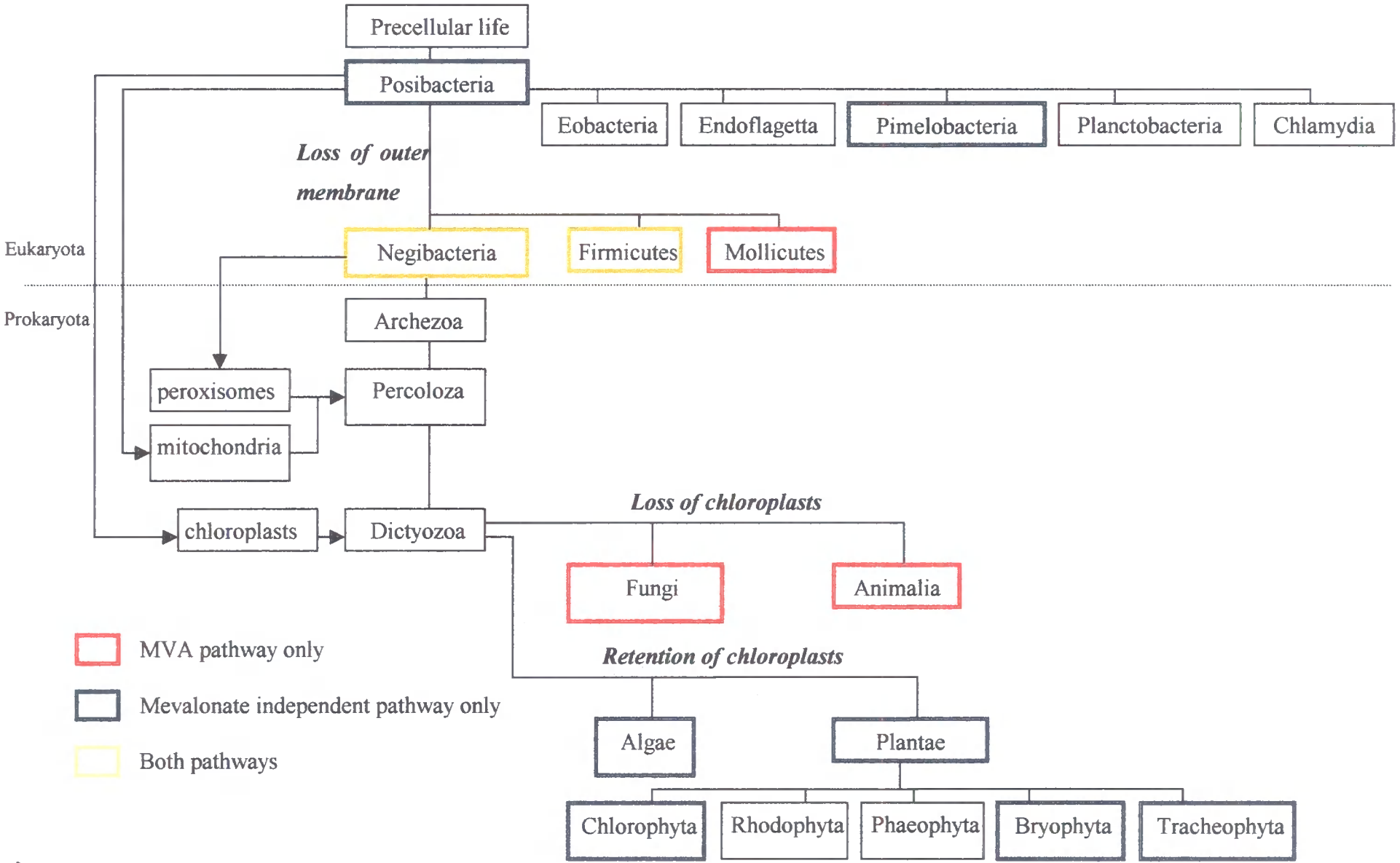

Scheme 1-32 Distribution of the two pathways in terpene biosynthesis

In evolutionary terms the distribution of the mevalonate independent pathway correlates with current thinking about how organisms evolved. Gram Negative bacteria are thought to have been assimilated into cells that would later evolve to become plant cells. The Gram Negative bacteria, and all their biosynthetic pathways, then constitute the chloroplasts of *Dictyozoa*. The evolution of fungi and animals, and plants and algae, represent a divergence in the pathways to terpene biosynthesis. The chloroplasts of *Dictyozoa* were retained in plants and algae, and hence the mevalonate independent pathway is found in these organisms. This contrasts with fungal and animal cells which lost their chloroplasts and hence the ability to manafacture terpenes by the mevalonate independent pathway.

1.7.6 Post ME-2,4-CDP intermediates and IPP formation

As yet, no other features of the mevalonate independent pathway are known. Hypotheses relating to putative intermediates and issues regarding the interconversion of IPP and DMAPP are discussed in Chapter 2.

1.8 Précis

This thesis is divided into four main chapters. Chapter 2 relates to studies on the mevalonate independent pathway that operates in the plant *Mentha citrata* and the bacterium *Escherichia coli*. Feeding studies and synthesis of labelled intermediates are discussed. Chapter 3 concerns the growth and isolation of a meroterpene from the fungus *R. necatrix*. Structure analysis and biosynthetic studies are also described. Isolation and structure elucidation of a metabolite from *Xylaria grammicin* completes the chapter. Chapter 4 is the experimental section.

Chapter 2

The biosynthesis of linalyl acetate by M. citrata *and ubiquinone-8 by* E. coli

2 *The biosynthesis of metabolites by the mevalonate independent pathway*

This chapter describes studies that have been performed on the mevalonate independent pathway using whole plant cultures of *Mentha citrata* and cultures of the bacterium *Escherichia coli*. Initially the chapter describes the isolation and purification of linalyl acetate and the assignment of proton and carbon NMR resonances. The chapter then reports the results of feeding experiments using ^{13}C and ^{2}H labelled compounds to *M. citrata* and *E. coli* and information about the extent that the mevalonate independent pathway operates in the context of compartmentalisation. The synthesis and feeding of stable isotope labelled compounds concludes the chapter.

2.1 Introduction to M. citrata

For this study of the mevalonate independent pathway, plant tissue cultures of *M. citrata* and whole cell cultures of *E. coli* were used. It is pertinent to briefly describe each system in turn.

Plant tissue cultures have many advantages over whole plant cultures in biosynthetic studies as outlined below.

Plant tissue cultures	**Whole plant culture**
Maturity in ~30 days	Maturation in 1-4 months
Can be grown easily in simple medium	Typically require soil
Easy introduction of labelled precursors	Complex transport mechanism via roots
Low maintenance	Require regular tending

Table 2-1 Comparison between plant tissue and whole plant cultures

2.1.1 *The production of linalyl acetate by* M. citrata

The cultures of *M. citrata* were a gift from Dr Richard Robins (CNRS, Nantes) and were initially generated by Hamill and co-workers[79]. In order to enhance terpenoid production, shooty *M. citrata* cultures were transformed with a variety of strains of *Agrobacterium tumefaciens*. The use of *Agrobacterium* to effect secondary metabolite production is well described[80] although the mechanism is not well understood. Transformation involves infecting the plant with *Agrobacterium* which transfers T-DNA which, in turn, decreases the auxin/cytokynin ratio in the transformed plant. This results in the retardation in growth of stem tissue with a concordant increase in leaf growth. Previous studies with *M. citrata* cultures had shown that linalyl acetate (**78**) production is localised in terpenoid producing glands that are situated on the underside of the leaf [79] and thus enhanced leaf growth leads to increased terpenoid production. The work had also investigated the effect of external physical conditions on the rate of growth and terpenoid production[81]. Linalyl acetate production was found to be maximal when the transformed cultures were grown in 3% sucrose and Murashige and Skoog medium. Under these conditions, it was reported that after 41 days growth up to 800μg of linalyl acetate per flask was produced. Linaloöl **46**, the parent alcohol of linalyl acetate, was also produced, but at much lower level (21μg/flask).

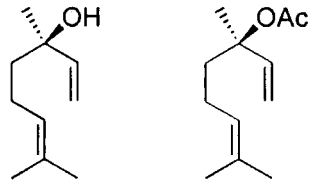

46 **78**

2.1.2 *Extraction of linalyl acetate from* M. citrata

One of the primary objectives in this programme was to isolate and fully characterise linalyl acetate. Intially the method of Hamill[81] was used in which the plant tissue was collected and dried between filter papers and air dried for one hour. The tissue was then homogenised three times in a Waring blender with HPLC grade heptane at 4°C and the heptane decanted into a centrifuge tube. Following centrifugation at 4°C, the supernatant liquid was decanted and the solvent removed under reduced pressure. The

last traces of heptane were removed under high vacuum for one minute. This method proved to be very successful as it repeatably delivered 10mg of linalyl acetate per flask and was quick and effective. This method (Procedure 1) was employed for all of the initial experiments but was stopped when it was the result of a fire when the blender cracked.

Other extraction procedures were explored to modify the procedure. The method found to be the best replacement was the soxhlet extraction of plant tissue with heptane. However, the amount of linalyl acetate that was extracted was found to be approximately half that when using the Waring blender (5mg/flask). The soxhlet method is herein-described as procedure 2. Both procedures gave samples of linalyl acetate that were identical to commercial linalyl acetate (GC-MS, NMR).

2.1.3 Analysis of linalyl acetate

It was important to have fully assigned ^{1}H and ^{13}C NMR spectra of linalyl acetate.

A DEPT experiment allowed assignment of the resonance at 83 ppm to C-3 and the olefinic signal at 113ppm to C-1. The carbon signal at 132 ppm did not appear in the DEPT spectrum and could thus be assigned to C-7.

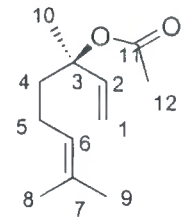

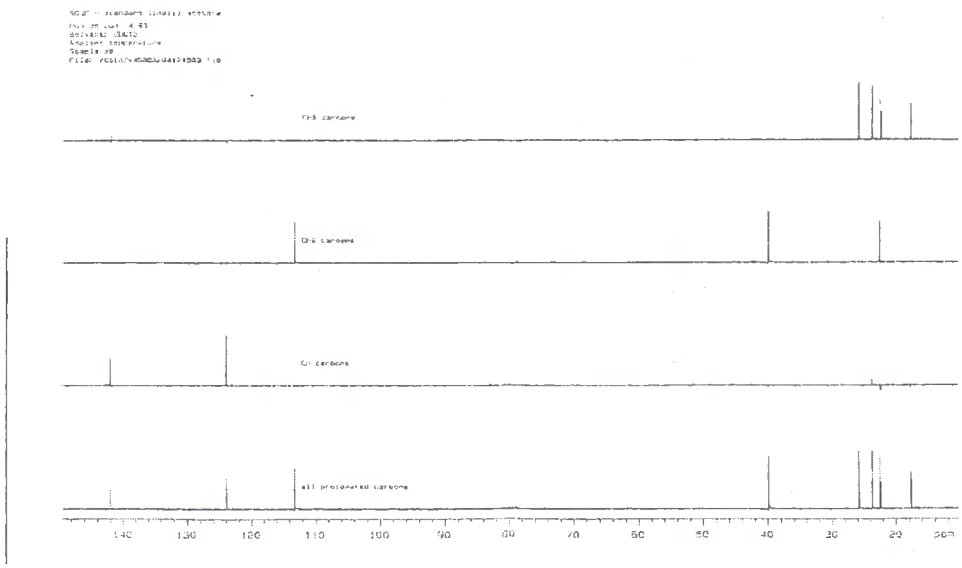

Figure 2-1 DEPT of linalyl acetate showing the degrees of protonation of each carbon

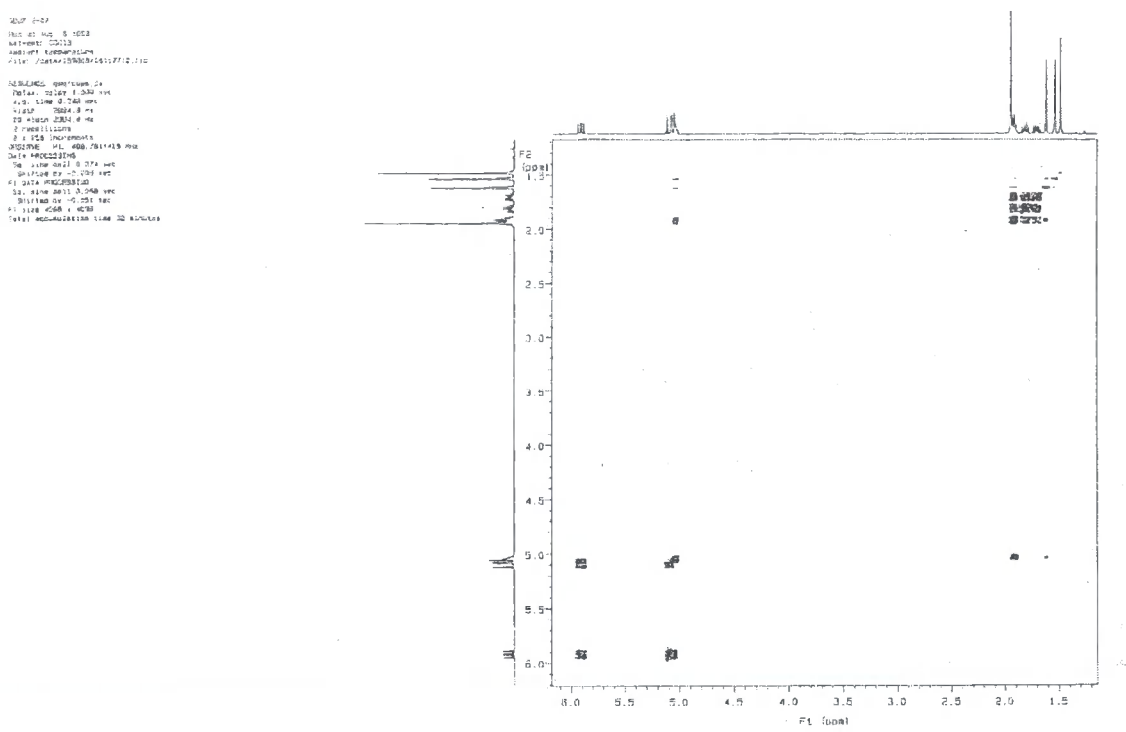

Figure 2-2 ^{1}H-^{1}H COSY of linalyl acetate

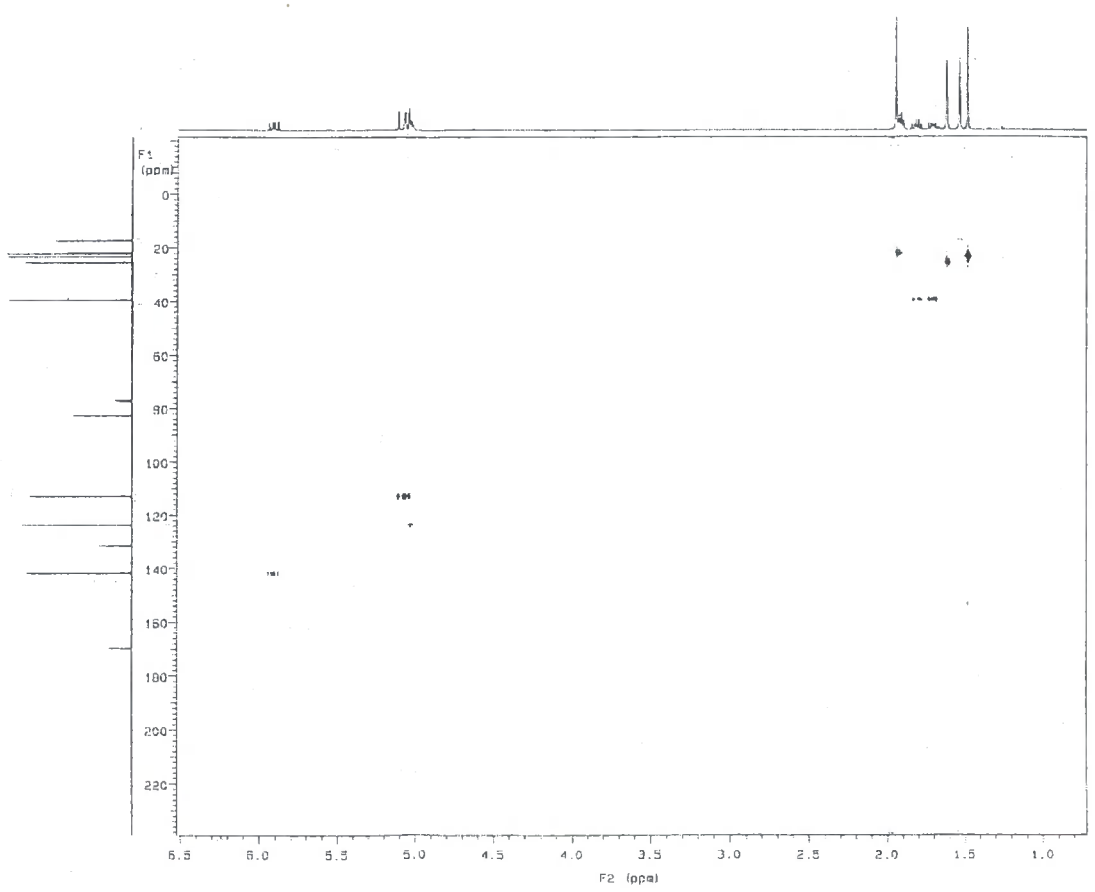

Figure 2-3 HETCOR Of linalyl acetate

COSY and HETCOR analysis in tandem enabled differentiation of the olefinic protons of C-2 and C-6. As the carbon resonance of C-1 had been assigned to the signal at 113ppm, it was obvious from analysis of the HETCOR spectrum to assign the signals at 5.0 ppm to C-1. The COSY spectrum showed clear coupling to proton resonances at 4.9 ppm which were shown in the HETCOR spectrum to correlate to the resonance at 142 ppm. Thus the 142ppm resonance was assigned to C-2. Examination of the resonance at 124 ppm showed that it was attached to protons at 4.9 ppm which gave off diagonal coupling to resonances in the COSY spectrum to signals at 2.0 ppm. Hence, the signals at 124 and 2.0 ppm represent the carbon and proton resonances respectively of C-6. Assignment of the aliphatic protons at C-4 and C-5 was made easier by the fact that the proton at C-6 couples to the diastereomeric protons at C-5. Analysis of the COSY spectrum showed coupling of C-6 to the centre of a pair of muliplets at 1.8ppm , both of which correlate to the resonance at 22.5 ppm in the HETCOR. This is entirely consistent with those resonances being derived from C-5. Hence the remaining methylene resonances at 40.0 and 1.9 ppm are from C-4. This is further demonstrated by the proton multiplicity (a doublet of doublets corresponding to coupling to the two non equivalent protons of C-5). Difficulties were encountered when assigning the methyl resonances however. A literature search for similar structural motifs as those found in linalyl acetate revealed an assignment to chinesin I (**79**), a plant phloroglucinol[82]. Chinesin possesses a pendant terpenoid derived unit that is identical to that in linalyl acetate.

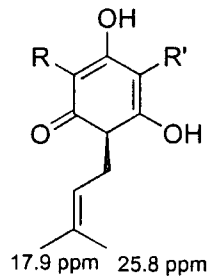

79

Figure 2-4 Terpenoid motif in chinesin (**79**). ^{13}C-NMR shifts of the terpene unit are shown

The carbon NMR of chinesin showed that the *cis* and *trans* methyl groups gave signals at 17.9 and 25.8 ppm respectively. These corresponded almost exactly to two methyl resonances at 17.8 and 25.9 ppm in the spectrum of linalyl acetate, which tentatively suggested that the signals were due to C-8 and C-9 respectively. This was confirmed by

nOe analysis which showed that irridiation of the C-6 proton gave enhancement of the protons corresponding to the carbon at 25.9 ppm.

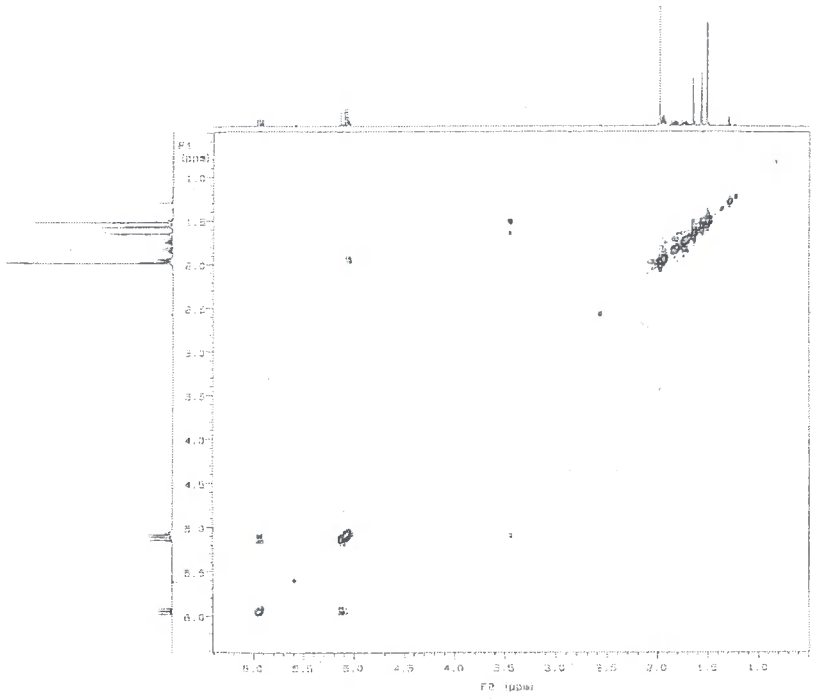

Figure 2-5 NOESY of linalyl acetate

Carbon number	δ_C/ppm	δ_H/ppm
1	113.3	5.25
2	124.0	5.89
3	83.1	-
4	39.9	1.75
5	22.5	1.85
6	142.0	5.10
7	132.0	-
8	17.8	1.58
9	25.9	1.69
10	23.9	1.55
11	170.1	-
12	22.4	2.01

Table 2-2 ^{1}H and ^{13}C-NMR resonances of linalyl acetate

NMR is very useful as an analysis technique for biosynthetic studies, but is only moderately sensitive. In order to assess low levels of incorporation, a GC-MS protocol

was developed and samples of linalyl acetate were analysed by Dr Jack Hamilton (Queen's University, Belfast). GC-EIMS of linalyl acetate proved to be unfruitful as neither the molecular ion nor any useful daughter fragments were observed. However, when GC-CIMS was performed with methane as the carrier gas, an ion corresponding to the loss of acetic acid was detected. This pseudo molecular ion was used throughout the course of the experiments to determine levels of incorporation. In order to produce accurate results, GC-CIMS was recorded 10 times and the values were averaged to give levels of incorporation when corrected for natural abundance.

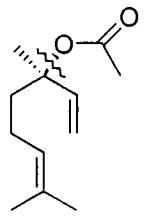

137

Figure 2-6 Illustration of the formation of the pseudo molecular ion of linalyl acetate **(78)**

2.2 *Biosynthesis of ubiquinone in* E. coli

In addition to whole plant cultures of *M. citrata*, *E. coli* was selected to investigate the mevalonate independent pathway as it was being used concurrently by other research groups. *E. coli* has many features that make it attractive for use in biosynthetic investigations such as the rate of cell growth (2-3d), the ease of maintenance and its ready availability. Of the broad spectrum of idolites that are produced by *E. coli*, ubiquinone (**80**) and menaquinone (**81**) are probably the most important in terms of biological activity and they have been used as tools for determining features of the mevalonate independent pathway in bacteria.

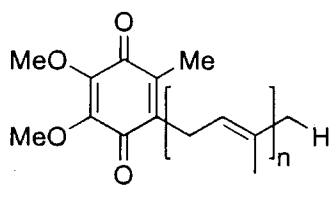

80

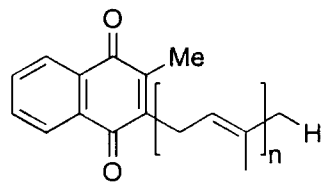

81

Arguments have been put forward that categorise the quinones as primary, rather than secondary metabolites. This reasoning, however, does not consider that ubiquinones are delivered by secondary metabolic pathways such as the shikimate, mevalonate and mevalonate independent pathways. Both of the quinones are used to mediate respiratory electron transfers owing to the redox ability of the quinone nucleus.

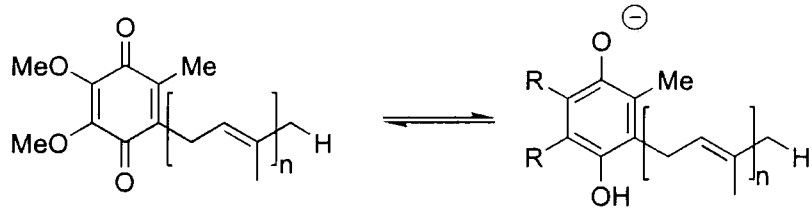

Scheme 2-1 Reduction of the quinone nucleus

Ubiquinones are described by the number of IPP derived building blocks that form the prenyl chain. Ubiquinone-8, for example, has eight repeat units in the prenyl unit resulting in a C_{40} sidechain. Prenyl chain lengths between ten and fifty carbon atoms have been reported.

Ubiquinone-10 was the first ubiquinone to be isolated, and was extracted from bovine heart by Morton and coworkers[83] in 1958. The name ubiquinone was coined by Morton owing to its universal distribution. Indeed, the only organisms in which ubiquinones have not been detected are blue green algae and Gram-positive bacteria.

In bacteria, ubiquinones are biosynthesised from chorisimic acid, with extensive functionalistion afforded by molecular oxygen and SAM.

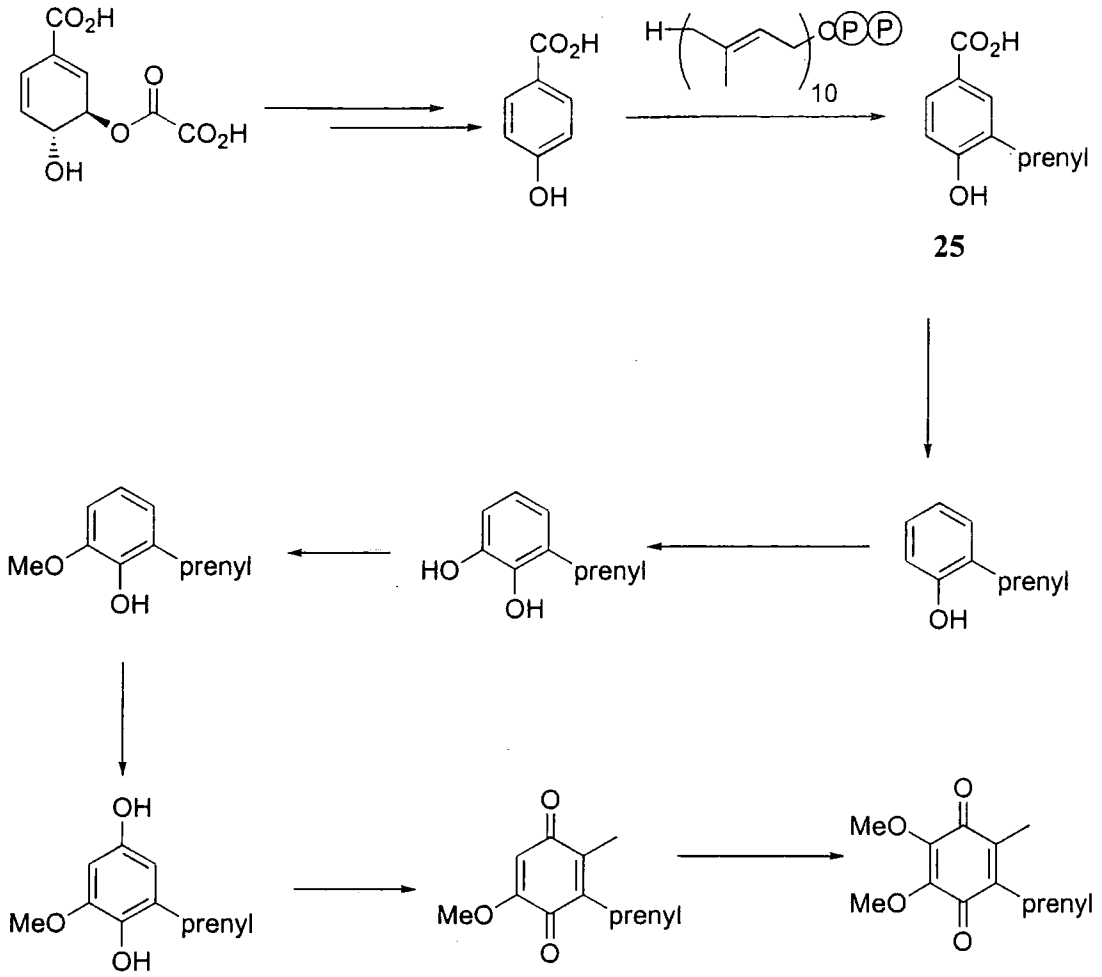

Scheme 2-2 Biosynthesis of ubiquinone from chromismate (**25**) in bacteria

2.2.1 Growth of E. coli

Cultures of *E. coli* DH5α were obtained from Dr Tony Fawcett (Biological Sciences, Durham) and were grown in standard LB medium. In accordance with standard practice, starter cultures (35ml) were seeded and grown for three days. Starter cultures were initially inoculated from an agar plate, and subsequently from cultures stored in glycerol solution (10%) at –20°C. Production cultures (500ml) were inoculated from starter cultures (5ml) and grown for three days. At the outset a time course study of cell density was undertaken. The most straightforward method to record cell density is *via* absorbance at 600nm and a maximal absorbance of 1.96 A was found after 26 hours, which corresponds to the beginning of the stationary phase.

2.2.2 Extraction of ubiquinone

The extraction and purification of ubiquinone is well documented although most literature methods describe its extraction from mammalian hearts. In this programme the procedure described by Rohmer[53] from *E. coli* was followed. Cells were collected by centrifugation which were then freeze-dried overnight to afford 1g/l of cells. The cells were then extracted three times into chloroform/methanol by heating under reflux. Removal of the solvent yielded a brown oil which, after extraction with heptane and column chromatography, gave ubiquinone-8. Initially, purification was performed using preparative TLC, but this was found to be unsuitable owing to poor chromatographic resolution and the need to run multiple plates if large amounts (200mg) of crude extract were obtained. This procedure allowed the isolation of relatively pure ubiquinone-8 (NMR).

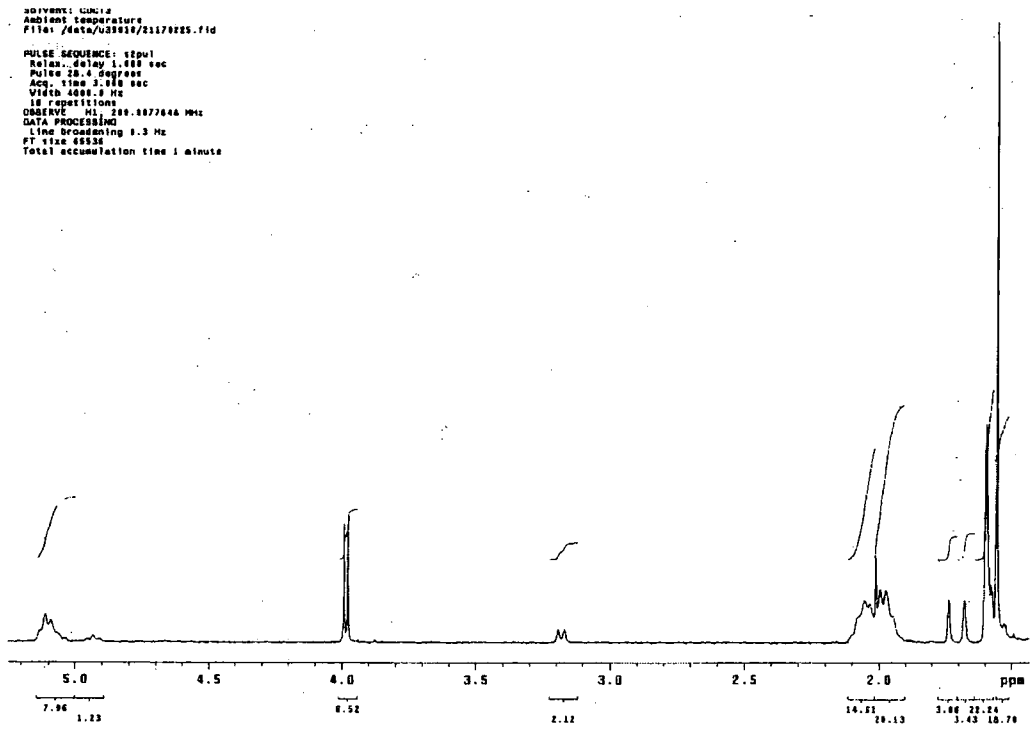

Figure 2-7 ^{1}H NMR spectrum of ubiquinone-8 isolated from *E. coli*

Ubiquinone-8 was routinely isolated at a level of ~800μg/l, which required that 4 litres of broth were innoculated in order to obtain sufficient ubiquinone for ^{2}H NMR analysis.

2.3 Preliminary feeding experiments

The first objective of the program was to determine whether linalyl acetate was biosynthesised using the mevalonate independent pathway or MVA pathway by *M. citrata.* The feeding of sodium [1,2-^{13}C]-acetate and [1-^{13}C]-glucose were identified as key experiments to establish which pathway produced the terpene fragment of linalyl acetate. It is was known that ubiquinone-8 from *E. coli* is produced *via* the mevalonate independent pathway, and consequently only [6,6-$^{2}H_2$]-glucose and [$^{2}H_3$-*methyl*]-methionine were fed in order to establish whether the cultures were behaving in a similar manner to those in the reported literature.

2.3.1 Feeding of sodium [1,2-^{13}C]-acetate (82) to M. citrata

Sodium [1,2-$^{13}C_2$]-acetate was fed to two cultures of *M. citrata* to a final concentration of 10mM. The cultures were grown under standard conditions with fructose as the sugar source. At the end of the incubation, linalyl acetate was extracted using procedure 1. The resultant ^{13}C-NMR spectrum (Figure 2-8) showed that all of the intact acetate was located in C-11 and C-12 as evident from the J_{13C13C} coupling of 58.9 Hz between C-11 and C-12. No incorporation into the terpene moiety was evident from this experiment.

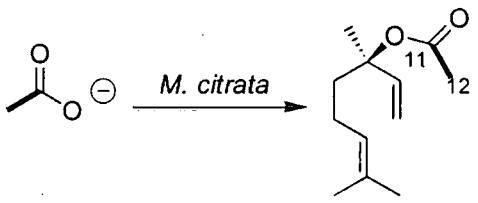

Scheme 2-3 Incorporation of [1,2-$^{13}C_2$]-acetate into linalyl acetate

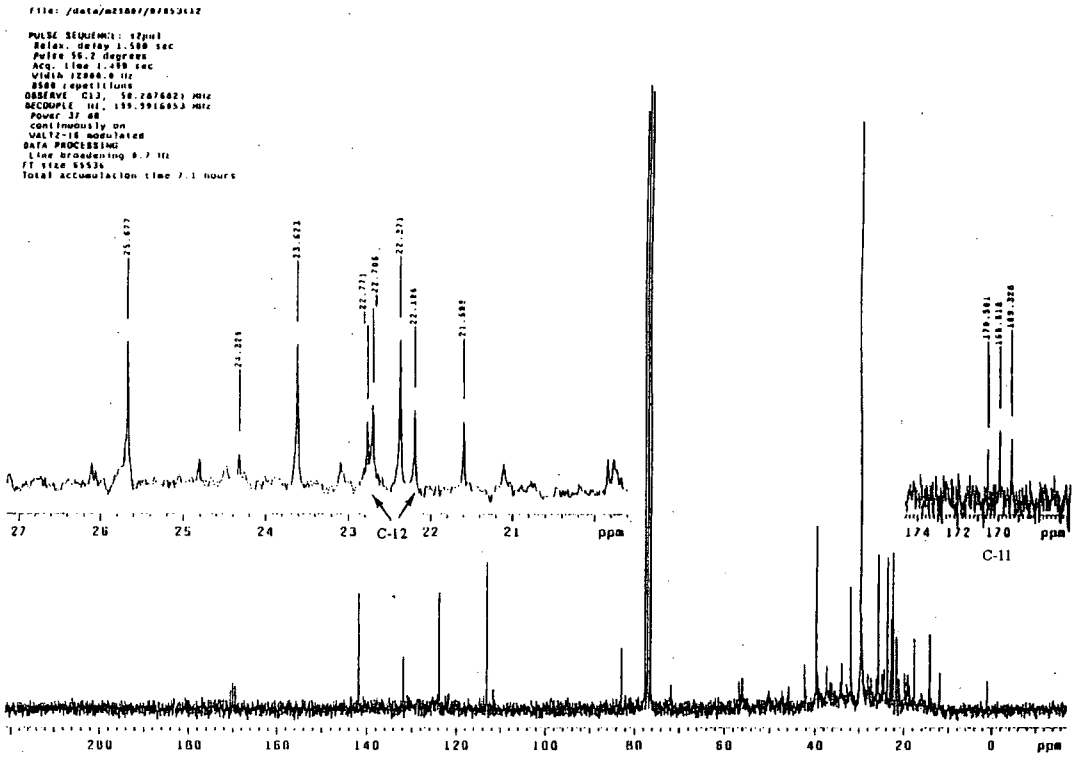

Figure 2-8 ^{13}C-NMR of linalyl acetate after feeding [1,2-$^{13}C_2$]-acetate. ^{2}J ^{13}C-^{13}C Coupling corresponding to the intact incorporation of an acetate unit are shown in the inset plots.

2.3.2 *Feeding of [1-^{13}C] glucose (83) to* M. citrata – *operation of the mevalonate independent pathway*

The feeding of [1-^{13}C]-glucose emerged as a key experiment to delineate which pathway produced the terpene fragment of linalyl acetate. Almost all organisms are capable of using glucose as a carbon source, which makes it ideal for biosynthetic investigations. [1-^{13}C]-Glucose is processed *via* glycolysis through known intermediates, as described in chapter one, which means that the biosynthetic route of the label can be elucidated from the incorporation pattern.

[1-^{13}C]-Glucose labels IPP differently depending on which pathway is involved as shown below in Scheme 2-4. Thus, [1-^{13}C]-glucose is a powerful tool for determining which is the dominant pathway for terpene biosynthesis.

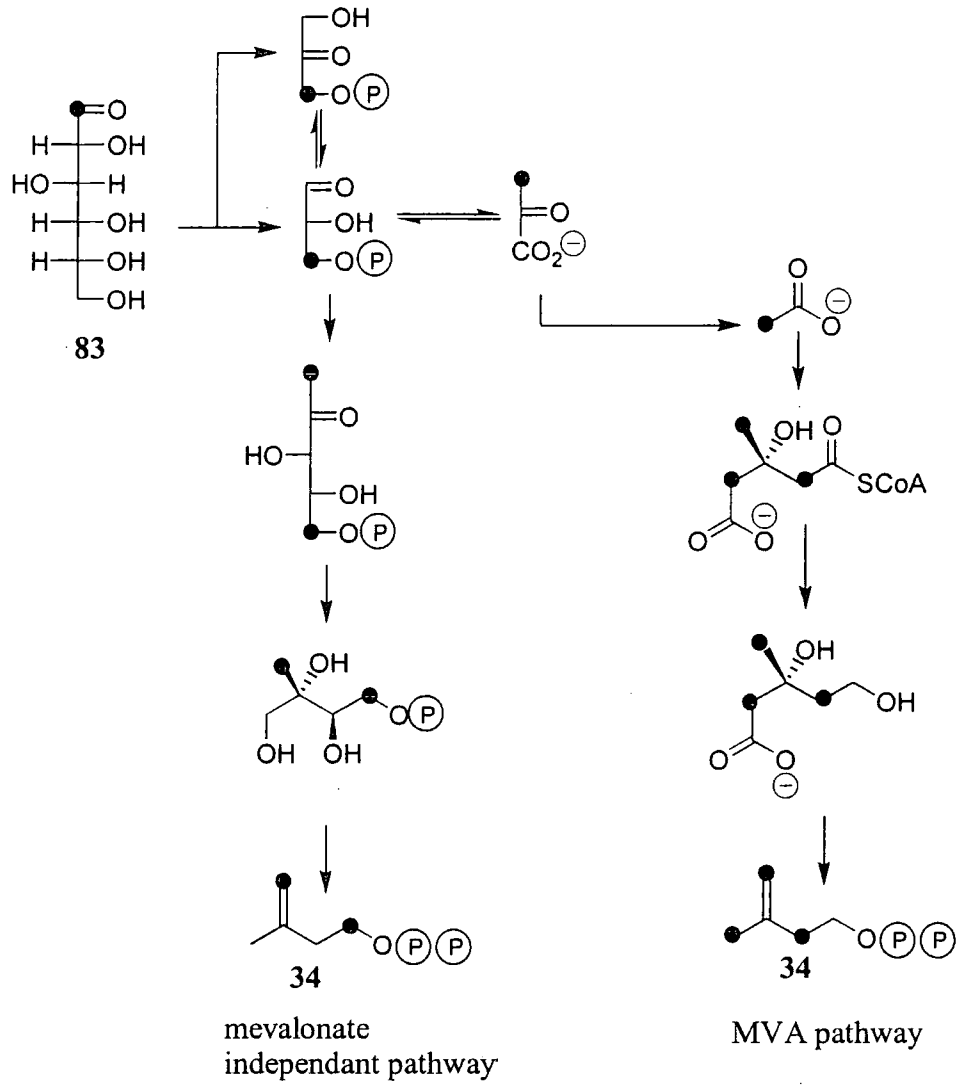

Scheme 2-4 Processing of [1-^{13}C] glucose (**83**) to IPP (**34**) *via* the mevalonate independent pathway and the MVA pathway

[1-^{13}C]-Glucose was administered to two flasks of *M. citrata* to a final concentration of 8.4 mM and the cultures were harvested after 25 days. Linalyl acetate was extracted using procedure 1 and analysed by ^{13}C NMR spectroscopy.

In order to estimate the level of isotopic enrichment it was necessary to normalise the peak heights of the resultant spectrum relative to the natural abundance spectrum. C-3 of linalyl acetate was selected a reference peak as it is labelled by neither pathway. Accordingly, each peak height in the spectrum that was obtained after feeding [1-^{13}C]-glucose was divided by the height of C-3. Finally, each peak height was corrected for natural abundance ^{13}C by dividing each peak height of the labelled linalyl acetate by the peak height of the same signal in the ^{13}C-NMR of an unlabelled sample of linalyl acetate. This analysis provided the enrichments as shown in Table 2-3.

Carbon no	*Level of enrichment*
1	**2.50**
2	1.60
3	1.10
4	1.40
5	**2.29**
6	1.31
7	1.58
8	**2.44**
9	1.66
10	**2.31**
11	1.13
12	**3.90**

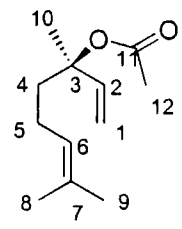

Table 2-3 Enrichment of carbon signals after feeding with [1-^{13}C]-glucose relative to C-3. Values in bold type indicate significantly enriched ^{13}C signals

There is a clear enrichment of carbon atoms 1, 5, 8,10 and 12 and a small enhancement of carbons 2, 7 and 9. The labelling pattern is consistent with [1-^{13}C]-glucose being processed *via* the mevalonate independent pathway as outlined in Scheme 2-4. The enrichments into C-2 and C-4, which are not a result of incorporation *via* the mevalonate independent pathway, are due to incorporation of C-1 of glucose through mechanisms other than those shown in Scheme 2-4.

2.3.3 *Feeding of sodium [2,2,3,3-$^2H_4$]-succinate to* M. citrata *and* E. coli

Sodium succinate (**84**) was fed to *M. citrata* owing to its availability as a pyruvate surrogate. Succinate (**84**) is processed to pyruvate (**7**) *via* the TCA cycle.

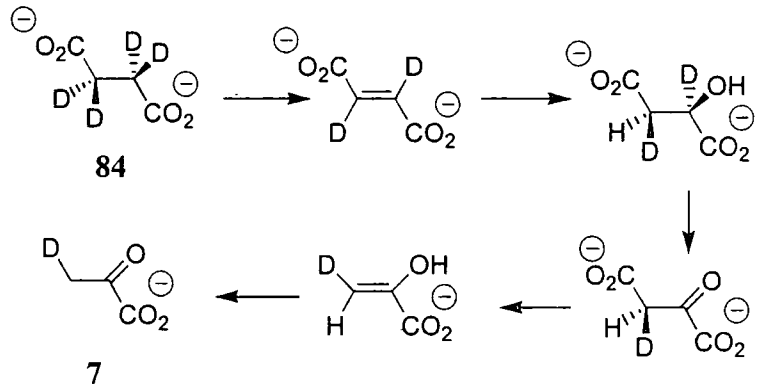

Scheme 2-5 Processing of sodium [2,2,3,3-$^2H_4$]-succinate (**84**) to pyruvate (**7**)

It was anticipated that the feeding of succinate would result in deuterium incorporation into linalyl acetate and provide information about the concentrations of precursors that were required for successful enrichments.

Accordingly, sodium [2,2,3,3-$^2H_4$]-succinate was pulse fed to two cultures of *M. citrata* on days 7, 14, and 19 and the plant tissue was extracted using procedure 1. GC-MS analysis was performed ten times and the results were averaged to ensure that enhancements were statistically significant. Analysis of the linalyl acetate after feeding sodium [2,2,3,3-$^2H_4$]-succinate showed an enhancement of the M+1 ion (0.14%). The data is shown in Figure 2-9.

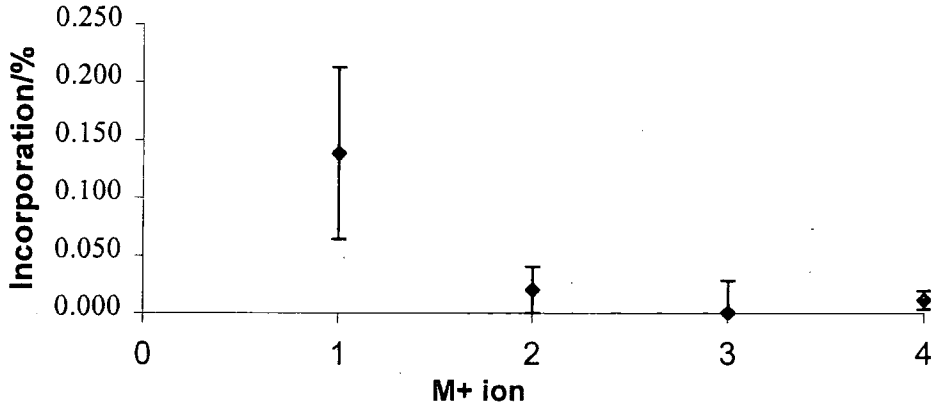

Figure 2-9 GC-MS Determined incorporation *vs* molecular weight after feeding [2,2,3,3-$^2H_4$]-succinate (**84**) to *M. citrata*

The level of incorporation is low but significant and represents the incorporation of one deuterium atom into linalyl acetate. This is consistent with the processing of succinate *via* the TCA cycle and incorporation into linalyl acetate from [3-^{2}H]-pyruvate as shown in Scheme 2-5. The result was very encouraging as it demonstrated that the GC-CIMS protocol was capable of detecting very low levels of enrichment and that whole cell plant tissue cultures of *M. citrata* were capable of using exogenously administered substrates. Furthermore, the incorporation showed that the pyruvate end of DXP was amenable to investigation by the use of surrogate substrates. This prompted an investigation using a number of potential precursors that would allow the origin of the methyl hydrogen atoms of DXP to be traced.

In the analogous experiment in bacteria, sodium [2,2,3,3-$^2H_4$]-succinate (**84**) was fed to eight production cultures (500ml) of *E. coli* to a concentration of 1.1mM. Ubiquinone-8 was extracted according to standard procedures and was analysed *via* ^{2}H-NMR. However, no enrichment of deuterium was observed. This is possibly due to the low concentration at which sodium [2,2,3,3-$^2H_4$]-succinate was fed to *E. coli*

2.3.4 *Feeding of alanine*

Previous work in Durham[84] had demonstrated the use of alanine as an excellent pyruvate surrogate in fungus. Alanine is processed *in vivo* to pyruvate by transamination.

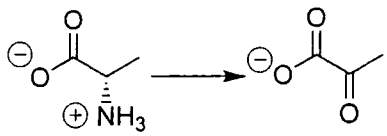

85 **7**

Scheme 2-6 Formation of pyruvate (**7**) from alanine (**85**)

One of the attractive features about the use of labelled alanine was that both [3-^{13}C] and [3-$^{2}H_3$]-alanine were commercially available and the preparation of enatiopure [3-$^{13}C^{2}H_3$]-alanine was reported in the literature. It was anticipated that alanine would provide a method of determining whether the methyl protons of MEP were abstracted during the conversion of MEP to IPP.

2.3.5 *Synthesis of D-[3-$^{13}C^{2}H_3$]-alanine (86)*

The synthesis of D-[3-$^{13}C^{2}H_3$]-alanine (**86**) was followed using Seebach's oxazolidinone methodology[85] as modified by Chesters and O'Hagan[84]. Treatment of benzoyl-2-(*t*-butyl)-3-methylimidazolidin-4-one (**87**) with LDA at –78^{O}C yields the anion which can then be reacted with a suitable electrophile. In the case of methyl iodide, the methylation proceeds with stereochemical control owing to the steric bulk of the *tert*-butyl group that hinders attack from one face to give benzoyl-2-(*t*-butyl)-3,5-dimethylimidazolidin-4-one (**88**). Acid hydrolysis at elevated temperature and pressure yields alanine (**85**).

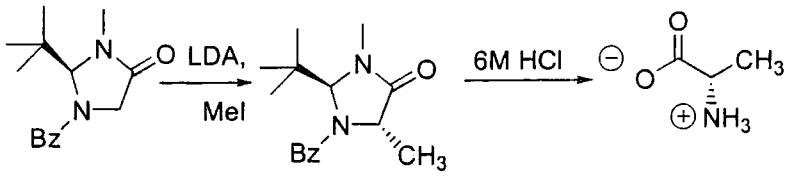

Scheme 2-7 Synthesis of alanine (**85**) from benzoyl-2-(*t*-butyl)-3-methylimidazolidin-4-one (**87**)

Treatment of benzoyl-2-(*t*-butyl)-3-methylimidazolidin-4-one (**87**) with methyl iodide gave benzoyl-2-(*t*-butyl)-3,5-dimethylimidazolidin-4-one (**88**) in a moderate yield (65%). Unreacted starting material was recovered by column chromatography. Hydrolysis in a sealed tube with 6M HCl at 180°C yielded a black powder, which after purification over Dowex, gave alanine as a white crystalline solid.

The synthesis was repeated using [$^{13}C^{2}H_3$]-methyl iodide with a similar yield for the first step to give benzoyl-2-(*t*-butyl)-3-methyl-5-[$^{13}C^{2}H_3$]-imidazolidin-4-one (**89**). ydrolysis with 6M at 180°C and purification by Dowex yielded [3-$^{13}C^{2}H_3$]-alanine (**86**) as a white crystalline solid.

2.3.6 Feeding of [3-^{13}C]-alanine (90) to M. citrata

The feeding of [3-^{13}C]-alanine (**90**) was a key experiment as it was essential to determine the regiochemistry of the incorporation of alanine into linalyl acetate. Processing of alanine to acetate and incorporation *via* the MVA pathway would result in the retention of all three acetate methyl protons and hence an isolated M+3 incorporation from [3-^{2}H]-alanine could not be conclusively interpreted as the retention of all three protons of pyruvate *via* the mevalonate independent pathway.

Alanine was found to be acutely toxic to *M. citrata* and chronically toxic to cultures of *E. coli*. When cultures of *M. citrata* were supplemented with alanine at 5mM, the shoots blackened and died within 3 days. Feeding alanine above 5mM caused death within 24 hours. Ultimately, labelled substrates were fed at 3mM to cultures of *M. citrata*, which caused significant growth retardation and a much lower yield of linalyl acetate (3mg/flask compared to a typical 10mg/flask). This is partly due to the onset of necrosis which required that the cultures were harvested on day 17 rather than day 23. A similar sensitivity to nitrogen was observed by Hamill[81] who observed that the use of a medium with a high nitrogen content diminished the yield of linalyl acetate. Incubation of *E. coli*

with unlabelled alanine at 2mM resulted in the cessation of ubiquinone production and a concomitant decrease in dry cell mass (250mg/l rather than 1g/l). Consequently, experiments with labelled alanine and *E. coli* were not pursued.

Accordingly, [3-^{13}C]-alanine was fed to two cultures of *M. citrata* that were harvested using procedure 1 and analysed *via* ^{13}C-NMR. In order to assess incorporation, the peak heights were measured and normalised by dividing each individual peak height by the height of the C-3 peak. Each peak height was corrected for natural abundance ^{13}C by dividing each peak height of the labelled linalyl acetate by the peak height of the same signal in the ^{13}C-NMR of an unlabelled sample of linalyl acetate. This gives incorporations that are reported in Table 2-4. The peaks corresponding to C-7 and C-11 were not observed in the ^{13}C-NMR owing to the small amount of linalyl acetate that was isolated (3mg/flask).

Carbon no	*Level of incorporation*
1	1.10
2	1.25
3	1.54
4	1.22
5	1.50
6	1.28
7	n.d.
8	**2.00**
9	1.22
10	**1.90**
11	n.d.
12	**2.33**

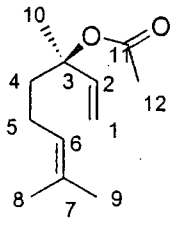

Table 2-4 Incorporation of [3-^{13}C]-alanine (**90**) into linalyl acetate. Bold figures indicate significant incorporation

Enrichment was observed into C-8, C-10 and C-12. This corresponds to processing of [3-^{13}C]-alanine (**90**) to pyrvuate (**7**) and incorporation *via* the mevalonate independent pathway as shown in Scheme 2-8.

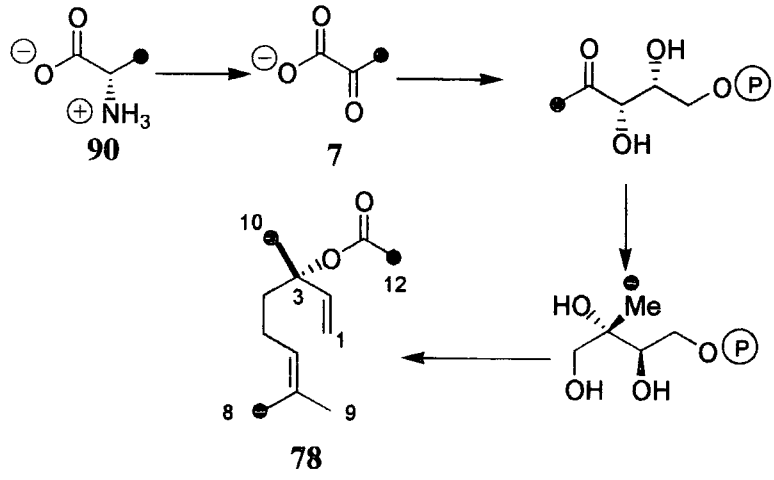

Scheme 2-8 Incorporation of [3-^{13}C]-alanine (**90**) into linalyl acetate (**78**)

In separate experiments, [3-$^{2}H_3$] and [3-$^{13}C^{2}H_3$]-alanine were fed to two cultures of *M. citrata*. Both experiments showed identical growth retardation and yielded similarly low levels of linalyl acetate (3mg/flask). GC-MS Analysis of linalyl acetate isolated after feeding [3-$^{2}H_3$]-alanine showed enhanced M+1 and M+3 ions. The feeding of [3-$^{13}C^{2}H_3$]-alanine gave enhanced M+2 and M+4 ions. Each sample was examined ten times and the mean incorporations are shown in Figure 2-10.

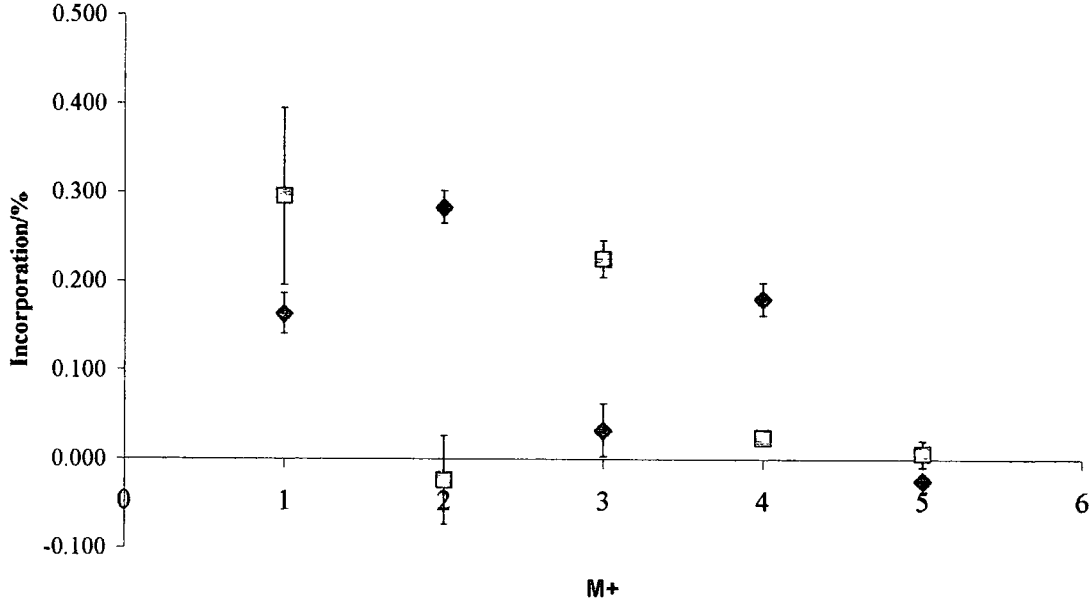

Figure 2-10 GC-MS Incorporation of [3-$^{2}H_3$] (■) and [3-$^{13}C^{2}H_3$]-alanine (♦) into linalyl acetate

The enrichment in the M+3 ion after feeding [3-$^{2}H_3$]-alanine and incorporation into the M+4 ion after feeding [3-$^{13}C^{2}H_3$]-alanine correspond to the incorporation of $^{2}H_3$ and $^{13}C^{2}H_3$ respectively. This shows that all three deuterium atoms were retained during the conversion of DXP to IPP by the mevalonate independent pathway. Furthermore, there is a significant M+1 enrichment after feeding [3-$^{2}H_3$]-alanine and a corresponding M+2 enrichment after feeding [3-$^{13}C^{2}H_3$]-alanine. In both cases, this corresponds to incorporation of one deuterium, which is due to the processing of [3-$^{2}H_3$]-pyruvate (**91**) *via* the TCA cycle to succinate and incorporation of [3-^{2}H]-pyruvate (**92**) as described in Scheme 2-9.

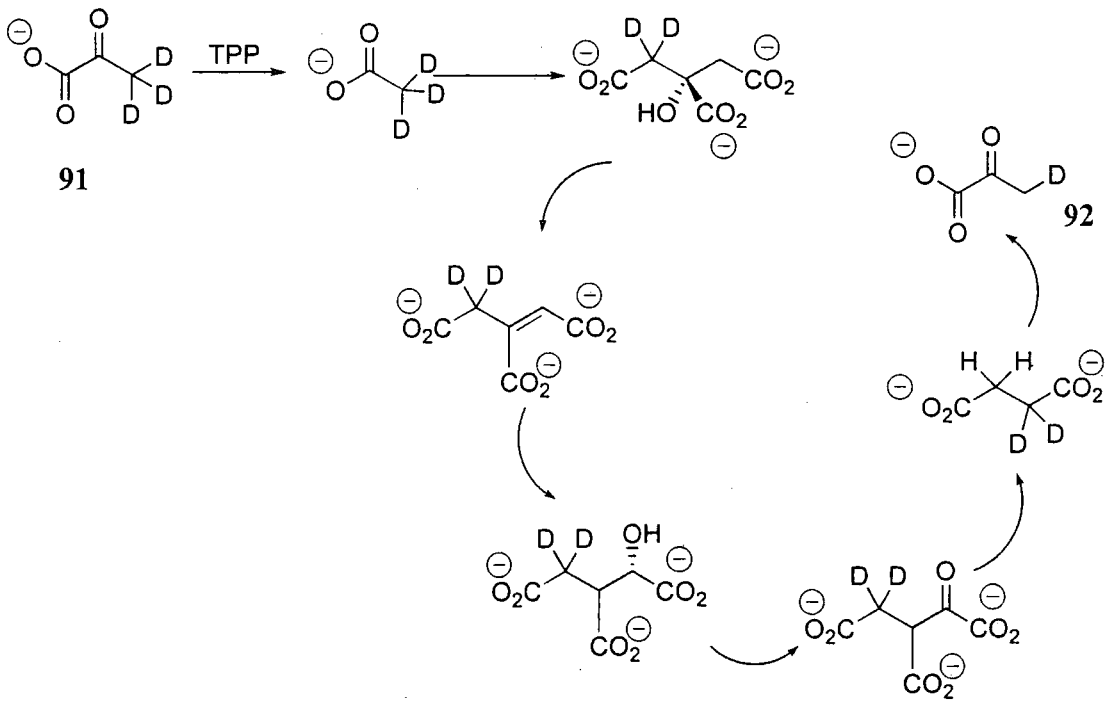

Scheme 2-9 Loss of two deuterium atoms from pyruvate after processing *via* the TCA cycle

As all three deuterium atoms are retained and thus the mevalonate independent pathway does not remove the methyl protons of MEP during linalyl acetate biosynthesis. This limits the processes by which MEP is converted to IPP by precluding a dehydration involving any of the methyl protons.

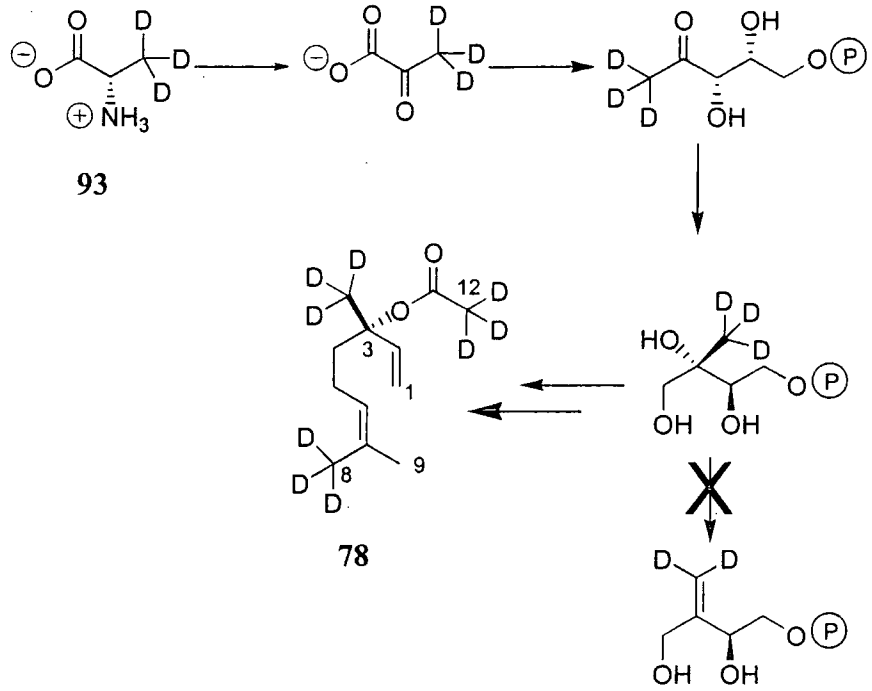

Scheme 2-10 Incorporation of deuterium into linalyl acetate (**78**) from [3-$^2H_3$]-alanine (**93**) which precludes the dehydration shown

2.3.7 Feeding of [6,6-$^2H_2$]-glucose to M. citrata

Although the terminal protons of DXP had been shown to be retained during bacterial terpene biosynthesis by Rohmer analogous studies in plants had not been performed. Thus the origin of the C-5 protons of DXP in plants were unknown and this was approached by feeding [6,6-$^2H_2$]-glucose (**94**). As already demonstrated with [1-^{13}C]-glucose, [6,6-$^2H_2$]-glucose will be processed *via* glycolysis to dihydroxyacetone phosphate (**70**) and GAP (**3**), which are interconverted by triose phosphate isomerase. Accordingly, [6,6-$^2H_2$]-glucose was administered to two cultures of *M. citrata* to a final concentration of 8.4mM. Linalyl acetate was extracted using procedure 1 and analysed *via* GC-CIMS. The sample was run ten times and the mean values are shown in Figure 2-11.

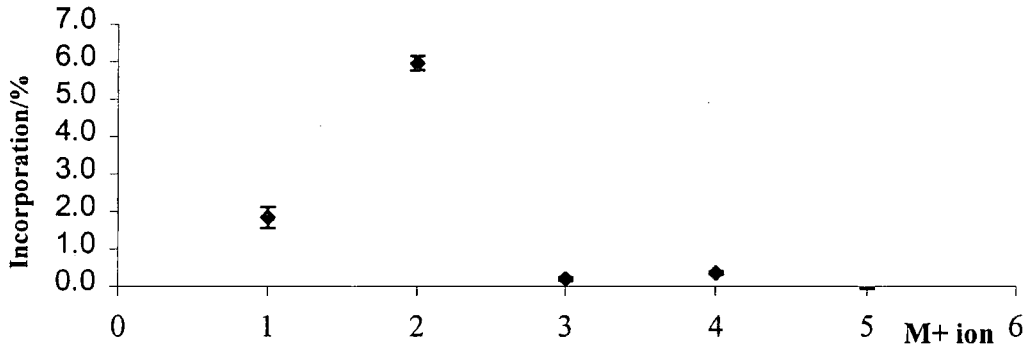

Figure 2-11 GC-MS Incorporation of deuterium from [6,6-$^2H_2$]-glucose into linalyl acetate

There is an enrichment of M+1 and M+2 ions and a small but significant incorporation into the M+4 ion. Significantly, the M+2 ion shows the highest level of incorporation (5.97%) representing retention of both deuterium atoms. Accordingly it can be deduced that both C-5 protons of DXP (**6**) are retained during plant terpene biosynthesis.

The high level of enrichment of the M+2 ion also gave rise to a statistically significant enhancement of the M+4 ion. This arises from a small population of linalyl acetate molecules which are derived from the statistical combination of two C_5 units both of which are labelled with two deuterium atoms (5.97% x 5.97%= 0.36%).

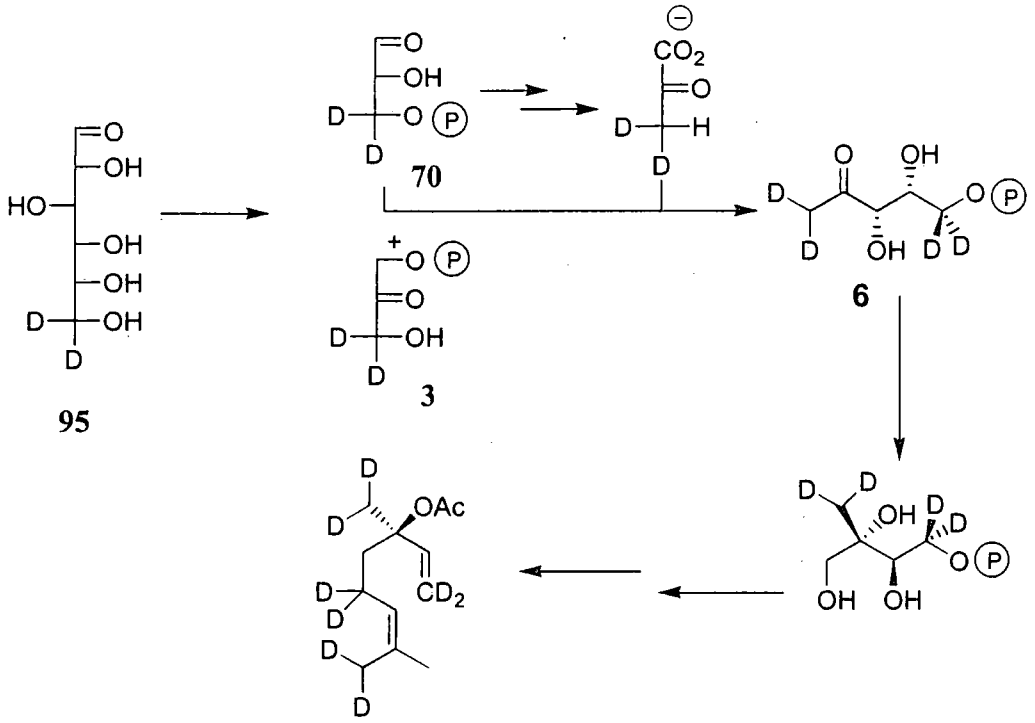

Scheme 2-11 Incorporation of deuterium from [6,6-$^2H_2$]-glucose (**95**) into linalyl acetate (**78**) by *M. citrata*

The retention of both deuterium atoms shows that the conversion of MEP to IPP *via* the mevalonate independent pathway does not proceed *via* dehydration involving the C-4 protons of MEP.

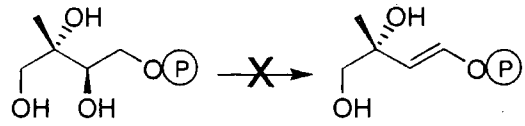

Figure 2-12 Disallowed transformation

These findings were consistent with those reported in bacteria and from the feeding of [6,6-$^{2}H_2$]-glucose to cyanobacteria[86].

The level of incorporation in this experiment was significantly higher than that observed after feeding [1-^{13}C]-glucose. This is presumably due to the competing operation of the oxidative pentose phosphate pathway that significantly metabolises C-1 of glucose.

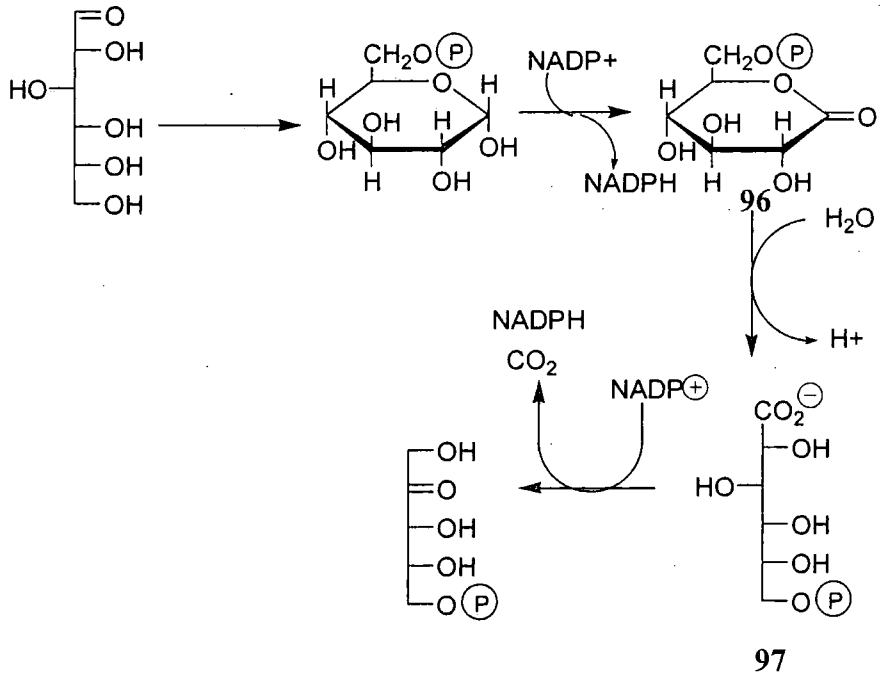

Scheme 2-12 Loss of C-1 of glucose by the pentose phosphate pathway

The oxidative pentose phosphate pathway uses glucose to generate NADPH and ribose-5-phosphate for nucleic acid biosynthesis and can be upregulated to supply NADPH when required. Following oxidation to 6-phosphonogluconolactone (**96**) and 6-

phosphonogluconate (**97**) the carbon derived from C-1 of glucose is lost as CO_2 and would account for ^{13}C loss from [1-^{13}C]-glucose.

2.3.8 Feeding of [6,6-$^2H_2$]-glucose to E. coli

Although the mevalonate independent pathway has recently been shown to operate in *E. coli*, it appeared appropriate to conduct an initial feeding experiment with a substrate for which the results were already known. Accordingly [6,6-$^2H_2$]-glucose was fed to *E. coli.* to a final concentration of 1.4 mM to *E. coli* and the cultures were grown under standard conditions for 3 days. Ubiquinone was isolated and purified according to the standard method. ^2H NMR Analysis of the sample revealed incorporation of deuterium, which was evident from the peaks at 1.6 and 2.0 ppm.

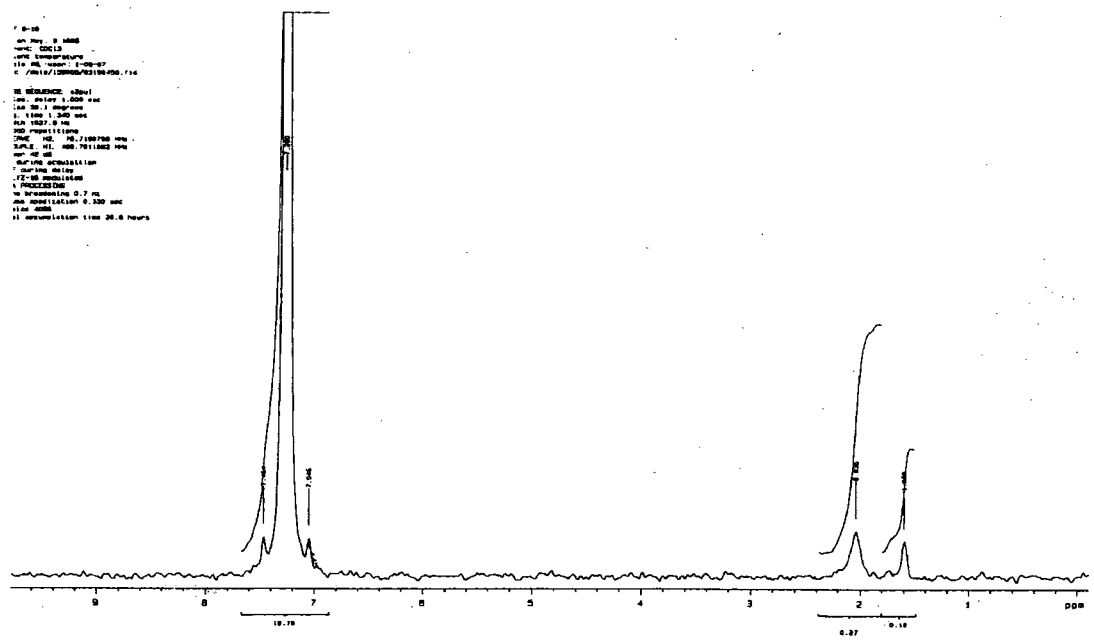

Figure 2-13 ^2H NMR Showing incorporation of deuterium from [6,6-$^2H_2$]-glucose into ubiquinone-8 by *E. coli*

These peaks represent incorporation of deuterium into the methyl and methylene protons of the prenyl chain after processing of glucose to [3,3-$^2H_2$]-GAP (**98**) and [3,3-$^2H_2$]-pyruvate (**99**) *via* the mevalonate independent pathway.

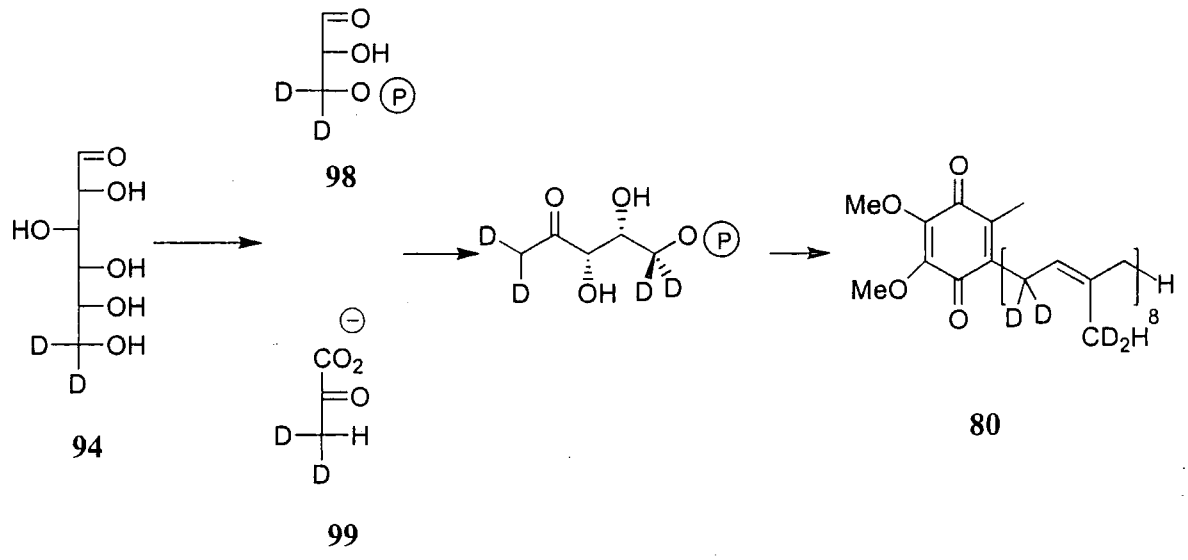

Scheme 2-13 Incorporation of [6,6-$^2H_2$]-glucose (**94**) into ubiquinone (**80**) by *E. coli*

2.3.9 *Incorporation of [*methyl-$^2H_3$*]-methionine into ubiquinone by* E. coli

S-Adenosyl methionine (SAM) is the source of the methoxy methyl groups of the quinone nucleus in ubiquinone. The feeding of methionine was a valid experiment as it was anticipated that it would provide a another sample of ubiquinone for ^{2}H-NMR analysis. Accordingly, [*methyl*-$^2H_3$]-methionine was fed to eight cultures (500ml) of *E. coli* and the ubiquinone extracted according to the standard procedure. ^{2}H-NMR showed two peaks in an approximate ratio of 2:1 (Figure 2-14). This represents incorporation into the methoxy groups and quinone methyl groups. Although the two methoxy groups are resolvable by ^{1}H NMR, quadrapolar line broadening causes coalescence into a broad peak at 3.97 ppm. No incorporation of deuterium into the prenyl chain was observed.

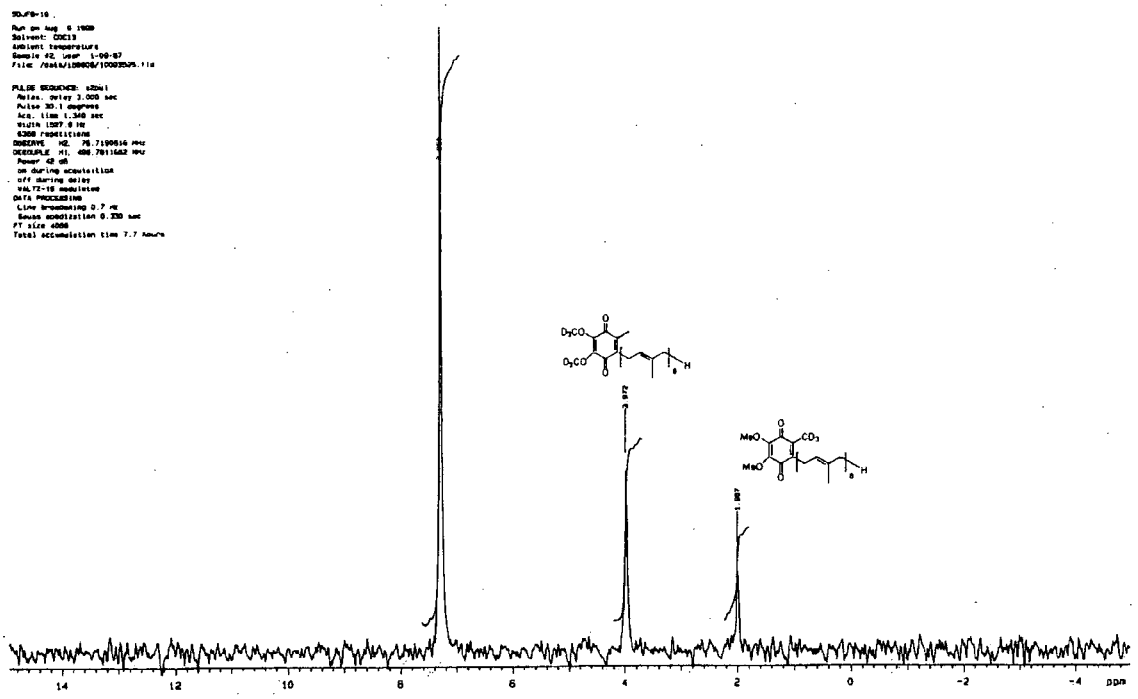

Figure 2-14 ^{2}H NMR of ubiquinone after feeding of [*methyl*-$^{2}H_3$]-methionine to *E. coli*

This confirmed that the methoxy methyl groups are derived from methionine and, in turn from SAM. The experiment was encouraging as it reaffirmed that deuterium incorporation into ubiquinone could be readily observed by ^{2}H-NMR.

2.3.10 The fate of H-3 of DXP – feeding of labelled glycerols

Glycerol (**100**) has long been established as good surrogate for GAP (**3**). The conversion of glycerol (**100**) to GAP (**3**) *via* dihydroxyacetone phosphate (**70**) is mediated by triose phosphate isomerase.

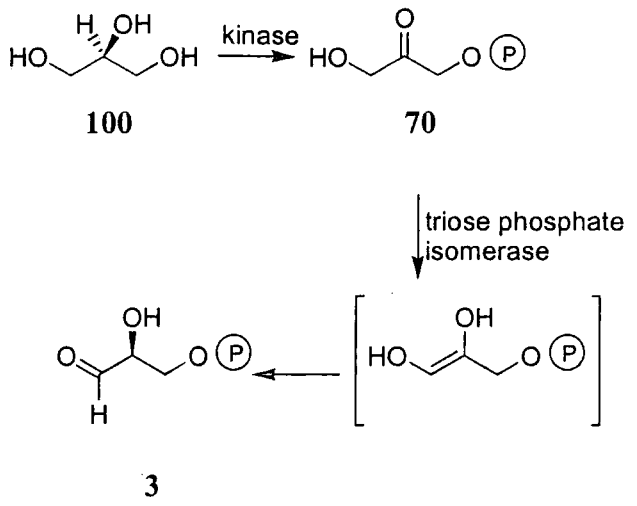

100 70 3

Scheme 2-14 Conversion of glycerol (**100**) to GAP (**3**)

As the conversion proceeds through oxidation of C-2, the deuterium atom at C-2 is lost which limits the use of [$^2H_5$]-glycerol as a probe to explore the fate of the C-4 hydrogen of DXP. As glycerol is prochiral, substitution of a proton by a deuterium at C-1 or C-3 renders the molecule chiral. This allows either the C-1 or C-3 protons to be mapped in pairs, in the case of chiral glycerols, or simultaneously, in the case of [$^2H_5$]-glycerol[87].

2.3.10.1 Feeding of glycerol to M. citrata

An initial experiment was performed to test the toxicity of glycerol to cultures of *M. citrata*. Pulse feeding on days 4,11 and 21 to a final concentration of 5mM was found to encourage growth with a concomitant 50% increase in the wet tissue mass.

A repeat experiment was performed using [$^2H_8$]-glycerol (**101**) (Sigma Aldrich chemicals, UK) which was fed as described above. The cultures were grown under standard conditions and harvested using procedure 2. GC-CIMS Analysis of the resulting linalyl acetate was performed ten times and the mean enrichment values are shown in Figure 2-15.

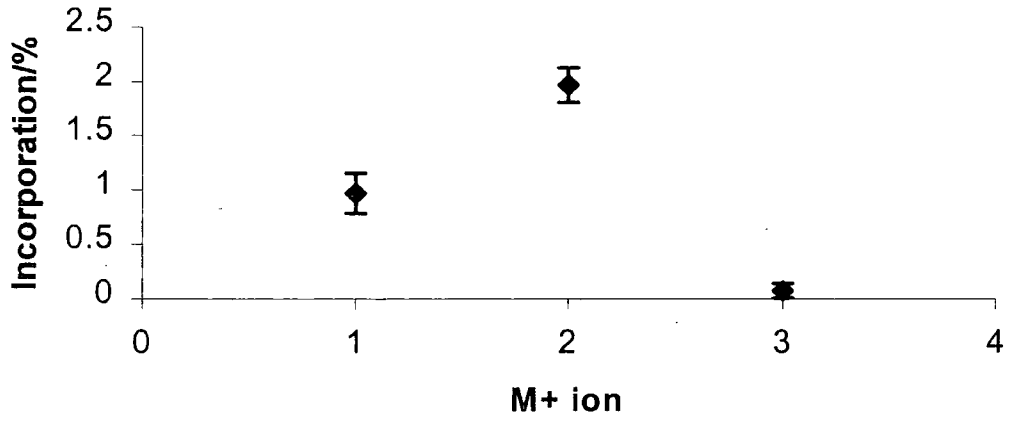

Figure 2-15 Incorporation of deuterium from [$^2H_5$]-glycerol

Both the M+1 and M+2 ions show significant enrichment and correspond to incorporation of one and two deuterium atoms respectively. The M+2 ion shows incorporation of only two deuterium atoms into linalyl acetate and, in the absence of an M+3 enrichment, revealed that only two deuterium atoms from [$^2H_5$]-glycerol (**101**) were incorporated into linalyl acetate.

When [$^2H_8$]-glycerol was fed at 3mM, the level of incorporation was much lower but mirrored the 5mM incorporations. The presence of an M+2 ion (0.45 ± 0.07%) was accompanied by a small M+1 (0.15 ± 0.11%) with no observable M+3 ion (0.04 ± 0.02%). This confirmed that two deuterium atoms were carried through from [$^2H_5$]-glycerol.

*2.3.10.2 Feeding of (2R)-[1,1-$^2H_2$]-glycerol (**102**) and (2S)-[1,1-$^2H_2$]-glycerol (**103**) to* **M. citrata**

There are two possible isotopomers of GAP that would lead to incorporation of two deuterium atoms into linalyl acetate. The incorporation of two deuterium atoms could be the result of glycerol delivering either [1,3-$^2H_2$]-GAP (**104**) or [3,3-$^2H_2$]-GAP (**98**) which could then be incorporated into linalyl acetate *via* the mevalonate independent pathway.

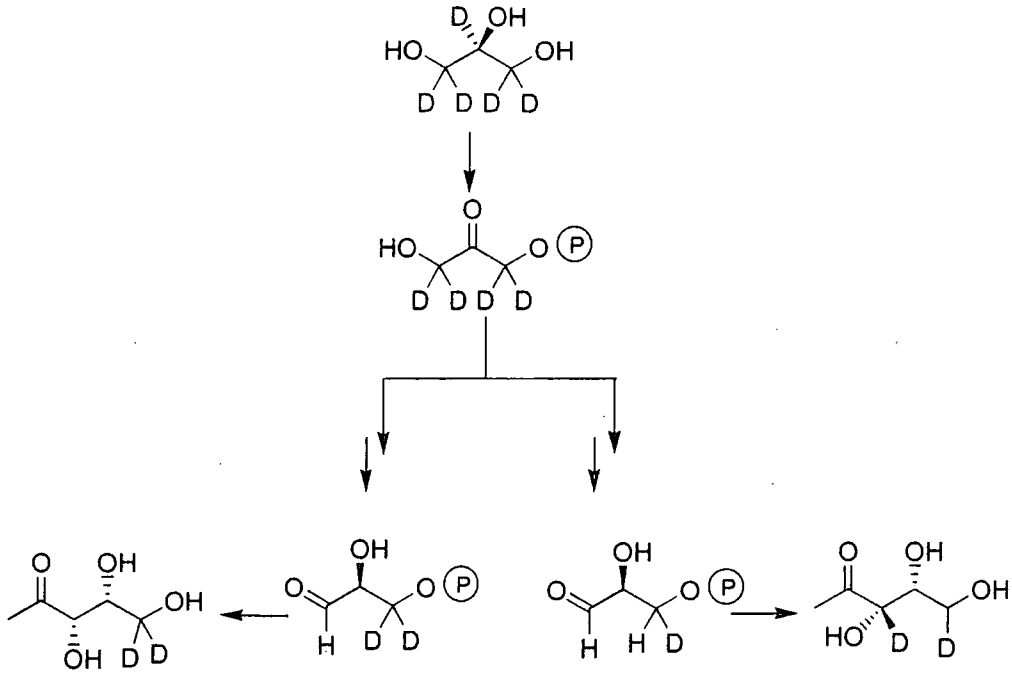

98 **104**

Scheme 2-15 Possible explanations for incorporation of two deuterium atoms

The difference in the two proposed isotopomers shown in Scheme 2-15 is the position of the deuterium atoms. Isotopomer **104** has one deuterium derived from the each of the *pro*-S and *pro*-R arms whereas **98** has both deuterium atoms from the *pro*-R arm of glycerol. Chiral glycerols bearing deuterium provide a convenient method of independently labelling each arm of glycerol and hence were identified as suitable substrates to determine which of the deuterium atoms had become incorporated.

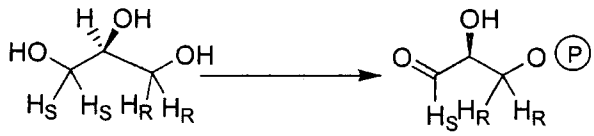

Scheme 2-16 The fate of the *pro* R and *pro* S protons of glycerol

Accordingly, both (2R)-[1,1-$^2H_2$]-glycerol (**102**) and (2S)-[1,1-$^2H_2$]-glycerol (**103**) (prepared by Dr Jens Nieschalk in Durham) were fed to cultures of *M. citrata*. (2R)-[1,1-$^2H_2$]-Glycerol (**102**) was fed to two cultures of *M. citrata* to a final concentration of 5mM and the linalyl acetate was extracted using procedure 2 and analysed *via* GC-CIMS. The sample was analysed ten times and the mean values are shown in Figure 2-16.

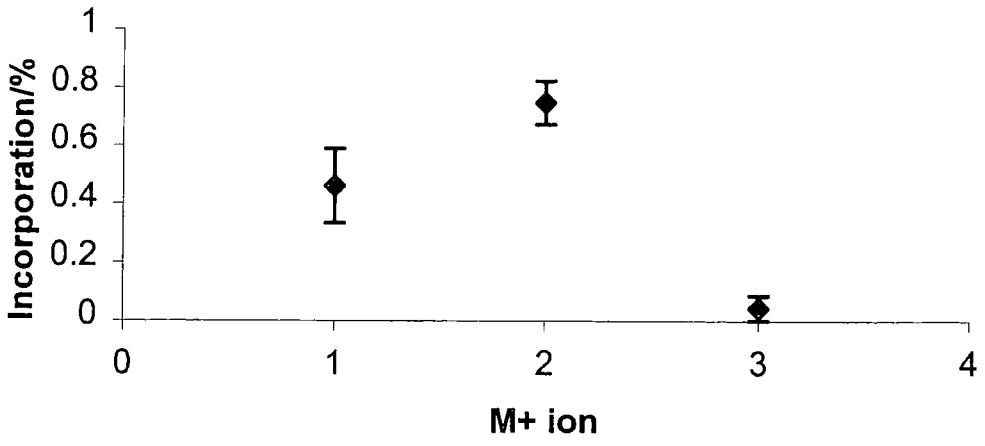

Figure 2-16 Incorporation of deuterium from (2*R*)-[1,1-$^2H_2$]-glycerol (**102**) into linalyl acetate

Both M+1 and M+2 ions showed enrichment, which corresponds to the incorporation of one and two deuterium atoms respectively. Significantly, the M+2 ion shows that both deuterium atoms were incorporated from the *pro*-R arm of glycerol.

In the complimentary experiment, (2S)-[1,1-$^2H_2$]-glycerol (**103**) to a final concentration of 5mM. The linalyl acetate was extracted by procedure 2 and was analysed *via* GC-CIMS. The mean values after ten runs showed that was no observable enrichment of either the M+1 or M+2 ion. This corresponds to the loss of both deuterium atoms from the *pro*-S arm of glycerol.

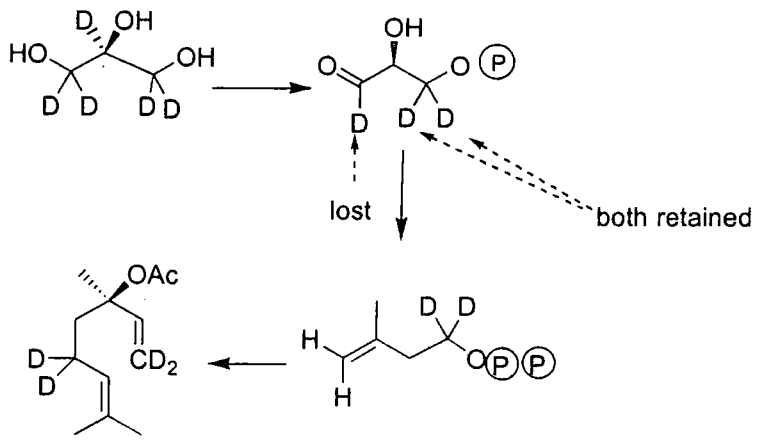

Scheme 2-17 Incorporation of deuterium from [$^2H_5$]-glycerol (**101**) into linalyl acetate (**78**) by *M. citrata*

This supported the result after feeding [6,6-$^2H_2$]-glucose (**94**) which had shown that both of the protons of C-3 of GAP are retained during the biosynthesis of linalyl acetate.

2.3.10.3 Feeding of [$^2H_8$]-glycerol (101) to E. coli

In the same experiment in bacteria, cultures of *E. coli* were supplemented with [$^2H_8$]-glycerol (1g) and the ubiquinone was harvested according to the standard procedure. ^2H NMR Analysis showed peaks at 1.59 and 2.04 ppm, which corresponded to incorporation of deuterium into the prenyl methyl and methylene groups as shown in Figure 2-17.

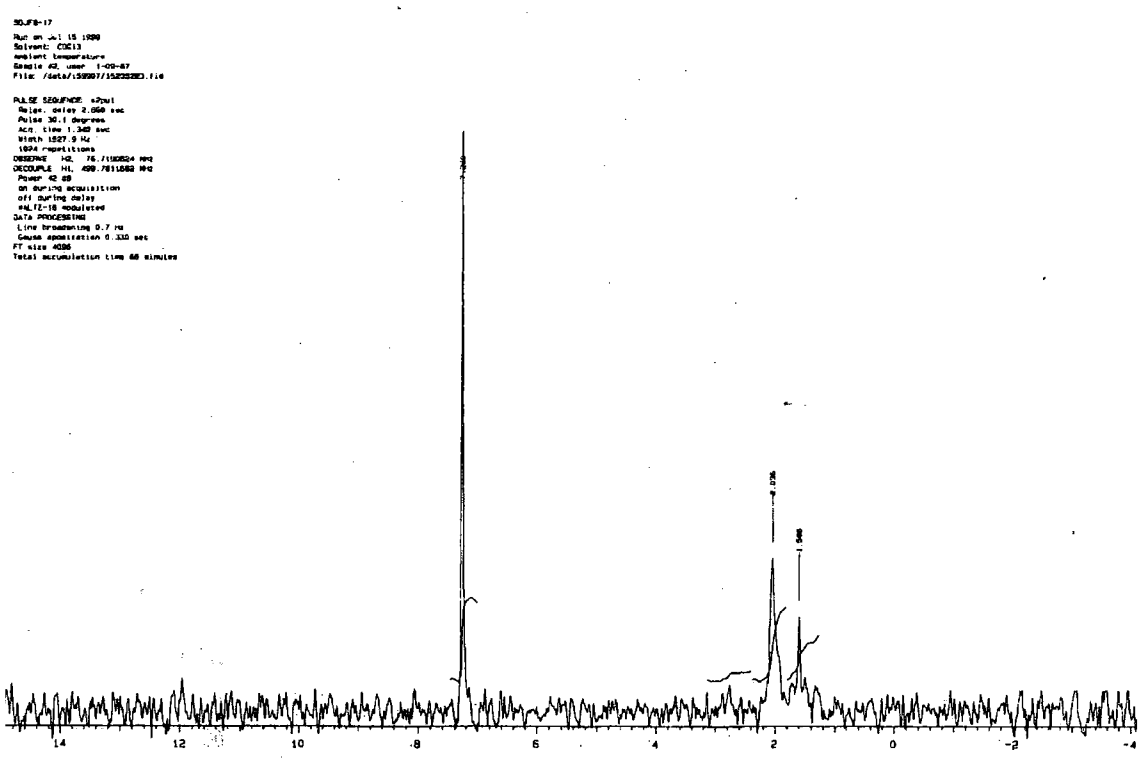

Figure 2-17 ^2H NMR Of ubiquinone after feeding [$^2H_8$]-glycerol (**101**) to *E. coli*

Two isotopomers of ubiquinone can reasonably be formed after feeding [$^2H_8$]-glycerol (**101**). These correspond to the loss or retention of the aldehydic deuterium of the subsequently formed GAP. Loss of the aldehydic hydrogen of GAP introduces deuterium into the methyl and terminal methylene groups of the prenyl chain (**105**) whereas retention of the aldehydic proton introduces an additional deuterium atom (**106**) into the prenyl chain as shown in Scheme 2-18.

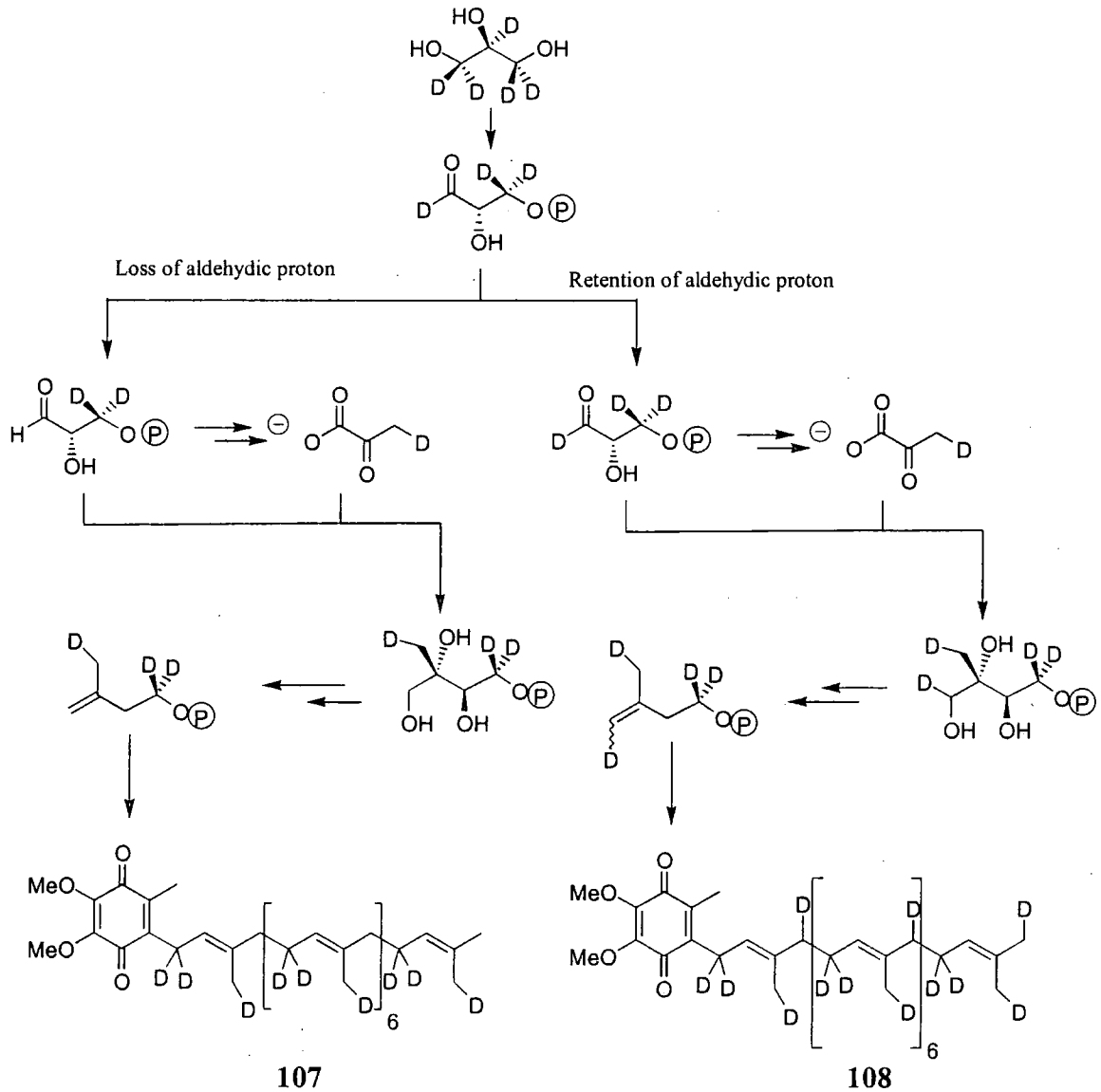

Scheme 2-18 Possible incorporation of deuterium from [$^2H_8$]-glycerol (**101**) showing the isotopomers of ubiquinone resulting from either loss or retention of the aldehydic hydrogen of GAP

The abundant isotopomer can be estimated by the integral ratios of the methylene protons to the methyl protons. The relative ratios of the methylene and methyl peak areas after feeding [6,6-$^2H_2$]-glucose was 2.25:1. The deviation from 2:1 represents higher incorporation from GAP than pyruvate.

Retention of the aldehydic proton would cause incorporation into the methylene groups and increase the ratio to approximately 3:1. However, loss of the aldehydic deuterium would cause labelling that is identical to that observed for [6,6-$^2H_2$]-glucose (2.25:1). Integration of the peaks of ubiquinone after feeding [$^2H_8$]-glycerol (**101**) showed that the ratio of methylene to methyl peak areas after feeding [$^2H_8$]-glycerol (**101**) was 1.62:1. As the ratio is significantly lower than 3:1, the incorporation suggests loss of the

aldehydic proton of GAP, just as was observed in *M. citrata*. The discrepancy between the expected ratio (2.25:1) and that which was observed (1.65:1) is perhaps due to a poor signal to noise ratio.

2.3.10.4 Discussion of feeding labelled glycerol to M. citrata *and* E. coli

It was anticipated that two deuterium atoms would be lost from glycerol when it was metabolised to GAP (**3**). The deuterium at C-2 is removed upon oxidation of glycerol (**100**) to DHAP (**70**), and one of the C-1 protons is removed by the action of triose phosphate isomerase. Incorporation of the two deuterium atoms into linalyl acetate (**78**) by *M. citrata* from (2*R*)-[1,1-$^2H_2$]-glycerol (**102**) and the corresponding absence of deuterium enrichment after feeding (2*S*)-[1,1-$^2H_2$]-glycerol (**103**) indicated that the aldehydic proton of GAP was lost. The incorporation of deuterium into the ubiquinone of *E. coli* suggested an identical enrichment corresponding to the loss of the aldehydic proton of [1,3,3-$^2H_3$]-GAP (**109**)

One of the more obvious mechanisms where the deuterium atom could be lost is through a reversible oxidation. GAP Is known to be converted to 1,3-biphosphoglycerate (BPG, **110**) by the action of glyceraldehyde-3-phosphate dehydrogenase in the presence of NAD^+. BPG Is biologically important as it is used in the manufacture of ATP.

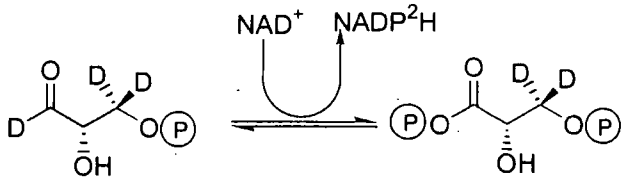

109 **111**

Scheme 2-19 Conversion of [1,3,3-$^2H_3$]-GAP (**109**) to [3,3-$^2H_2$]-BPG (**112**) with loss of the aldehydic deuterium atom of GAP

As GAP and BPG are in rapid equilibrium the action of glyceraldehyde-3-phosphate dehydrogenase would result in the complete loss of deuterium from C-1.

Deuterium could also be removed by DXP synthase. DXP synthase catalyses the formation of DXP from GAP (**3**) and pyruvate (**7**) and utilises TPP (**113**) as a co-factor. The mechanism of TPP mediated aldol type condensations is well established and the

formation of DXP (**6**) is shown in Scheme 2-20. Initially the thiazoline ring reacts with an electrophile to a form a Schiff's base. In the case of DXP synthase, the electrophile is pyruvate. The complex then undergoes decarboxylation to generate an "activated aldehyde" species. This negative charge is readily localised into the aromatic ring which confers stability on the acyl anion equivalent. Nucleophilic attack of GAP produces TPP bound DXP (**114**) and classically the reaction would be expected to proceed *via* the route marked A. Removal of a hydroxy proton by a base produces DXP and releases TPP.

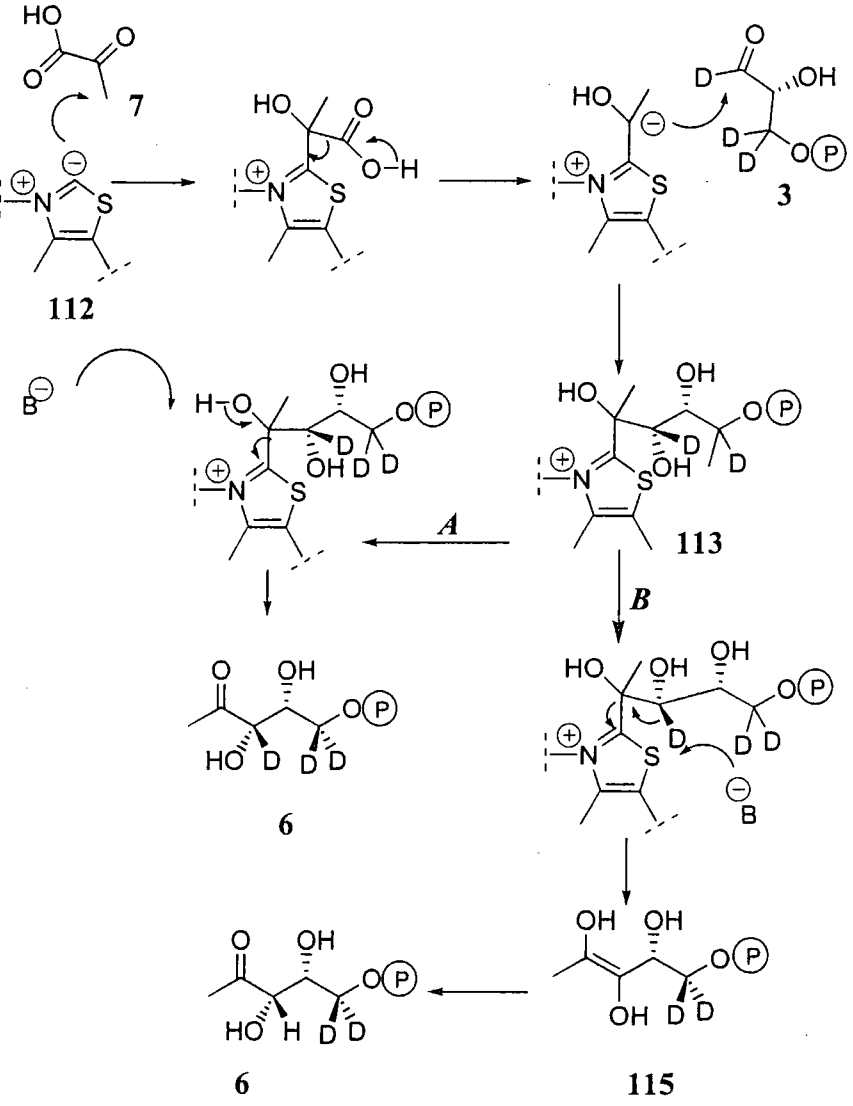

Scheme 2-20 Proposed mechanism of TPP mediated synthesis of DXP (**6**)

However, once the final Schiff's base complex has been formed, there is another site in addition to the hydroxy proton that can be attacked by the base. Rather than abstracting the hydroxy proton, the base could remove the deuterium atom at C-3 to generate a ene-diol (**115**) which could collapse to deliver DXP (**6**). This differs from the classical mechanism in that the proton (in this case a deuterium) that is removed is not the most

acidic proton. Given that this is a deviation from the classical mechanism, it seems more plausible that the deuterium is removed by reversible oxidation to DBG.

2.4 Tracing the fate of H-4 of DXP

The final proton that was amenable to biosynthetic investigation was H-4 of DXP which is derived from H-2 of GAP. Before describing experiments that were performed, it is pertinent to describe how the fate of H-4 differs in plants and bacteria. H-4 is implicated in the isomerisation and prenyl transferase reactions. Studies on the isomerase and prenyl transferase for mevalonate independent pathway are ongoing.

One of the first studies on the fate of H-4 of DX was performed using [4-^{2}H]-1-D-deoxyxylulose (**116**)[88]. When *E. coli* was fed labelled [4-^{2}H]-DX, deuterium incorporation into ubiquinone (**80**) was observed only into the terminal olefinic bond that corresponds to the DMAPP unit. No incorporation into the IPP derived chain was found by either MS or ^{2}H NMR.

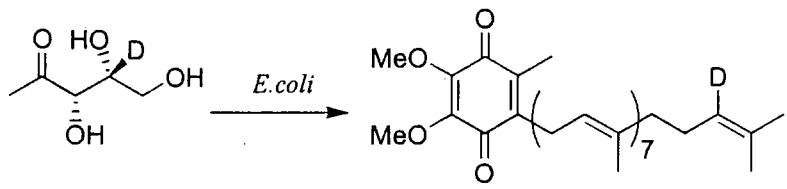

Scheme 2-21 Incorporation of deuterium into the DMAPP unit of ubiquinone (**80**)[88]

The authors argued that this demonstrated that if both a prenyl transferase and IPP isomerase operated on IPP derived from the mevalonate independent pathway in bacteria, then their relative stereochemistries must be opposite. This contrasts with the MVA pathway the same proton (*pro*-R) is abstracted by both the isomerase and prenyl transferase.

Poulter and co-workers[89] demonstrated that the interconversion of IPP (34) and DMAPP (35) results in the loss of the *pro*-R proton from C-2 of IPP (34), which is derived from H-4 of DXP. Whether the proton was retained during the course of the biosynthesis from DXP was not investigated as the work focused on the incubation of IPP with IPP isomerase from *E. coli*. Poulter argued that these experiments show that the *E. coli*

isomerase removes the *pro*-R proton and the *E. coli* prenyl transferase abstracts the *pro*-S proton.

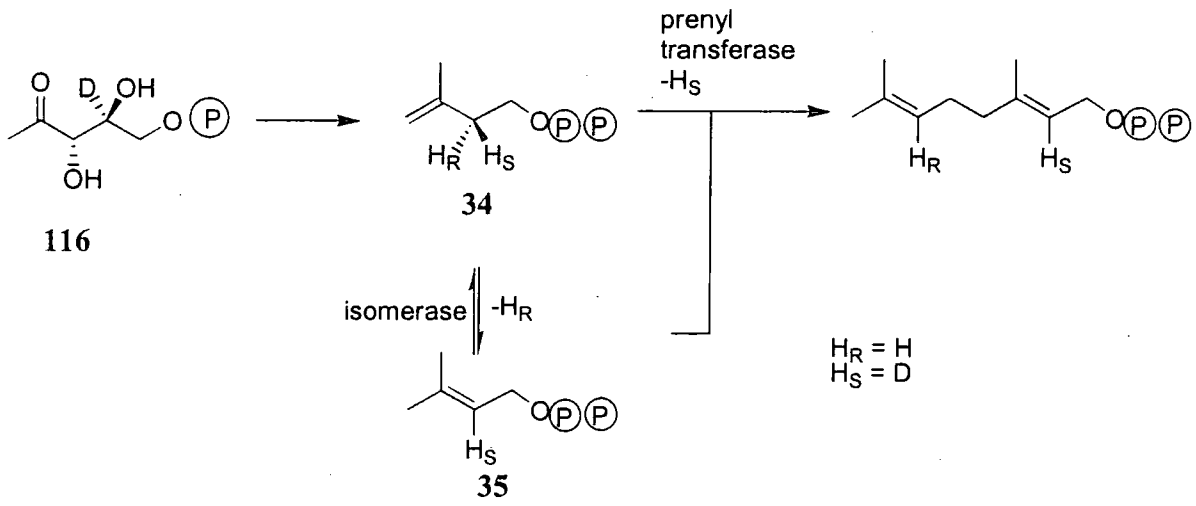

Scheme 2- 22 Incorporation of one deuterium (H_S) from [4-^{2}H]-DX (**116**) as a result of a prenyl transferase and isomerase which abstract different protons of IPP (*E. coli*)

Analogous studies have been performed in plant systems. The work of Arigoni[90] demonstrated that the relative stereochemistries of the prenyl transferase and isomerase of *Catharanthus roseus* are the same, just as in the MVA pathway. When [2-^{13}C,4-^{2}H]-deoxyxylulose (**117**) was fed to *Catharanthus roseus,* incorporation of ^{13}C but not ^{2}H was observed. This inferred that either the deuterium atom was lost as a result of unknown steps on the mevalonate independent pathway or was removed by both the prenyl transferase and the isomerase (Scheme 2-23).

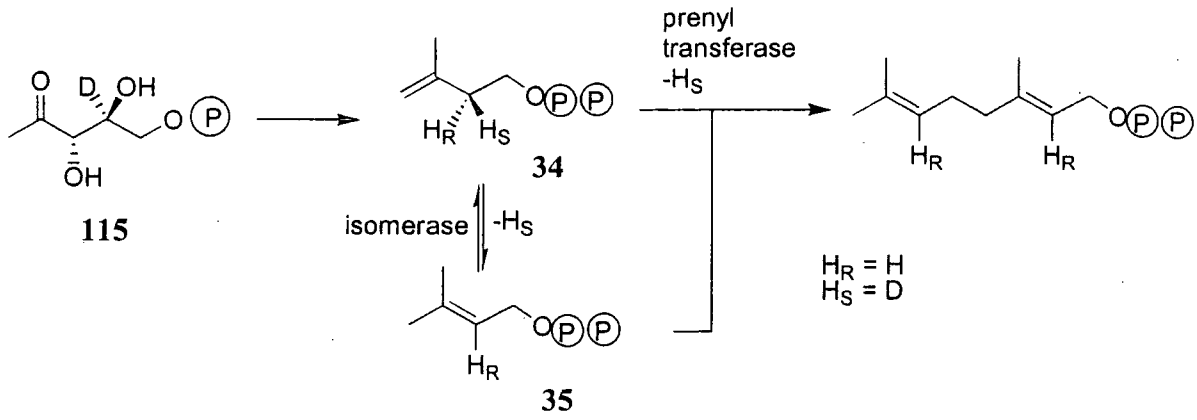

Scheme 2-23 Absence of deuterium incorporation (H_S) from [4-^{2}H]-DX (**116**) as a result of a prenyl transferase and isomerase which abstract the same protons of IPP (**34**) in *Catharanthus roseus*

Clearly, this contrasts with the case of incorporation of deuterium from [4-^{2}H] deoxyxylulose into *E. coli*. This could be rationalised by one of two hypotheses. The *E. coli* prenyl transferase and isomerase could stereoselectively abstract different protons of C-2 of IPP whereas in *Catharanthus roseus* the same proton is removed by both the prenyl transferase and isomerase. Alternatively, the incorporations could also be interpreted as being the result of a difference in the mevalonate independent pathways in bacteria and plants which have prenyl transferases and isomerases with identical stereochemistry. More work needs to be performed before a fuller understanding is gained.

2.4.1 The role of IPP isomerase in the mevalonate independent pathway

There is a growing opinion that the results of incorporation into *E. coli* represent the divergence of the mevalonate independent pathway into routes that deliver IPP and DMAPP separately.

Poulter and co-workers have identified the prenyl transferase of *E. coli* as having the same relative stereochemistry as the isomerase[91]. This is incompatible with the interconversion of IPP (**34**) and DMAPP (**35**) to introduce deuterium from [4-^{2}H]-DX (**116**) into the DMAPP derived chain of ubiquinone (**80**) and is represented in Scheme 2-24.

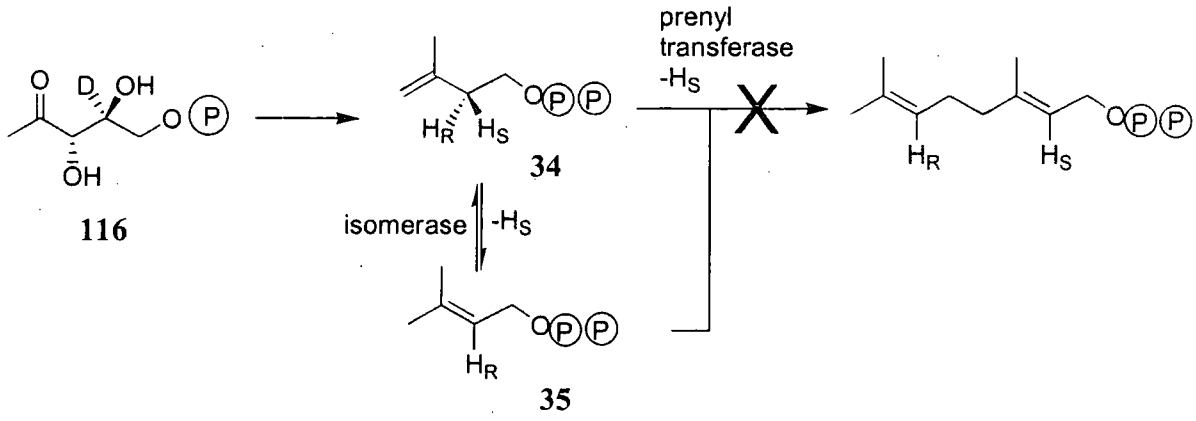

Scheme 2-24 Illustration that IPP isomerase is not significant in the mevalonate independent pathway in *E. coli*. H_S (deuterium) is found to be incorporated but would be removed in the isomerisation reaction

This is a clear demonstration that DMAPP (**35**) is not formed as the result of IPP isomerase in *E. coli*. Furthermore, studies by Rohmer[92] have indicated that only one IPP isomerase is present in *E. coli* and that no other enzyme caters for the interconversion of IPP (**34**) and DMAPP (**35**). This eliminates the possibility that numerous isomerases exist with alternative stereochemistry which would allow the incorporation of deuterium from [4-^{2}H]-DX (**116**) by Scheme 2-24. Conclusive proof that IPP isomerase is not essential for terpenoid formation in *E. coli* was provided when the *ipi* gene encoding for IPP isomerase was deleted[93]. Growth of the organism demonstrated that terpene production was occurring, as terpenoids such as ubiquinone are essential for growth. Furthermore, species such as *Synechocytis sp.*, a cyanobacterium which produces terpenes *via* the mevalonate independent pathway, are known to be deficient in IPP isomerase[94] and genome analysis shows no homologue for the enzyme. When an *ipi* gene from yeast was inserted into *Synechocytis* sp. carotenoid production was not found to be enhanced which suggests that *Synechocytis* has developed a method to produce terpenoids *via* the mevalonate independent pathway without the use of IPP isomerase. This contrasts with the pathway in plants and the bacterium *Zymomonas mobilis*[95] in which it has been demonstrated that IPP isomerase is essential to terpenoid formation.

2.4.2 Synthesis of DX

In order to investigate the fate of H-4 of DXP in *M. citrata*, a synthetic sample of [4-^{2}H]-DX was prepared..

Enzymatic methods had been used in the literature to prepare samples of DXP. The isolation of DXP synthase allowed preparation of samples of DXP carrying ^{13}C or ^{14}C from the appropriately labelled pyruvate or GAP. The methodogy has been used to prepare samples of [1-^{13}C] & [2,3,4,4-$^{13}C_4$][96], [1,2-$^{14}C_2$] & [2,3-$^{13}C_2$][97] and [2,4-$^{13}C_2$]-DXP[98]. This method is unsuitable for the preparation of [4-^{2}H]-DX as it would require [1-^{2}H]-GAP which is not commercially available. Furthermore, the product of the reaction, DXP, is not a suitable substrate for whole cell systems as cell walls are impermeable to phosphate esters.

Spenser and co-workers[99] prepared [2,3-$^{13}C_2$]-DX for use in studies on the biosynthesis of vitamins B_1 (**71**) and B_6 (**72**). The synthesis was completed in twelve steps with a net yield of 16%. The C-5 framework was built using a HWE coupling using *O*-benzylacetaldehyde (**118**) and triethyl-[1,2-$^{13}C_2$]-phosphonacetate (**119**). The stereogenic centres were established by the use of a Sharpless epoxidation which was followed by a Payne rearrangement. Functional group interconversions produced the acetonide protected tetrose (**120**) which was converted to a pentose by a Grignard reaction. Deprotection yielded [2,3-$^{13}C_2$]-DX (**121**). Whilst the stereochemical configuration of C-4 remained unchanged, C-3 was originally set up as an *R* centre. Hydrolysis of the *gem*-acetoxy sulphide results in inversion of configuration of C-3 which then retains its stereochemical integrity through the remaining steps (Scheme 2-25).

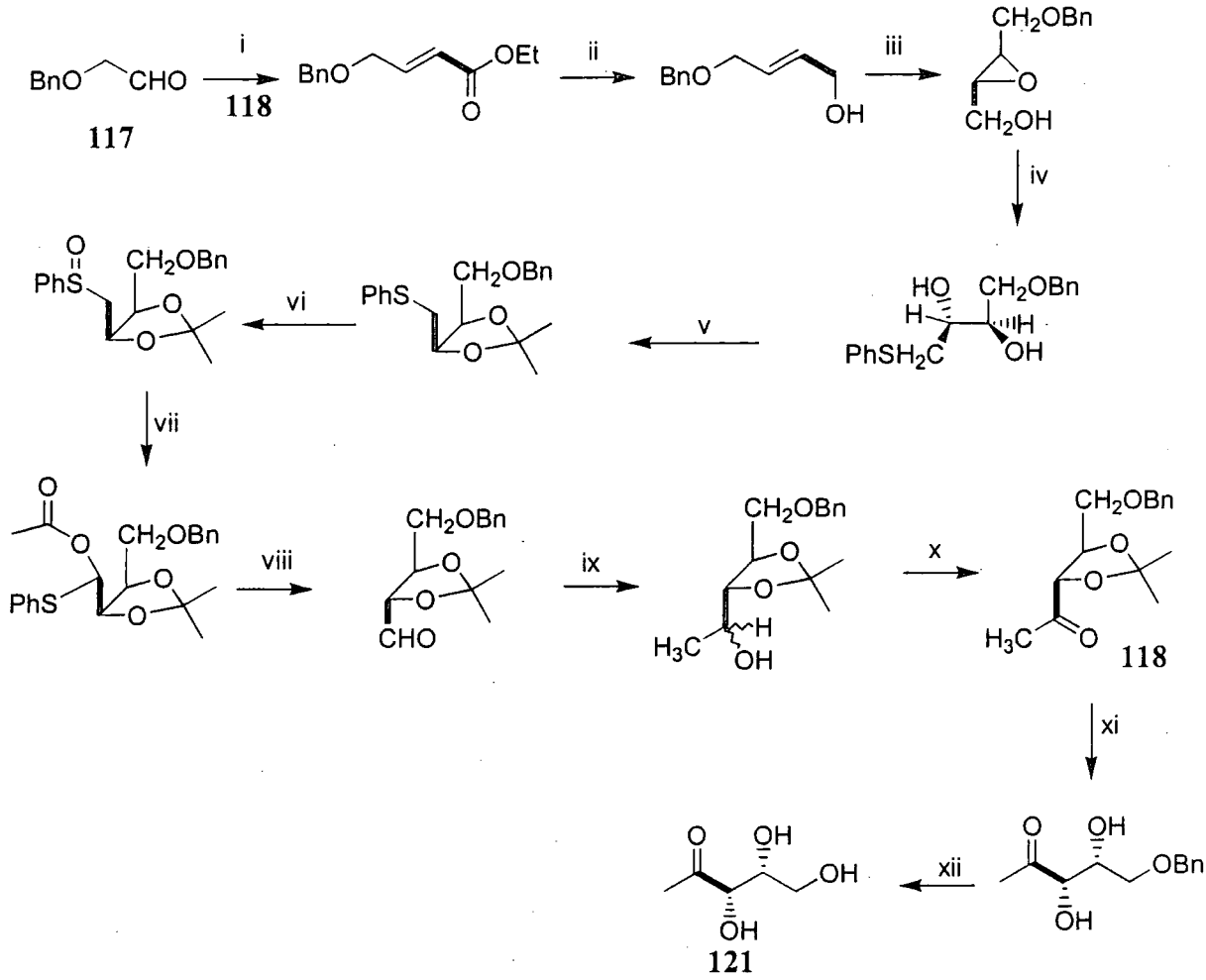

Scheme 2-25 Synthesis of [2,3-$^{13}C_2$]-DX **121**[99]

Reagents and conditions; i) $(EtO)_2PO^{13}CH_2{}^{13}CO_2C_2H_5$, ii) $LiAlH_4$, DCM iii) Sharpless oxidation iv) NaOH then PhSH v) $(CH_3)_2C(OCH_3)_2$, $POCl_3$ vi) MCPBA vii) NaOAc, Ac_2O viii) K_2CO_3 ix) MeMgBr x) Swern oxidation xi) 2M HCl, MeCN xii) H_2, Pd/C

However, this route was unsuitable for the synthesis of [4-^{2}H]-DX (**116**) as the label would need to be introduced from the first step.

A different approach was taken by Poulter and Blagg[100] to produce both DX (**122**) and DXP (**6**). Rather than using synthetic protocols to build in the required stereochemistry, a chiral starting material was used. Using (-)-2,3-*O*-isopropylidene-D-threitol (**123**), DX (**122**) and DXP (**6**) were synthesised in five and eight steps respectively in overall yields of 69% and 58%. The synthesis initially employed protection of the primary alcohol as TIPS followed by oxidation and Grignard addition to yield the C-5 alcohol. Oxidation by TPAP and subsequent deprotections gave DX. DXP was produced using a similar

strategy except that the aldehyde was masked as a 1,2 dioxolane to enable phosphate ester formation with trimethyl phosphite (Scheme 2-26).

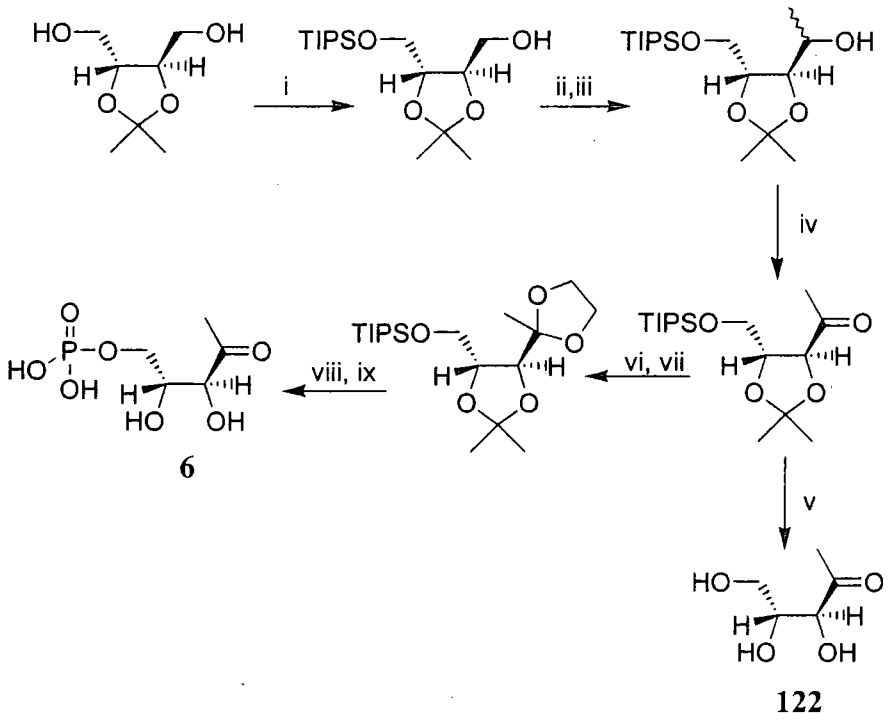

Scheme 2-26 Synthesis of DX (**122**) and DXP (**6**) (Poulter and Blagg)

Reagents; i) NaH, TIPS-Cl, 96% ii) Swern oxidation iii) MeMgBr, 88% iv) TPAP, NMO, 97% v) AcOH, THF, H_2O, 84% vi) $HO(CH_2)_2OH$, TsOH, 88% vii) TBAF, THF, 99% viii) $P(OMe)_3$, $TeCl_4$ ix) TMSBr, H_2O, HCl, 90%

Again, this method did not allow for a facile introduction of deuterium into C-4 although it did provide an efficient route to [1-$^2H_3$]-DX and DXP.

A similar methodolgy was employed by Boland and Piel[101] whereby the stereochemistry was set from the outset using diastereomerically pure 2,3-*O*-isopropylidene-D-tartrate (**124**).

In order to differentiate between the two ester groups whilst maintaining stereochemical integrity, the dimethyl ester of 2,3-*O*-isopropylidene-D-tartrate (124) was treated with pig liver esterase (PLE). Reduction of the remaining ester group using "superhydride" allowed facile introduction of deuterium and left the acid functionality unchanged. After treatment with methyl lithium to afford the methyl ketone the isopropylidene group was hydrolysed under standard conditions.

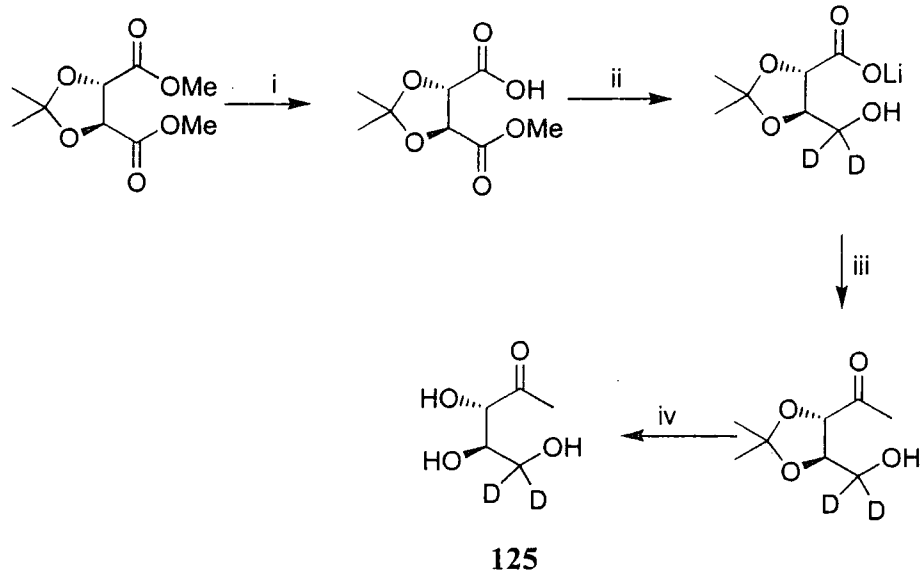

125

Scheme 2-27 Synthesis of [5,5-$^2H_2$]-DX **125** (Boland)

Reagents i) PLE, 25°C ii) $LiBEt_3D$/THF, 1h iii) MeLi iv) 2M $HCl/H_2O/CH_3CN$

Later work[102] revised the procedure to combine the reduction and alkylation into a one pot procedure which reduced the number of equivalents of methyl lithium that were required. Again, the introduction of deuterium onto the C-4 position by this route was impractical.

The most versatile syntheses of DX were outlined by Giner[103] who described three routes to DX bearing deuterium and ^{13}C in a variety of positions. These syntheses differ from the syntheses using tartrate as in the preparations described by Giner, the stereochemistry is built in using a diastereoselective reaction and an achiral substrate.

The syntheses use (E)-5-benzyloxy-3-pentanone (**126**) as an intermediate that can be converted to DX (**122**) in two steps. Stereoselective formation of 5-benzyl-1-deoxy-D-xylulose (**127**) is achieved by the use of an asymmetric Sharpless dihydroxylation.

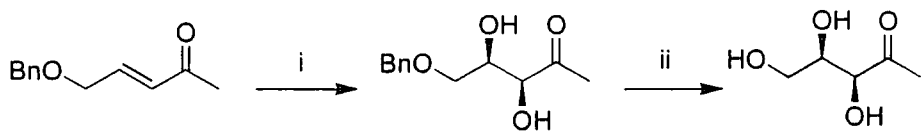

128 **129** **122**

Scheme 2-28 Synthesis of DX (**122**) from (E)-5-benzyloxy-3-pentanone (**126**)

Reagents i) AD-Mix β ii) H_2, Pd/C

Three different routes to (E)-5-benzyloxy-3-pentanone (**126**) have been described which allow great synthetic flexibility. By the first route, the C-5 skeleton was built by the addition of methylmagnesium bromide with (E)-4-benzyloxy-2-butenal (**130**). Subsequent oxidation of the resulting primary alcohol (**131**) gave the required pentanone.

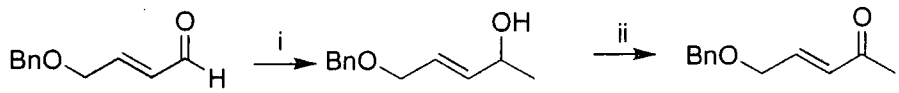

130 **131** **126**

Scheme 2-29 Synthesis of (E)-5-benzyloxy-2-pentanone (**126**) from (E)-4-benzyloxy-2-butenal (**130**)

Reagents i) MeMgBr ii) Swern oxidation

This route enabled labelling of C-1 with either ^{13}C, ^{2}H or a combination of ^{13}C and ^{2}H if a labelled Grignard reagent was used.

The routes that were most convenient were the use of a Wittig coupling or functionalisation of *O*-benzylacetylene (**132**) to produce (E)-5-benzyloxy-2-pentanone (**126**). The latter route enabled introduction of deuterium at either the 3 or 4 position by the use of either $LiAlH_4$ or D_2O. Reduction of propagyl alcohol (**133**) with $LiAl^2H_4$ introduces deuterium into the 3 position whilst the 4 position is deuterated upon the use of $LiAlH_4$ and quenching the reaction with D_2O.

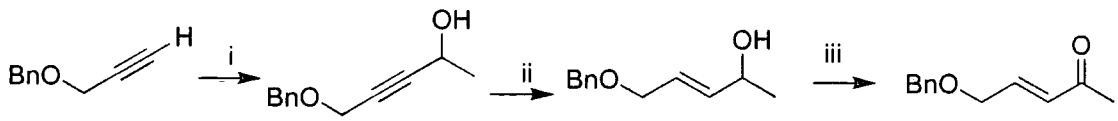

(132 **(133** **131** **126**

Scheme 2-30 Synthesis of (E)-5-benzyloxy-2-pentanone (**126**) from benzylacetylene (**133**)

Reagents i) Acetaldehyde ii) $LiAlH_4$ iii) Swern oxidation

The third route started with benzyloxyacetaldehyde (**118**) and delivered (E)-5-benzyloxy-2-pentanone in one step (**126**).

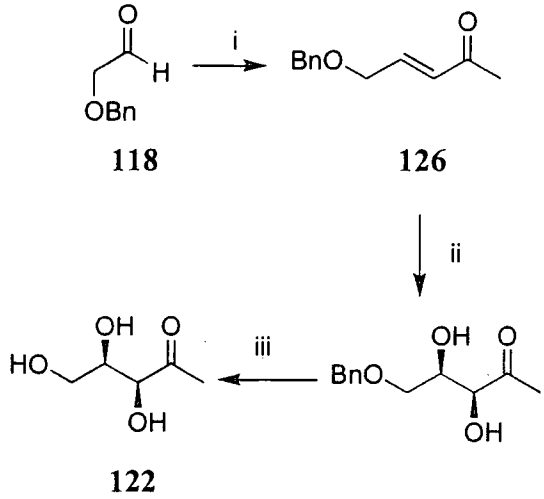

Scheme 2-31 Synthesis of DX (**122**) from benzyloxyacetaldehyde (**118**)[103]

Reagents i) $Ph_3P{=}CHCOCH_3$ ii) Ad-Mix β iii) H_2, Pd/C

This latter route appeared the most amenable to the introduction of deuterium at C-4 as the use of [1-^{2}H]-*O*-benzylacetaldehyde (**134**) would enable straightforward access to [4-^{2}H]-(E)-5-benzyloxy-2-pentanone (**135**) and thus [4-^{2}H]-DX (**116**).
Benzyloxyacetaldehyde (**118**) is unstable to decomposition and thus must be prepared as required. There are several reports that describe the preparation of benzyloxyacetaldehyde (**118**) of which the most attractive appeared the deprotection of benzyloxyacetaldehyde diethyl acetal (**136**)[104] (Scheme 2-32)

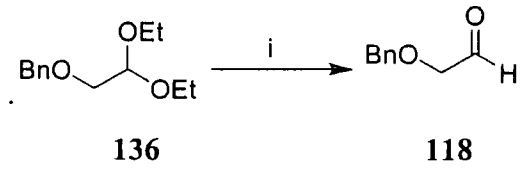

Scheme 2-32 Synthesis of benzyloxyacetaldehyde (**118**) from benzyloxyacetaldehyde diethyl acetal (**136**)

Reagents i) TFA, H_2O, $CHCl_3$

Accordingly, benzyloxyacetaldehyde diethyl acetal (**136**) was treated with TFA, water and chloroform for 90 minutes. Work-up of the reaction after this time gave a 48% yield of benzyloxyacetaldehyde (**118**), which was purified by column chromotography.

Longer reaction times resulted in a lower yield corresponding to the formation of by-products due to decomposition.

The aldehyde was then promptly reacted with 1-triphenylphosporanylidene-2-propanone in THF to yield (E)-5-benzyloxy-2-pentanone (**126**) as outlined in Scheme 2-31[105]. None of the (Z) isomer was observed by ^{1}H-NMR analysis.

Incubation of the olefin with AD-Mix β overnight at 0°C cleanly produced a product with a lower R_f than that of (E)-5-benzyloxy-2-pentanone (**126**) which, after workup, gave 5-benzyl-1-deoxy-D-xylulose (**127**) as a white semisolid[106]. In order to establish the stereochemical purity of **127** a chiral shift reagent was employed. Titration of the diol against $Eu(hfc)_3$ showed increased line broadening and shifting of the methyl resonance as the concentration of $Eu(hfc)_3$ increased. However, even at a concentration of 20mg ml^{-1} of $Eu(hfc)_3$ only one methyl resonance was observed which suggested that the product was enantiomerically pure. This was supported by optical rotation measurements. The optical rotation ($[\alpha]_D$=53.4, c 0.1, $CDCl_3$) of the (E)-5-benzyloxy-2-pentanone (**126**) was found to be almost identical to the material reported by Giner[103] ($[\alpha]_D$=52.9, c 0.1, $CHCl_3$) which was in turn identical to the optical rotation from the same material derived from D-tartaric acid[99].

Removal of the benzyl protecting group *via* hydrogenolysis in the presence of catalytic Pd/C afforded DX (**122**) as a colourless oil[107]. In spite of a seemingly clean reaction for the AD-mix reaction it was essential to purify the diol *via* column chromatography as a constituent of the crude diol mixture prevented benzyl removal.

DX (**122**) was found to decompose on standing to a complex mixture of products. DX (**122**) Is known to readily cyclise to give β-1-deoxy-D-xylulofuranose (**137**) which can then eject a hydroxyl group and dimerise to from di-β-1-deoxy-D-xylulofuranose-2,3':3,2'-dianhydride (**138**)[99].

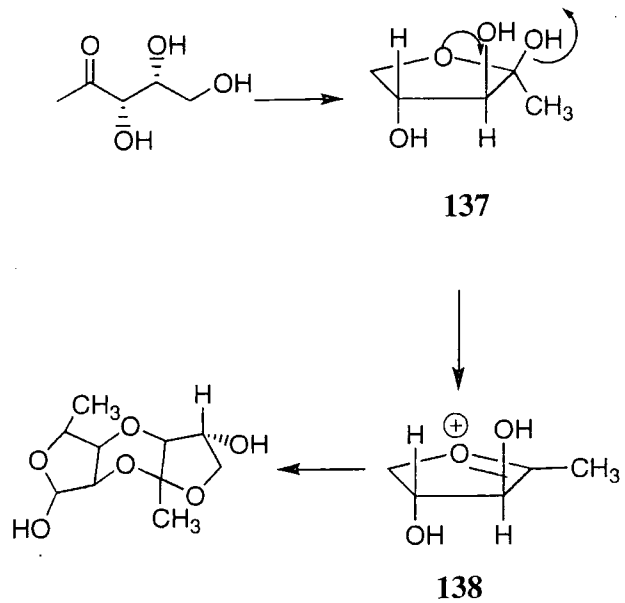

Scheme 2-33 Cyclisation of DX [99]

Free DX was not amenable to GC-MS analysis and in order to obtain a suitable mass spectrum, DX was per-acetylated. Treatment of DX with a 1:1 mix of acetic anhydride and pyridine produced the per-acetylated sugar with a corresponding molecular ion at 278. The reaction was halted by the removal of pyridine under high vacuum and the crude mixture was analysed by GC-MS. A GC-MS protocol was an essential prerequisite for this study it allowed which calculation of the level of deuterium enrichment for the labelled product.

One of the easiest methods to introduce deuterium is *via* reduction of a carbonyl group with a deuterated reducing reagent. Accordingly benzyloxyacetaldehyde (**118**) was reduced with $LiAl^2H_4$ to generate [1,1-$^2H_2$]-benzyloxyethanol (**139**). This enabled deuterium to be effectively incorporated into the alcohol terminus.

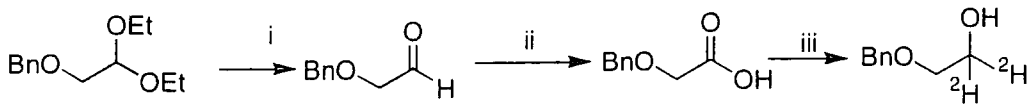

Scheme 2-1 Synthesis of [1,1-$^2H_2$]- benzyloxyethanol (**139**)

Reagents i) TFA, H_2O, $CHCl_3$ ii) $KMnO_4$ iii)$LiAlH_4$

Treatment of [1,1-$^2H_2$]-benzyloxyethanol (**139**) under Swern conditions[108] produced [1-^{2}H]-benzyloxyacetaldehyde (**134**) in moderate yield (64%) and with complete retention of deuterium (GC-MS, ^{13}C-NMR).

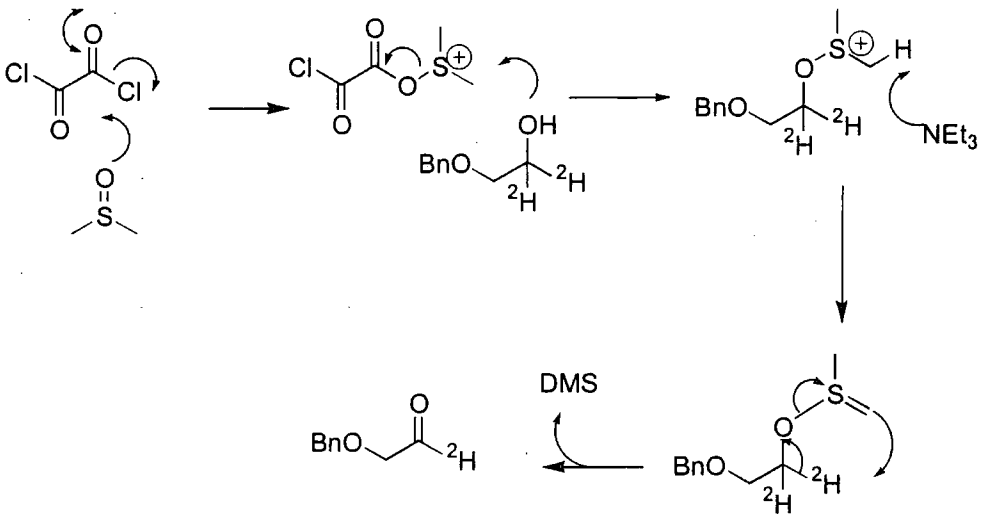

Scheme 2-35 Swern oxidation of [1,1-$^2H_2$]-benzyloxyethanol (**139**)

Wittig coupling with 1-triphenylphosporanylidene-2-propanone produced [4-^{2}H]-(E)-5-benzyloxy-2-pentanone (**135**) in good yield. Successful dihydroxylation with AD-mix β gave [4-^{2}H]-5-benzyl-DX (**140**) which had an identical optical rotation to the unlabelled product. Removal of the benzyl protecting group *via* hydrogenolysis gave [4-^{2}H]-DX (**116**). As [4-^{2}H]-DX (**116**) was pulse fed over the course of the growth period, fresh [4-^{2}H]-DX (**116**) had to be prepared on the day of feeding.

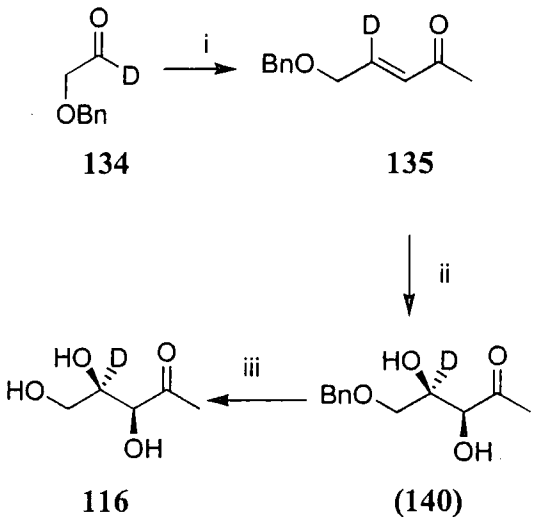

Scheme 2-36 Summary of the synthesis of [4-^{2}H]-DX (**116**)

Reagents i) Ph_3P=$CHCOCH_3$ ii) Ad-Mix β iii) H_2, Pd/C

2.4.3 *Feeding of [4-^{2}H]-DX (116) to* M. citrata

[4-^{2}H]-DX (**116**) Was fed to two cultures of *M. citrata* at a final concentration of 7mM on days 4, 11 and 18, and the crude extract was collected by procedure 2. Analysis of the resulting linalyl acetate by ^{2}H NMR showed a region of intensity at 5.1 ppm.

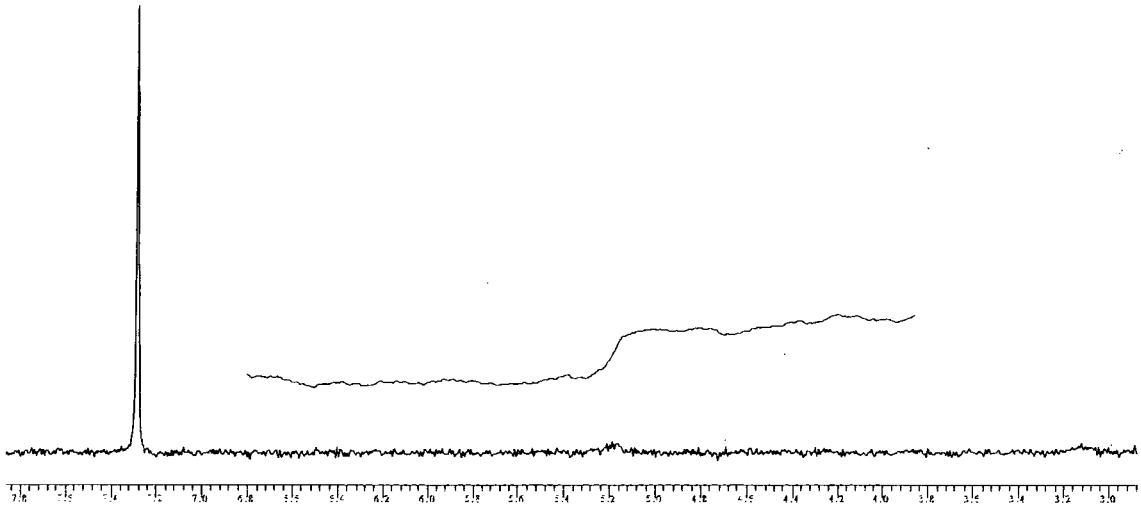

Figure 2-18 ^{2}H-NMR Of linalyl acetate (**78**) after feeding [4-^{2}H]-DX (**116**)

The weak signal intensity at 5.1 ppm suggested incorporation into the protons at 5.14 ppm of linalyl acetate, corresponding to incorporation into the DMAPP derived unit. No incorporation into H-2 at 5.88 ppm was observed. However, this enrichment could also be due to deuterium incorporation into another metabolite in the product mixture. Confirmation of incorporation of deuterium into linalyl acetate (**78**) was pursued by GC-MS analysis. The analysis was performed ten times and mean values are presented in Figure 2-19.

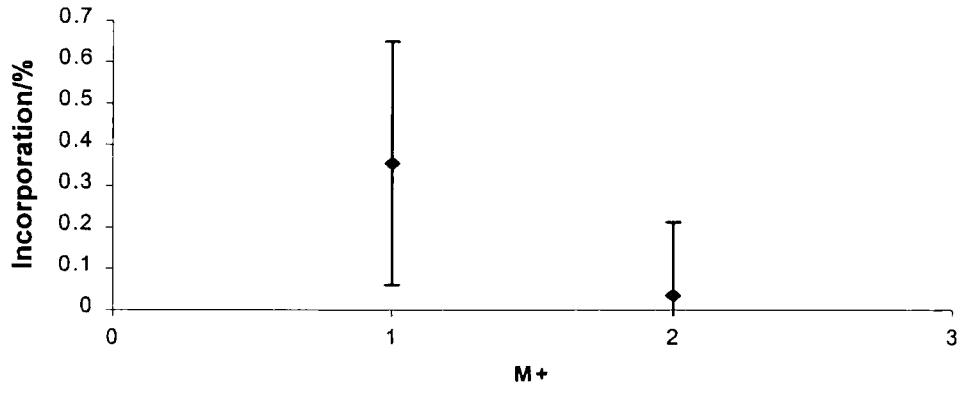

Figure 2-19 Incorporation of [4-^{2}H]-DX (**116**) into linalyl acetate (**78**)

GC-MS analysis suggested enrichment of the M+1 ion although the level of incorporation was complicated by a large standard error that accompanied the data. Similarly, there is a large margin of error associated with the M+2 ion. The standard error of the M+1 ion is caused by two of the ten runs that have relatively high M+ ions. This data is presented in Table 2-5.

Run no.	*M*	*M+1*	*M+2*
1	99.66	0.52	-0.18
2	**100.31**	**-0.21**	**-0.09**
3	99.72	0.50	-0.22
4	**100.24**	**-0.35**	**0.11**
5	99.78	0.23	0.00
6	99.79	0.35	-0.14
7	99.32	0.44	0.24
8	99.65	0.19	0.17
9	99.41	0.38	0.22
10	99.57	0.23	0.20

Table 2-5 Data for each individual GC-MS analysis of linalyl acetate (**78**) after feeding [4-^{2}H]-DX (**116**). High M+ ions are shown in bold

Although the enrichment of the M+1 ion suggests the retention of one deuterium atom, due to the standard deviation the retention of neither or both deuterium atoms cannot be dismissed on the basis of GC-MS analysis.

2.5 Synthesis of [4,5,5,-$^2H_3$]-DX (141)

One of the problems when assessing incorporation into the M+1 ion is to determine a statistical significance above natural abundance. The problem is less significant for M+2 and M+3 as their natural abundance values are much lower. Accordingly, more accurate incorporations can often be obtained from double or triple labelled precursors. Feeding [6,6-$^2H_2$]-glucose (**94**) to *M. citrata* had already shown that the C-5 protons of DXP were retained during the biosynthesis of linalyl acetate and accordingly [4,5,5-$^2H_3$]-DX (**141**) became a synthetic target. It was expedient to synthesise [4,5,5-$^2H_3$]-DX

using the same strategy that was used to make [4-^{2}H]-DX (**116**). Retrosynthetic analysis of [4,5,5-$^2H_3$]-(E)-5-benzyloxy-3-pentanone (**142**) offered a synthesis from commercial [$^2H_6$]-ethylene glycol (**143**)

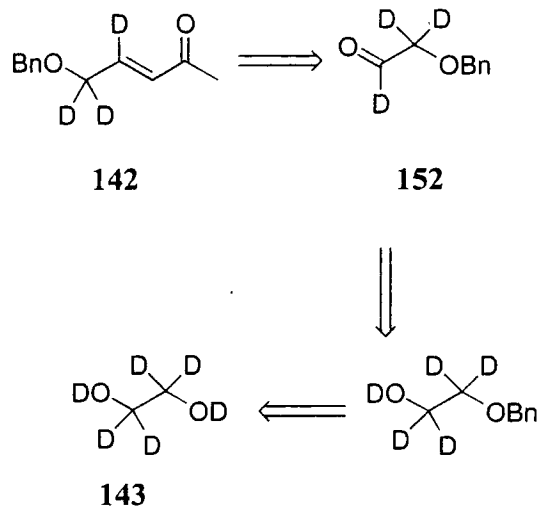

142 **152** **143**

Scheme 2-37 Retrosynthesis of [4,5,5-$^2H_3$]-(E)-5-benzyloxy-3-pentanone (**142**)

A survey of the literature revealed that the monobenzyl protection of ethylene glycol (**144**) had been performed previously with benzyl bromide (**145**) and sodium hydride[109]. However, when ethylene glycol was treated with one equivalent of NaH and one equivalent of benzyl bromide only the diprotected product (**146**) was isolated (Scheme 2-38). When the reaction was monitored *via* TLC it was clear that the di ether was formed preferentially to the monoether (**147**). Attempts to introduce kinetic control by performing the reaction at 0°C and –78°C resulted in identical product profile but at a slower rate.

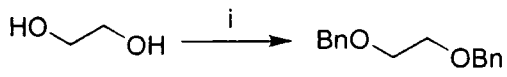

144 **146**

Scheme 2-38 Formation of 1,2-*O*-dibenzyl ethylene glycol (**146**)

Reagents i) NaH, BnBr

In the event it was found that treatment of ethylene glycol with half an equivalent of potassium hydroxide and one equivalent of benzyl bromide (**145**) generated the mono ether (**147**). This was adapted from a procedure which used equivalent ratios to prepare 3-(3-phenylprop-2-enyloxy)propanol (**148**) from cinnamyl bromide (**149**) and 1,3-propandiol (**150**)[110].

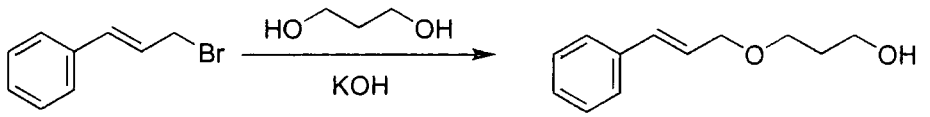

149 **148**

Scheme 2-39 Use of cinnamyl bromide (**149**) to prepare 3-(3-phenylprop-2-enyloxy)propanol (**148,** Kizil[110])

When ethylene glycol (**144**) and benzyl bromide (**145**) were substituted in the reaction in a 1:1 ratio in THF, none of the benzyl ether was formed. However, when DMSO was used as the reaction solvent a product was formed by TLC that possessed a lower R_f than the dibenzyl ether (**146**). After 30 minutes the reaction worked up. NMR Analysis showed that the new spot corresponded to the mono benzyl ether (**147**). When the reaction time was increased, formation of the dibenzyl ether (**146**) was observed until it was the only product. Attempts to enforce kinetic control by cooling the reaction and increasing the reaction time caused the products to be formed at a reduced rate, but in the same ratio as for the reaction under ambient conditions. In spite of a low yield (40% based on the amount of benzyl bromide), these conditions were used to prepare [1,1,2,2-$^2H_4$]-benzyloxyethanol (**151**) from [1,1,2,2-$^2H_4$]-ethylene glycol (**143**).

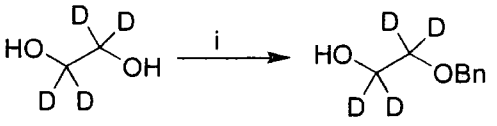

143 **151**

Scheme 2-40 Synthesis of [1,1,2,2-$^2H_4$]-benzyloxyethanol (**151**) from [1,1,2,2-$^2H_4$]-ethylene glycol (**143**)

Reagents i) BnBr (1eq), KOH (0.5 eq), DMSO

Treatment of [1,1,2,2-$^2H_4$]-benzyloxyethanol (**151**) with Swern conditions gave [1,2,2-$^2H_3$]- benzylacetaldehyde (**152**). However, it was necessary to perform the oxidation using deuterium labelled reactants as triethylamine was found to abstract the acidic α-protons. When the reaction was quenched by the addition of H_2O, subsequent tauteromerisation gave rise to a distribution of [1,2-$^2H_2$] (**153**) and [1-$^2H_2$]-benzylacetaldehyde (**134**) in the ratio of 1:3 (^{13}C-NMR).

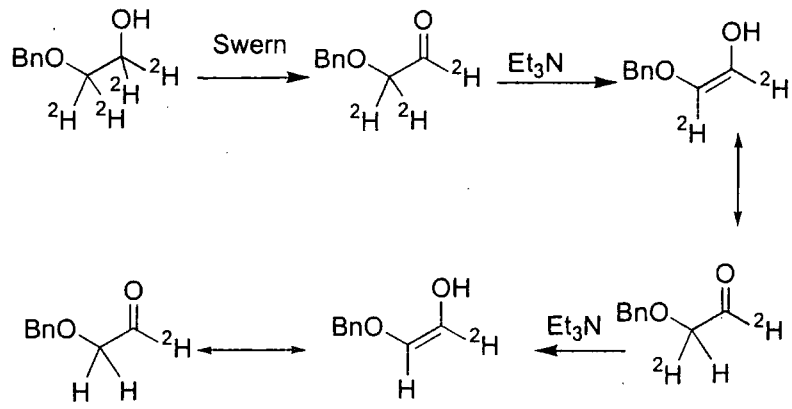

153 134

Scheme 2-41 Loss of deuterium during the Swern oxidation of by the action of residual triethylamine

Standard Wittig coupling yielded [4,5,5-$^2H_3$]-(E)-5-benzyloxy-2-pentanone (**142**) and successful dihydroxylation delivered [4,5,5-$^2H_3$]-5-benzyl-DX (**154**).

Hydrogenolysis of [4,5,5-$^2H_3$]-5-benzyl-DX (**154**) in EtOH with Pd/C gave rise to significant loss (~60%, NMR) of deuterium from C-5. This was possibly due to radical abstraction of deuterium and quenching by nascent hydrogen or transfer of the hydroxyl proton from ethanol.

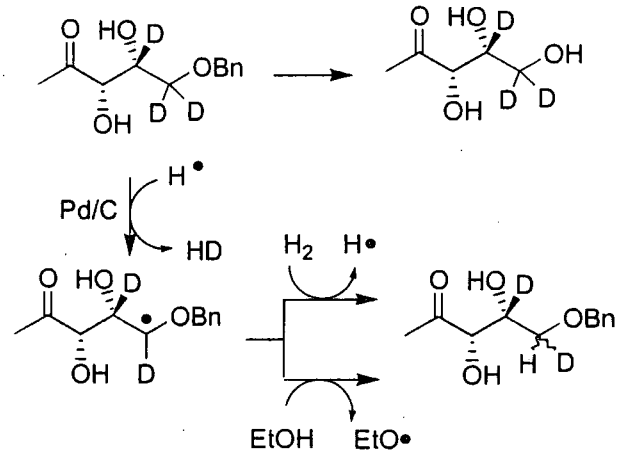

Scheme 2-42 Suggested loss of deuterium by radical abstraction in Pd/C/H_2 reaction

When hydrogenolysis was performed using EtOD, formation of DX was accompanied with a greater retention of deuterium. GC-MS analysis of the triacetate derivative showed that the major isotopomer was [4,5,5-$^2H_3$]-DX (**141**, 67%). Lower populations of [4,5-$^2H_2$]-DX (**155**, 31%) and [4-^2H]-DX (**116**, 2%) were also present.

The mixture was fed to two sets of *M. citrata* cultures and each was worked up separately *via* procedure 2. Each sample was then analysed ten times *via* GC-MS and the mean incorporation values are shown in Figure 2-20.

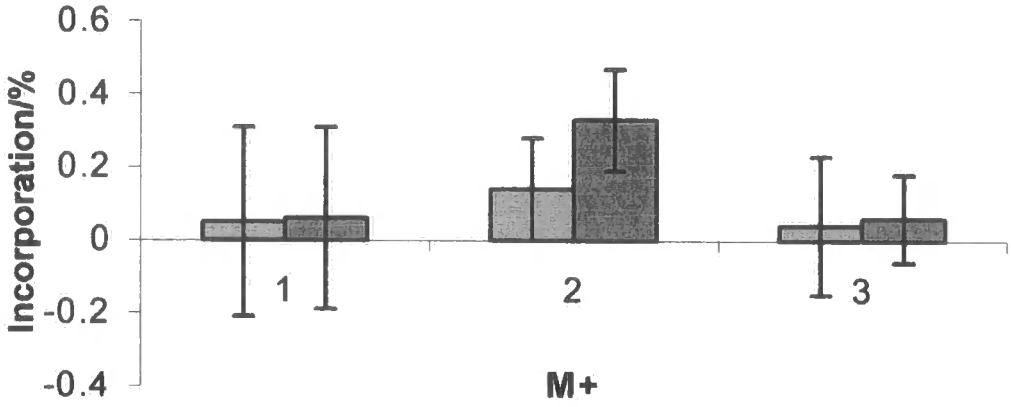

Figure 2-20 Incorporation of deuterium into linalyl acetate after feeding [4,4,5-$^2H_2$]-DX (**141**). Separate experiments are shown by adjacent bars

On both sets of M+1 data, the standard error is large, and thus no conclusion can be drawn about whether a single deuterium atom was incorporated. Similarly, the M+3 enhancements, which would correspond to retention of all three deuterium atoms, have small mean values and have large associated errors. Analysis of the M+2 ions does however suggest incorporation of two deuterium atoms, although in both cases the potential enrichment is subject to a wide margin of error. From these results, no definite conclusion can be draw; although the M+2 ion appears to indicate incorporation of two deuterium atoms the standard deviation is too large to have confidence that the enrichment represents a *bona fide* incorporation into linalyl acetate.

2.6 Working hypothesis for the conversion of MEP to IPP

A revised working hypothesis was subsequently developed based on the discovery that the mevalonate independent pathway proceeds *via* the cyclo-diphosphate (**76**, Figure 2-43). Removal of the tertiary hydroxyl group yields a carbocation (**156**) that can be stabilised by the formation of an epoxide (**157,158**) from either of the two hydroxyl groups. Attack by NADPH (**159**) yields a source of hydride that can be used to effect dehydrations – in this scheme, the same hydrogen is added and removed and the hydrogen atoms that originate from MEP are left intact. Mapping of the protons of DXP and MEP showed that all the protons that were present in DXP and MEP were retained in the final isoprenoid, but did not shed light on any processes that would introduce and remove the same proton. Dehydration can proceed *via* the hydroxyl at either C-2 or C-4 to produce a vinylic alcohol (**160, 161**). Attack of hydride, which may be preceded by activation of the alcohol to a good leaving group, yields IPP (**34**) or DMAPP (**35**).

This would offer a rational account for the formation of the pyrophosphate group and mechanisms by which IPP and DMAPP are formed independently. Four of the putative intermediates were identified as synthetic targets for feeding experiments, in addition to ME, isopentenyl alcohol and dimethylallyl alcohol and are shown in Figure 2-6.

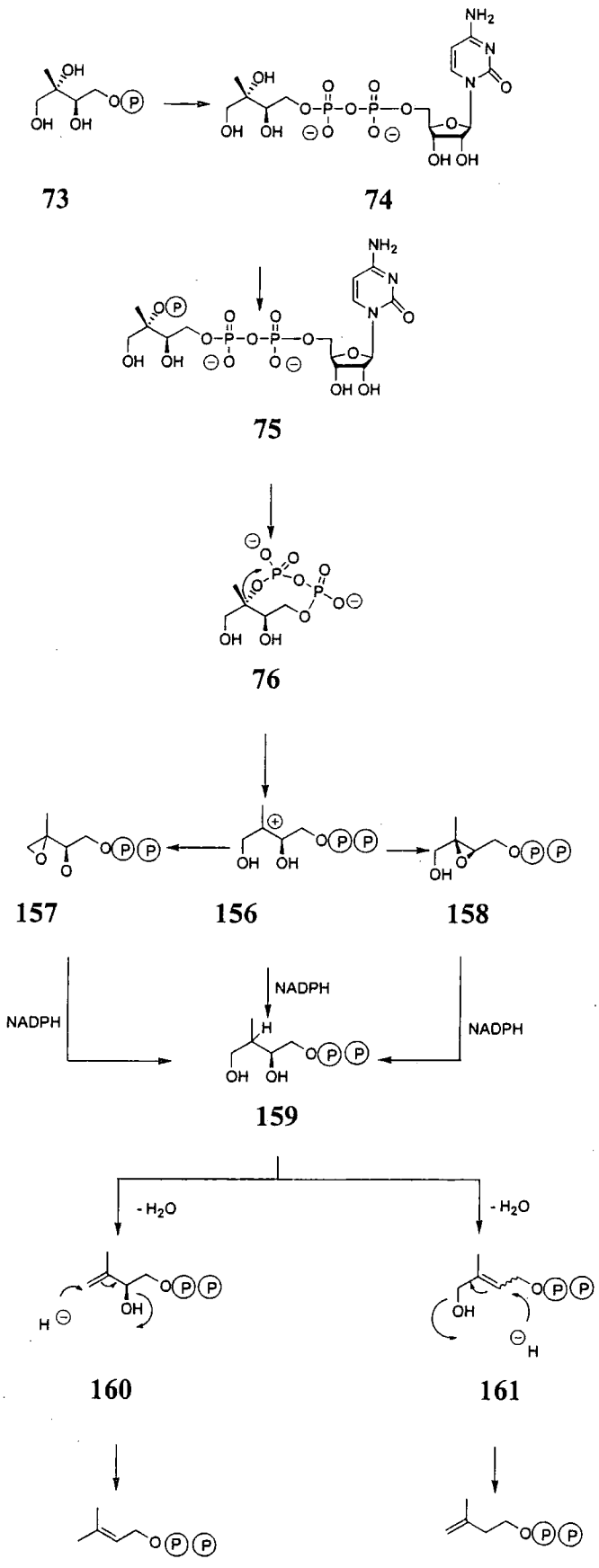

Scheme 2-43 A working hypothesis for the formation of IPP and DMAPP *via* the mevalonate independent pathway in bacteria

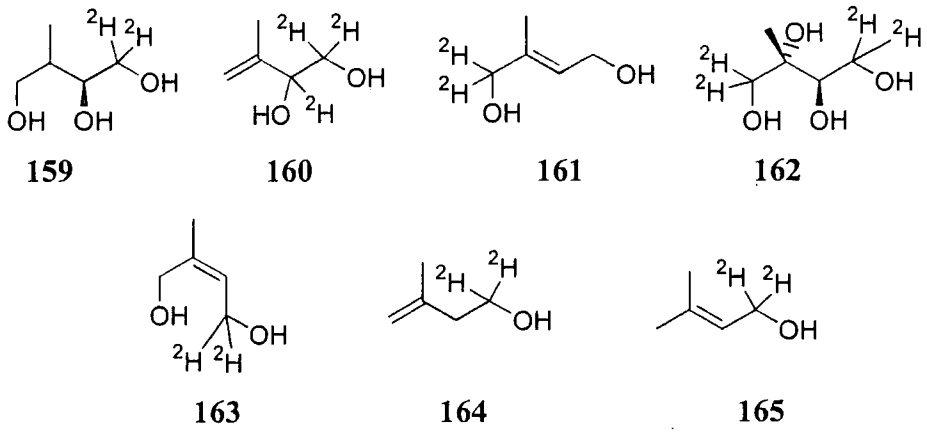

Figure 2-6 Synthetic targets

ME (**166**) was chosen as a target as it is the last known intermediate that is incorporated on the mevalonate independent pathway and would test whether incorporation into linalyl acetate could be detected.

A potentially limiting feature of this strategy was whether free alcohols can be activated to the phosphate level for inclusion in the biosynthesis. To determine if a kinase was present that could activate the alcohols to the required phosphate level, the parent alcohols of IPP and DMAPP were chosen as substrates. It was anticipated that these would be a gauge of which substrates could be expected to be incorporated when fed as alcohols.

2.6.1 Synthesis of putative intermediates

2.6.1.1 [1,1-$^2H_2$]-DMAA (167)

3-Methyl-but-2-ene-1-ol (dimethyl allyl alcohol, DMAA), was synthesised in a one step reduction from the ethyl ester of 3-methyl-but-2-ene-1-oic acid (**168**) using lithium aluminium hydride[111].

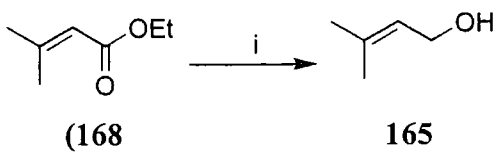

(**168** **165**

Scheme 2-44 i) $LiAlH_4$, ether

The reaction proceeded in good yield and prompted synthesis using $LiAl^2H_4$ which delivered 2g of [1,1-$^2H_2$]-DMAA (**167**)[112].

2.6.1.2 Synthesis of [1,1,2-$^2H_3$]-1,2 dihydroxy 4-methyl but-3-ene (160)

A synthetic scheme for the synthesis of 1,2 dihydroxy-4-methyl-but-3-ene (**160**) was devised, starting from D-mannitol (**169**). It was anticipated that either ^{13}C or ^2H could be incorporated into the olefinic methylene group during the Wittig coupling reaction.

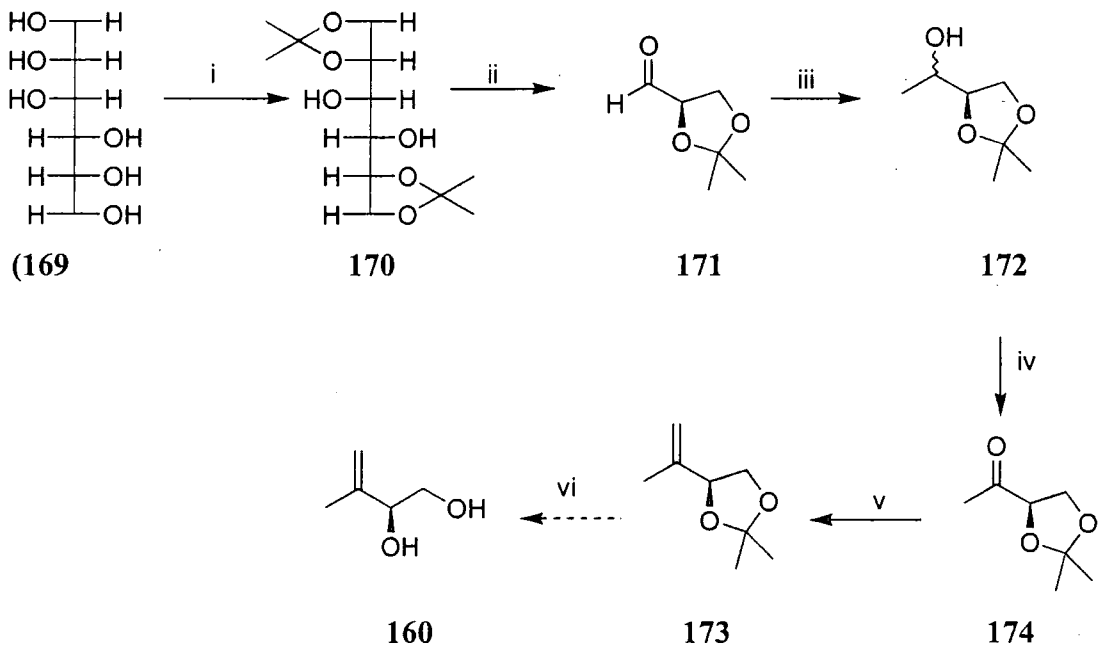

Scheme 2-45 i) Zn,acetone,3h ii) $NaIO_4$, DCM, 1h iii) MeMgBr, ether iv) PDC, 3A Molecular sieves, acetic acid, DCM, 12h v) $Ph_3P{=}CH_2$, THF

Protection of D-mannitol ((**169**) to form the acetonide (**170**) was achieved using zinc and acetone[113] and was oxidised to D-glyceraldehyde acetonide (**171**) by sodium metaperiodate[114]. Grignard addition gave the alcohol (**172**) in moderate yield (58%) as a mix of diastereomers (3:1)[115].

Oxidation of the secondary alcohol proved to be difficult. A variety of oxidising conditions were tested (MnO_2 , pyridinium chlorochromate and Swern conditions) but these did not afford oxidation to the ketone and only gave recovery of the starting material. The method that was found to work most efficiently used pyridinium

dichromate (PDC) with catalytic acetic acid and dry molecular sieves[116]. Under these conditions, ketone **174** was produced cleanly.

The Wittig olefination proved unsatisfactory and gave low yields (10-15%) of **174**. This contrasts with literature reports which describes a 30% isolated yield, albeit on an 11 gram scale[26]. The low yield is undoubtedly due to the product being held in the triphenyl phosphine oxide solid which is a byproduct of the reaction. Furthermore, the crude product readily decomposes on silica, and made isolation and purification very difficult. In light of this, an alternative strategy for **160** was employed.

The synthesis of **160** was achieved by Dr Andy Humphrey (Durham). The carbon skeleton was built from the Grignard addition of isopropenyl magnesium bromide to diethyl oxalate (**175**). The crude product was treated with $LiAl^2H_4$ to afford **176** bearing three deuterium atoms.

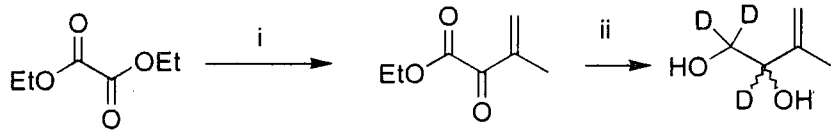

175 **176**

Scheme 2-46 i) $MeC(CH_2)MgBr$ ii) $LiAl^2H_4$

2.6.1.3 Synthesis of 177

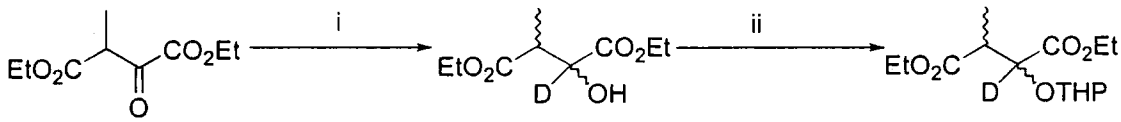

178 **179** **180**

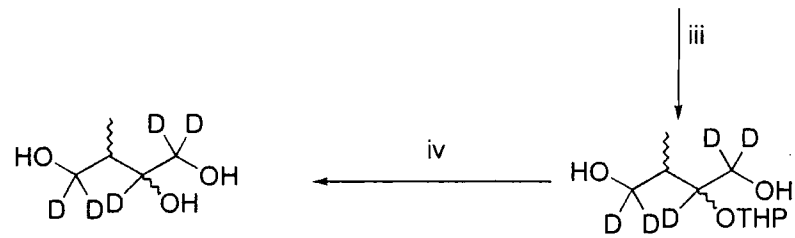

177 **181**

Scheme 2-47 i) NaB^2H_4 ii) THP, H^+ iii) $LiAl^2H_4$ iv) MeOH, H^+

Compound **177** was synthesised by Dr Andy Humphrey with five deuterium atoms starting from diethyl 3-oxoglutarate as outlined in Scheme 2-47.

2.6.1.4 ***Synthesis of* 182**

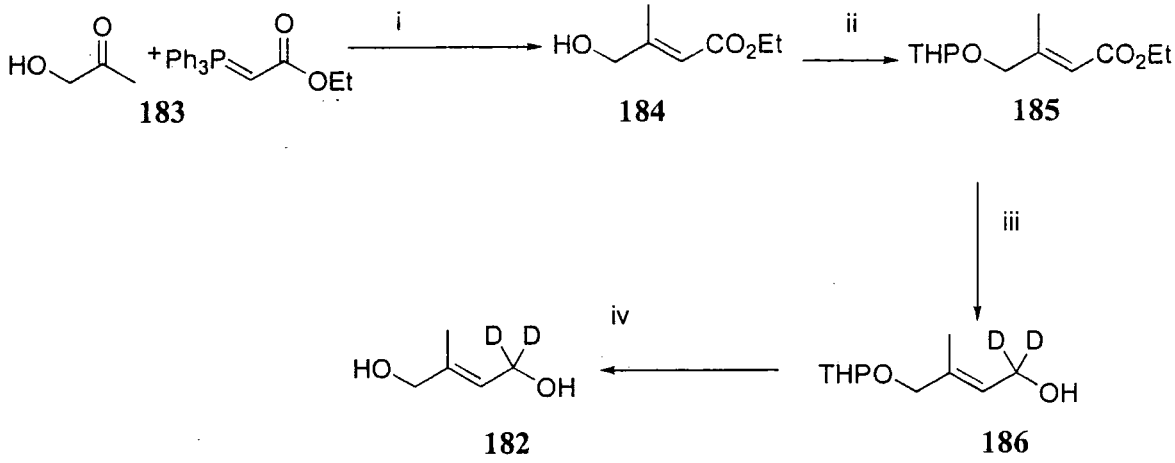

183 **184** **185** **186** **182**

Scheme 2-48 i) $CHCl_2$, Δ; ii) THP, H^+; iii) $LiAl^2H_4$; iv)H^+, MeOH

Compound **182** was synthesised by Dr Andy Humphrey in four steps from acetol. The carbon skeleton was built from a Wittig coupling which was protected by THP. Reduction by $LiAl^2H_4$ followed by deprotection gave **182**.

2.6.1.5 ***Synthesis of* 187**

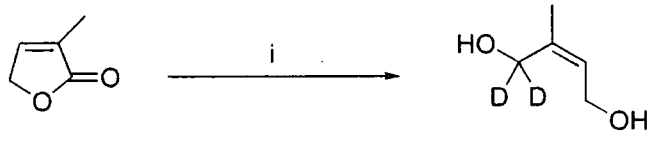

187

Scheme 2- 49 i) $LiAl^2H_4$

Compound **187** was prepared by Dr Andy Humphrey in a one step reduction of 3-methyl-2(5 H)-furanone with lithium aluminium deuteride.

2.6.1.6 ***Synthesis of [1,1-$^2H_2$]-isopentenyl alcohol (*188)**

[1,1-$^2H_2$]-Isopentenyl alcohol (**188**) was synthesised by Dr Andy Humphrey in two steps from allyl bromide **189**. Conversion of allyl bromide to the Grignard (**190***)* by refluxing with magnesium was followed by reaction with solid CO_2. A standard $LiAl^2H_4$ reaction gave (**188**) in 45% yield.

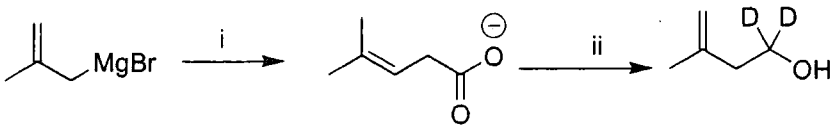

189 **190** **(188)**

Scheme 2-50 i) CO_2 ; ii) $LiAl^2H_4$

2.6.2 Feeding of putative intermediates to E. coli

The intermediates were fed at the concentrations outlined below and worked up following the standard protocol.

Substrate	*Structure*	*Conc*
176	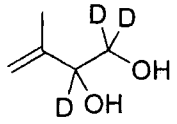	1.3mM
177	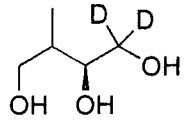	1.1mM
182	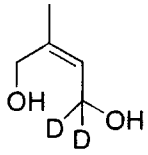	1.2mM
187	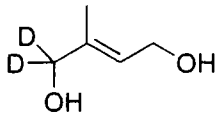	1.4mM

Table 2-6 Table showing the concentration of putative intermediates fed to *E. coli*

In each experiment, ubiquinone was collected according to the standard procedure and analysed *via* ^{2}H-NMR. The ^{2}H-NMR spectrum of ubiquinone after feeding **176** , **182** and **187** are shown in Figure 2-7.

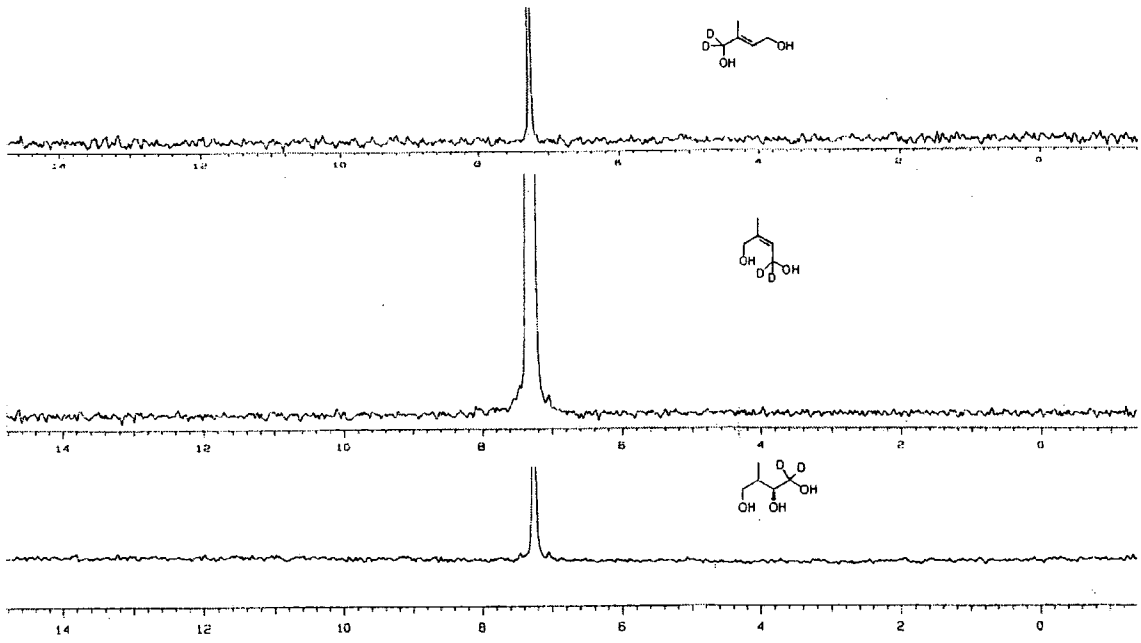

Figure 2-7 ^{2}H NMR of ubiquinone after feeding **177, 182** and **187** to *E. coli*

None of the three spectra show significant signals that could be due to incorporation of deuterium into ubiquinone. However, ^{2}H NMR of the ubiquinone after feeding **176** to *E. coli* showed a sharp peak at 4.0ppm and regions of intensity at 3.7 and 1.7 ppm (Figure 2-8). The peak at 3.7 ppm is due to deuterium from residual ethanol used in the extraction process.

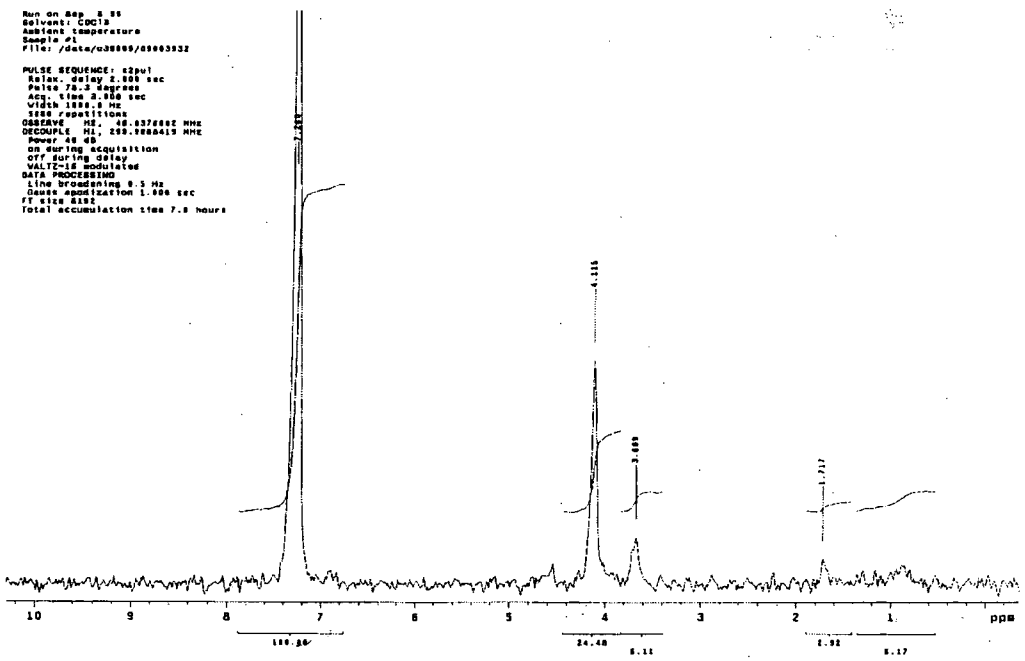

Figure 2-8 ^{2}H NMR Spectrum of ubiquinone after feeding **176** to *E. coli*

Incorporation into the methoxy groups is evident from the signal at 4.1 ppm. As the methyl groups are derived from SAM, the incorporation of deuterium corresponds to labelling of SAM and hence methionine. A possible method by which deuterium could be incorporated into methionine is after oxidation of **177** to yield [1,1-$^2H_2$]-formaldehyde (**191**). Loading of methionine (**192**) and incorporation into the methoxy groups would account for the observed peak.

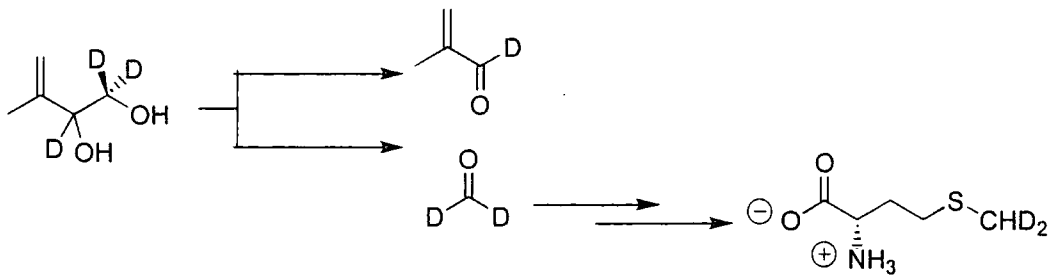

191 **192**

Scheme 2-51 Suggested labelling of methionine from **177**

The peak at 1.7 ppm could represent incorporation into the prenyl chain but also could be due to incorporation of deuterium into lipids that contaminated the sample. From these results, no conclusion about whether **177** is an intermediate can be drawn.

2.6.3 *Feeding of [4,4-$^2H_2$]-ME (162) to* E. coli

[4,4-$^2H_2$]-ME was fed to *E. coli* in order to determine whether the cultures developed in Durham could incorporate ME in a similar manner to as those described in the literature. Accordingly, [4,4-$^2H_2$]-ME (**162**) was fed to *E. coli* to a final concentration of 1.4mM and the resultant ubiquinone was analysed *via* ^{2}H NMR. The spectrum is shown in Figure 2-9.

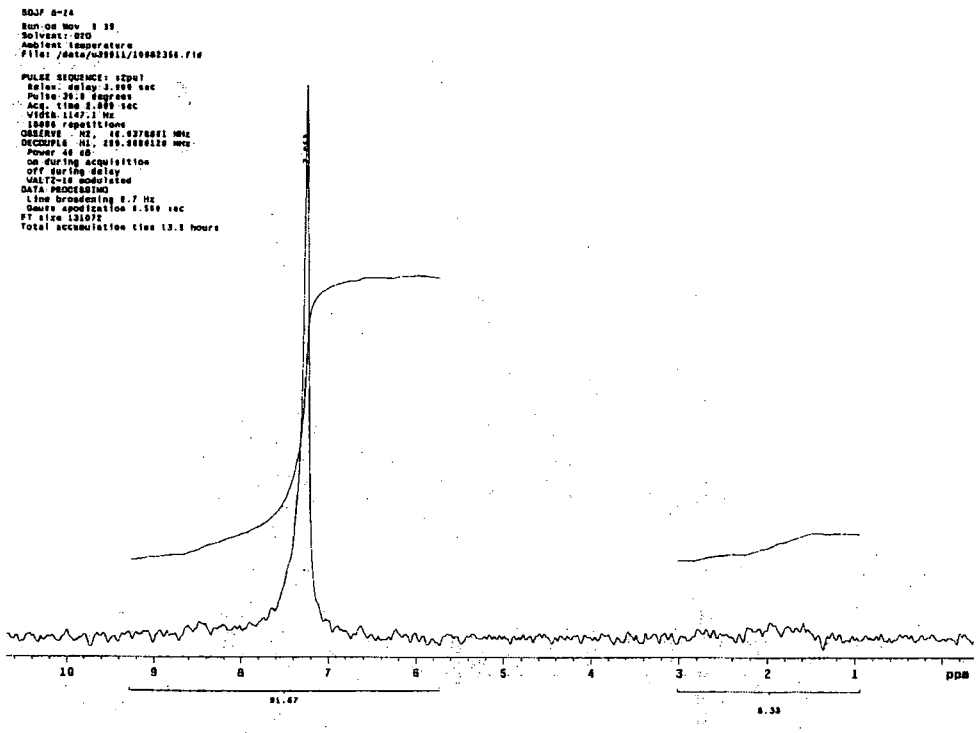

Figure 2-9 ^{2}H NMR of ubiquinone (**80**) after incubating of [4,4-$^{2}H_2$]-ME (**162**) with *E. coli*

A region of intensity between 1.8-2.3 ppm suggests labelling of the prenyl chain. The signal could correspond to deuterium being carried through and incorporated into the prenyl chain as shown in Scheme 2-52.

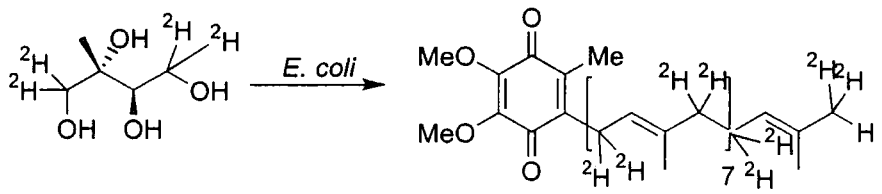

162 **80**

Scheme 2-52 Possible mode of incorporation of [4,4-$^{2}H_2$]-ME (**162**) into ubiquinone (**80**)

However, the weakness of the experiment is the low level of incorporation. The peak could be accounted for by contamination from small amounts (50 μg) of highly labelled (40%) metabolites. Literature reports[58] describe incorporation of deuterium from deuterium labelled ME and show that *E. coli* is capable of accepting free ME as an

exogenously administered substrate. In these reports, significant signals in the ^{2}H-NMR are reported. However, this may have been a consequence of the larger amounts of ubiquinone that were isolated in the literature examples (6-8mg) compared to 3mg from this study.

2.6.4 *Feeding of [1,1-$^2H_2$]-DMAA (167) and [1,1-$^2H_2$]- isopentenyl alcohol (188) to* E. coli *and* M. citrata

In order to establish whether latter intermediates on the pathway could be incorporated, [1,1-$^2H_2$]-DMAA (**167**) and [1,1-$^2H_2$]-isopentenyl alcohol (**188**) were fed to *E. coli* and *M. citrata*. Accordingly, [1,1-$^2H_2$]-DMAA (**167**) was pulse fed separately to two sets of *M. citrata* cultures to final concentrations of 3mM and 5mM and the cultures were harvested *via* procedure 2 on day 17. Each sample was analysed ten times and the mean incorporations are shown in Figure 2-21.

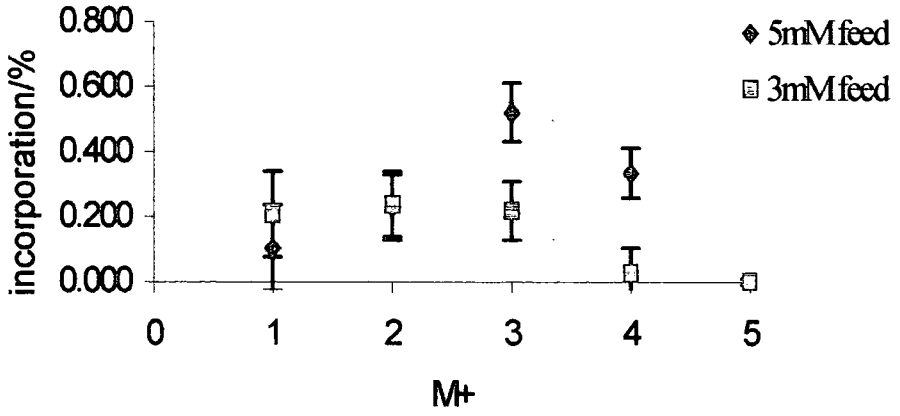

Figure 2-21 Incorporation of [1,1-$^2H_2$]-DMAA (**167**) into linalyl acetate by *M. citrata*

Feeding of [1,1-$^2H_2$]-DMAA (**167**) at 3mM showed enrichments of the M+1, M+2 and M+3 ions which suggested incorporation of one, two and three deuterium atoms respectively. This contrasts with the incorporation into linalyl acetate after feeding DMAA at 5mM, which showed incorporation into the M+2, M+3 and M+4 ions. The relatively large standard errors and differences in the incorporations between each experiment do not provide any confidence that DMAA had been incorporated into linalyl acetate. Hence, the enrichments do not represent the straightforward

incorporation of deuterium into linalyl acetate by a prenyl transferase/isomerase mechanism. The incorporations could be due to metabolism and re-introduction of deuterium.

In the same experiment in bacteria, [1,1-$^2H_2$]-DMAA (**167**) was fed to eight cultures of *E. coli* to a final concentration of 1.1mM. The resultant ubiquinone was harvested according to the standard procedure and analysed *via* ^{2}H-NMR. No signals or areas of intensity were observed, indicating no significant incorporation of DMAA (**167**) into ubiquinone by *E. coli.*

In a parallel experiment, [1,1-$^2H_2$]-isopentenyl alcohol (**188**) was fed to two cultures of *M. citrata* to a final concentration of 1.8 mM, and the resulting linalyl acetate analused by GC-MS. No enhancement of the M+1 or M+2 ions was observed.

Likewise, cultures of *E. Coli* were supplemented with [1,1-$^2H_2$]-isopentenyl alcohol (**188**). Analysis of the resultant ubiquinone by ^{2}H-NMR did not show any ^{2}H signals.

2.6.5 Analysis of results after feeding putative intermediates

There is no evidence that the mevalonate independent pathway does not deliver IPP and DMAPP. Hence the lack of incorporation of [1,1-$^2H_2$]-isopentenyl alcohol (**188**) and [1,1-$^2H_2$]-DMAA (**167**) indicates that there is no kinase to activate exogenously administered alcohols to the required phosphate level. In the light of this, alcohols **176** , **177, 182, 187**, would not be incorporated as they lack the phosphate or pyrophosphate motif.

These results also suggest that *E. coli* is capable of activating ME to MEP *in vivo*. In the case of ME, only monophosphorylation is required to produce the relevant intermediate, whereas post MEP intermediates require the introduction of at least a pyrophosphate group. Furthermore, if the pyrophosphate is delivered intramolecularly as depicted in the working hypothesis, all post MEP intermediates would be present *in vivo* as the pyrophosphate and hence the organism is less likely to recognise intermediates fed as the free alcohol. Although feeding of intermediates as their pyrophosphate esters seems like a feasible method of study, cell walls are impenetrable to phosphate and pyrophosphate esters.

These findings are summarised in Figure 2-21. Dashed lines indicate that substrates fed as free alcohols are transported into the cell, converted to the phosphate and used. The bold lines indicate that all intermediates on the pathway are present as pyrophosphates.

Hence, although intermediates may be transported into the cell, they are not recognised or activated as pyrophosphates. Pyrophosphates are not transported into the cell.

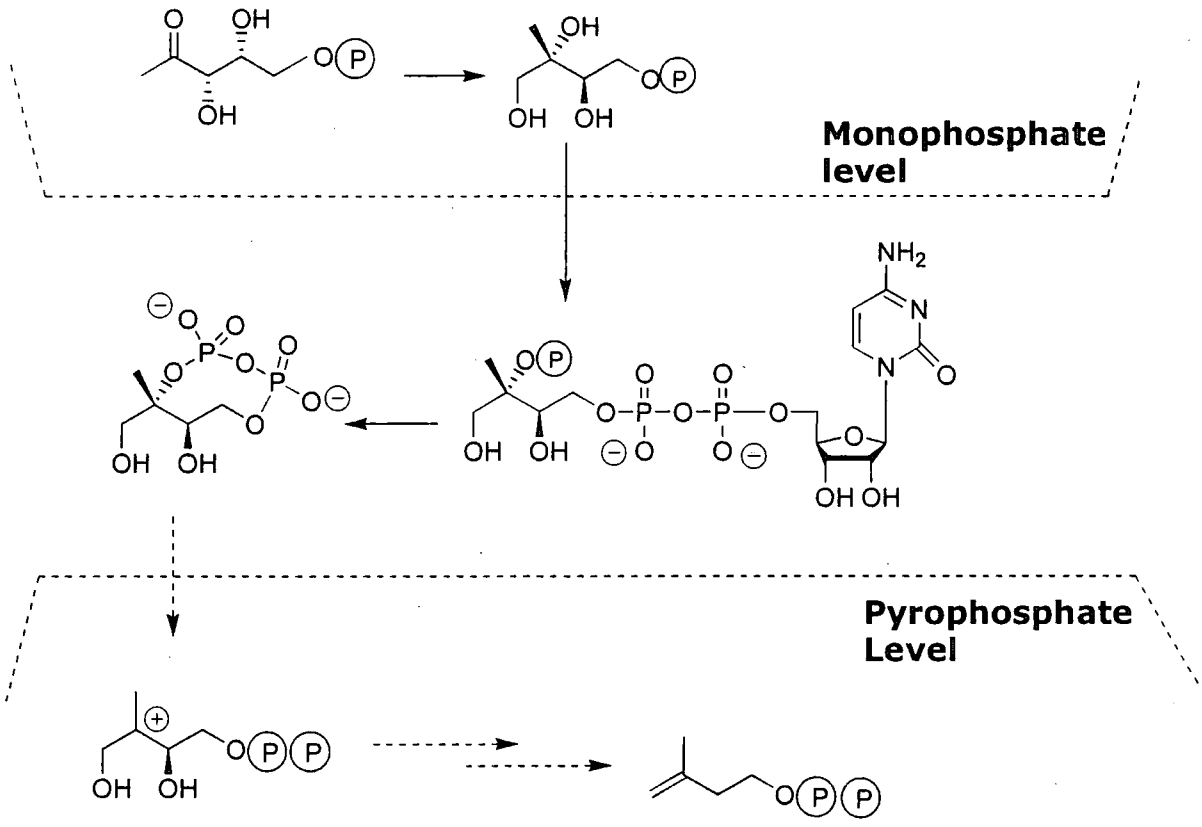

Figure 2-21 Working hypothesis of the mevalonate independent pathway and the activation to the pyrophosphate level

2.7 Conclusions

The feeding of [1,2-$^{13}C_2$]-acetate and [1-^{13}C]-glucose to *M. citrata* reveal that linalyl acetate is biosynthesised exclusively *via* the mevalonate independent pathway. The results of feeding [3-^{13}C]-alanine to *M. citrata* show that alanine is processed *via* the mevalonate independent pathway and the incorporation of [3-$^{2}H_3$]-alanine and [3-$^{13}C^{2}H_3$]-alanine show retention of all three methyl protons during the biosynthesis of linalyl acetate. Similarly, [6,6-$^{2}H_2$]-glucose and [$^{2}H_8$]-glycerol show retention of the C-5 protons of DX. These results place limitations on the processes by which MEP can be converted to IPP in plants.

The incorporation of deuterium into ubiquinone after feeding [6,6-$^{2}H_2$]-glucose to *E. coli* verify that ubiquinone is biosynthesised *via* the mevalonate independent pathway.

Synthesis and feeding of [4-^{2}H]-DX to *M. citrata* suggests partial retention of deuterium although the level of incorporation is low and has a large variance.

Feeding of synthetically prepared DMAA and isopentenyl alcohol bearing deuterium did not give any incorporation into linalyl acetate or ubiquinone. Likewise, putative intermediates bearing deuterium were fed to *E. coli* and showed no incorporation of deuterium into the terpenoid unit of ubiquinone. Perhaps these intermediates could not be activated to their pyrophosphate esters.

Chapter 3

Studies on fungal metabolites

3 Studies on fungal metabolites

This chapter describes the isolation and characterisation of a meroterpene, rosnecatone, from *Rosellinia necatrix* and studies on metabolite production as a function of growth conditions. The feeding of stable isotope labelled compounds and their incorporation is also discussed.

The identification of a metabolite, epoxydon, from *Xylaria grammicin* is described and studies on metabolite production in *X. grammicin* conclude the chapter. Results of screening rosnecatone and epoxydon against Human cancer cell lines are described.

3.1 Fungal metabolites

Fungi produce a vast array of unique secondary metabolites, the distribution of which is very different to that in plants and bacteria. The majority of polyketides isolated have been obtained from fungal sources, particularly fungi imperfecti. Most fungal polyketides are aromatic and are derived from one of three aromatic sources; acetylphloroglucinol (**193**) , orsellinic acid (**194**) and 6-methylsalicylic acid (**195**).[117]

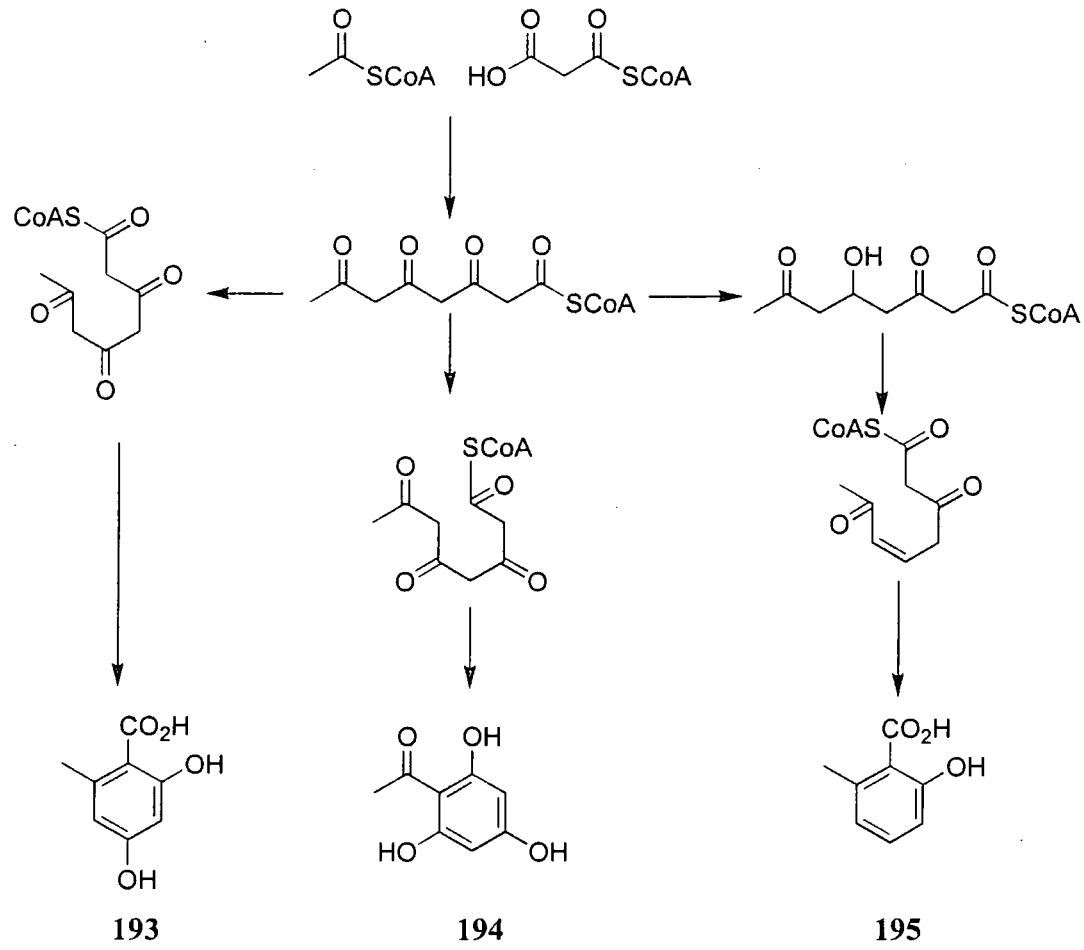

193 **194** **195**

Scheme 3-1 Biosynthesis of acetylphloroglucinol (**193**), orsellinic acid (**194**) and 6-methylsalicylic acid (**195**)

Fungal aromatics are largely polyketide rather than shikimate in origin, and hence the shikimate pathway is much less widely used in fungi than in bacteria and plants. Nevertheless, the pathway is still used to deliver aromatic amino acids such as L-phenylalanine (**22**) and L-tyrosine (**23**), as described in chapter 1.

Far fewer fungal terpenes than fungal polyketides are known and although fungal terpenes have a limited distribution, fungi often represent a unique source of the few terpenes they produce. Monoterpenes and sesquiterpenes are rare, and collectively number less than forty. Those that are known demonstrate a variety of bi and tri cyclic structures, which are similar to sesquiterpenes observed in plants. Likewise, diterpenes and sesterterpenes have similarly limited distributions, of which the gibberillins are the most important examples. Steroids and triterpenoids account for the majority of the fungal terpenoids. All fungal sterols possess the standard tetracyclic skeleton and are often found in bacteria.

3.2 Mixed metabolites

In the context of this project, two of the most important classes of metabolites that are derived from more than one biosynthetic pathway are the meroterpenoids and the cytochalasins.

3.2.1 Meroterpenes

Meroterpenoids are a diverse class of secondary metabolites that exhibit a wide range of structures and biological activity. Over 700 such compounds have been reported[118], some of which demonstrate antifungal and larvicidal activities[119], whilst others are inhibitors of mammalian acetylcholinesterase and protein farnesyltransferase[120]. Originally the name "meroterpene" was coined by Cornforth[121] to describe all mixed metabolites containing a terpene fragment. More recently Simpson's definition, that meroterpenes are mixed metabolites containing terpenoid and polyketide fragments[122] has been gaining acceptance.

Surprisingly few biosynthetic studies have been performed on meroterpenes. The most thorough study was performed by Staunton on metabolites produced by *Aspergillis variecolor, Aspergillis ustus* and *Aspergillis terreus*. Isotopic labelling studies showed that the *Aspergillis* meroterpenes **196** and **197** were produced by the condensation of orsellinic acid (**194**) with FPP (**37**). Most significantly though, incorporation of [1,2-$^{13}C_2$]-acetate (**63**) into the terpenoid derived units showed that the terpene moiety was delivered by the MVA pathway[123,124].

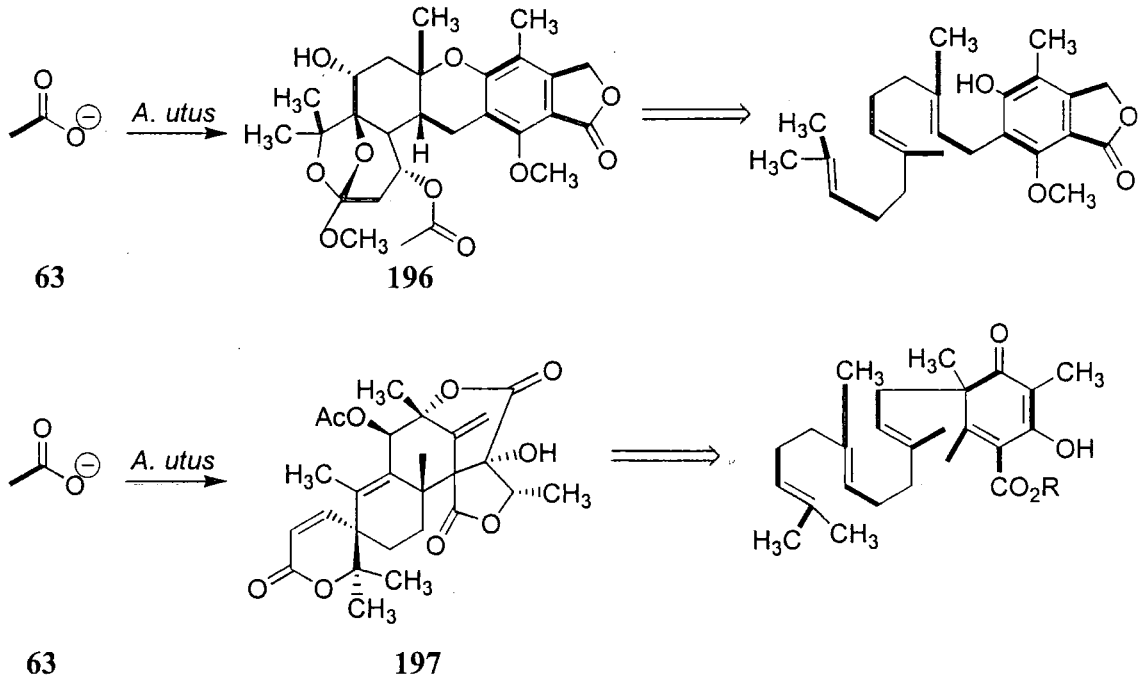

63 196

63 197

Scheme 3-2 Incorporation of [1,2-$^{13}C_2$]-acetate (**63**) into meroterpenes produced by *A. utus*

More recently, incorporation of [1-^{13}C]-glucose showed that the prenyl chain in boviquinone (**198**), a metabolite of *Chrogomphus rutilus*, was produced by the MVA pathway[125]. Meroterpenoid quinones fulfil the same role as ubiquinones in bacteria and animals and appear to be membrane associated electron transfer agents.

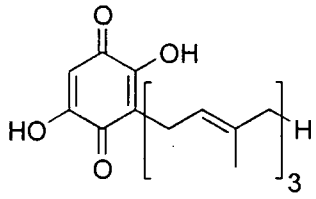

198

Surprisingly little is known about the extent to which the mevalonate independent pathway operates in fungi. Previous work[126] in fungi feeding labelled glucose and acetate revealed exclusive operation of the mevalonic acid pathway in a study on hopanoid (**199**) biosynthesis.

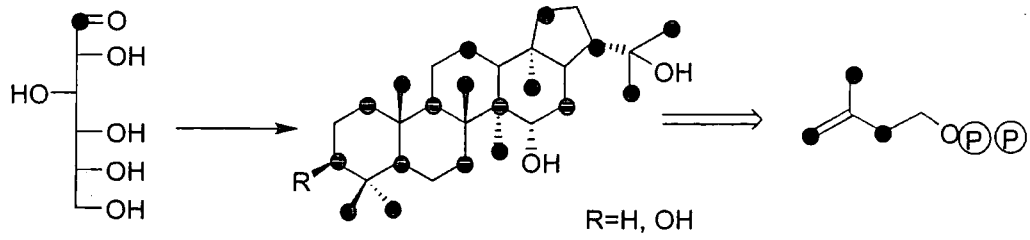

68 **199**

Scheme 3-3 Feeding of [1-^{13}C]-glucose (**68**) to *A. aleyrodis* shows incorporation into the hopanoid (**199**) *via* the MVA pathway

If the hypothesis that the mevalonate independent pathway is largely localised in chloroplasts is correct, then as fungi do not have chloroplasts, all fungal terpenes would be expected to be biosynthesised *via* the MVA pathway.

3.2.2 Cytochalasins

Cytochalasins are a class of compounds that are derived from acetate and L-phenylalanine. They possess fused tricyclic structures comprising a fused pyrrole-cyclohexane ring substituted with a macrocylic ring. The first cytochalasins A (**200**) and B (**201**) were isolated in 1966 by Tamm and Rothweiler[127] and were shown to have the structures below.

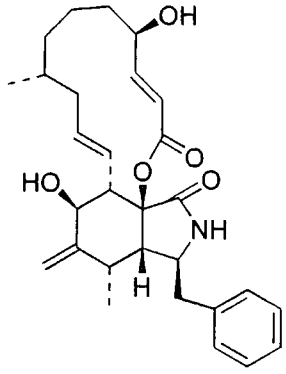

200

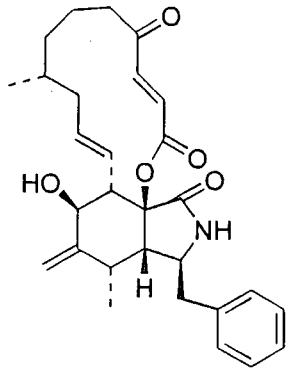

201

Nearly thirty cytochalasins have been isolated and characterised and have attracted attention because of their biological properties. The name cytochalasin is derived from the Greek κντος, meaning cell, and χαλασις, meaning relaxation and refers to the action of cytochalasins on mammalian cells. All cytochalasins inhibit cell division *in vivo* and, at high concentrations, cause ejection of the cell nucleus. In particular,

cytochalasin B inhibits cell movement by altering cells' shapes to that of a thin disc and cytochalasin E causes cells to develop bearing a "thick scalloped margin"[128].

By virtue of their nitrogen atom, cytochalasins are formally alkaloids, but it is most helpful to consider their biosynthesis in terms of a phenylalanine/polyketide pathway. Work by Tamm, Vederas and coworkers showed that cytochalasin B is built from acetate[129] and phenylalanine[130]. Two pendant methyl groups are derived from methionine and the lactone oxygen is derived from a Bayer-Villiger oxidation .

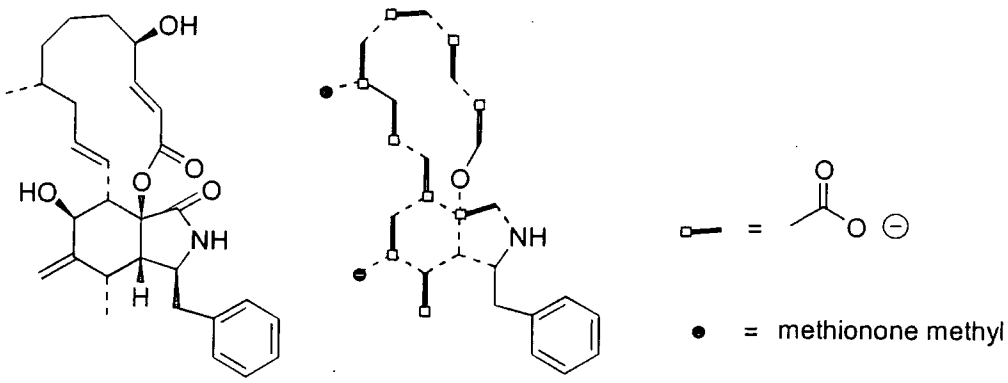

Figure 3-1 The origin of cytochalasin B (**201**) from acetate, methionine and phenylalanine.

3.3 Fungal growth techniques

There are two techniques that are commonly employed for growing fungi in the laboratory. The first is to grow the mycelium on the surface of the static medium where the mycelium grows to cover the surface of the liquid. This method is widely employed, as it is straightforward and is very efficient in terms of space utilisation. However, it does suffer from a number of disadvantages, of which the most significant is inhomogeneous growth. As the mycelium spreads across the surface by sporulation, the mycelium mat contains patches of mature and immature mycelia. This can be used to advantage to ensure that the feeding of a substrate is concomitant with the appropriate period of growth. In a static culture, there is a significant nutrient gradient within the mycelium as the areas on the surface of the mat rely on nutrients being transported through the fungus. This results in static cultures growing much slower than submerged cultures.

Submerged cultures represent an alternative method. In a submerged culture, the broth is inoculated with mycelium and shaken rapidly so that growth occurs within the

medium. As there is no nutrient gradient and there is increased aeration and greater dispersion of spores, submerged cultures grow at a much faster rate than static cultures. Subsequently, accelerated growth results in growth homogeneity. However, the production profile of submerged cultures may be radically different from the same strain incubated as a static culture.

3.4 Rosnecatone

Rosnecatone was first isolated by Edwards[131] in 1997 from *Rosellinia necatrix* The strain had been collected from Portugal and represents one of over one hundred *Rosellinia* species that have been described to date[132]. The structure of rosnecatone was determined by X-ray crystallography and notably possesses a hemiterpene moiety substituted with a hydroxyl group. The central nucleus displays extensive functionalistion and oxygenation.

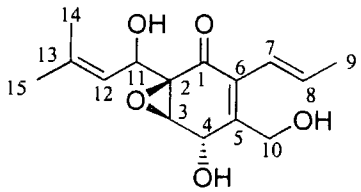

202

The primary basis for selecting rosnecatone as a candidate for biosynthetic study was the presence of the terpene derived moiety in this metabolite. The primary aim of the programme was to investigate the origin of the hemiterpenoid moiety from either the MVA or mevalonate independent pathway. In addition, the presence of a polyketide or shikimate derived nucleus afforded an additional detail of biosynthetic enquiry.
Edwards had also found that in mature cultures of *R. necatrix*, rosnecatone production was accompanied by the production of cytochalasin E (**203**) [133].

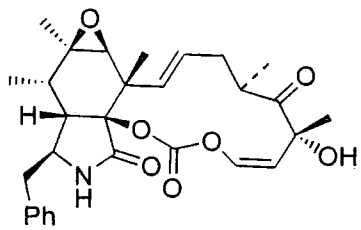

203

Cytochalasin E is structurally different from other cytochalasins in that it possess a carbamate residue. It had also been isolated previously from *R. necatrix*[134] and *Aspergillis clavatus*[135] and possesses antibiotic and cytotoxic properties that are typical of the other cytochalasins. Although there is no formal report on the biosynthesis of cytochalasin E (**203**), it is almost certainly related to cytochalasin B (**201**) in that it is formed from phenylalanine, methionine and a polyketide chain. In the case of cytochalasin E (**203**), the polyketide derived chain is one acetate unit smaller than cytochalasin B (**201**). The presence of two oxygen atoms in the macrocycle suggests the intervention of a further Bayer- Villiger oxidation during the biosynthesis.

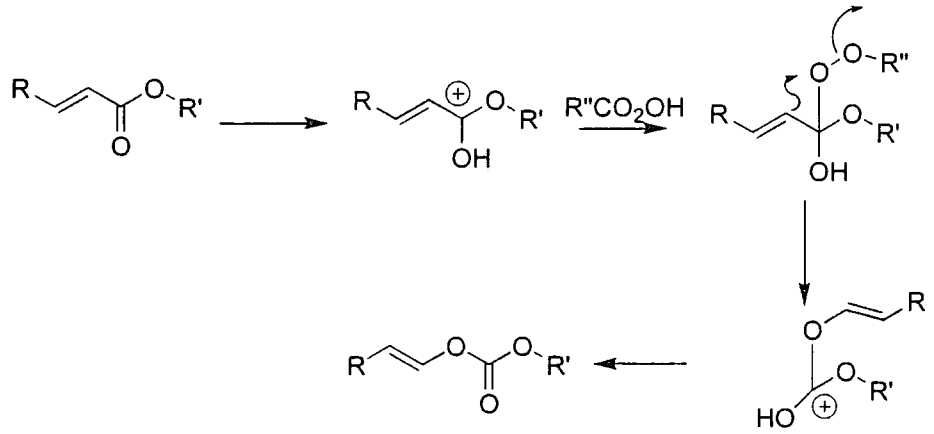

Scheme 3-4 Bayer-Villiger formation of the carbamate residue of cytochalasin E (**203**)

3.4.1 Growth of R. necatrix

Rosellinia are slow growing fungi and require six to eight weeks to achieve cell maturity. One of the first objectives of the project was to determine the maximal growth conditions for rosnecatone production as a static culture. Using malt broth supplemented with 6% glucose, mycelial growth ceased after six weeks. This was evident by the formation of dark areas on the mycelium mat.

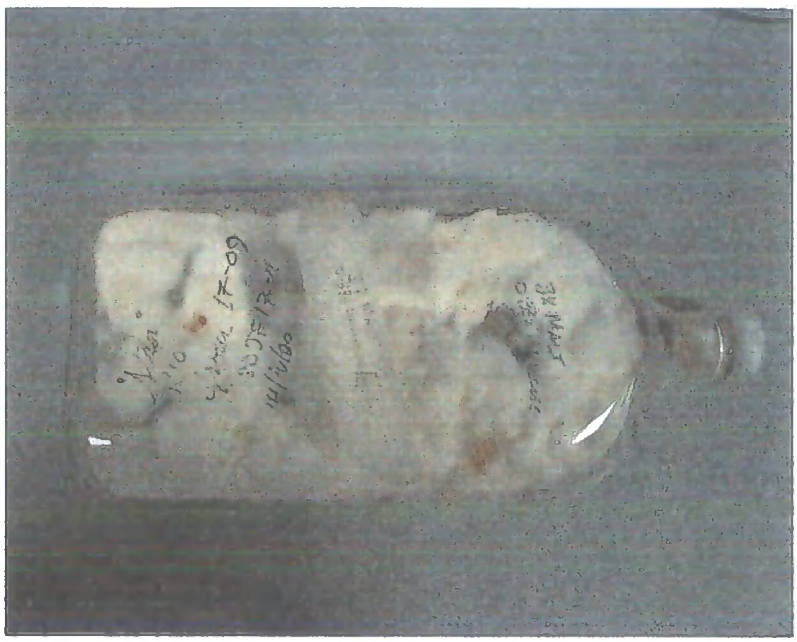

Figure 3-2 Six-week-old culture of *R. necatrix* showing the upper side mycelial mat and spores

Extraction of the broth with ethyl acetate yielded a tacky brown oil that gave rosnecatone as a white crystalline solid after column chromatography. During initial investigations, rosnecatone production ceased after one generation with a concomitant decrease in the mycelial mat thickness. Repeated attempts to elicit rosnecatone production failed as subsequent generations did not grow. Fresh cultures were grown from a slant that had been used previously to seed the producing cultures. Rosnecatone production was restored, but at very low levels (3-5mg per 300ml flask) which decreased vanishingly in subsequent generations.

A new sample of *R. necatrix* was obtained from Edwards (Bradford) and was initially found to yield rosnecatone in batches of 250mg from each flask (300ml). However, upon repeated subculturing from flask to flask, the amount of rosnecatone dramatically decreased with each subculturing, in spite of apparently healthy growth.

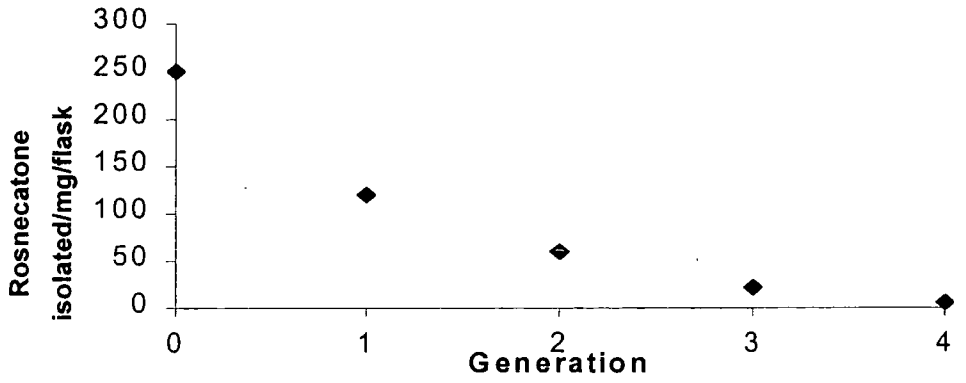

Figure 3-3 Rosnecatone production (mg/flask) as a function of the number of times subcultured (generation)

When the cultures were inoculated from a new slide containing *R. necatrix* spores, rosnecatone production was resumed but at much lower levels, typically no more than 20mg of pure rosnecatone per flask (300ml). Thus, it appeared that rosnecatone production decreases as a function of time.

Edwards also found that rosnecatone production was maximal at 23°C but halted at 27°C[133]. Although this is difficult to rationalise it does support experimental findings as cultures of *R. necatrix* that were grown below 27°C produced rosnecatone more consistently than cultures grown at 31°C. Other external factors also caused variations in rosnecatone production. For example, light had a significant effect, as cultures grown in darkness were slow to reach maturity (typically 12 weeks), had correspondingly thin mycelium beds and did not produce rosnecatone.

The propensity of fungi to alter their production profile is well known. Localised mutations can occur in a mycelium, which although may cause no apparent physical differences, can cause biochemical variations. These variations can manifest themselves as the cessation of secondary metabolite production. Subculturing from such a mutated mycelium area causes subsequent generations to lack the capacity for secondary metabolite production. Such mutations could account for the decreasing yields of rosnecatone although it was beyond the scope of this project to investigate this.

3.4.2 Extraction and purification of rosnecatone

Following the procedure described by Edwards, the broth of a mature culture of *R. necatrix* was extracted several times with ethyl acetate. Removal of the solvent generated a dark brown oil which, after purification by preparative TLC, gave rosnecatone as a white crystalline solid. This initial method was of limited use as prep. TLC is only appropriate for small amounts of material. Furthermore, it was often difficult to perform EtOAc extractions due to the formation of emulsions caused by small mycelium fragments. This problem was overcome by saturating the broth with sodium chloride prior to extraction. If a large amount of debris was present then a filtration under gravity was performed. Column chromatography of the crude extract gave rosnecatone that was of higher purity (^{1}H, ^{13}C NMR) than that obtained by prep. TLC and afforded separation when large amounts of crude extract were delivered. The recovery of rosnecatone from the cells was insignificant.

3.4.3 Spectral assignment of rosnecatone

The structure of rosnecatone is secure from an X-ray crystal structure solved in Bradford. However, the ^{13}C and ^{1}H NMR spectra had not been assigned unambigously. In order to conduct a biosynthetic study, a secure assignment of the ^{1}H and ^{13}C NMR spectra was required.

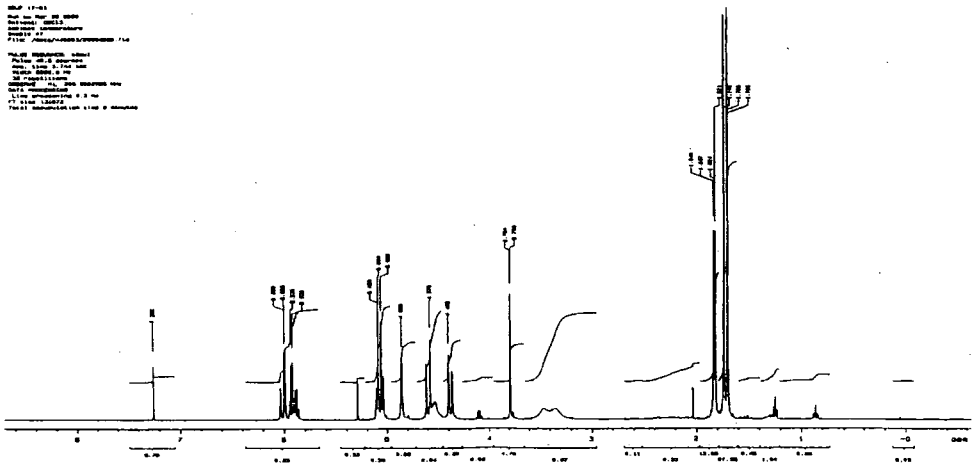

Figure 3-4 ^{1}H-NMR of rosnecatone (**202**)

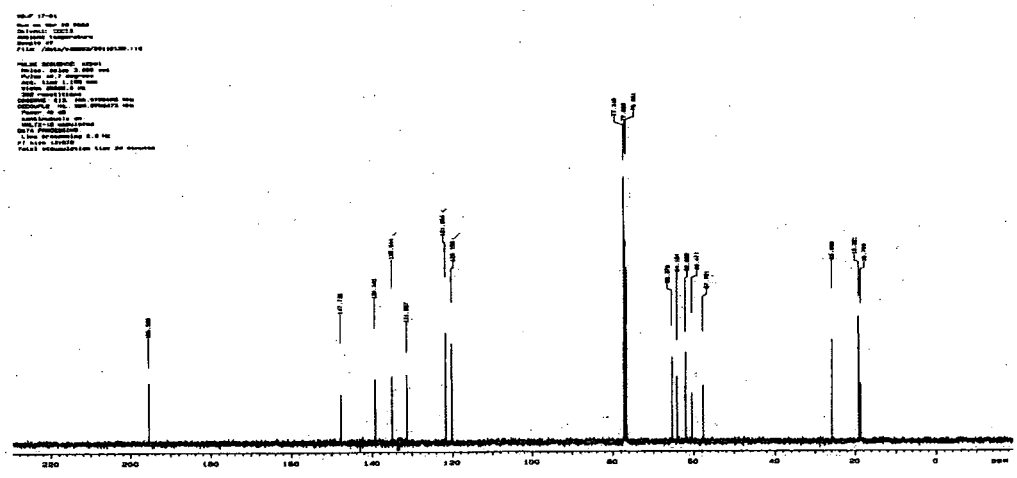

Figure 3-5 ^{13}C-NMR spectrum of rosnecatone (**202**)

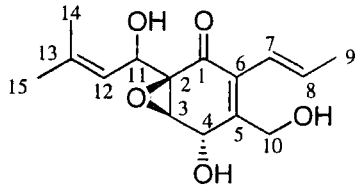

202

Assignment of the proton methyl resonances was trivial as the ^{1}H NMR shows two singlets and one doublet in the high field region. Integration showed that each peak corresponds to three protons. The doublet is derived from C-9 and revealed coupling to the olefinic proton of C-8. A ^{1}H-^{1}H COSY spectrum of rosnecatone showed the proton resonance at C-9 gave an off diagonal peak at 19.2 ppm whilst the two singlets correlated with carbon resonances at 25.9 and 18.7 ppm. These were in good agreement with the assignment of the terminal methyl groups in linalyl acetate.

Once C-9 and H-9 had been assigned, it was relatively straightforward to assign the peaks for C-7 and C-8. Off diagonal coupling between the protons of C-9 and the multiplet at 5.92 ppm demonstrated that the C-8 proton came at 5.92 ppm. As expected, H-8 gave a further off diagonal resonance that corresponded to coupling to H-7. On this basis, H-7 was assigned as the resonance at 6.00 ppm. ^{13}C-^{1}H HETCOR Analysis confirmed that C-7 and C-8 resonances were those at 121.6 and 135.0 ppm respectively. Further examination of the HETCOR spectrum revealed that the carbon peak at 62.0ppm gave rise to a correlation that was directly between the two proton resonances at 4.40 and 4.58 ppm. This could only arise from a diastereotopic methylene group

i.e. C-10. This left only two pairs of peaks that were left unassigned in the proton spectrum; a pair of doublets at 3.79 and 4.87 ppm and another pair downfield at 5.08 and 5.10 ppm. The major difference between the signals was that although both H-3 and H-4 protons that were bonded to a tertiary alcohol, H-12 was olefinic. This was apparent in the HETCOR spectrum whereby the proton resonance at 5.10 ppm correlated with an olefinic signal at 120.2 ppm. From this the H-12 resonance was assigned to 5.10 ppm and the H-11 resonance to 5.08 ppm. Using the HETCOR spectrum, C-11 was found contribute the signal at 65.4 ppm.

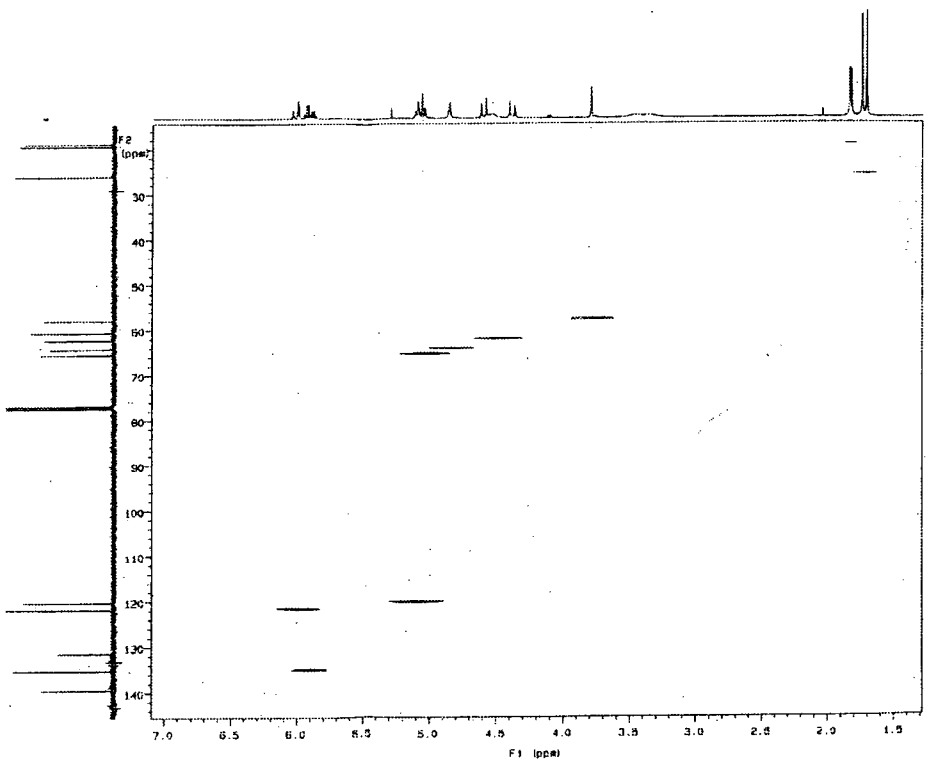

Figure 3-6 HETCOR of rosnecatone (**202**)

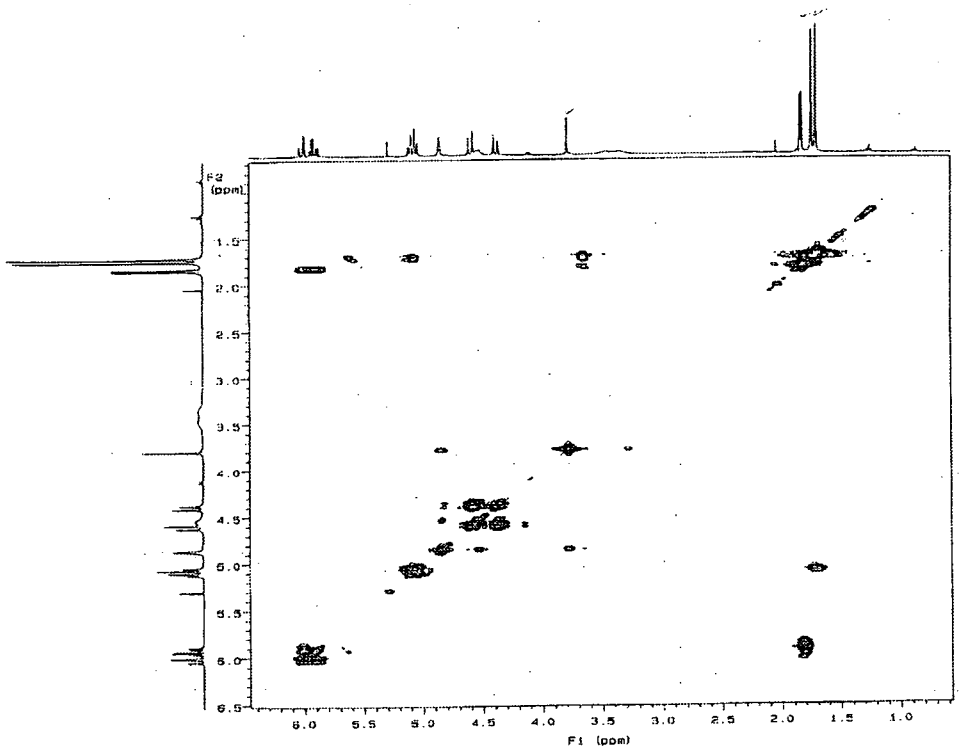

Figure 3-7 COSY of rosnecatone (**202**)

By deduction, the remaining proton resonances were due to H-3 and H-4, which gave correlations in the HETCOR spectrum at 57.7 and 64.1 ppm respectively. Of the non-protonated carbons, the carbonyl peak at 195.5 could be assigned in a straightforward manner to C-1. The remaining centres, C-5, C-6 and C-13, could however, not be assigned unambiguously without recourse to an HMQC experiment.

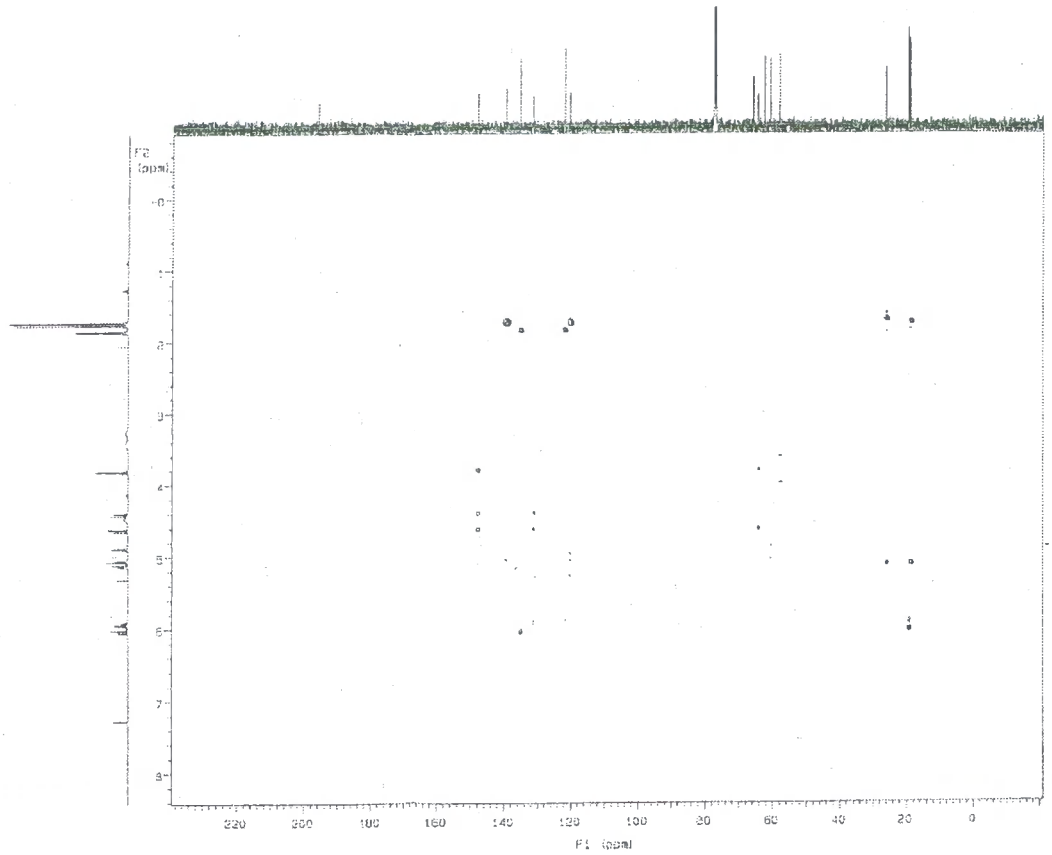

Figure 3-8 HMQC of rosnecatone (**202**)

HMQC Analysis revealed the enhancements as shown below by correlation peaks.

Proton number	*Enhanced signal*
12, 14, 15	139.3
4,10a, 10b	147.7
7	131.0

Table 3-1 Results from HMQC of rosnecatone (**202**)

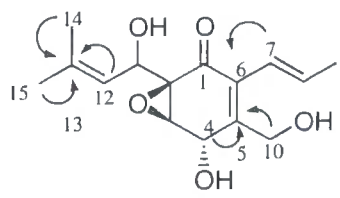

Figure 3-9 Selected HMQC couplings

This data revealed that C-5 is assigned to 147.7, C-6 as 131.0 and C-13 as 139.3. The complete assignment of rosnecatone is described below.

Atom	δ_C	δ_H
1	195.5	-
2	60.5	-
3	57.7	3.79
4	64.1	4.87
5	147.7	-
6	131.0	-
7	121.6	6.00
8	135.0	5.92
9	19.2	1.83
10	62.1	4.40, 4.58
11	65.4	5.08
12	120.2	5.10
13	139.3	-
14	25.9	1.74
15	18.7	1.70

Table 3-2 ^{1}H and ^{13}C resonances of rosnecatone **202**)

3.5 Biosynthetic studies on rosnecatone (202)

The biosynthetic origin of rosnecatone is not clear. The pendant C-5 unit is clearly of terpenoid origin whilst the remaining structure could be delivered from either the shikimate or polyketide pathways.

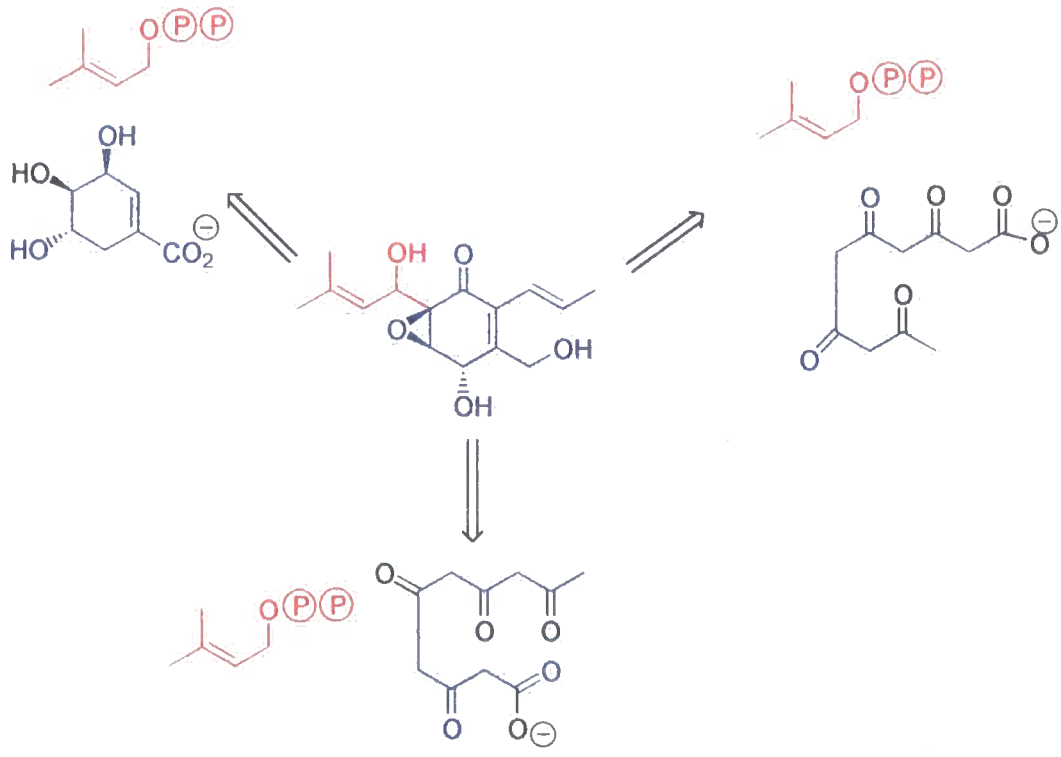

Scheme 3-5 Three putative biosynthetic origins for rosnecatone (**202**)

Furthermore, there are two possible ways in which a polyketide skeleton could arise. The hydroxymethyl carbon, C-10, could derive from either a carboxylate carbon or a acetate methyl carbon depending on which way the polyketide chain is assembled. Clearly there are two pathways by which the terpenoid moiety could be generated either *via* the MVA pathway or the mevalonate independent pathway.

The most straightforward way to determine the origin of the non terpenoid moiety was to feed isotopically labelled acetate to the fungus and assess the labelling pattern in rosnecatone.

3.5.1 Feeding of sodium [1,2-$^{13}C_2$]-acetate

The feeding of sodium [1,2-$^{13}C_2$]-acetate emerged as a key experiment to delineate the pathway by which the terpene fragment was biosynthesised. As described in chapter 2, the MVA pathway delivers two intact acetate units into IPP whereas the mevalonate independent pathway delivers only one intact unit. Furthermore, the level of incorporation of acetate by the mevalonate independent pathway is usually very low as a consequence of processing *via* the TCA cycle, and hence the incorporation is often not observed.

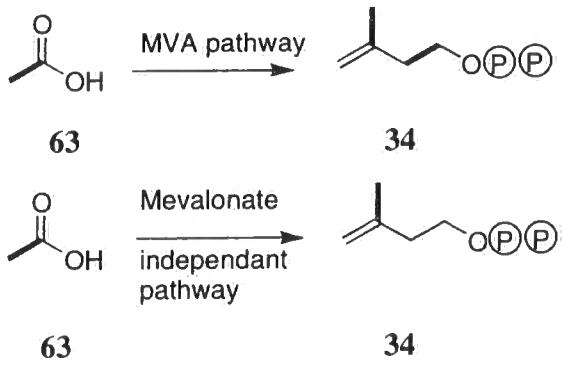

Figure 3-10 Incorporation of [1,2-$^{13}C_2$]-acetate (**63**) into IPP (**34**) *via* the MVA or mevalonate independent pathway

The feeding of sodium [1,2-$^{13}C_2$]-acetate was also anticipated to delineate a shikimate or polyketide origin for the remainder of the molecule. The difference between the shikimate and polyketide pathways is the connectivities that each would employ to deliver the core of rosnecatone. Polyketide assembly from acetate units will maintain the integrity of the all carbon-carbon bonds of the non terpene unit whereas a shikimate origin would result in intact incorporation into only two bonds.

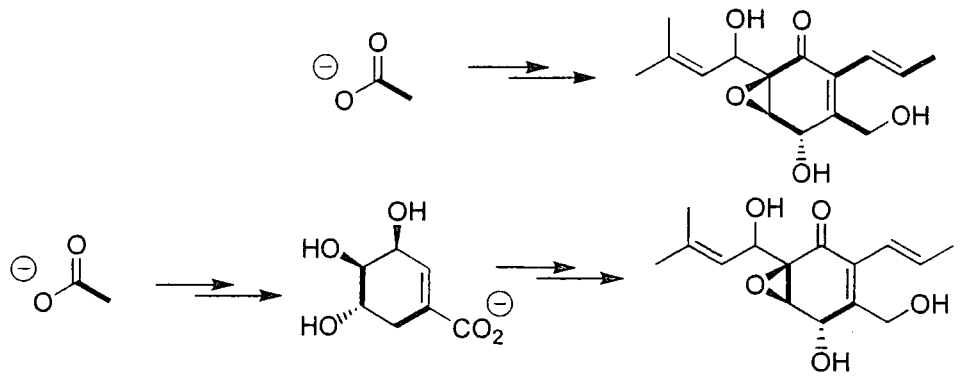

Scheme 3-6 Predicted incorporation patterns from sodium [1,2-$^{13}C_2$]-acetate (**63**) into rosnecatone (**202**) by polyketide and shikimate assembly

Sodium [1,2-$^{13}C_2$]-acetate was pulse fed in three doses to cultures of *R. necatrix* to a final concentration of 4mM, and the rosnecatone was extracted after 36 days following the standard protocol. ^{13}C NMR Analysis of the resultant rosnecatone showed incorporation of intact carbon-carbon bonds consistent with a polyketide assembly.

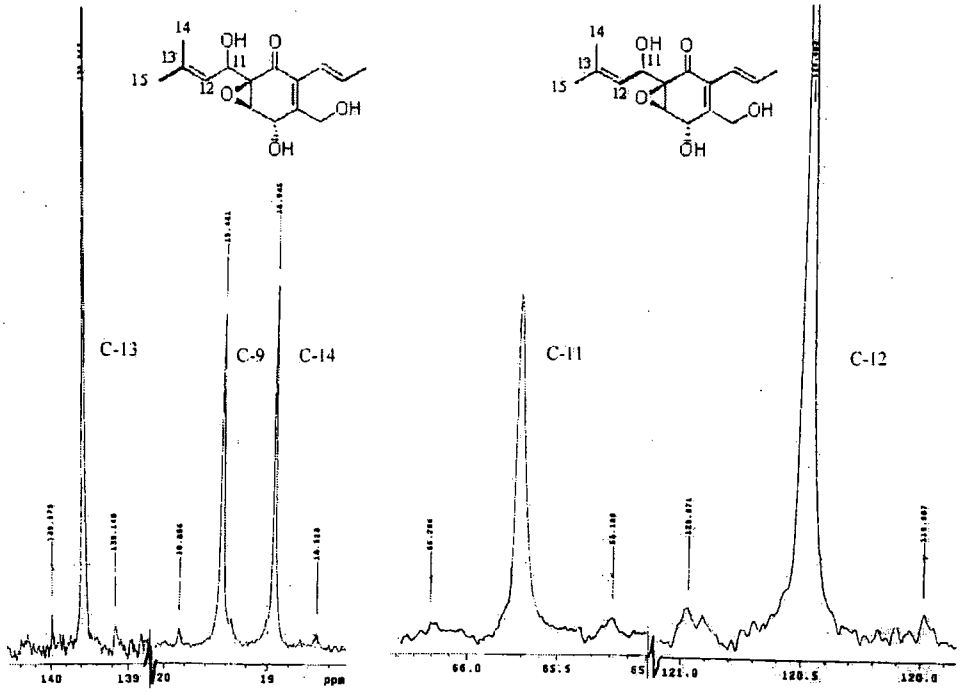

Figure 3-11 ^{13}C NMR resonances of the terpene unit of rosnecatone showing $^{1}J_{13C\text{-}13C}$ coupling. The peaks correspond to the bonds shown in bold on the structures

Carbon atom	*δ_c /ppm*	*$^1J(^{13}C\text{-}^{13}C)$/ Hz*
1	195.5	42.1
2	60.5	42.4
3	57.7	56.9
4	64.1	56.9
5	147.7	55.0
6	131.0	54.6
7	121.6	49.7
8	135.0	48.6
9	19.2	49.9
10	62.1	49.5
11	65.4	50.1
12	120.2	50.1
13	139.3	41.3
14	25.9	41.3
15	18.7	-

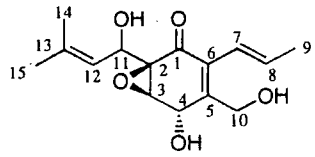

Table 3-3 $^1J_{13C\text{-}13C}$ Coupling constants from rosnecatone after ^{13}C data (125.7 MHz) for rosnecatone showing [1,2-$^{13}C_2$]-acetate incorporation.

$^{13}C\text{-}^{13}C$ Couplings between C-11 and C-12 and between C-13 and C-14 was evident from the ^{13}C NMR spectrum and indicated intact incorporation into four carbons of the terpenoid moiety. No coupling was observed to C-15. These enrichments are consistent with the incorporation of acetate into the terpene unit *via* MVA (**9**) and the MVA pathway. Furthermore, the $^1J_{13C\text{-}13C}$ coupling constants of the non-terpenoid derived enrichments revealed contiguous incorporation of acetate as each carbon was coupled to one of its neighbouring carbon atoms. This pattern is consistent with a polyketide origin of the non terpenoid moiety of rosnecatone.

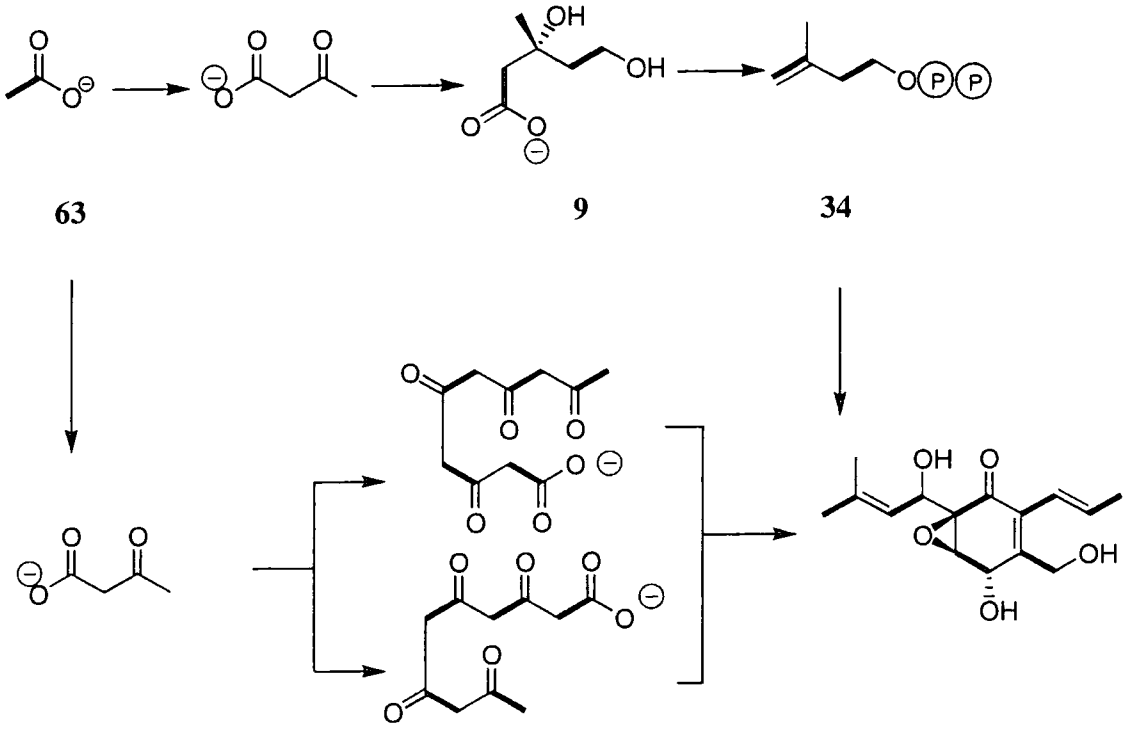

Scheme 3-7 Incorporation of ^{13}C from [1,2-$^{13}C_2$]-acetate (**63**) into rosnecatone (**202**)

This biosynthetic outcome adds further support to the hypothesis that the mevalonate independent pathway is localised in chloroplasts as fungi do not possess chloroplasts.

3.5.2 Determining the orientation of the acetate assembly in the polyketide chain

The feeding of sodium [1,2-$^{13}C_2$]-acetate (**63**) to a culture of *R. necatrix* indicated that the non-terpenoid derived nucleus of rosnecatone was polyketide derived, but the result does not delineate which carbon atoms were derived from C-1 and C-2 of acetate. As described in Scheme 3-7, there are two general ways by which a putative pentaketide can fold to form rosnecatone. Each carbon atom can be derived from either a methyl group or a carboxylate carbon depending on the orientation of the polyketide assembly. The classical method of determining which carbon atoms are derived from the methyl group of acetate is to feed acetate bearing an isotopic label at either C-1 or C-2. For this investigation, single label ^{13}C was unsuitable as the levels of incorporation were very low. An enrichment of similar magnitude (0.3-0.4%) to that observed after feeding [1,2-$^{13}C_2$]-acetate would result in an undetectable increase in ^{13}C-NMR peak height. In an alternative approach, sodium [2-$^{2}H_3$]-acetate (**28**) was chosen as a potential probe as

deuterium has a low natural abundance (0.016%) and deuterium incorporations can be measured by ^{2}H NMR.

In the event, sodium [2-$^{2}H_3$]-acetate (**28**) was added to a culture of *R. necatrix* to a final concentration of 4mM. After 36 days the flask was worked up and the resultant crystalline rosnecatone was analysed *via* deuterium NMR. The spectrum is shown in Figure 3-12.

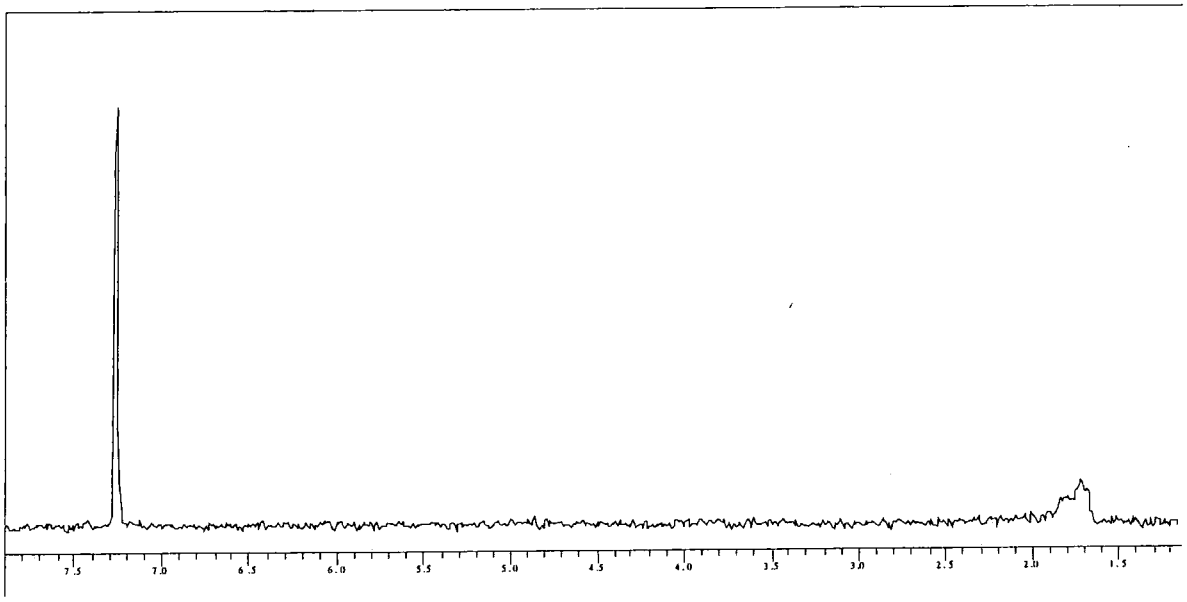

Figure 3-12 ^{2}H NMR Of rosnecatone after feeding sodium [$^{2}H_3$]-acetate (**28**)

There is a region of intensity in the methyl group region between 1.7-1.9 ppm. The peak at 1.7 ppm is accompanied by a peak at 1.8ppm which is approximately half the intensity indicating possible incorporation of deuterium into the three methyl groups at C-9, C-14 and C-15. The isolation of a crystalline sample of rosnecatone gave us confidence that the enrichment was due to deuterium that was incorporated into rosnecatone rather than deuterium incorporation into a contaminating metabolite, such as a lipid.

Most significant is the apparent deuterium incorporation into C-9. If this is the case then the incorporation of acetate from a putative pentaketide can be summarised as shown in Scheme 3-8.

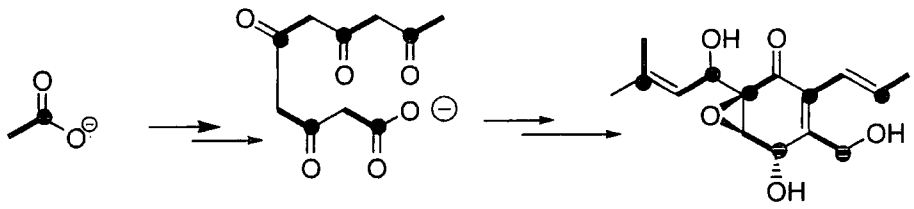

28 202

Scheme 3-8 Conversion of acetate (**28**) to rosnecatone (**202**)

The incorporation of deuterium from [$^2H_3$]-acetate into C-14 and C-15 of the terpenoid group is again consistent with processing of acetate *via* the MVA pathway.

In view of the low incorporation of deuterium from sodium [$^2H_3$]-acetate, another experiment was undertaken to reinforce this result. [6,6-$^2H_2$]-Glucose (**94**) is metabolised to acetate and delivers deuterium into the C-2 of acetate *in vivo*. Accordingly, [6,6-$^2H_2$]-glucose was pulse fed to cultures of *R. necatrix* to a final concentration of 7mM. The sample of rosnecatone that was isolated after feeding [6,6-$^2H_2$]-glucose was crystalline, which again gave confidence that signals in the ^2H NMR spectrum were due to incorporation into rosnecatone. Analysis by ^2H NMR revealed a similar spectrum to that recorded after feeding [$^2H_3$]-acetate. The ^2H NMR is shown in Figure 3-13

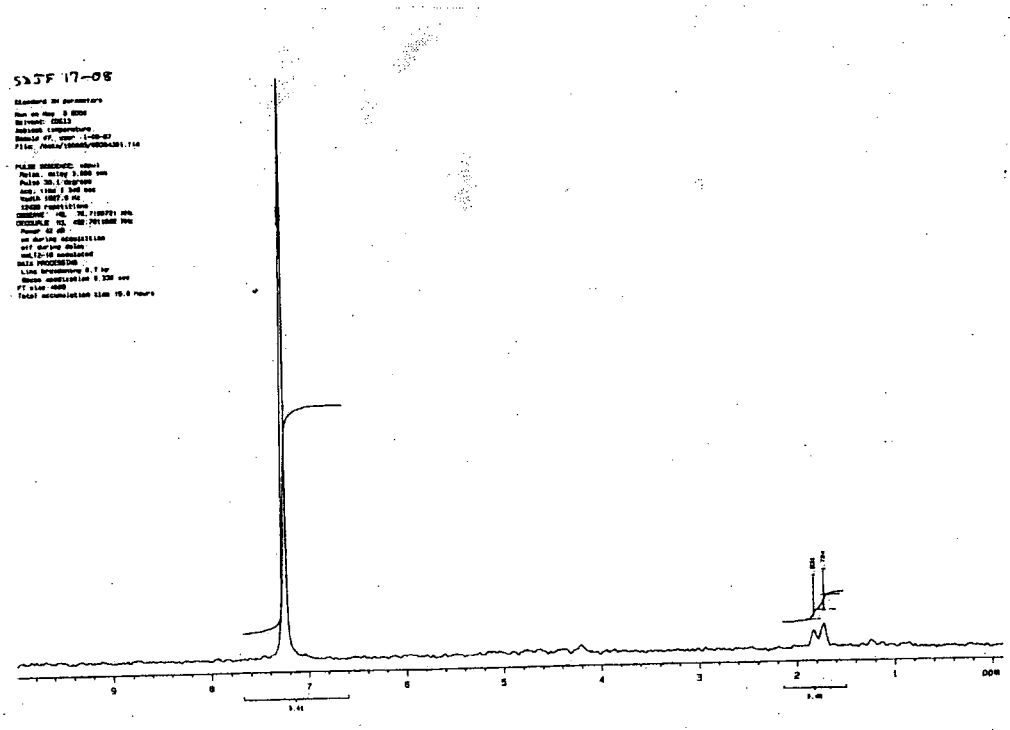

Figure 3-13 ^2H NMR of rosnecatone (**202**) after feeding [6,6-$^2H_2$]-glucose (**94**)

The ^2H NMR spectrum of the resulting rosnecatone showed signals at 1.7 and 1.8 ppm which again indicated incorporation of deuterium into the three methyl groups C-9, C-14 and C-15. No other deuterium signals were apparent.

Clearly, the signals in the ^2H NMR after feeding [6,6-$^2H_2$]-glucose are more intense than those in the ^2H NMR after feeding sodium [$^2H_3$]-acetate. This is a direct consequence of isolating more rosnecatone (43mg) from the flask supplemented with [6,6-$^2H_2$]-glucose than the flask fed with [$^2H_3$]-acetate (23mg) which gives an increased signal to noise ratio and provides a more accurate and reliable indication of deuterium incorporation. It may also represent a higher level of incorporation, however a quantitative assessment of this was not carried out. The incorporations after feeding [6,6-$^2H_2$]-glucose into the terpenoid derived unit are again consistent with the processing of acetate *via* the MVA pathway.

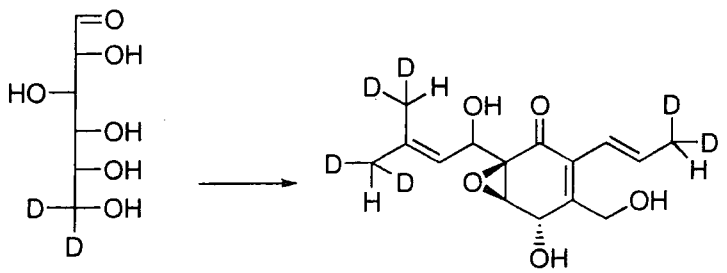

94 **202**

Scheme 3-9 Incorporation of deuterium from [6,6-$^2H_2$]-glucose (**94**) into rosnecatone 202)

3.5.3 Analysis of deuterium incorporation into rosnecatone

The polyketide origin of rosnecatone has some similarity to the biosynthesis of mellein (**204**). Mellein (**204**) was shown to originate from acetate by Simpson and Holker[136] and it bears a structural similarity to rosnecatone. Common structural features are the C_3 and C_1 groups that correspond to C-7 to C-10 of rosnecatone and a central six membered ring.

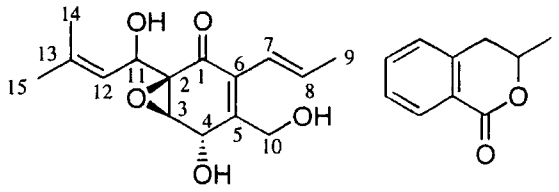

202 **204**

The incorporation of acetate into mellein suggests that it is delivered from a putative pentaketide (**205**) which then undergoes modifications to mellein (**204**).

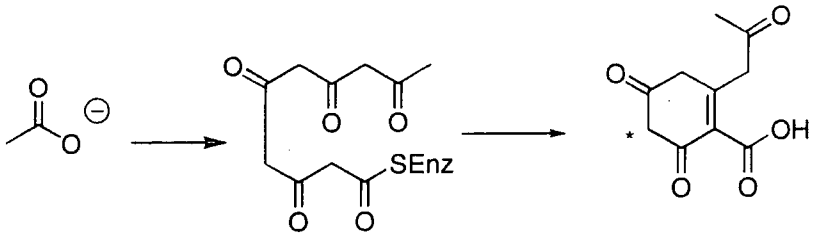

63 **205** **206**

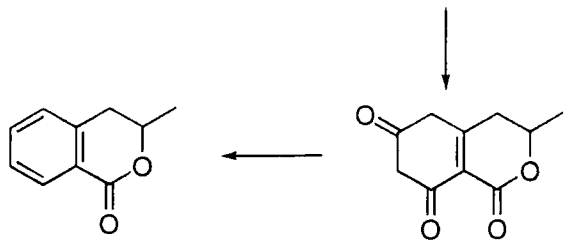

204

Scheme 3-10 Outline of the biosynthesis of mellein (**204**)

Investigations with [2-$^2H_3$]-acetate revealed that a substantial loss of deuterium occurred. The methylene site marked * of **206** lost almost all the deuterium from acetate, presumably due to enolisation during the biosynthesis. This would correspond to the loss of deuterium from C-3 of rosnecatone, and indeed no deuterium was retained at that site in the experiment. Enolisation would also explain the loss of deuterium from C-7 in rosnecatone. The similarity between mellein and rosnecatone both in structure and biosynthesis allows a hypothesis to be developed in which mellein is a biosynthetic precursor to rosnecatone (Figure 3-11).

An elimination of water establishes the pendant chains that form C-7 to C-10 of rosnecatone. Reduction of the carboxylic acid (**207**) followed by hydroxylation and oxidation would yield the polyketide nucleus (**208**). Epoxydation, electrophilic substitution of DMAPP and hydroxylation complete the transformation.

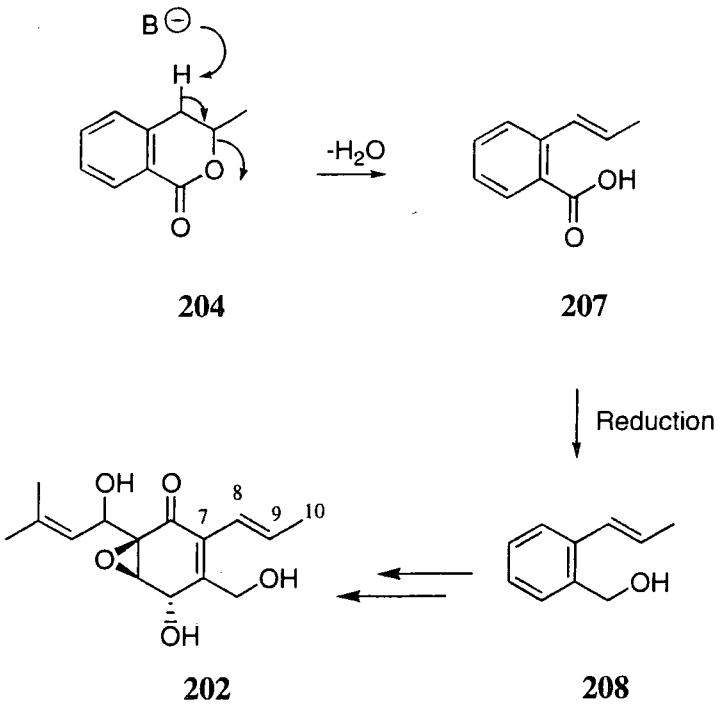

Scheme 3-11 Proposed biosynthesis of rosnecatone from mellein (**204**)

3.6 The effect of changing from a static culture of R. necatrix *to a submerged culture*

Static cultures of *R. necatrix* required six weeks to reach the stage at which they could be harvested for metabolite isolation. It would have been advantageous if this time period could have been reduced and accordingly a method was sought which would facilitate faster growth. As described in section 3.3, shaken cultures generally grow much faster than static cultures due to improved aeration, spore dispersal and nutrient supply, and thus an experiment was undertaken to establish a submerged culture of *R. necatrix.*

Both spores and mycelium were used as inoculate Erlenmeyer flasks containing either standard culture medium or defined medium. The defined medium contained 2% glucose and a trace mineral solution which had previously been developed for use with another submerged fungus, *Beavaria bassiana*, which was used in Durham[137]. No growth was observed for any conditions in which the defined medium was used. Initially the cultures grown in the standard medium were very slow to grow. After ten days a thin mycelium formed on the surface of the broth which, after extraction, gave the same metabolite profile as a static culture.

However, when a sample of innoculum from this culture was used to seed flasks containing standard medium, growth of the submerged culture proceeded very rapidly.

Within three days a thick suspension of white mycelium had formed with a significant decolourisation of the broth. After five days the broth was highly viscous and no further decolourisation or growth was observed.

Figure 3-14 Five day old submerged culture of *R. necatrix*

One of the key objectives was determine if submerged cultures of *R. necatrix* produced rosnecatone. The easiest way to compare the metabolite production profile was *via* TLC. Using EtOAc as the eluent and anisaldehyde stain, rosnecatone appears as a deep red spot with an R_f value of 0.66 and cytochalasin E (**203**) produces a blue spot with an R_f value of 0.73.

Accordingly, samples of crude extracts of a six and twelve week old static cultures of *R. necatrix* were compared by TLC to a crude extract of a five day old submerged culture of *R. necatrix.* The crude extract of the submerged culture was prepared by extraction of the broth and mycelium with EtOAc to give a brown oil. TLC Showed that rosnecatone was not produced in the submerged culture of *R. necatrix* and that metabolite production had been channelled entirely towards cytochalasin E. which was confirmed by visualisation of the plate under UV prior to staining with anisaldehyde. Column chromatography of the crude extract of the subemerged cutlure gave cytochalasan E as a colourless oil which gave ^{13}C and ^{1}H-NMR spectra which were identical to those reported in the literature[138].

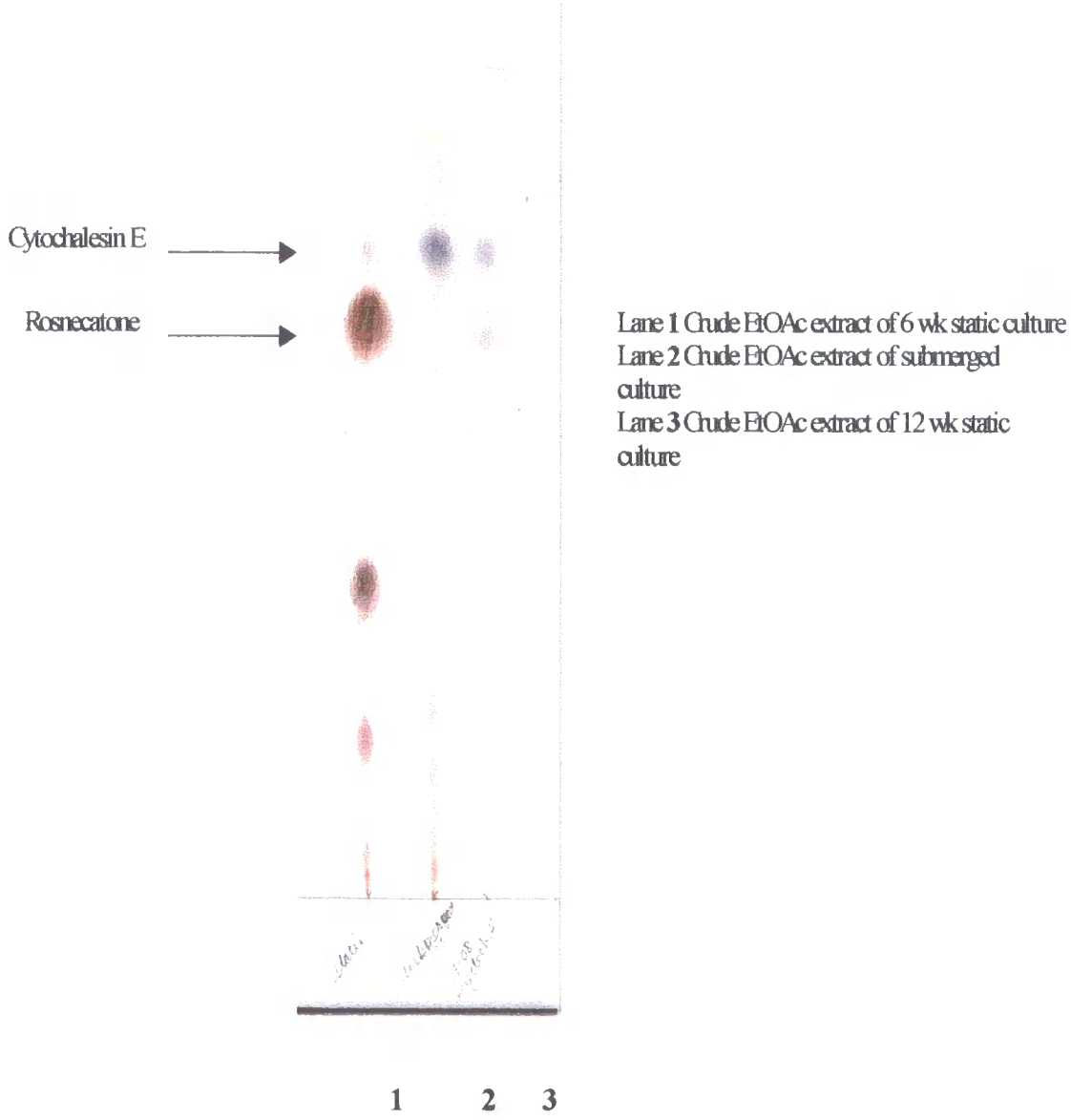

Figure 3-15 TLC of broth extracts showing cytochalasin E production from a submerged culture of *R. necatrix* (lane 2).

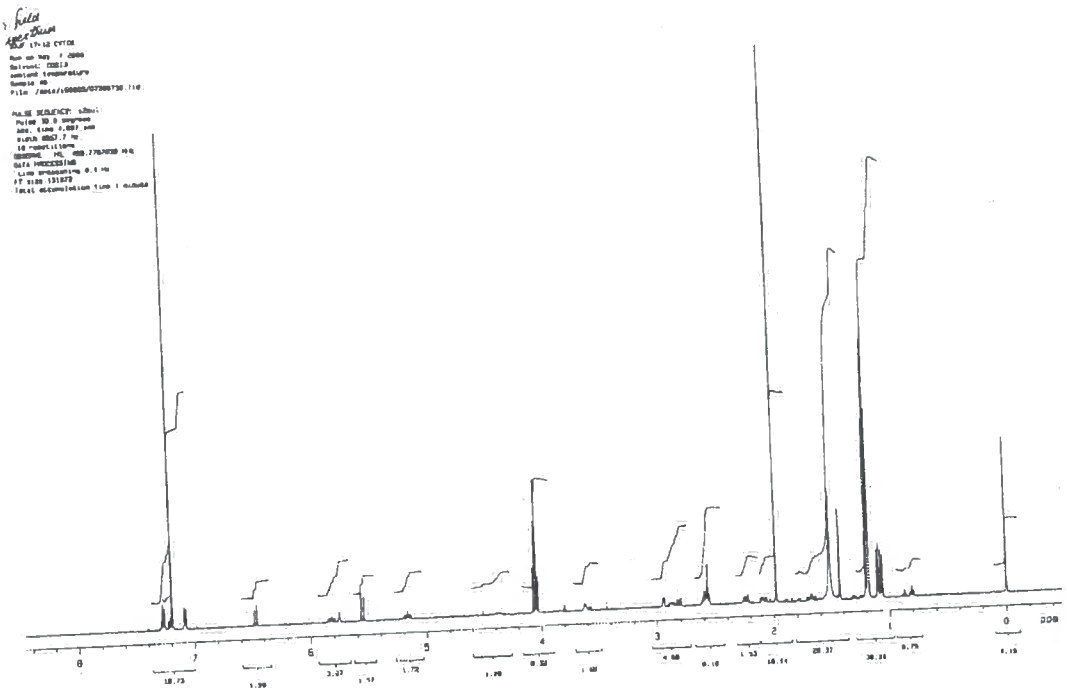

Figure 3-16 ^{1}H NMR spectrum of cytochalasin E (**203**) isolated from a submerged culture of *R. necatrix*

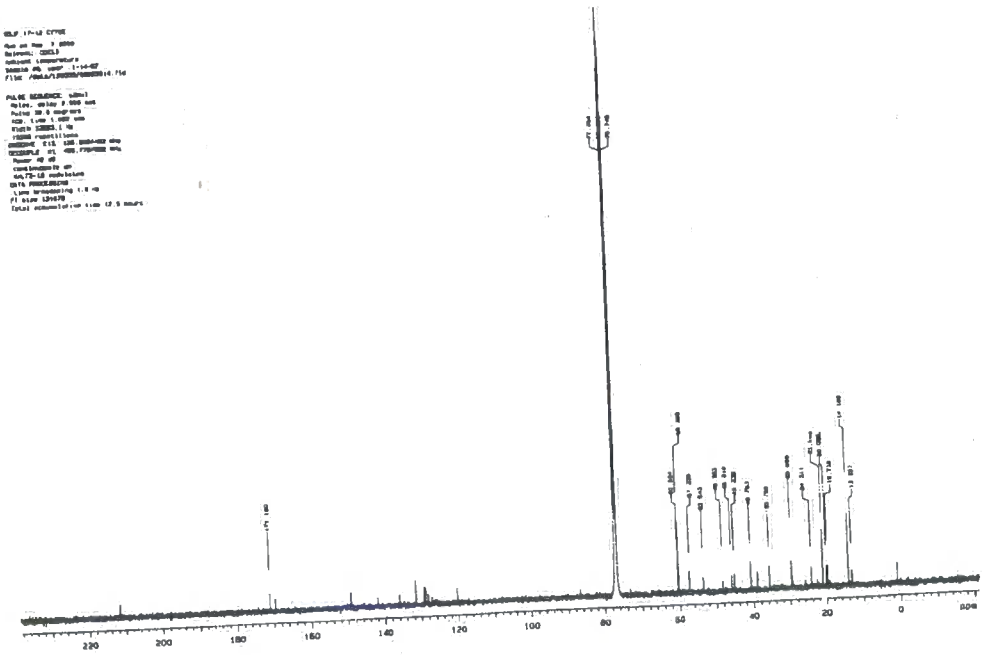

Figure 3-17 ^{13}C NMR spectrum of cytochalasin E (**203**) isolated from a submerged culture of *R. necatrix*

Cytochalasin E generally emerges only after six week in a static culture. The production of cytochalasin E within five days under submerged culture conditions, suggests that the rapid growth rate of the submerged culture caused production of the late onset metabolites rather than rosnecatone, which is observed during the course of growth. Alternatively, the production of cytochalasin E within five days by a submerged culture can also be rationalised in terms of a response to the conditions and represent the formation of a stress metabolite. If this is the case, then the production of cytochalasin E in week six from a static culture represents a sudden stress to the organism. Such a stress could be caused if all the nutrients in the medium became exhausted.

3.7 Biological testing of fungal metabolites

One of the significant features of natural products is their biological toxicity. In view of the low molecular weight and high level of functionality found in rosnecatone it appeared appropriate to screen rosnecatone for potentially useful activity

In collaboration with workers at the Patterson Institute for Cancer Research, Manchester, rosnecatone was tested against two cancer cell lines. The National Cancer Institute protocol was followed whereby a fixed number of cells is plated in a 96 well plate with a titration of the compound under investigation. These were incubated for 5 days and the IC_{50} (the concentration of compound with inhibits 50% of cell growth) was measured.

In experiments with two cell lines, rosnecatone was found to display micromolar levels of toxicity. The IC_{50} against Human ovarian carcinoma cells in DMSO was 4.48 μM and that for Human chronic myelogenous leukaemia was 5.78μM. For a compound to progress to further testing against lung and colon cancer, compounds generally have an IC_{50} below 1μM. The values for rosnecatone are low and suggest that analogues may possess desirable chemotherapeutic properties.

Another fungus, *Xylaria grammica,* provided an additional candidate for screening. A culture of *X. grammica* was obtained from Edwards (Bradford) and extraction of the broth of *X. grammica* resulted in the isolation of a metabolite, which was shown to be epoxydon (**209**). A survey of the literature revealed that the metabolite had been previously isolated from *Penicillium uritcae*[139].

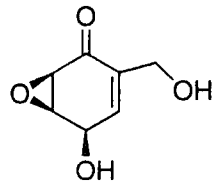

Figure 3-18 Epoxydon (**209**)

3.8 Structure determination of epoxydon (**209**)

^{13}C NMR Spectroscopy showed the new compound had seven carbon atoms of which one was clearly a carbonyl and two others were olefinic. These assignments were made on the basis of chemical shifts. The remaining four carbon signals were clustered in the 53-63 ppm region, suggesting carbon atoms bonded to oxygen.

The ^{1}H NMR indicated that there were six chemically distinct protons, of which two were clearly coupling to each other. Other proton signals were seen as broad doublets with small coupling constants. The presence of an AB system suggested a methylene group in a chiral environment.

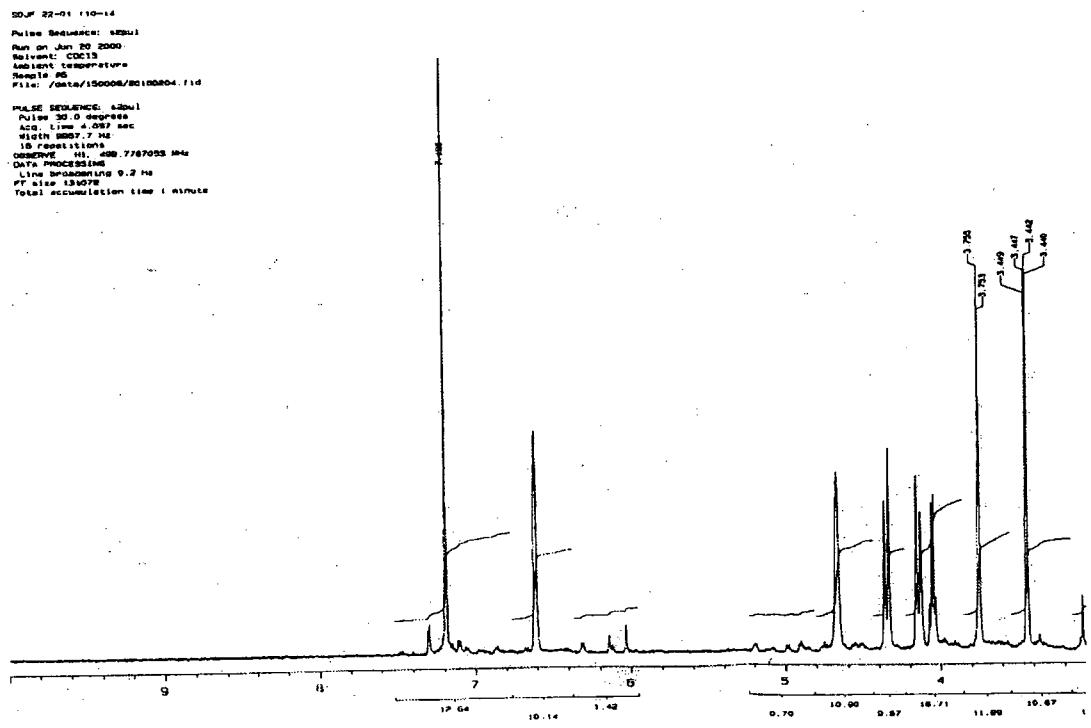

Figure 3-19 ^{1}H NMR spectrum of epoxydon (**209**) isolated from *X. grammicin*

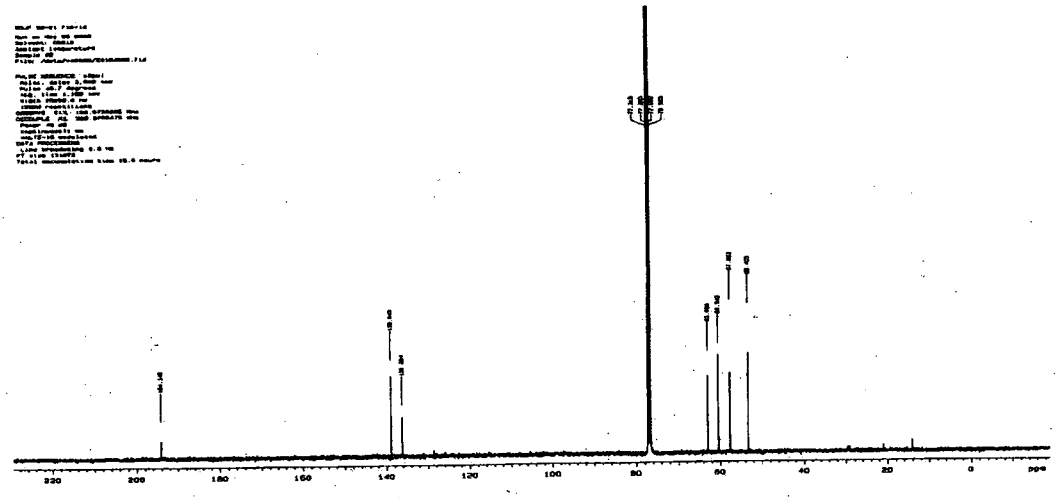

Figure 3-20 ^{13}C NMR spectrum of epoxydon (**209**) isolated from *X. grammicin*

^{1}H-^{1}H COSY NMR Indicated coupling of the signal at 3.40 to 3.78, 3.78 to 4.65 and 4.65 to 6.74. This suggested three protons that were adjacent to one another. However,

coupling was also observed between the olefinic proton and the diastereotopic methylene protons.

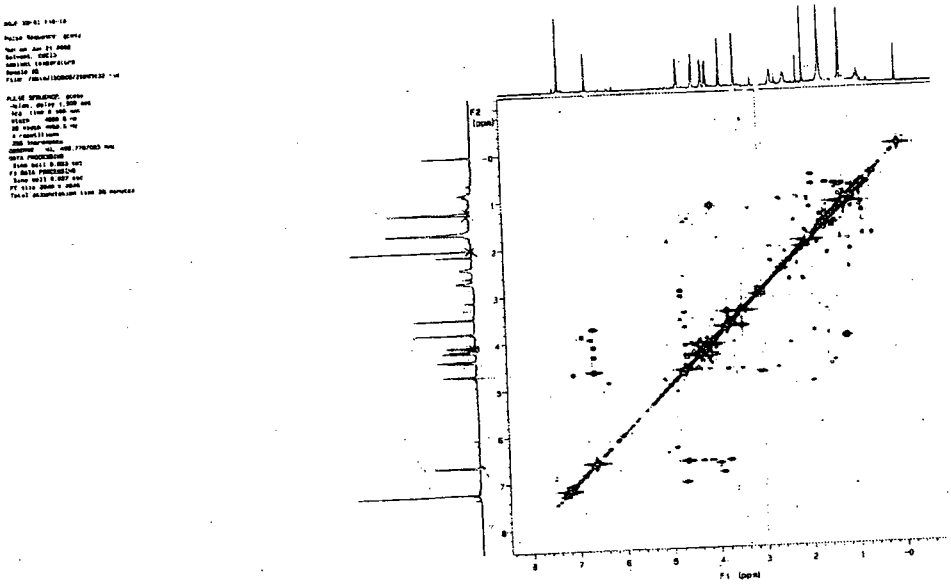

Figure 3-21 ^{1}H-^{1}H COSY spectrum of epoxydon (**209**) isolated from *X. grammicin*

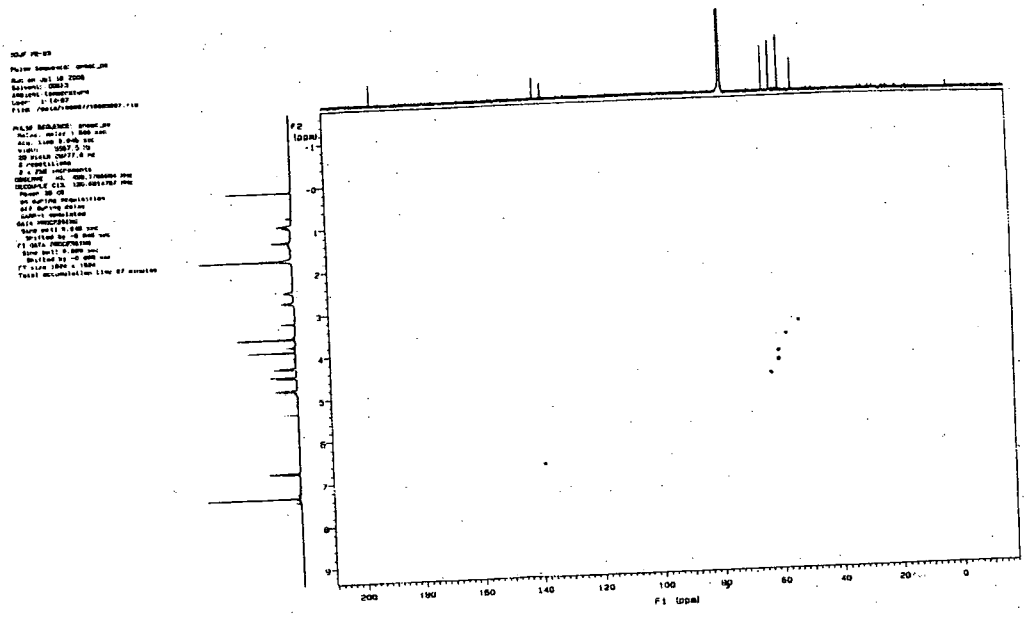

Figure 3-22 ^{1}H-^{13}C HETCOR Of epoxydon (**209**) isolated from *X. grammicin*

The ^{1}H-^{13}C HETCOR spectrum showed that only one olefinic proton was present, which demonstrated that it was a substituted αβ-unsaturated ketone. Two different diastereomers, epoxydon (**209**) and epiepxoydon (**210**), had been isolated from *Penicillium uritcae*[139]

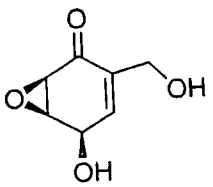

209

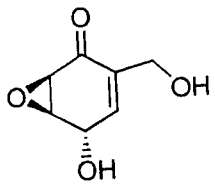

210

In order to determine whether the metabolite was epoxydon (**209**) or epiepoxydon (**210**), it was necessary to determine the relative configuration at C-4. Both epoxydon and epiepoxydon (**210**) have been prepared by synthesis and thus data was available from a number of sources. Epiepoxydon (**210**) has an optical rotation that is nearly double that of epoxydon[140] ($[\alpha]_D$ (epiepoxydon) +256.4° whereas $[\alpha]_D$ (epoxydon) +106.7°). The coupling constants between H-3and H-4 are also diagnostic. The *trans* relationship in epiepoxydon results in a coupling constant between H-3 and H-4 of 5Hz whereas the same coupling in epoxydon is smaller (4Hz). The optical rotation was found to be identical to that of epoxydon ($[\alpha]_D$ +102.2°, c 0.1, MeOH) and the coupling constant between H-2 and H-3 was 4Hz.

It is concluded that the strain of *X. grammicin* that was used produced epoxydon (**209**).

3.8.1 Growth of and extraction of X. grammicin *as a static culture*

X. grammicin was grown on standard medium to produce a mycelium bed very similar in appearance to that of R. necatrix. Six weeks of growth manifested a thin mat with a dark underside. Extraction of the mat with EtOAc yielded 20mg of epoxydon.

3.8.2 Growth of X. grammicin *as a submerged culture*

In light of the unexpected result of transferring *R. necatrix* to a submerged cutlure, the same experiment with *X. grammicin* was repeated. Both mycelium and spores from mature cultures were used to inoculate standard medium and the cultures were shaken

(170rpm) with constant illumination. As in the analogous experiment with *R. necatrix* the first generation culture grew slowly whereas the second generation culture reached maturity within five days. Analysis by TLC showed that the metabolite production was identical to the static culture.

3.8.3 Biological testing of epoxydon

Epoxydon was screened at the Paterson Cancer Institute. The IC_{50} against Human ovarian carcinoma cells in DMSO was 2.54 μM and 16.97 μM against Human chronic myelogenous leukaemia.

These figures are low and are similar to the results found for rosnecatone and suggest that analogues of epoxydon may also possess desirable chemotheraputic properties.

3.9 *Conclusions*

Static cultures of *R. necatrix* produce rosnecatone but production is difficult to control and ceases if the incubation temperature is greater than 31°C. This could represent the presence of mutations in the mycelium that are incapable of rosnecatone production. Rosnecatone is produced by the polyketide and mevalonate pathways, and the orientation of the polyketide chain is such that C-10 is derived from an acetate methyl group. Mature cultures of *R. necatrix* produce the amino acid-polyketide derived metabolite cytochalasin E.

Submerged cultures of *R. necatrix* produce cytochalasin E rather than rosnecatone and grow at an enhanced rate relative to static cultures. This suggests that cytochalasin E is produced as a stress metabolite and is a response to the exhaustion of nutrients in the medium.

Biological testing of rosnecatone and epoxydon against cancer cell lines showed rosnecatone and epoxydon to possess significant cytostatic activity.

	Human ovarian carcinoma/IC_{50} (μM)	Human chronic myelogenous leukaemia/ IC_{50} (μM)
Rosnecatone	4.48	5.78
Epoxydon	2.54	16.97

Table 3-4 Bioactivity table summarising effecy of rosnecatone and epoxydon against two cancer cell lines

Chapter 4

Experimental

4 Experimental

4.1 General

All NMR were recorded on Varian Mercury 200MHz (^{1}H at 199.99 MHz, ^{13}C at 50.30 MHz), Varian Unity 300MHz (^{1}H at 299.908 MHz, ^{13}C at 75.45MHz), Varian VXR 400(S) (^{1}H at 399.95 MHz, ^{13}C at 100.58 MHz), or Varian 500MHz (^{1}H at 500.137 MHz, ^{13}C at 125.76 MHz, ^{2}H at 76.77 MHz). Chemical shifts are reported in parts per million quoted relative to the residual proton peak of $CDCl_3$ at 7.27ppm or central ^{13}C triplet peak at 77.0 ppm. Coupling constants are reported in hertz.

Infra red spectra were recorded with absorbance values in cm^{-1} using a Perkin Elmer 257 between NaCl plates.

Mass spectra of synthetic samples were performed using a VG Analytical 7070E mass spectrometer. Mass spectra of samples of linalyl acetate were recorded using a VG TRIO 1000 mass spectrometer equipped with a HP 1 Ultra column.

The solvents used in reactions were dried, distilled and stored under nitrogen prior to use: diethyl ether (sodium, benzophenone), dichloromethane (calcium hydride), THF (sodium, benzophenone), acetone (phosphorus pentoxide), and pyridine (calcium hydride). Petrol refers to the 40-60°C boiling fraction of petroleum ether. HPLC grade heptane was used throughout.

Reaction glassware was oven dried (120°C) prior to use and cooled under nitrogen. Where anhydrous conditions were required, reactions were carried out under dry nitrogen atmosphere.

Thin layer chromotography was performed using Kieselgel 60 glass backed plates and preparative thin layer chromotography using Merck F_{254} glass backed plates with a 1cm thickness. Plates were visualised by the use of a UV lamp or by the use of permanganate, phosphomolybdic acid or anisaldeyde stains.

Flash chromotography was performed using Merck, Kieselgel 60 (230-400 mesh).

Melting points were measured on a Gallenkamp variable heater and are uncorrected.

4.2 *Growth and maintenance of M. citrata C18*

A solution of Murashige and Skooge medium (2.2g) and glucose (15g) or fructose (15g) in distilled water (500ml) was adjusted to pH 5.5 by the addition of 1M NaOH. Transformed cultures of *M. citrata* were subcultured at ≈ 2g per flask (50ml of medium) after 20-25 days growth and grown under a 24h day at 29.1°C on an orbital shaker (99rpm).

4.2.1 *Extraction of linalyl acetate M. citrata C18 (78)*

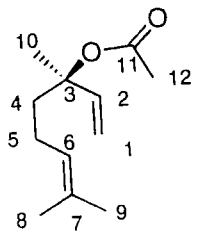

4.2.1.1 *Procedure 1*

After 28 days of growth, the shooty teratoma were harvested, dried between filter papers and air dried for one hour to yield 11g of material per flask. The dry plants were then blended using a Waring blender into heptane (3 x 200ml) in short bursts (5x1min) and the heptane decanted into a centrifuge bottle. The heptane was centrifuged (4°C, 6000rpm, 10min) and removed to produce a green oil containing linalyl acetate (11mg of linalyl acetate per flask).

δ_H ($CDCl_3$) 1.55 (3H, s, H-10), 1.58 (3H, s, H-8), 1.69 (3H, s, H-9), 1.75 (4H, m, H-4, H-5), 2.01 (3H, s, H-12), 5.10 (1H,m, H-6), 5.25 (2H, m, H-1), 5.89 (1H, d, J 7.4, 7.6, H-2)

δ_C ($CDCl_3$) 17.8 (C-8), 23.9 (C-10), 22.4 (C-12), 22.6 (C-5), 25.9 (C-9), 39.9 (C-4), 83.1 (C-3), 113.3 (C-1), 124. 0 (C-2), 132.0 (C-7), 142.0 (C-6), 170.1 (C-11)

4.2.1.2 *Procedure 2*

After 28 days of growth, the shooty teratoma were harvested, dried between filter papers and air dried for one hour to yield 11g of material per flask. After chopping into 1 cm^2 pieces, the tissues were soxhlet extracted into heptane (500ml) for 24 h. Removal of the solvent under reduced pressure followed by removal of residual heptane under high vacuum (1 min.) yielded a green oil containing linalyl acetate (6mg of linalyl acetate per flasks).
Analytical data is described in 4.2.1.1.

4.2.2 *Feeding of substrates to* M. citrata

4.2.2.1 *Feeding of [1-^{13}C]-glucose* (68)

On days 7, 13 and 19, [1-^{13}C]-glucose (49 mg) was dissolved in water (2ml) and administered through a sterile filter unit to two flasks of *M. citrata* to a final concentration of 8.4 mM. The cultures were worked up using procedure 1.

4.2.2.2 *Feeding of sodium [1,2-$^{13}C_2$]-acetate* (63)

On days 7, 13 and 19, sodium [1,2-$^{13}C_2$]-acetate (16 mg) was dissolved in water (2ml) and administered through a sterile filter unit to two cultures of *M. citrata* to a final concentration of 5.6 mM. The cultures were worked up using procedure 1.

4.2.2.3 *Feeding of [6,6-$^{2}H_2$]-glucose* (94)

On days 7, 13 and 19, [6,6-$^{2}H_2$]-glucose (49 mg) was dissolved in water (2ml) and administered through a sterile filter unit to two cultures of *M. citrata* to a final concentration of 8.4 mM. The cultures were worked up using procedure 1.

4.2.2.4 Feeding of [3-^{13}C]-alanine(**90**)

On days 5, 11 and 17, [3-^{13}C]-alanine (10 mg) was dissolved in water (2ml) and administered through a sterile filter unit to two cultures of *M. citrata* to a final concentration of 3.2 mM. The cultures were worked up using procedure 1.

4.2.2.5 Feeding of [3-$^{2}H_3$]-alanine (**93**)

On days 5, 11 and 17, [3-$^{2}H_3$]-alanine (11 mg) was dissolved in water (2ml) and administered through a sterile filter unit to two cultures of *M. citrata* to a final concentration of 3.3 mM. The cultures were worked up using procedure 1.

4.2.2.6 Feeding of [3-$^{13}C^{2}H_3$]-alanine (**86**)

On days 5, 11 and 17, [3-$^{13}C^{2}H_3$]-alanine (11 mg) was dissolved in water (2ml) and administered through a sterile filter unit to two cultures of *M. citrata* to a final concentration of 3.3 mM. The cultures were worked up using procedure 1.

4.2.2.7 Feeding of [$^{2}H_8$]-glycerol (**101**)

On days 6, 13 and 18, [$^{2}H_8$]-glycerol (17 mg) was dissolved in water (2ml) and administered through a sterile filter unit to two cultures of *M. citrata* to a final concentration of 5 mM. The cultures were worked up using procedure 1.
A repeat experiment was also performed using the above procedure to feed to a final concentration of 8.8 mM

4.2.2.8 Feeding of R-[$^{2}H_2$]-glycerol (**102**)

On days 7, 13 and 19, *R*-[$^{2}H_2$]-glycerol (31 mg) was dissolved in water (2ml) and administered through a sterile filter unit to two cultures of *M. citrata* to a final concentration of 9.7 mM. The cultures were worked up using procedure 1.

4.2.2.9 Feeding of S-[$^2H_2$]-glycerol (**103**)

On days 7, 13 and 19, *S*-[$^2H_2$]-glycerol (28 mg) was dissolved in water (2ml) and administered through a sterile filter unit to two cultures of *M. citrata* to a final concentration of 9.1 mM. The cultures were worked up using procedure 1.

4.2.2.10 Feeding of sodium [2,2,3,3-$^2H_4$]-succinate (**84**)

On days 7, 13 and 19, sodium [2,2,3,3-$^2H_4$]-succinate (38 mg) was dissolved in water (2ml) and administered through a sterile filter unit to two cultures of *M. citrata* to a final concentration of 7.1 mM. The cultures were worked up using procedure 1.

4.2.2.11 Feeding of [1,1-$^2H_2$]-isopentenyl alcohol(**188**)

On days 7, 13 and 19, [1,1-$^2H_2$]-isopentenyl alcohol (15.3 mg) was dissolved in water (2ml) and administered through a sterile filter unit to two cultures of *M. citrata* to a final concentration of 5.2 mM. The cultures were worked up using procedure 1.

4.2.2.12 Feeding of [1,1-$^2H_2$]-dimethylallyl alcohol (**167**)

On days 7, 13 and 19, [1,1-$^2H_2$]-dimethyl allyl alcohol (14 mg) was dissolved in water (2ml) and administered through a sterile filter unit to two cultures of *M. citrata* to a final concentration of 4.8 mM. The cultures were worked up using procedure 1.

4.2.2.13 Feeding of [4-^2H]-DX (**116**)

On days 7, 13 and 19, [4-^2H]-DX (20 mg) was dissolved in water (2ml) and administered through a sterile filter unit to two cultures of *M. citrata* to a final concentration of 4.4 mM. The cultures were worked up using procedure 1.

4.2.2.14 Feeding of [4,5,5-$^2H_3$]-DX (141)

On days 7, 13 and 19, [4,5,5-$^2H_3$]-DX (21 mg) was dissolved in water (2ml) and administered through a sterile filter unit to two cultures of *M. citrata* to a final concentration of 4.7 mM. The cultures were worked up using procedure 1.

4.3 *Growth and maintenance of* E. coli

E. coli cultures were grown in standard Luria-Bertani medium containing tryptic soy broth (10g/l), yeast extract (5g/l) and NaCl (10g/l) and the pH adjusted to pH 7.5 by the addition of 0.2M NaOH. Starter cultures were grown in 100ml conical flasks containing 35ml of medium and production cultures were grown in 1l flasks containing 500ml of medium.

Cultures were incubated at 29°C and 130rpm under constant illumination.

4.3.1 Extraction of ubiquinone (80) *from E. coli*

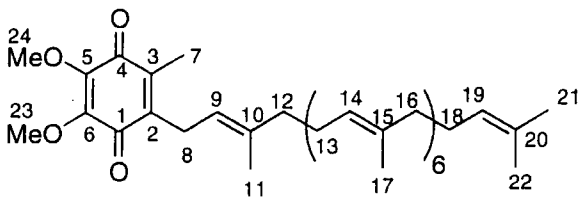

80

Mature cultures of *E. coli* were decanted into centrifuge bottles and centrifuged at 14000rpm at 4°C for 35 min. The cells were collected (1g/l), combined and freeze-dried overnight and crushed to give a free flowing yellow powder. The cells were extracted by refluxing in a 3:1 mixture of DCM/MeOH (250ml) three times and the extracts combined. Removal of the solvent under reduced pressure yielded a dark yellow solid (up to 150mg). The solid was extracted using heptane (3 x 50ml) and the solvent removed to yield a tacky oil (typically 75mg). Column chromotography with EtOAc as the eluent gave ubiquinone-8 (**80**) (R_f = 0.29) as a yellow solid (4mg).

δ_H ($CDCl_3$) 1.56-1.59 (21H, br s, H-11, H-17), 1.69 (3H, s, H-21), 1.78 (3H, s, H-22), 1.98-2.07 (28H, m, H-12, H-13, H-16, H-18), 3.20 (2H, d, J 7, H-8), 3.98 (3H, s, H-23), 3.99 (3H, s, H-24), 4.95 (1H, t, J 7, H-9), 5.05 (7H, s, H-14, H-19).

4.3.2 Feeding of labelled substrates to E. coli

4.3.2.1 Feeding of [6,6-$^2H_2$]-glucose (94) to E. coli

[6,6-$^2H_2$]-Glucose (500 mg) was dissolved in water (2ml) and administered through a sterile filter unit to eight production cultures (500ml) f *E. coli* to a concentration of 0.7mM. The cultures were worked up using the standard procedure.

*4.3.2.2 Feeding of [*methyl-$^2H_3$*]-methionine (192) to* E. coli

[*methly*-$^2H_3$]-Methionine (200mg) was dissolved in water (2ml) and administered through a sterile filter unit to eight production cultures (500ml) of *E. coli* to a concentration of 0.3 mM. The cultures were worked up using the standard procedure.

4.3.2.3 Feeding of [$^2H_5$]-glycerol (101) to E. coli

[$^2H_5$]-Glycerol (766 mg) was dissolved in water (2ml) and administered through a sterile filter unit to eight production cultures (500ml) of *E. coli* to a concentration of 1.9 mM. The cultures were worked up using the standard procedure.

4.3.2.4 Feeding of [1,1-$^2H_2$]-ME (211) to E. coli

[1,1-$^2H_2$]-ME (640 mg) was dissolved in water (2ml) and administered through a sterile filter unit to eight production cultures (500ml) of *E. coli* to a concentration of 1.2 mM. The cultures were worked up using the standard procedure.

4.3.2.5 Feeding of [1,1-$^2H_2$]-isopentenyl alcohol (34) to E. coli

[1,1-$^2H_2$]-Isopentenyl alcohol (880 mg) was dissolved in water (2ml) and administered through a sterile filter unit to eight production cultures (500ml) of *E. coli* to a concentration of 2.5mM. The cultures were worked up using the standard procedure.

4.3.2.6 Feeding of [1,1-$^2H_2$]-dimethyallyl alcohol (167) *to* E. coli

[1,1-$^2H_2$]-Dimethylallyl alcohol (800 mg) was dissolved in water (2ml) and administered through a sterile filter unit to eight production cultures (500ml) of *E. coli* to a concentration of 2.3mM. The cultures were worked up using the standard procedure.

4.3.2.7 Feeding of [1,1,2-$^2H_3$]-3-methyl-but-3-ene-1,2-diol (176 *to* E. coli

[1,1,2-$^2H_3$]-3-Methyl-but-3-ene-1,2-diol (430 mg) was dissolved in water (2ml) and administered through a sterile filter unit to eight production cultures (500ml) of *E. coli* to a concentration of 1.1mM. The cultures were worked up using the standard procedure.

4.3.2.8 Feeding of [4,4-$^2H_2$]-erythritol (177) *to* E. coli

[4,4-$^2H_2$]-Erythritol (820 mg) was dissolved in water (2ml) and administered through a sterile filter unit to eight production cultures (500ml) of *E. coli* to a concentration of 1.7 mM. The cultures were worked up using the standard procedure.

4.3.2.9 Feeding of [1,1-$^2H_2$]-(E)-2-methyl-but-2-ene-1,4-diol (182) *to* E. coli

[1,1-$^2H_2$]-(E)-2-methyl-but-2-ene-1,4-diol (980 mg) was dissolved in water (2ml) and administered through a sterile filter unit to eight production cultures (500ml) of *E. coli* to a concentration of 2.4 mM. The cultures were worked up using the standard procedure.

4.3.2.10 Feeding of [4,4-$^2H_2$]-(Z)-2-methyl-but-2-ene-1,4-diol (187) *to* E. coli

[4,4-$^2H_2$]-(Z)-2-methyl-but-2-ene-1,4-diol (600 mg) was dissolved in water (2ml) and administered through a sterile filter unit to eight production cultures of *E. coli* to a concentration of 1.5 mM. The cultures were worked up using the standard procedure.

4.4 Growth of Rosellinia sp. *and* Xylaria grammicin

4.4.1 Preparation of standard fungal broth

A solution of glucose (18g) and Oxoid malt broth (9g) in distilled water (300ml) and the solution autoclaved at 110°C for one hour in the appropriate flask. After autoclaving, the bottles were allowed to cool to ambient temperature in a laminar flow hood.

4.4.2 Growth of static cultures

Mycelia (3 pieces, 6cm^2 total area) from established cultures or from slants was used to inoculate P bottles or 20/20 bottles (Bottoms Up, Durham) containing standard fungal broth (300ml). Cultures were grown at an angle of 10° under constant illumination between 24-27°C and harvested after eight weeks.

4.4.3 Growth of submerged cultures

For the first generation of submerged cultures, 250ml conical flasks were charged with standard fungal broth (75ml), inoculated with mycelium (4 x 3cm^2) from static cultures and grown at 29°C, 170 rpm under constant illumination. After 10 days growth a produce a thin mycellial suspension was used which was used to innoculate (5ml) 250ml conical flasks containing standard fungal broth (75ml). Subsequent generations were inoculated flask to flask with 10% innoculum.

4.4.4 Isolation of rosnecatone (202) from static cultures of R. necatrix

Culture supernatant of mature cultures of *Rosellinia sp* was decanted from the bottle and filtered under gravity. The supernatant was then saturated with sodium chloride and extracted with EtOAc (3 x 300ml). Removal of the solvent under reduced pressure afforded a dark brown tacky oil (typically 200mg) which was purified by column chromotography (silica, EtOAc) to yield rosnecatone (202) (up to 20mg) as a white crystalline solid (R_f = 0.66).

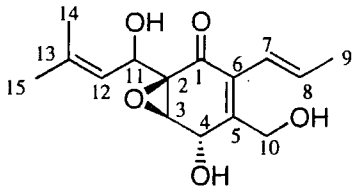

M/z (EI) 280 (12.6%, $[M]^+$), 263 (5.7%, $[M-H_2O]^+$)

δ_H ($CDCl_3$) 1.70 (3H, s, H-15), 1.74 (3H, s, H-14), 1.83 (3H, d, ^2J 6.4, H-9), 3.80 (1H, d, ^2J 5.2, H-3), 4.40 (1H, d, ^1J 14.8, H-10), 4.58 (1H, d, ^1J 14.8, H-10), 4.87 (1H, d, ^2J 5.2, H-4), 5.08 (1H, d, ^2J 8.8, H-11), 5.10 (1H, d, ^2J, 8.4, H-12), 5.92 (1H, dq, J 6.4, 15.6, H-8), 6.00 (1H, d, ^2J 15.6, H-7)

δ_c($CDCl_3$) 18.7 (C-15), 19.2 (C-9), 25.9 (C-14), 57.7 (C-3), 60.5 (C-2), 62.1 (C-10), 64.1 (C-4), 65.4 (C-11), 120.2 (C-12), 121.6 (C-7), 131.3 (C-6), 135. (C-8), 139.3 (C-13), 147.7 (C-5), 195.5 (C-1).

*4.4.5 Isolation of cytochalasan E (**203**) from submerged cultures of* R. necatrix

A mycelium suspension of submerged cultures of *R. necatrix* was removed after 5 days growth by centrifugation (6000rpm, 4°C, 10 min) to produce a mycelium pellet and a yellow supernatant. Extraction of the supernatant with EtOAc (3x 100ml) followed by removal of the solvent yielded a pale brown oil (50mg). Column chromotography (silica, EtOAc) yielded cytochalasan E (**203**) as a colourless oil (6mg, R_f=0.77).

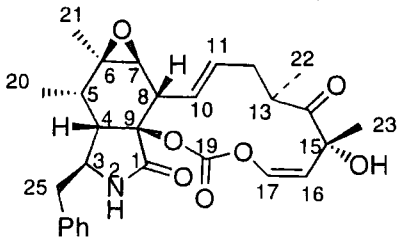

m/z (EI) 495 (5.5%, $[M]^+$)

δ_H($CDCl_3$)1.12 (3H, d, J 7.2, H-20), 1.15 (3H, d, J 7.3, H-22), 1.24 (3H, H-21), 1.42 (3H, s, H-23), 2.14 (1H, m, H-12), 2.26 (1H, m , H-5), 2.63 (3H, m , H-7, H-8, H-12), 2.70 (1H, d, J 12.3, H-25), 2.90 (1H, d, J 12.3, H-25), 2.95 (1H, m , H-13), 3.03 (1H, dd, J 3, 5, H-4), 3.76 (1H, m, H-3), 5.22 (1H, ddd, J 5,5 8, H-11), 5.59 (1H, d, J 11, H-

16), 5.89 (1H, dd, J 8, 15, H-10), 6.43 (1H, d, J 11, H-17), 7.15 (2H, d, Ar), 7.29 (1H, t, Ar), 7.36 (2H, t, Ar)

δ_C 13.2 (C-20), 19.7 (C-21), 20.1 (C-22), 24.3 (C-23), 35.8 (C-5), 39.1 (C-12), 40.8 (C-13), 45.2 (C-8), 45.9 (C-25), 48.3 (C-8), 53.6 (C-3), 60.6 (C-7), 87.1 (C-9), 120.3 (C-16), 127.2 (Ar), 128.4 (C-10), 128.9 (Ar), 129.7 (Ar), 131.4 (C-11), 135.9 (Ar), 142.1 (C-17), 149.3 (C-19), 170.2 (C-1), 211.9 (C-14)

*4.4.6 Isolation of epoxydon (**209**) from static cultures of X. grammicin.*

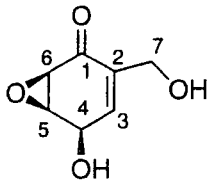

Culture supernatant of mature cultures of *X. grammici.* was decanted from the bottle and filtered under gravity. The supernatant was then saturated with sodium chloride and extracted into EtOAc (3 x 300ml). Removal of the solvent under reduced pressure afforded a dark brown tacky oil (typically 120mg) which was purified by silica column chromotography to yield epoxydon (**209**) (up to 20mg) as a white semisolid (R_f = 0.38).

M/z (EI)156 (1.7%, $[M]^+$)

$[\alpha_D]$ +102.2° (c 0.1, MeOH) lit: +106.7° (c 0.1, MeOH)[139]

δ_H ($CDCl_3$) 3.40 (1H, d, J 3.6, H-6), 3.76 (1H, br s, H-5), 4.25 (2H, dd, C-7, J 4.2, 1.4, H-7), 4.67 (1H, d, J 4.2, H-4), 6.61 (1H, br s, H-3)

δ_C ($CDCl_3$) 53.4 (C-6), 57.7 (C-5), 60.5 (C-7), 63.0 (C-4), 136.4 (C-2), 138.9 (C-3), 194.1 (C-1)

4.4.7 Feeding of labelled compounds to R. necatrix

4.4.7.1 Feeding of sodium [1,2-$^{13}C_2$]-acetate (82)

On days 7, 13 and 19, sodium [1,2-$^{13}C_2$]-acetate (100 mg) was dissolved in water (2ml) and administered through a sterile filter unit to cultures of *R. necatrix* to a final concentration of 4.1 mM. The cultures were worked up using according to the standard protocol.

4.4.7.2 Feeding of [6,6-$^{2}H_2$]-glucose (94)

On days 7, 13 and 19, sodium [6,6-$^{2}H_2$]-glucose (1g) was dissolved in water (2ml) and administered through a sterile filter unit to a culture of *R. necatrix* to a final concentration of 19 mM. The cultures were worked up using according to the standard protocol.

4.4.7.3 Feeding of sodium [2-$^{2}H_3$]-acetate (28)

On days 7, 13 and 19, sodium [2-$^{2}H_3$]-acetate (100 mg) was dissolved in water (2ml) and administered through a sterile filter unit to a culture of *R. necatrix* to a final concentration of 4.1 mM. The cultures were worked up using according to the standard protocol.

4.5 *Synthesis*

4.5.1 Synthesis of dimethylallyl alcohol (165)[111]

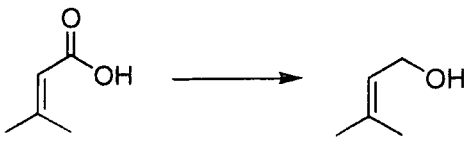

(168 165

Acrylic acid (**168**) (5.0g, 50mM) in ether (25ml) was added to a stirred solution of $LiAlH_4$ (5.4g, 160mM) in ether (30ml) at 0°C over 1.5h *via* a dropping funnel. The reaction was quenched by the careful addition of iced water (5ml), followed by NaOH (15%, 4ml) and water (3ml). The slurry was filtered through silicon impregnated filter papers (Whatman) and the solvent removed to give a colourless oil. Distillation afforded dimethyl allyl alcohol (**165**) (3.35g, 78%).

Bpt 140-143^0 (lit 141-142°)[111]

M/z(EI) 86 (M+, 28.0%), 71 (M-CH_3, 100%), 69 (M-OH, 16.7%)

δ_H ($CDCl_3$) 1.64 (3H, s, CH_3), 1.70 (3H, s, CH_3), 4.76 (2H, d, ^{1}J=6.9, CH=C$\underline{H}_2$OH), 5.36 (1H, m, C$\underline{H}$=CH_2OH)

δ_c ($CDCl_3$) 17.7 ($\underline{C}H_3$), 25.6 ($\underline{C}H_3$), 59.1 ($\underline{C}H_2$OH), 123.6 ($\underline{C}$H=CH(CH_3)$_2$), 136.0 (CH=$\underline{C}$H(CH_3)$_2$)

4.5.2 Synthesis of [1,1-$^2H_2$]-dimethyl allyl alcohol (167)[112]

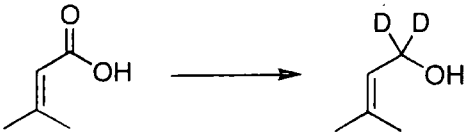

165 **167**

Acrylic acid (**165**) (5g, 50mM) in ether (25ml) was added to a stirred solution of $LiAlD_4$ (6.4g, 160mM) in ether (30ml) at 0°C over 1.5h *via* a dropping funnel. The reaction was quenched by the careful addition of iced water (5ml), followed by NaOH (15%, 4ml) and water (3ml). The slurry was filtered through silicon impregnated filter papers

(Whatman) and the solvent removed to give a colourless oil. Distillation afforded dimethyl allyl alcohol **167** as a colourless oil (2.75g, 64%)

Bpt 142-143^0 (lit 142-143[112])

M/z(EI) 88 (M+, 30.4%), 73 (M-CH_3, 100%), 71 (M-OH, 20.1%)

δ_H ($CDCl_3$) 1.65 (3H, s, CH_3), 1.71 (3H, s, CH_3), 5.36 (1H, br, C<u>H</u>=CD_2OH)

δ_c ($CDCl_3$) 17.8 (<u>C</u>H_3), 25.7 (<u>C</u>H_3), 58.5 (pentet, $^1J_{C\text{-}D}$ 21.4 Hz, <u>C</u>D_2OH), 123.4 (<u>C</u>H=$CH(CH_3)_2$), 136.3 (CH=<u>C</u>$H(CH_3)_2$)

4.5.3 Benzoyl-2-(t-butyl)-3,5-dimethylimidazolidin-4-one (88) [84]

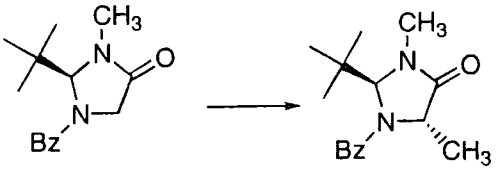

87 **88**

Benzoyl-2-(t-butyl)-3-methylimidazolidin-4-one (0.5g, 1.91mM) was added to a solution of LDA (2.11mM) generated from diisopropylamine (0.21g, 0.29ml, 2.11mM) and *n*-butyllithium (1.32ml, 1.6M in hexanes) at –78°C, and the reaction stirred at –78°C for 1h to produce a deep red solution. MeI (0.13ml, 1.91mM) was added dropwise and stirred at –78°C for 45min, allowed to warm to room temperature and stirred for a further 16h. The reaction was quenched by the addition of half saturated ammonium chloride (20ml) and the layers separated. The aqueous layer was extracted with ether (3x25ml) and the organic layers combined, dried ($MgSO_4$) and the solvent removed to afford a pale yellow powder. Column chromotography (silica, ether:petrol:methanol 60:35:5) afforded **88** (374mg, 71%) as a white amorphous solid.

mp: found 145-146°C (lit: 145.6-146.2°[84])

ν_{max} 2960, 2888, 1707, 1634

δ_H($CDCl_3$) 0.98 (3H, d, J=6.5, CH_3), 1.09 (9H, s, *-t-Bu*), 3.11 (3H, s, NCH_3), 4.30 (1H, q, J=6.5, CH), 5.65 (1H, s, CH), 7.55 (5H, m, Ar)

$\delta_C(CDCl_3)$ 20.57 ($\underline{C}H_3$), 27.43 ($C(\underline{C}H_3)_3$), 33.02 ($\underline{C}(CH_3)_3$), 41.88 (NCH_3), 58.59 (Ar, C-5), 80.50 (Ar, C-2), 129.1 (Ar, C-3), 129.9 (Ar, C-4), 132.8 (Ar, C-5), 137.6 (Ar, C-2), 173.4 (Ar,C-1)

4.5.4 L-Alanine (90) [84]

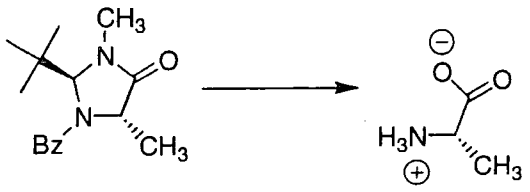

87 **90**

Benzoyl-2-(*t*-butyl)-3,5-dimethylimidazolidin-4-one (**87**) (300mg, 1.08mM) was heated in a sealed tube with 6M HCl (4ml) and heated at 180°C for 15 hours. The solution was removed from the tube by washing with dichloromethane (20ml) and water (20ml) and the solvents removed to produce a brown solid. Purification over Dowex gave **90** as a white solid (235mg, 78% yield).

Mp 289-290 °C (decomp) [lit.,[84] 289-290 °C (decomp)]

$\delta_H(D_2O)$ 1.37 (3H, d, J 8.0, $C\underline{H}_3$), 3.60 (1H, q, J 8.0, $C\underline{H}$)

δ_C (D_2O) 18.6 (C-3), 53.8 (C-2), 178.7 (C-1)

4.5.5 Benzoyl-2-(t-butyl)-3-methyl-5-[$^{13}C^2H_3$]-methylimidazolidin-4-one (89)[84]

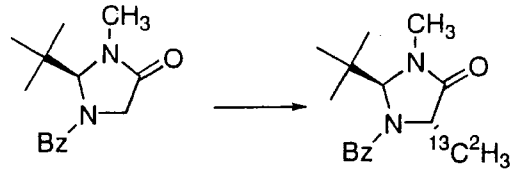

87 **89**

Benzoyl-2-(t-butyl)-3-methylimidazolidin-4-one (0.5g, 1.91mM) was added to a solution of LDA (2.11mM) generated from diisopropylamine (0.21g, 0.29ml, 2.11mM) and *n*-butyllithium (1.32ml, 1.6M in hexanes) at –78°C, and the reaction stirred at for 1h to produce a deep red solution. [$^{13}C^2H_3$]-MeI (0.13ml, 1.91mM) was added dropwise and stirred at –78°C for 45min, allowed to warm to room temperature and stirred for a further 16h. The reaction was quenched by the addition of half saturated ammonium chloride (20ml) and the layers separated. The aqueous layer was extracted with ether

(3x25ml) and the organic layers combined, dried ($MgSO_4$) and the solvent removed to afford a pale yellow powder. Column chromotography (silica, ether:petrol:methanol 60:35:5) afforded pure **89** (374mg, 71%)

mp 145.5-146.7°C (lit.,[84] 145.6-146.2°)

ν_{max}2960, 2888, 1707, 1634

$\delta_H(CDCl_3)$ 0.98 (3H, d, J 6.5, C<u>H</u>$_3$), 1.09 (9H, s, -*t*-*Bu*), 3.11 (3H, s, NC<u>H</u>$_3$), 4.30 (1H, br s, J 6.5, C<u>H</u>), 5.65 (1H, s, C<u>H</u>), 7.55 (5H, m, Ar)

$\delta_C(CDCl_3)$ 20.6 (septet, $J_{^{13}C\text{-}^2H}$ 19.9, <u>C</u>^{2}H$_3$), 27.4 (C(<u>C</u>H$_3$)$_3$), 33.0 (<u>C</u>(CH$_3$)$_3$), 41.9 (N<u>C</u>H$_3$), 58.6 (d, J $_{^{13}C^{13}C}$ 34.8, C-5), 80.50 (C-2), 129.1 (Ar, C-3), 129.9 (Ar, C-4), 132.8 (Ar, C-5), 137.6 (Ar, C-2), 171.3 (C-4'), 173.4 (C-1),

4.5.6 [3-$^{13}C^2H_3$]-L-Alanine (86) [84]

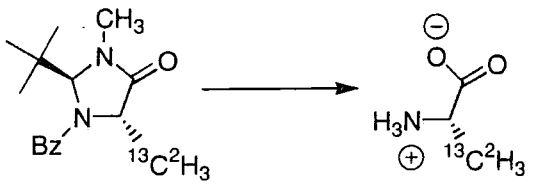

87 **86**

Benzoyl-2-(*t*-butyl)-3,5-dimethylimidazolidin-4-one **87** (300mg, 1.08mM) was heated in a sealed tube with 6M HCl (4ml) and heated at 180°C for 15 hours. The solution was removed from the tube by washing with dichloromethane (20ml) and water (20ml) and the solvents removed to produce a brown solid. Purification over Dowex gave **86** as a white solid (229mg, 71% yield).

Mp 290-292 °C (decomp) [lit.,[84] 289-290 °C (decomp)]

M/z (CI) 94 (100%, $[M+1]^+$)

$\delta_H(D_2O)$ 3.60 (1H, br, C<u>H</u>)

δ_C (D_2O) 18.4 (septet, $J_{^{13}C\text{-}^2H}$ 19.4, C-3), 53.4 (d, $J_{^{13}C\text{-}^{13}C}$ 34.9, C-2), 178.6 (C-1)

4.5.6.1 D-Mannitol acetonide(**170** [113]

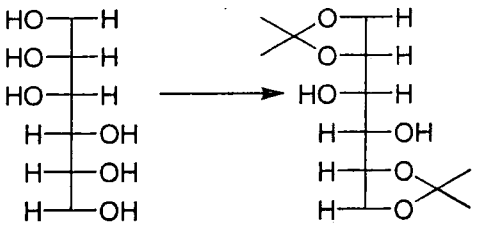

(169 **170**

D-Mannitol (**169** (20g, 110 mM) was added to a stirred solution of anhydrous zinc chloride (30g, 220 mM) in dry acetone (100ml) and the mixture stirred for 4h. Filtration to remove unreacted D-mannitol was performed and the filtrate dropped into a bi phasic solution containing potassium carbonate (34g) in water (50ml) and ether (150ml) and the mixture stirred for one hour. A slurry was precipitated upon concentration and then extracted into dichloromethane (3 x75ml). The extracts were combined, filtered and dried ($MgSO_4$) and the solvent removed to produce **170** as a white powder (11.4g, 39%).

ν_{max}/cm^{-1} 3324, 3376, 2978, 2933, 2890, 1456, 1371, 1258, 1206, 1158, 1125, 1063, 1005, 941.4,855.7, 650.1

δ_H (D_2O) 1.38 (6H, d, J 0.92, $C\underline{H}_3$), 1.41 (6H, d, J 0.92, $C\underline{H}_3$), 2.81 (2H, dd, J 1.28, 6.74, C<u>H</u>OH), 3.74 (2H, td, J 1.52, 6.50, C<u>H</u>(O)CH_2O), 3.980 (4H, m, CH(O)C<u>H</u>$_2$O). δ_C(D_2O) 25.2 (CH_3), 26.7 (CH_3), 66.7 (<u>C</u>H(O)CH_2O), 71.1 (<u>C</u>HOH), 76.1 (CH(O)<u>C</u>H_2O), 109.3 (<u>C</u>(CH_3)$_2$)

4.5.6.2 D-Glyceraldehyde acetonide (**171**)[114]

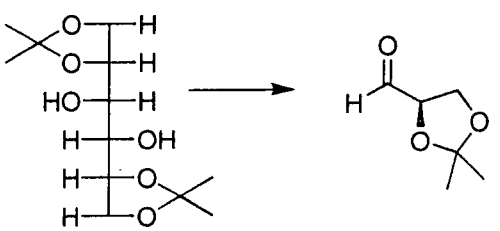

170 **171**

$NaIO_4$ (8.10g, 37 mM) was added to a solution of **170** (5g, 19mM) in dichloromethane (50ml) and water (2ml) with vigorous stirring. The reaction was monitored via TLC (silica, 85:15 DCM:acetone) and found to be complete after 1h. Dry $MgSO_4$ (2g) was

added and the reaction stirred for a further 15min and then filtered to produce a clear, colourless solution. The solvent was removed by distillation through a 6'' Vigreux column and the residue distilled to produce **170** as a clear, colourless oil (3.13g, 63%)

m/z (EI+) 130 (M^+ 28.09 %)

bp 40-42 °C (10 torr)

ν_{max}/cm^{-1} 2985, 1732, 1456, 1370, 1257, 1211, 1152, 1063, 844.4

δ_H ($CDCl_3$) 1.37 (6H, s, $C\underline{H}_3$), 1.45 (3H, s, $C\underline{H}_3$), 4.01 (2H, m, $C\underline{H}_2$), 4.17 (1H, dd, J 1.53, 6.45,C<u>H</u>), 9.68 (1H,s, C<u>H</u>O)

δ_C ($CDCl_3$) 25.3 ($\underline{C}H_3$), 26.4 ($\underline{C}H_3$), 65.8 ($\underline{C}H_2$), 80.0 (<u>C</u>H), 111.5 ($\underline{C}(CH_3)_2$), 198.4 (<u>C</u>HO)

$[\alpha]^{21}_D$=+63.2° (c=0.03, EtOH)

4.5.6.3 1-(2,2 Dimethyl-[1,3]-dioxolan-4-yl)-ethanol (172) [115]

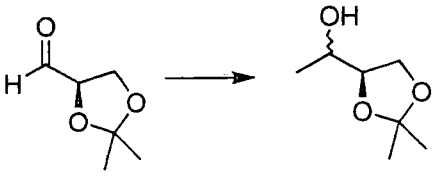

171 **172**

Aldehyde **171** (3.13g, 24mM) was added to a 3M solution of methylmagnesium bromide in ether (10.7 ml, 32mM) at 0°C under nitrogen and the reaction mixture stirred at 0°C for 1h. After warming to room temperature stirring was continued for 3h during which time the reaction was monitored by TLC (silica, 2:1 DCM:acetone) and IR. The reaction was quenched by pouring into iced water (25ml) and the layers separated. The aqueous phase was extracted with diethyl ether (3x75ml) and the organic fractions combined, dried ($MgSO_4$) and the solvent removed to produce a clear colourless oil. Distillation afforded **172** (1.58g, 48%)

m/z (EI^+) 146 (M^+ 4.52%)

bp 60-63°C (10 torr)

ν_{max}/cm^{-1} 3439, 2977, 2886, 1456, 1369, 1252, 1211, 1152, 1053, 903, 849, 794, 726, 645

δ_H ($CDCl_3$) 1.13 (3H, d, J 6.4, CH_3), 1.17(3H, d, J 6.3, CH_3), 1.38 (3H, s, $C(C\underline{H}_3)(CH_3)$), 1.43 (3H, s, $C(CH_3)(C\underline{H}_3)$), 3.50-4.30 (2H, m, C<u>H</u>O<u>H</u>)

δ_C ($CDCl_3$) 18.5 ($\underline{C}H_3CHOH$), 25.3 ($\underline{C}H_3CHOH$)', 25.5 ($C(\underline{C}H_3)(CH_3)$), 26.6 ($C(\underline{C}H_3)(CH_3)$)', 26.7 ($C(CH_3)(\underline{C}H_3)$), 26.8 ($C(CH_3)(\underline{C}H_3)$)', 67.0 ($\underline{C}H_2$), 68.9 ($CH_3$)', 79.6 ($\underline{C}H$), 80.5 ($\underline{C}H$), 109.2 ($\underline{C}(CH_3)(CH_3)$), 109.6 ($\underline{C}(CH_3)(CH_3)$)'

4.5.6.4 1-(2,2 Dimethyl-[1,3] dioxolan-4-yl)-ethanone(**174**) [116]

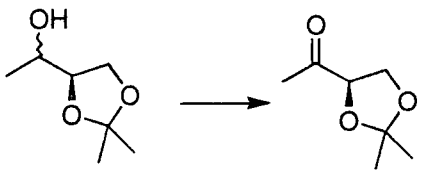

172 **174**

To a solution of **172** (1.58g, 10.7mM) in dry dichloromethane (100ml) was added pyridinium dichromate (6.60g, 17.6 mM), 3Å activated molecular sieves (8g) and dry acetic acid (300µl) and the reaction stirred under nitrogen for 48h. Hyflo (2g) was added, the mixture stirred for a further 20 mins and filtered through a $MgSO_4$ (2g) plug. After removal of the solvent the dark residue was extracted into diethyl ether (3x75ml) which after solvent removal afforded a pale yellow oil. Purification was performed using column chromotography (silica, 9:1 petrol:acetone) to produce **174** as a clear, colourless oil (791mg, 50%).

ν_{max} 2360, 1714, 1379, 1211, 1066, 907.8, 727.1, 645.6.

m/z (EI^+) 144 (M^+ 5.6%)

δ_H 1.32 (3H, s, $C\underline{H}_3$), 1.42 (3H, s, $C\underline{H}_3$), 2.19 (3H, s, $C\underline{H}_3CO$), 3.94 (1H,dd, J 5.6, 8.6, $C\underline{H}$), (1H, t, J 7.8, $C\underline{H}$), 4.34 (1H, dd, J 5.4, 7.6, $C\underline{H}$)

δ_C ($CDCl_3$) 25.1 ($\underline{C}H_3$), 26.7 ($\underline{C}H_3$), 28.4 ($\underline{C}H_3$), 65.8 ($\underline{C}H_2$), 80.0 ($\underline{C}H$), 111.5 ($\underline{C}(CH_3)_2$), 198.4 ($\underline{C}HO$)

$[\alpha]^{24}_D$=+101.2° (c=0.029, $CDCl_3$)

4.5.7 *Synthesis of benzyoxyacetaldehyde* (**118**) *from benzyloxyacetaldehyde diethyl acetal* (**136**)[104]

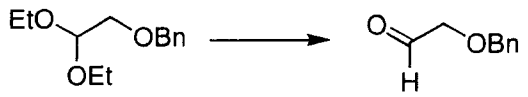

136 **118**

Benzyloxyacetaldehyde diethyl acetal (2.95g, 13.2mM) was stirred with TFA (5ml), water (5ml) and $CHCl_3$ (5ml) at ambient temperature for 1h. The mixture was extracted with $CHCl_3$ (3 x 100ml), dried over $MgSO_4$ and the solvent removed under reduced pressure to afford a colourless oil. Column chromatography (silica, 5:1 EtOAc:Petrol) yielded benzyoxyacetaldehyde *(***118***)* as a viscous oil (0.92g, 46%).

M/z (EI) 150 (5.8%, $[M]^+$), 107 (86.2 %, $[M\text{-}CH_2CHO]^+$)

δ_H ($CDCl_3$) 3.94 (2H, s, $\underline{C}H_2CHO$), 4.45 (2H, s, $O\underline{C}H_2Ph$), 7.21 (5H, m, Ar), 9.52 (1H, s, $C\underline{H}O$)

δ_C ($CDCl_3$) 73.3 ($\underline{C}H_2CHO$), 75.5 ($O\underline{C}H_2Ph$), 128.1 (Ar), 128.5 (Ar), 128.7 (Ar), 137.2 (Ar), 200.4 ($C\underline{H}O$)

4.5.8 *Synthesis of benzyloxyacetaldehyde (***118***) from O-benzyloxyethanol* (**147**) [108]

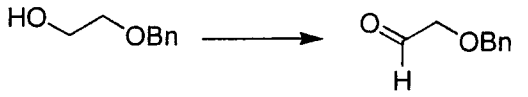

118 **147**

Oxalyl chloride (320µl, 466mg, 3.7mM) was dissolved in $CHCl_3$ (10ml) and cooled to –78°C. To the solution was added a solution of DMSO (440µL, 484mg, 6.2mM) in dry $CHCl_3$ and the mixture stirred at –78°C for 15 min after which *O*-benzyloxyethanol (480mg, 3.0mM) was dissolved in $CHCl_3$ (10ml) and added dropwise. Stirring was maintained at –78°C for 20 min. Et_3N (2.00ml, 1.45g, 14.4mM) was added and the reaction stirred at –78°C for 30 min. and allowed to warm to RT overnight. The mixture was quenched with water (50ml) and the organic layer separated. The aqueous layer was extracted with $CHCl_3$ and the organic extracts were combined and dried over $MgSO_4$. Removal of the solvent yielded a yellow oil which was purified by column chromatography (silica, 1:1 EtOAc:Petrol) to give benzyloxyacetaldehyde (**118**) as a colourless oil. Analytical data was identical to that described in 4.5.7.

4.5.9 Synthesis of benzyloxyethanol (147) [110]

144 **147**

To a suspension of KOH (796mg, 16mM) in DMSO (4ml) and benzyl bromide (0.90mL, 1.36g, 8mM) was added ethylene glycol **144** (1g, 16mM). The mixture was stirred for 0.5h, poured into water (25ml) and extracted into DCM (3x100ml). The aqueous phase was acidified with HCl and extracted into DCM (3x50ml). The organic phases were combined, washed with water (3x100ml) and dried over $MgSO_4$. Removal of the solvent afforded a pale yellow oil. Column chromatography (silica, 1:1 EtOAc:Petrol) gave benzyloxyethanol **147** as a colourless oil (644mg, 53%).

IR (neat) 3345, 3028, 2946, 1640, 1486, 1447, 742

δ_H 3.54 (2H, t, J=5.1 Hz, $C\underline{H}_2OH$), 3.70 (2H, t, J=5.1 Hz, $C\underline{H}_2OBn$), 4.53 (2H,s, $OC\underline{H}_2Ph$) 7.34 (5H, m, Ar)

δ_c 61.8 ($\underline{C}H_2OH$), 71.8 ($C\underline{H}_2OBn$), 73.4 ($OC\underline{H}_2Ph$), 128.0 (Ar), 128.1 (Ar), 128.7 (Ar), 138.3 (Ar)

4.5.10 (E)-5-Benzyloxy-3-penten-2-one (126)[105]

147 **126**

To a suspension of 1-triphenylphosphoranylidene-2-propanone (3.20g, 10.0mM) in THF (20ml) was added benzyloxyacetaldehyde (**147**) (750mg, 5.0mM) and the mixture refluxed for 20h. The solvent was removed under reduced pressure to give a white tarry solid which was extracted into ether (4x150ml). The solution was filtered through a silica plug to remove triphenylphosphine oxide and the solvent was removed to afford a brown oil. Column chromotography (silica, PE:EtOAc 5:1) gave (E)-5-benzyloxy-3-penten-2-one (**126**) as a colourless oil (817 mg ,86%)

M/z (EI) 190 (13%, $[M]^+$), 147 (7.28%, $[M\text{-}COCH_3]^+$)

IR (film) 3049, 2865, 1683, 1116, 742

δ_H ($CDCl_3$) 2.24 (3H, s, C<u>H</u>$_3$), 4.20 (2H, d, J=4.6 Hz, C<u>H</u>$_2$OBn), 4.55 (2H, s, OC<u>H</u>$_2$Ph), 6.30 (1H, d, C<u>H</u>=CHCH$_2$), 6. 80 (1H, dt, J=2.1, 4.6Hz, CH=C<u>H</u>CH$_2$)

δ_C ($CDCl_3$) 27.4 (CH_3), 70.0 (C<u>H</u>$_2$OBn), 73.3 (OC<u>H</u>$_2$Ph), 127.7 (Ar), 127.9 (Ar), 128.8 (Ar), 130.4 (<u>C</u>H=CHCH$_2$), 137.7 (Ar), 143.3 (CH=C<u>H</u>CH$_2$), 193.2 (<u>C</u>OCH$_3$)

4.5.11 5-Benzyl-1-deoxy-D-xylulose (**127**)[106]

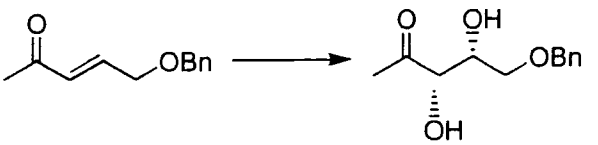

126 **127**

(E)-5-Benzyloxy-3-penten-2-one (**126**) (500mg, 2.42mM) was added to a solution containing Ad Mix β (5.92g), Na_2CO_3 (1.06g, 12.5mM), methanesulphonamide (402mg, 4.32mM) in ^{t}BuOH/water (30ml/30ml) and the mixture stirred overnight at 0°C. EtOAc (50 ml) was added and the reaction was quenched by the addition of $NaSO_3$ (8g) and allowed to warm to room temperature. The aqueous layer was separated and extracted with EtOAc (3x300ml). The organic fractions were combined, washed with water (30ml) and dried over $MgSO_4$. Removal of the solvent afforded a colourless oil which was purified over silica (3:1 EtOAc:Petrol) to give 5-benzyl-1-deoxy-D-xylulose (**127**) as a colourless semisolid (417mg ,77%)

M/z (CI) 242 ($[M+NH_4]^+$, 88%), 224 ($[M]^+$, 12.6%)

δ_H ($CDCl_3$) 2.19 (3H, s, C<u>H</u>$_3$), 3.57 (2H, m, C<u>H</u>$_2$OBn), 4.14 (2H, m, C<u>H</u>(OH)-C<u>H</u>(OH)), 4.53 (2H, s, OC<u>H</u>$_2$Ph), 7.31 (Ar)

δ_C ($CDCl_3$) 25.8 (CH_3), 70.6 (CH(OH)<u>C</u>H$_2$OBn), 71.5 (CH(OH)<u>C</u>H$_2$OBn), 73.9 (O<u>C</u>H$_2$Ph), 77.3 (<u>C</u>H(OH)CH$_2$OBn), 127.3 (Ar), 127.9 (Ar), 128.3 (Ar), 137.8 (Ar), 208.6 (<u>C</u>OCH$_3$)

4.5.12 1-Deoxy-D-xylulose (122)[107]

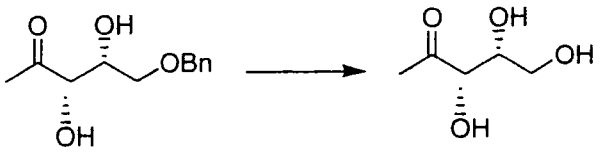

127 **122**

10% Pd/C (Degaussa type, 50% water by weight) was added to a solution of 5-benzyl-1-deoxy-D-xylulose (**127**) (35mg, 0.16mM) in 95% EtOH (10ml) The flask was filled with hydrogen three times and then evacuated, and the mixture was stirred for 3 hours. The catalyst was removed by filtration through Hyflo and the solvent removed under reduced pressure to afford DX (**122**) (18mg, 86%) as a colourless oil.

$\delta_H(CDCl_3)$ 2.31 (3H, s, $C\underline{H}_3$), 3.80 (2H, br, $C\underline{H}_2OH$), 4.25-4.56 (2H, m, $COC\underline{H}(OH)$,$C\underline{H}(OH)COMe$)

4.5.13 Analytical determination of DX (122) *as DX-triacetate*

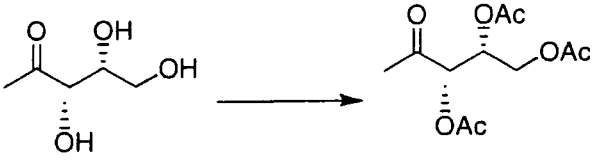

Acetic anhydride (2ml) was added to a solution of DX (5mg) in pyridine (2ml) and the reaction was stirred until the formation of product was evident by TLC (EtOAc, R_f (triacetate) = 0.73). The reaction was quenched by the addition of water (400µl) and the solvents removed under high vacuum for 3h. The crude mixture was applied neat to the GC column.

M/z (CI) 276 (100%, $[M+NH_4]^+$)

4.5.14 Synthesis of [1-^{2}H]-benzyloxyacetaldehyde (134)[108]

139 **134**

DMSO (472μL, 519mg, 6.65mM) In dry $CHCl_3$ (5ml) was added to a solution of oxalyl chloride (343μl, 500mg, 3.97mM) in $CHCl_3$ (5ml) at –78°C and the mixture stirred at –78°C for 15 min. A solution of [1,1-$^2H_2$]-benzyloxyethanol (**139**) (515mg, 3.21mM) in $CHCl_3$ (10ml) was added dropwise to the reaction and stirring was maintained at –78°C for 20 min. Et_3N (2.14ml, 1.56g, 15.4mM) was added and the reaction stirred at –78°C for 30 min. and allowed to warm to RT for 12h. The reaction was quenched by the addition of water (50ml) and the organic layer was separated. The aqueous layer was extracted into $CHCl_3$ and the combined organic extracts were dried over $MgSO_4$. Removal of the solvent gave a yellow oil which was purified over silica (1:1 EtOAc:Petrol) to give [1-^{2}H]-benzyloxyacetaldehyde (**134**) as a colourless oil (309mg, 63%).

M/z (EI) 151 (3.7%, $[M]^+$), 106 (75.2%, $[M\text{-}CH_2CDO]^+$)

$\delta_H(CDCl_3)$ 4.07 (2H, t, $J_{H\text{-}D}$ 0.48, $C\underline{H}_2OBn$), 4.53 (2H, s, $OC\underline{H}_2Ph$), 7.32 (5H, m, Ar)

$\delta_C(CDCl_3)$ 73.7 ($OC\underline{H}_2Ph$), 73.4 ($\underline{C}H_2OBn$), 127.3 (Ar), 127.9 (Ar), 128.3 (Ar), 137.8 (Ar), 200.1 ($\underline{C}HO$, t, $^1J_{C\text{-}D}$ 27Hz).

4.5.15 [3-^{2}H]-(E)-5-Benzyloxy-3-penten-2-one (135)[103]

134 **135**

To a suspension of 1-triphenylphosphoranylidene-2-propanone (1.44g, 4.49mM) in THF (20ml) was added [1-^{2}H]-benzyloxyacetaldehyde **134** (337mg, 2.25mM) and the reaction heated under reflux for 23h. The solvent was removed under reduced pressure to give a white tarry solid which was extracted into ether (4x200ml). The solution was filtered through a silica plug to remove triphenylphosphine oxide and the solvent

removed to afford a brown oil. Purification over silica (PE:EtOAc 5:1) gave [3-^{2}H]-(E)-5-benzyloxy-3-penten-2-one (**135**) as a colourless oil (292mg, 68%).

M/z (EI) 191 (18%, $[M]^+$), 148 (9.3%, $[M\text{-}COCH_3]^+$)

IR (film) 3027, 2868, 1685, 1102, 738

$\delta_H(CDCl_3)$ 2.09 (3H, s, $C\underline{H}_3$), 4.01 (2H, br, $C\underline{H}_2OBn$), 4.40 (2H, s, $C\underline{H}_2Ph$), 6.10 (1H, br, $C\underline{H}$=COMe), 7.20 (5H, Ar)

$\delta_C(CDCl_3)$ 27.2 ($\underline{C}H_3$), 68.8 ($OC\underline{H}_2Ph$), 72.9 ($\underline{C}H_2OBn$), 127.7 (Ar), 127.9 (Ar), 128.4 (Ar), 130.2 (Ar), 137.9 ($\underline{C}H$=COMe), 143.1 (t, $J_{C\text{-}D}$ 23.4, CH=$\underline{C}$D), 199.0 ($\underline{C}OCH_3$)

4.5.16 [3-^{2}H]-5-benzyl-1-deoxy-D-xylulose (140) [103]

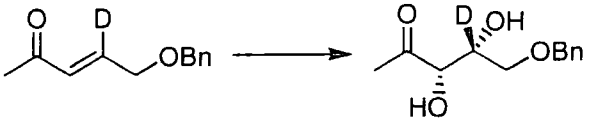

135 **(140)**

[3-^{2}H]-(E)-5-Benzyloxy-3-penten-2-one (**135**) (280mg, 1.39mM) was added to a solution containing Ad Mix β (3.31g), Na_2CO_3 (0.59g, 7mM), methanesulphonamide (225mg, 2.37mM) in ^{t}BuOH/water (20ml/20ml) and the mixture stirred overnight at 0°C. EtOAc (50 ml) was added and the reaction was quenched by the addition of $NaSO_3$ (5g) and allowed to warm to room temperature. The aqueous layer was separated and extracted into EtOAc (3x300ml). The organic fractions were combined, washed with water (30ml) and dried over $MgSO_4$. Removal of the solvent afforded a colourless oil which was purified *via* column chromatography (silica, 3:1 EtOAc:Petrol) to give [3-^{2}H]-5-benzyl-1-deoxy-D-xylulose (140) as a colourless semisolid (238mg,76%)

M/z (CI) 243 ($[M+NH_4]^+$, 94%), 225 (M+, 18.2%)

$\delta_H(CDCl_3)$ 2.27 (3H, s, $C\underline{H}_3$), 3.62 (2H, s, $C\underline{H}_2Ph$), 4.25 (1H, br, $C\underline{H}$(OH)C(OH)D), 4.47 (2H, br, $C\underline{H}_2OBn$), 7.20 (5H, Ar)

$\delta_C(CDCl_3)$ 25.6 ($\underline{C}H_3$), 70.5 (t, $J_{C\text{-}D}$ 31.5, CH(OH)$\underline{C}$(OH)D), 71.0 ($OC\underline{H}_2Ph$), 73.6 ($\underline{C}H_2OBn$), 77.5 ($\underline{C}$H(OH)C(OH)D), 127.8 (Ar), 128.0 (Ar), 128.3 (Ar), 138.4 (Ar), 208.1 ($\underline{C}OCH_3$)

4.5.17 [4-^{2}H]-1-Deoxy-D-xylulose (116)[103]

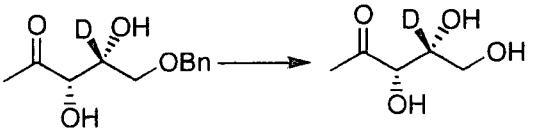

(140) **116**

[3-^{2}H]-5-Benzyl-1-deoxy-D-xylulose (140) (46mg, 0.20mM) was dissolved in 95% EtOH (10ml) was 10% Pd/C (Degaussa type, 50% water by weight,10mg) added. The flask was flushed with hydrogen and then evaporated three times and the mixture was stirred under H_2 for 3 hours. The catalyst was removed by filtration through Hyflo and the solvent removed under reduced pressure to afford [4-^{2}H]-DX (**116**) as a colourless oil (24mg, 89%)

$\delta_H(CDCl_3)$ 2.25 (3H, s, C<u>H</u>$_3$), 3.85 (2H, br, C<u>H</u>$_2$OH), 4.25 (1H, br, C<u>H</u>(OH)COMe)

4.5.18 [4-^{2}H]-DX-triacetate

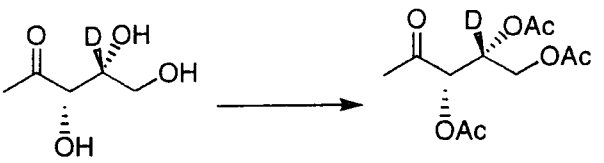

[4-^{2}H]-DX (**116**) (3mg) was stirred in pyridine (2ml) and acetic anhydride (2ml) until formation of product was evident by TLC (EtOAc, R_f (triacetate) = 0.77). The reaction was quenched by the addition of water (300µl) and the solvents removed under high vacuum for 3h. The crude mixture was applied neat to the GC column.

M/z (CI) 279 (100%, $[M+NH_4]^+$), 160 (18.6%, $[M+NH_4]^+$-2 x CO_2CH_3)

4.5.19 Synthesis of [1,1,2,2-$^2H_4$]-benzyloxyethanol (151)[110]

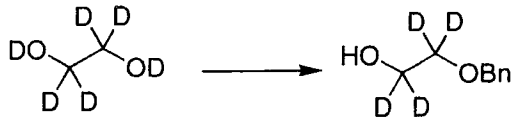

143 **151**

[$^2H_6$]-Ethylene glycol (**143**) (2g, 29mM) was added to a suspension of KOH (1.64g, 29mM and benzyl bromide (1.69ml, 2.56g, 15mM) in DMSO (6ml) and the mixture was stirred for 0.5h. The mixture was poured into water (40ml) and extracted with DCM (3x100ml). The aqueous phase was acidified with HCl and extracted with DCM (3x50ml). The organic phases were combined, washed with water (3x100ml) and dried over $MgSO_4$. Removal of the solvent afforded an oil which was purified by column chromatography (silica, 1:1 EtOAc:Petrol) to give [1,1,2,2-$^2H_4$]-benzyloxyethanol (**151**) as a colourless oil (1.01g, 43%).

IR (neat) 3343, 3020, 2941, 1645, 1472, 1438, 740

Mz 156 (72%, [M^+])

$\delta_H(CDCl_3)$ 4.43 (2H, s, $OC\underline{H}_2Ph$) 7.26 (5H, m, Ar)

$\delta_C(CDCl_3)$ 64.6 (pentet, $J_{C\text{-}D}$ 22.5Hz, $\underline{C}D_2OH$), 74.6 (pentet, $J_{C\text{-}D}$ 23.2Hz, $\underline{C}D_2OBn$) 76.9 ($OC\underline{H}_2Ph$), 127.9 (Ar), 128.3 (Ar), 128.5 (Ar), 138.6 (Ar),

4.5.20 Synthesis of [1,2,2-$^2H_3$]-benzyloxyacetaldehyde (152) [108]

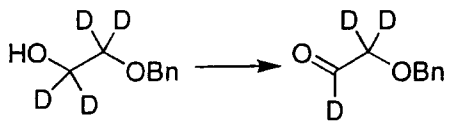

151 **152**

[$^2H_6$]-DMSO (434µL, 564mg, 6.12mM) In dry $CDCl_3$ (5ml) was added to a solution of oxalyl chloride (315µl, 460mg, 3.64mM) in $CDCl_3$ (5ml) at –78°C and the mixture stirred at –78°C for 15 min. **151** (474mg, 2.95mM) in $CDCl_3$ (10ml) and added dropwise. Stirring was maintained at –78°C for 20 min. Et_3N (1.97ml, 1.44g, 14.2mM) was then added and the reaction stirred at –78°C for 30 min. and allowed to warm to RT

overnight. The mixture was quenched with water (50ml) and the organic layer separated. The aqueous layer was extracted with $CHCl_3$ and the organic extracts combined and dried over $MgSO_4$. Removal of the solvent yielded a yellow oil which was purified by column chromatography (silica, 1:1 EtOAc:Petrol) to give [1,2,2-$^2H_3$]-benzyloxyacetaldehyde (**152**) as a colourless oil which was stable to decomposition for 2 days at 0°C. (321mg ,71%)

M/z (EI) 153 (2.3%, $[M]^+$), 106 (86.1%, $[M\text{-}CD_2CDO]^+$)

$\delta_H(CDCl_3)$ 4.56 (2H, s, $OC\underline{H}_2Ph$) 7.30 (5H, m, Ar)

$\delta_C(CDCl_3)$ 73.8 ($OC\underline{H}_2Ph$), 72.0 (t, $^1J_{C\text{-}D}$ 23, $\underline{C}D_2OBn$), 127.8 (Ar), 128.0 (Ar), 128.3 (Ar), 138.4 (Ar), 200.1 ($\underline{C}HO$, t, $^1J_{C\text{-}D}$ 27).

4.5.21 [4,5,5-$^2H_3$]-(E)-5-Benzyloxy-3-penten-2-one (142) [105]

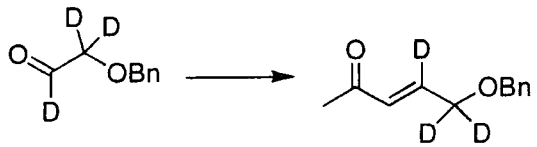

152 **142**

To a suspension of 1-triphenylphosphoranylidene-2-propanone (1.24g, 3.89mM) in THF (20ml) was added [1,3,3-$^2H_3$]-benzyloxyacetaldehyde (**152**) (292mg, 1.94mM) and the mixture refluxed for 23h. The solvent was removed under reduced pressure to give a white tarry solid which was extracted with ether (4x200ml). The solution was filtered through a silica plug to remove triphenylphosphine oxide and the solvent removed to afford a brown oil. Column chromotography (silica, PE:EtOAc 5:1) gave [4,5,5-$^2H_3$]-(E)-5-benzyloxy-3-penten-2-one (**142**) as a colourless oil (303mg, 81%)

M/z (EI) 193 (11%, $[M]^+$), 150 (4.4%, $[M\text{-}COCH_3]^+$)

IR (film) 3027, 2868, 1685, 1100, 738

$\delta_H(CDCl_3)$ 2.26 (3H, s, $C\underline{H}_3$), 4.45 (2H, s, $C\underline{H}_2Ph$), 7.34 (5H, Ar)

$\delta_C(CDCl_3)$ 25.6 ($\underline{C}H_3$), 70.5 (pentet, $J_{C\text{-}D}$ 22.6, $\underline{C}D_2OBn$), 71.0 ($OC\underline{H}_2Ph$), 137.9 ($\underline{C}H$=COMe), 143.1 (t, $J_{C\text{-}D}$ 23.4, CH=$\underline{C}D$), 127.8 (Ar), 128.0 (Ar), 128.3 (Ar), 138.4 (Ar), 199.6 ($\underline{C}OCH_3$)

4.5.22 [4,5,5-$^2H_3$]-5-Benzyl-1-deoxy-D-xylulose (154) [106]

142 **154**

[4,5,5-$^2H_3$]-(E)-5-Benzyloxy-3-penten-2-one **142** (200mg, 0.99 mM) was added to a solution containing Ad Mix β (2.36g), Na_2CO_3 (420mg, 5.0 mM), methanesulphonamide (161mg, 1.69mM) in ^{t}BuOH/water (17ml/17ml) and the mixture stirred overnight at 0°C. EtOAc (50 ml) was added and the reaction was quenched by the addition of $NaSO_3$ (5g) and allowed to warm to room temperature. The aqueous layer was separated and extracted with EtOAc (3x300ml). The organic fractions were combined, washed with water (30ml) and dried over $MgSO_4$. Removal of the solvent afforded a colourless oil which was purified *via* column chromatography (3:1 EtOAc:Petrol) to give [4,5,5-$^2H_3$]-5-benzyl-1-deoxy-D-xylulose (**154**) as a colourless semisolid (127mg, 55%).

M/z (CI) 245 ([M+NH_4]$^+$, 96%), 227 (M+, 12.5%)

δ_H($CDCl_3$) 2.17 (3H, s, C$\underline{H}_3$), 4.15 (1H, br, C$\underline{H}$(OH)C(OH)D), 4.74 (2H, s, C$\underline{H}_2$Ph), 7.26 (5H, Ar)

δ_C($CDCl_3$) 25.6 (C$\underline{H}_3$), 70.5 (t, $J_{C\text{-}D}$ 31.5, CH(OH)$\underline{C}$(OH)D), 71.0 (OC$\underline{H}_2$Ph), 73.6 (pentet, $J_{C\text{-}D}$ 22.5, $\underline{C}D_2$OBn), 77.5 ($\underline{C}$H(OH)C(OH)D), 127.8 (Ar), 128.0 (Ar), 128.3 (Ar), 138.4 (Ar), 208.1 ($\underline{C}OCH_3$)

4.5.23 [4,5,5-$^2H_3$]-1-deoxy-D-xylulose (141)[107]

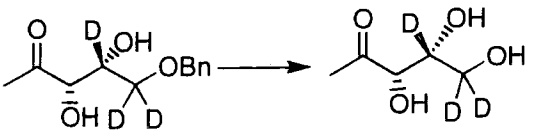

154 **141**

[4,5,5-$^2H_3$]-5-Benzyl-1-deoxy-D-xylulose (**154**) (40mg, 0.30mM) was dissolved in 95% EtOH (10ml) was 10% Pd/C (Degaussa type, 50% water by weight,) added. The flask was flushed with hydrogen and evacuated three times and the mixture was stirred under H_2 for 3 hours. The catalyst was removed by filtration through Hyflo and the solvent removed under reduced pressure to afford [4,5,5-$^2H_3$]-DX (**141**) as a colourless oil (36 mg, 91%)

$\delta_H(CDCl_3)$ 2.25 (3H, s, C<u>H</u>$_3$), 4.25 (1H, br, C<u>H</u>(OH)COMe)

4.5.24 [4,5,5-$^2H_3$]-DX-triacetate

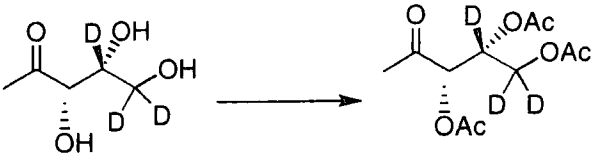

[4,5,5-$^2H_3$]-DX (**141**) (2mg) was stirred in pyridine (2ml) and acetic anhydride (2ml) overnight until a the reaction showed the formation of product by TLC (EtOAc, R_f (triacetate) = 0.72). The reaction was quenched by the addition of water (200µl) and the solvents removed under high vacuum for 2h. The crude mixture was applied neat to the GC column.

M/z (CI) 281 (100%, $[M+NH_4]^+$), 162 (19.2%, $[M+NH_4]^+$-2 x CO_2CH_3)

[1] A Lucas, *Ancient Egyptian Materials and Industries,* 1962, 4th Ed, Arnold, London

[2] The Bible, Matthew 2:10

[3] J.D. Bu'lock, *The biosynthesis of natural products,* 1st Ed. (1965), McGraw Hill Publishing, London

[4] J. Mann, *Secondary metabolism*, 2nd Ed. (1987), Clarendon Press, Oxford

[5] J. Davies, *Mol. Microbiol*, 1990, **43**, 207

[6] J. Cavalier-Smith, *Secondary Metabolites: their function and evolution*, 1st Ed. (1992), John Wiley, Chichester, 64-87

[7] L.C. Vining, *Annu. Rev. Microbiol.*, 1990, **44**, 395

[8] D. O'Hagan, D. B. Harper, *J. Fluorine Chem.,* 1999, **100**, 127

[9] J.N. Collie, *J. Chem. Soc.,* 1907, **91**, 1806

[10] A.J. Birch, *Proc. Chem. Soc.*, 1962, 3

[11] G Flesch, M, Rohmer,. *Eur. J. Biochem.,* **1988**, *175*, 405

[12] H. Lodish, D. Baltimore, A. Berk, S. A. Zipursky, P. Matsudiara, J. Darnell, *Molecular Cell Biology*, 3rd ed. (1995), Scientific American Books, New York

[13] C. Abell, M.J.Garson, F.J.Leeper, J. Staunton, *J. Chem. Soc., Chem. Comm.,* 1982, 1011

[14] R. Duran-Patron, D.O'Hagan , J.T.G. Hamilton , C.W. Wong, *Phytochemistry.*, **53**,777-784

[15] M. Tanabe, H. Seto, L. Johnson, *J. Am. Chem. Soc.*, **92**, 2157

[16] P.C. Lauterbur, *J. Chem. Phys.,* 1957, **26**, 217

[17] H. Seto, T. Sato, H. Yonehara, *J. Am. Chem. Soc.*, 1973, **95**, 8461

[18] M.J Garson and J. Staunton, *Chem. Soc. Rev.*, 1979, 539

[19] W. Templeton, *The chemistry of terpenes and steroids*, 1st Ed (1969), Butterworths, London

[20] A. R Penfold, J.L Simonsen, *J. Chem. Soc.*, 1939, 37

[21] L. Ruzicka, *Experimentia*, 1953, **9**, 357

[22] L. Jaenicke, F-J. Marner, *Pure and Appl. Chem.,*1990, **62**, 1365-1368

[23] I. P. Street, H. R. Coffman, J. A. Baker, C. D. Poulter, *Biochemistry*, 1994, **33**, 4212

[24] J. W. Cornforth, R. H. Cornforth, G. Popjak, L. Yengoyan, *J. Biol. Chem.*, **241**, 3970-3987

[25] Collins English Dictionary, 4th edition (1999), Harper Collins, Glasgow

[26] E.J.Corey, M. Ohno, P.A. Vatakencherry, R.B. Mitra, *J. Am. Chem. Soc.*, 1961, **83**, 1251

[27] L. Ruzicka, *Expermentia*, **9**, 357

[28] K. Bloch, *Science*, 1965, **150**, 19

[29] R. Sanderhoff, H. Thomas, *Annalen,* 1937, **530**, 195

[30] D. H. R. Barton, W. D. Ollis, *Comprehensive Organic Chemistry*, 1st Ed. (1979), Volume 6, Chapter 6, Pergammon Press, Oxford, England

[31] J. W. Cornforth, G. D. Hunter, G. Popjâk, *Biochem. J.*, 1952, **54**, 597

[32] F. Lynen, L. Wessely, O. Wieland, L. Reuff. E. Riechart, *Angew. Chem.*, 1952, **64**, 687

[33] D. Arigoni, M. Eberle, *Helv. Chem. Acta*, 1960, **43**, 1508

[34] K. J. Treharne, E. I. Mercer, T. W. Goodwin, *Biochem. J.*, 1966, **99**, 239

[35] L.J Rogers, S. Shah, T. W. Goodwin, *Biochem. J.* 1965, **96**, 7p

[36] J. Battaile, W. D. Loomis, *Biochem. Biophys. Acta.*, 1961, **51**, 545

[37] D.V. Banthorpe, B. V. Charlwood, M. J. O. Francis *Chem. Rev.*, 1972, **72**, 115

[38] A. J. Birch, D. Boulter, R. I. Fryer. P. J. Tomson, J. L. Wills, *Tetrahedron Letts*, 1959, **3**, 1

[39] D. V. Banthorpe, J. Mann, K. W. Turnbull, *J. Chem. Soc. C.*, 1970, 2689

[40] D. V. Banthorpe, D. Baxendale, *J. Chem. Soc. C.*, 1970, 2694

[41] E. von Rudloff, E. W. Underhill, *Phytochemistry*, 1965, **4**, 11

[42] G. Flesch, M. Rohmer, *Eur. J. Biochem.*, 1988, **175**, 405

[43] M. Rohmer, M. Knani, P. Simonin, B. Sutter, H. Sham, *Biochem. J.*, 1993, **295**, 517

[44] D. Zhou and R.H White, *Biochem. J.*, 1991, **273**, 627

[45] M. Rohmer, M. Seeman, S. Horbach, S. Bringer, H. Sahm, *J. Am.. Chem. Soc.*, 1996, **118**, 2564

[46] L. Slechta, L. F. Johnson, *J. Antibiot.*, 1976, *29*, 685

[47] A. Yokota, K.I. Sasajima, *Agric. Biol. Chem.*, 1984, **48**, 149

[48] A. Yokota, K.I. Sasajima, *Agric. Biol. Chem.*, 1986, **50**, 2517

[49] K. Himmeldirk, I. A. Kennedy, R. E. Hill, B. G. Sayer, I. D. Spenser, *Chem. Comm.*, 1996, 1187

[50] B. Alber, W. Maurer, S. Scharf, K, Stepusin, F. Schmidt, *FEBS Letts.*, 1999, **449**, 45

[51] S.T.J. Broers, Ph D thesis Nb 10978, E. T.H. , Zurich, Switzerland, 1994

[52] G. A. Sprenger, U. Schörken, T, Wiegert, S. Grolle, A. de Graaf, S. V Taylor, T. P. Begley, S. Bringer-Meyer, H. Sahm, *Proc. Natl. Acad. Sci. USA*, 1997, **94**, 12857

[53] L. M. Lois, N. Campos, S. R. Putra, K. Danielsen, M. Rohmer, A. Boronat, *Proc. Natl. Acad. Sci. USA*, 1998, **95**, 2105

[54] M. Harker, P. M. Bramley , *FEBS Letts.*, 1999, **448**, 115

[55] F. Bouvier, A. d'Harlingue, C. Sure, R.A. Backhouse, B. Camera, *Plant Physiol.*, 1998, **117**, 1423

[56] B. M.Lange, M. R. Wilding, D. McCaskill, R. Croteau, *Proc. Natl. Acad. Sci. USA*, 1998, **85**, 2100

[57] T. Duvold, J-M. Bravo, C. Pale-Grosdemange, M. Rohmer, *Tetrahedron Letts*, 1997, **38**, 4769

[58] T. Duvold, P. Cali, J-M. Bravo, M. Rohmer, *Tetrahedron Letts,* 1997, **38**, 6181

[59] S. Sanger, W. Eisenreich, M. Fellermeier, C. Laztel, A. Bacher, M. Zenk, *Tetrahedron Letts*, 1998, **39**, 2091

[60] M. Fellermeier, K. Kis, S. Sanger, U. Maier, A. Bacher, M. Zenk, *Tetrahedron Letts*, 1999, **40**, 2743

[61] D. Arigoni, J-L. Giner, S. Sanger, J. Wungsintaweekul, M. Zenk, K. Kis, A. Bacher, W. Eisenreich, *Chem. Comm.*, 1999, 1127

[62] J. Schwender, C. Müller, J. Zeidler, H. K. Lichenthaler, *FEBS Letts.*, 1999, **455**, 140

[63] B. M. Lange, R. Croteau, *Arch. Biochem. Biophys.*, 1999, **365**, 170

[64] T. Radykewicz, F. Rohdich, J. J. Wungsintaweekul, S. Herz, K. Kis, W. Eisenreich, A. Bacher, M. Zenk, D. Arigoni, *FEBS Letts.*, 2000, **465**, 157

[65] F. Rodich, J. Wungsintaweekul, M. Fellermeier, S. Sanger, S. Herz, K. Kis, W. Eisenreich, A. Bacher, M. Zenk, *Proc. Natl. Acad. Sci. USA*, 1999, **96**, 11758

[66] T. Kuzuyama, M. Takagi, K. Kaneda, T. Dairi, H. Seto, *Tetrahedron Letts.*, 2000, **41**, 703

[67] H. Lüttgen, F. Rodich, S. Herz, J. Wungsintaweekul, S. Hecht, C. A. Schur, M. Fellermeier, S. Sanger, M. Zenk, A. Bacher, *Proc. Natl. Acad. Sci. USA*, 2000, **97**, 1062

[68] M. Takagi, T. Kuzuyama, K. Kaneda, H. Watanabe, T. Dairi, H. Seto, *Tetrahedron Letts.*, 2000, **41**, 3395

[69] S. Herz, J. Wungsintaweekul, C. A. Schur, S. Hecht, H. Lüttgen, S. Sanger, M. Fellermeier, W. Eisenreich, M. Zenk, A. Bacher, F. Rodich, *Proc. Natl. Acad. Sci. USA*, 2000, **97**, 2486

[70] L. L. Turner, H. Santos, P. Fareleria, I. Pacheco, J. Le Gall, A. V. Xavier, *Biochem. J.*, **1992**, *285*, 367

[71] J. Schwender, M. Seeman, H. K. Lichtenthaler, M. Rohmer, *Biochem. J.*, 1996, **316**, 73

[72] K. Nabeta, T. Ishikawa, H. Okuyama, *J. Chem. Soc. Perkin Trans. 1*, 1995, 3111

[73] K. Nabeta, T. Kawae, T. Saitoh, H. Okuyama, *J. Chem. Soc. , Chem. Comm.*, 1997, 261

[74] H.K. Litchenhaler, J. Schwender, A. Ditsch, M. Rohmer, *FEBS Lett.*, 1997, **400**, 271

[75] M. K. Schultz, Ph D thesis, 1994, ETH, Zurich, Switzerland. Cited in M. Rohmer [79]

[76] J. Piel, J. Donath, K. Bandemer, W. Boland, *Angew. Chem., Int. Ed. Engl.*, 1998, **37**, 2478

[77] H. Seto, H. Watanabe, K. Furihata, *Tetrahedron Letts.*, 1996, **37**, 7979

[78] S. Rosa Putra, A. Ditsch, J-M Bravo, M. Rohmer, *FEMS Microbiol. Lett.*, 1998, **164**, 169

[79] A. Spencer, J.D. Hamill, M.J.C. Rhodes, *Plant Cell Reports*, 1990, **8**, 601

[80] J. D. Hamill, A. J. Parr, M. J. C. Rhodes, *Biotechnology*, 1987, **5**, 800

[81] A. Spencer, J. D. Hamill, M. J. C. Rhodes, *Phytochemistry*, 1993, **32**, 911

[82] Y. Aramaki, K. Chiba, M. Tada, *J. Chem. Soc. Perkin Trans. 1*, 1995, 683

[83] R.A. Morton, U. Gloss, O. Schindler, G. M. Wilson, L. H. Choppard-dit-Jean, F. W. Hemming, O. Isler, W. M. F. Leat, J. F. Pennock, R. Rüegg, U. Schwneter, O. Wiss *Helv. Chem. Acta*, 1958, **41**, 2343

[84] N.J.C.E. Chesters, D. O'Hagan, *J. Chem. Soc., Perkin Trans. I*, 1997, 833

[85] D. Seebach, E. Juaristi, Dd. Miller, C. Schickli, T. Weber, *Helv. Chim. Acta*, 1987, **70**, 237-261

[86] P.J. Proteau, *Tetrahedron Lett.*, 1998, **39**, 9373

[87] J. Nieschalk, J. T. G. Hamilton, C. D. Murphy, D. B. Harper, D. O'Hagan, *J. Chem. Soc., Chem. Comm.*, 1997, 799

[88] J-L Giner, B. Jaun, D. Arigoni, *Chem. Comm.*, 1998, 1857

[89] A. E. Leyes, J. A. Baker, F. M. Hahn, C. D. Poulter, *J. Chem Soc. Chem. Comm.*, 1999, 717

[90] D. Arigoni, W. Eisenreich, C. Latzel, S. Sanger, T. Radykewicz, M. H. Zenk, A. Bacher, *Proc. Natl. Acad. Sci. USA*, 1999, **96**, 1309

[91] A. E. Leyes, J. A. Baker, C. D. Poulter, *Org. Lett.*, 1999, 1071

[92] M. Rodríguez-Concepción, N. Campos. L. M. Lois, C. Maldonaldo, J-F. Hoeffler, C. Grosdemange-Billiard, M. Rohmer, A. Boronat, *FEBS Letts.*, 2000, **473**, 328

[93] F.M. Hahn, A. P. Hurlbut, C. D. Poulter, *J. Bacteroil.*, 1999, **181**, 4499

[94] Y. Ershov, R. R. Gantt, F. X. Cunningham, E. Gantt, *FEBS Letts.*, 2000, **473**, 337

[95] L. Charon, C. Pale-Grosdemange, M .Rohmer, *Tetrahedron Letts.*, 1999, **40**, 7231

[96] D. Arigoni, S. Sanger, C. Latzel, W. Eisenreich, A. Bacher, M. H. Zenk, *Proc. Natl. Acad. Sci. USA*, 1997, **94**, 10600

[97] S. Rosa Putra, L. M. Lois, N. Campos, A. Boronat, M. Rohmer, *Tetrahedron Letts.*, 1998, **39**, 23

[98] S. Sanger, C. Latzel, W. Eisenreich, A. Bacher, M.H. Zenk, *Chem. Comm.*, 1998, 221

[99] I. A. Kennedy, T. Hemscheidt, J. F. Britten, I. D. Spenser, *Can. J. Chem.*, 1995, **73**, 1329

[100] B. S. J. Blagg, C. D. Poulter, *J. Org. Chem.*, **1999**, 1508

[101] J. Piel, W. Boland, *Tetrahedron Letts.*, 1997, **38**, 6387

[102] A. Jux, W. Boland, *Tetrahedron Letts.*, 1999, **40**, 6913

[103] J-L . Giner, *Tetrahedron Letts.*, 1998, **39**, 2479

[104] L-Y. Hsu, C-H. Lin, *Heterocycles*, 1996, **43**, 2687

[105] A. Gossauer, K. Suhl, *Helv. Chim. Acta*, 1976, **59**, 1698

[106] P. J. Walsh, K.B. Sharpless, *Synlett.*, 1993, 605

[107] S. V. Taylor, L. D. Vu, T. P. Begley, *J. Org. Chem.*, 1998, **63**, 2375

[108] D. Taber, R. Walter, R. Meagley, *J. Org. Chem.*, 1994, **59**, 6014

[109] L-S. Li, Y. Wu, Y-J. Hu, L-Jun Xia, Y-L. Wu, *Tetrahedron: Asymm.*, 1998, **9**, 2271

[110] M. Kizil, J. A. Murphy, *Tetrahedron*, 1997, **53**, 16847

[111] H. G. Richey Jnr, L. M. Moses, *J. Org. Chem.*, 1983, **48**, 4013

[112] G. Vassilikogiannakis, N. Chronokis, M. Orfanopoulos, *J. Amer. Chem. Soc.*, 1998, **120**, 9911

[113] L.W. Hertel, C. S. Grossman and J. S. Kroin, *Synth. Comm.*, 1991, **2**, 155

[114] D. Y. Jackson, *Synth. Comm.*, 1988, **18**, 337

[115] P. Munier, A. Krusinski, D. Picq and D. Anker, *Tetrahedron*, 1995, **51**, 1229

[116] S. Czernecki, C. Georgoulis, C .L. Stevens and K. Vijayakumaran, *Tetrahedron Letts.*, 1985, **26**, 1699

[117] D. O'Hagan, *The Polyketide Metabolites*, 1st Ed. (1991), Ellis Horwood Limited, Chichester, England

[118] Buckingham, J.,ed. *Dictionary of Natural Products*, 1994, London, Chapman & Hall

[119] Ioset, J-R., Marston, A., Gupta, M. P., Hostettmann, K., *Phytochemistry*, 1998, **47**, 729

[120] Shiomi, K., Tomoda, H., Otoguro, K., Omura, S., *Pure Appl. Chem.*, 1999, **71**, 1059

[121] J. W. Cornforth, *Chem. Br.*, 1968, **4**, 102

[122] T.J. Simpson, *Chem. Soc. Rev.*, 1987, **16**, 123

[123] T. J. Simpson, *Tetrahedron. Letts.*, 1981, **22**, 3785

[124] T. J. Simpson, S. A. Ahmed. C. R. McIntyre, F. E. Scott, I. H. Sadler, *Tetrahedron*, **53**, 4013

[125] A. Mühlbauer, J. Beyer, W. Steglich, *Tetrahedron Letts.*, 1998, **39**, 5167

[126] Disch, A., Rohmer, M., *FEMS Microbiology Letts.*, 1998, **168**, 201

[127] W. Rothweiler. Ch. Tamm, *Experimentia*, 1966, **22**, 750

[128] M. Binder, Ch. Tamm, *Angew. Chem. Int. Ed.*, 1973, **12**, 370

[129] W. Graf, J-L. Robert, J. C. Vederas, Ch. Tamm, P. H. Solomon, I. Miura, K. Nakanishi, *Helv. Chem. Acta.*, 1974, **57**, 190

[130] J. C. Vederas, Ch. Tamm, *Helv. Chem. Acta*, 1976, **59**, 558

[131]R. Edwards, Unpublished results

[132] W. B. Turner, *Fungal Metabolism*, 1971, Academic Press Inc., London

[133] Personal Communication

[134] G. Büchi, *J. Am. Chem. Soc.*, 1973, **95**, 5423

[135] D. C. Aldridge, *J. Chem. Soc., Chem. Comm.*, 1973, 551

[136] H. S. E. Holker, T. J. Simpson, *J. Chem. Soc., Perkin Trans. I*, 1981, 1397

[137] M.C. Moore, R.J. Cox, G.R. Duffin , D. O'Hagan *Tetrahedron,* 1998, **54**, 9195

[138] T. Kajimoto, Y. Imamura, M. Yahamshita, K, Takahashi, M. Shibata, T. Nohara, *Chem. Pharm. Bull.*, 1989, **37**, 2212

[139] A. Close, R. Mauli, H. P. Sigg, *Helv. Chem. Acta.*, 1966, **49**, 204

[140] T. Kamikubo, K. Hiroya, K. Ogasawara, *Tetrahedron Letts.*, 1996, **37**, 499